Reduction of sulphur dioxide

Author:
Foong, Soon Kheong

Publication Date:
1975

DOI:

License:

THE UNIVERSITY OF NEW SOUTH WALES

"REDUCTION OF SULPHUR DIOXIDE"

A THESIS SUBMITTED IN PARTIAL FULFILMENT

OF THE REQUIREMENT FOR THE DEGREE OF

DOCTOR OF PHILOSOPHY.

BY

SOON-KHEONG FOONG

SCHOOL OF CHEMICAL ENGINEERING

1975.

CANDIDATE'S CERTIFICATE

THIS IS TO CERTIFY THAT THE WORK PRESENTED IN THIS
THESIS WAS CARRIED OUT BY THE CANDIDATE WITHIN THE
UNIVERSITY OF NEW SOUTH WALES AND HAS NOT BEEN
SUBMITTED TO ANY OTHER UNIVERSITY OR INSTITUTION FOR
A HIGHER DEGREE.

....

S. K. FOONG

DATE: ....

ACKNOWLEDGEMENT

ABSTRACT

In this thesis the experimental programme regarding the reduction of SO_2 primarily occuring in smelter gases using activated carbon, brown coal and anthracite as reductants was described. The programme was conducted in three main stages:

(1)   Thermodynamic analysis of the C-O-S and C-O-S-H systems.

(2)   Experimental and theoretical investigation of the sulphur dioxide reduction process in a spouted bed.

(3)   Study of the characteristics of a multiple spouted bed (the system proposed for handling large volumes of flue gases).

(1)   Thermodynamic Analysis.

Two systems viz. C-O-S and C-O-S-H representing the carbon sulphur dioxide and carbon/coal sulphur dioxide reactions were thermodynamically analysed in the temperature range of 800-1600°K, using a general hill-climbing programme in an IBM 360/50 computer. It was concluded from the thermodynamics view point that a process using carbon/coal to reduce sulphur dioxide should be conducted at temperatures higher than 1400°K.

At these temperatures carbon disulphide was found to
be the predominating specie and formation of COS and
H_2S was low.

(2) Experimental and Theoretical Investigation of the
Sulphur Dioxide Reduction Process

Experiments were conducted to study the reactions
between sulphur dioxide and activated carbon and
sulphur dioxide and coals (Brown coal and anthracite)
in a spouted bed. The temperature range used for the
study was between 650-950°C. Clean simulated flue
gases containing 1-7% sulphur dioxide were prepared
from pure sulphur dioxide and nitrogen. The experi-
mental results indicated that anthracite was compara-
tively inactive in sulphur dioxide reduction while
brown coal had the highest reactivity. High sulphur
recovery was indicated when activated carbon and brown
coal in particular were used as reductants. It was
suggested that sulphur dioxide could possibly be
reduced with brown coal efficiently at some intermediate
temperatures (around 700-800°C).

Some important design variables had been studied for
their relative significance. It was found that reaction
temperature and gas flow rate were most important when
activated carbon was used as reductant. With coals, it
was found that particle porosity and volatile matter
content also influenced strongly the sulphur dioxide
reduction reaction.

Theoretical prediction of the performance of a
spouted bed was found possible. A flow model pro-
posed by Mathur and Lim (ref. 42) for gas phase cata-
lytic reactions was found to be able to describe the
present system quite successfully.

(3) Characteristics Study of a Multiple Spouted Bed.

A multiple spouted bed system has been prepared for
handling large volumes of flue gases. The flow
characteristics of a multi-ple bed have been investi-
gated. Bed stability was noted and was found to be
dependent on bed height and D_p/D_i ratio. The optimal
ratio was found to lie within 0.09-0.13. General
correlations developed for single spouted beds were
proven applicable to multiple spouted beds. A solids-
flow model based on the concept of "Mixed models" was
developed for the bed.

TABLE OF CONTENTS

Page No.

CHAPTER TWO

<u>THERMODYNAMIC ANALYSIS</u>   Page No.

CHAPTER THREE

<u>REDUCTION OF SULPHUR DIOXIDE IN A SPOUTED BED</u>

LIST   OF   APPENDICES

APPENDIX A

COMPUTER PROGRAMME FOR CALCULATING THERMODYNAMIC

PROPERTIES AND TYPICAL PRINTOUTS

APPENDIX   B

GENERAL   HILL-CLIMB   PROGRAMME

GENERAL INTRODUCTION

Sulphur Dioxide is one of the major pollutants which has been plaguing the world for many years. The main reasons are as follows:

(1)   Large amounts of sulphur dioxide are being emitted into the atmosphere from various man-made sources. In the years between 1860 and 1960 SO_2 emission from man-made sources was found to increase from 5×10^6 tons per annum to 128×10^6 tons with a projected emission in the year 2000 of 333×10^6 tons if no control is effected.

(2) SO_2 has an adverse effect on human and animal health, crops and forest growth and on materials such as metals, stone, cement, paint, paper, leather and textiles (1,2).

In recent years, the control of sulphur dioxide emission has received much attention. A survey of the literature indicates that techniques and proposals for controlling the emission of sulphur dioxide are numerous. These techniques and proposals can be broadly classified into four categories:

(1) Adsorption of sulphur dioxide on solids materials.

(2) Adsorption of sulphur dioxide in solutions or on solid materials.

(3)   Reduction of sulphur dioxide to elemental
      sulphur.

(4)   Oxidation of sulphur dioxide to produce
      sulphuric acid.

Within these processes again there are two major
divisions:

(1)   Recovering sulphur dioxide in a useful form, and

(2)   Reacting sulphur dioxide to a waste product.

Reacting sulphur dioxide to a waste product could be
problematic because a different form of pollution, i.e.
solid waste pollution, is produced. Dry and wet sulphur
dioxide scrubbing with lime are typical examples (6).
Methods that recover sulphur dioxide in a useful form,
therefore, appear more attractive because they tend to have
less waste disposal problems and in addition credit could
be obtained from products recovered. The potential pro-
ducts that could be recovered are elemental sulphur,
sulphuric acid, liquid sulphur dioxide and ammonium sul-
phate. Of these products, elemental sulphur is the most
desirable. This is because it can be handled easier and
the costs of storing and shipping are comparatively lower.
These features are particularly important when marketing
the product is a problem.

Reduction of sulphur dioxide with carbon to elemental
sulphur is a well known process and was investigated a few
decades ago. Fixed beds of coke were invariably used in
the process and high temperatures were needed (10,11,12).

From the standpoint of ease of control and operation and
for providing better gas-solids contacting a continuous-
flow bed is more desirable. Furthermore, coal or char is
the preferred reductant since both are cheap and abundant.
Under these circumstances the spouted bed appears to be
most suitable. This is because the bed has been success-
fully used in low temperature carbonization of a variety
of N.S.W. coals without agglomeration problems (13,14).
It has also been shown to be a good contacting device for
gas and solids. These characteristics could, therefore,
be used to provide an environment for reducing sulphur
dioxide with carbon/coal or char.

In order to develop the spouted bed technique as an alterna-
tive for reducing sulphur dioxide emission from man-made
sources, the following studies are required:

    (1) Establishment of the spouted bed conditions

            necessary to reduce significantly inlet sulphur

            dioxide concentration to elemental sulphur.

    (2) Development of a process design model.

    (3) Scaling up.

For ease of experimentation, aspects (1) and (2) were in-
vestigated in a single-spout bed. In industrial applica-
tions, it is necessary that the bed be able to handle large
volumes of flue gases (i.e. in the order of 10,000 m^3/hr).
The largest spouted bed in commercial use is only 610 mm in
diameter (62,63,46). Therefore, it is essential that the
information obtained in a single-spout bed could be used

for scale-up purposes and what form the commercial spouted bed would take (investigation on these aspects is very scant). A multiple spouted bed appears to be an answer and therefore was chosen to be investigated for its operational and design characteristics.

CHAPTER   ONE

LITERATURE   SURVEY

1.1 INTRODUCTION

Sulphur dioxide has been recognised as a major atmospheric contaminant for many years. The main reasons for this are firstly, because of the large amount of SO_2 emitted into the atmosphere from various man made sources and secondly because of its adverse effects on human and animal health, crops and forest growth and on materials such as metals, stone, cement, paint, paper, leather and textiles (1,2).

The increased production of sulphur dioxide has been of the consequences of industrialisation. In a period of one hundred years from 1860 to 1960, world wide emission of sulphur dioxide from stationary sources has increased from 5×10^6 tons per annum to 128×10^6 tons with a projected emission in the year 2000 of 333×10^6 tons if no control is effected (3). The 1970 estimated sulphur dioxide emission in the U.S. without abatement was 36.6×10^6 tons. The potential emission for the year 2000 has been estimated at 125.8×10^6 tons. (6)

In Australia the emission of sulphur dioxide is less severe than that of the United States. However, according to the analysis of Thomson and Strauss (4), the emission of sulphur dioxide in the United States and in Australia is comparable on a per capita basis. Their data indicated that in 1971, Australia emitted 0.12 tons of sulphur dioxide per annum per capita compared to 0.15 tons per annum per capita in the United States (1968).

As mentioned above, millions of tons of sulphur dioxide are emitted into the atmosphere annually from man made sources. Such emission not only reduces the quality of the air and the environment, but also wastes one of the most valuable raw materials--sulphur. It was estimated that if 90% of all the sulphur dioxide emitted were recovered, there would be a surplus of supply over demand even if no sulphur was mined. One part of the costs of sulphur dioxide pollution may be regarded as the value of sulphur which is potentially recoverable. Dependent on the market value, this could be worth many millions of dollars. In addition to this, there are costs incurred due to the damage effected by the sulphur dioxide emitted. In the United States alone, (1970) it was estimated that the total damage amounted to 8.3 billion dollars (5). This amounts to about $0.20 for each pound of sulphur emitted.

Now, in most industrialized countries control of the emission of sulphur dioxide has become a matter of great urgency. Government regulating bodies have been set up and various air quality standards established. This means that sulphur dioxide abating processes will have to be installed in all non-natural sulphur dioxide emitting sources in order to meet the emission regulations. In recent years, quite a number of sulphur dioxide abating processes have been pro- posed and developed (6,7). The technology in this area, however, is by no means mature and further endeavours are required.

1.2 SOURCE OF SULPHUR DIOXIDE EMISSION

Sulphur dioxide emission from man made sources comes from the burning of naturally occuring sulphur compounds, either as a constituent of an ore or of a fossil carbonaceous material. For example, the sulphur content of coal varies from less than 1% to more than 3%. The sulphur content in sulphide ores is rather high, being of the order of 30% of the ore. Major potential sources of sulphur dioxide, therefore, are coal or oil-fired power plants, sulphide ore smelters, petroleum refineries, sulphuric acid manufacturing plants and incinerators. Table 1.1 shows the contribution of various sulphur dioxide sources in Australia (4). From this Table, it is clear that sulphur dioxide emission in Australia substantially results from the combustion of fossil fuels for power generation and the smelting of sulphide ores.

Projected sulphur dioxide emission in Australia is not reported in the literature. However, the future situation could probably be predicted by the figure (see Table 1.2) given by the National Air Pollution Control Administration in the United States. There about 60% of the total SO_2 emission is produced from power generation and sulphide ore smelting (6).

The estimates in Table 1.2 were made on the basis that there will be development and wide adoption of the breeder reactor, which is generally considered essential for major conversion to nuclear energy power generation. Even under such circumstances, the sulphur dioxide emission in the year 2000 is still about three times higher than that for 1970.

TABLE 1.1

ANALYSIS OF SO$_2$ EMISSION IN AUSTRALIA (1971) (4)

SOURCE	THOUSAND TONS PER ANNUM	%
Coal Combustion and Coke	467	32
Fuel Oil Combustion	241	16
Other Stationary Sources	2	-
Motor Spirit (Motor cars)	8	-
Other Mobile Sources	22	2
Petroleum Refineries	91	6
Other Process Industries	48	3
Non-ferrous Metals	619	41
Waste Diposal	5	-
Total	1,503	100

TABLE 1.2

ESTIMATED SULPHUR DIOXIDE EMISSION IN U.S. WITHOUT
ABATEMENT (ANNUAL EMISSION OF SULPHUR DIOXIDE) (6)
(MILLIONS OF TONS)

SOURCE	1970	1980	1990	2000
Power Plant Operation (Coal and Oil)	20.0	41.1	62.0	94.5
Other Combustion of Coal	4.8	4.0	3.1	1.6
Combustion of Petroleum Products (excluding power plant oil)	3.4	3.9	4.3	5.1
Smelting Metallic Ores	4.0	5.3	7.1	9.6
Petroleum Refinery Operation	2.4	4.0	6.5	10.5
Miscellaneous Sources	2.0	2.6	3.4	4.5
Total	36.6	60.9	86.4	125.8

1.3 CONTROL OF SULPHUR DIOXIDE EMISSION

A survey of the literature indicates that techniques and proposals for controlling the emission of sulphur dioxide are numerous. Three different approaches have generally been considered.

The first approach to sulphur dioxide abatement involves the use of high stacks. This is perhaps the most economical and simplest solution to the problem. The idea is to discharge sulphur dioxide high above ground level so that it will be diluted and dispersed over a wide area. High stacks have been used quite successfully over several decades as a means for dispersing pollutants. In order to keep ground level sulphur dioxide concentration at a tolerable limit stacks have been built higher and higher. It is not uncommon for power plants of today to have stacks as high as 1000 feet or more. It is obvious that this technique can only be a short term remedy to the problem. In Australia, this approach is still quite practical since most coals have sulphur contents lower than 1%. In ore smelting operations, high stacks are widely used. It is estimated that more than 50% of all the sulphur dioxide generated from ore smelting in Australia is emitted into the air through stacks (9). This has been permissible because many smelters are located well away from populated centres.

The second approach is centred on the use and development of low sulphur or sulphur free fuel. The reserves of low sulphur coal (less than 1%) are quite high as indicated by the survey carried out in the United States (6). It is unfortunate that

most of these reserves are of the sub-bituminous type and
not readily usable in power plants because of their low
heating value and the difficulty in achieving good combust-
ion. Another serious problem facing this method of reducing
sulphur dioxide emission is that the demand for power is
growing so rapidly that sulphur dioxide emission could become
unacceptably high, even if these low sulphur coals were used.

An alternative solution to the problem of sulphur dioxide
emission would be the desulphurisation of the fuel before
combustion and the use of non-pyrometallurgical processes
for sulphide ore extraction. So far, quite a number of
methods have been proposed and tested. Fuel oil has been
desulphurised by hydrogenation reasonably successfully, but
the same is not true for coal. This is because all coals
contain some sulphur in organic and inorganic form. The
inorganic sulphur can be removed by physical processes, but
the removal of organic sulphur has been found to be impossi-
ble except through processes that materially change the state
of the coal, such as liquefaction and gasification (8). The
cost of desulphurising coal via such a route would be
unacceptably high, when coal is used for its heating value
only.

The third approach for reducing sulphur dioxide is to de-
sulphurise the flue gas. In recent years, innumerable methods
have appeared in the literature (6,7). Some are still in
their experimental stage, some have been pilot planted and
others are claimed to have reached the commercial stage.

Most of these processes are designed as add-on systems to
reduce costs.

1.4   TECHNIQUES FOR FLUE GAS DESULPHURISATION

Because of environmental pressures many processes have evolved
in the past few years. These techniques can be broadly
classified into four categories:

(i)   Adsorption of sulphur dioxide on solid materials.

(ii)   Absorption of sulphur dioxide in solutions or
         on solid materials.

(iii)   Reduction of sulphur dioxide to elemental sulphur.

(iv)   Oxidation of sulphur dioxide to produce sulphuric
         acid.

Within these processes again there are two major divisions:

(i)   Recovering sulphur dioxide in a useful form, and

(ii)   Reacting sulphur dioxide to a waste product.

As in most cases, the evaluation of a process is based on
the balance of capital investment and credit received from
products recovered, the former approach seems more attractive
than the latter. The potential by-products from these pro-
cesses are elemental sulphur, sulphuric acid, liquid
sulphur dioxide and ammonium sulphate. Of these products,
elemental sulphur is the most desirable. This is because it
can be handled easier and the costs of storing and shipping
are comparatively lower. These features are particularly im-
portant when marketing the by-product is a problem. Further,
the process used should not cool the flue gas so that there

is no loss of plume buoyancy and no gas condensation.

Reduction of sulphur dioxide with carbon is one of the techniques which will satisfy the above requirements. Char or coal is the preferred source of carbon, since both are cheap and abundant. This technique is not new and has been successfully used in treating smelter gas over twenty years ago (10,11,12). These processes used coke as the reductant and a packed bed as the contactor. From the stand-point of ease of control and operation and for providing better gas-solids contacting a continuous-flow bed is more desirable. To this end, a spouted bed, a fluidised bed or even an entrained bed all appear to be suitable.

Fluidised beds have been used in the process industries for many years and have proved most useful in processes where gas-solids contacting is important. The technique has been applied to processes involving coal, such as low temperature carbonization and coal gassification because of the great improvement in heat transfer rates compared with those rates using traditional methods. One of the major problems associ-ated with the process is the tendency of the coal particles to agglomerate in the bed. The fine particles used in a fluidised bed (usually minus 30 mesh) allow rapid heating and relatively strong inter-particle bonding to occur, re-sulting in a marked tendency towards agglomeration.

The entrained system offers an alternative to the fluidised bed. In this method, the particles used have to be finely divided so that they can be carried along with the bulk of

the gas stream. The carbon utilization efficiency and gas cleaning are the major considerations. As the residence time of the particles in the reaction zone is usually only a few seconds, the reaction temperature is therefore necessarily very high (over 1300°C) in order to achieve high usage of carbon. The costs of using a high temperature reaction system, of providing high temperature electro-precipitation for gas cleaning and of operation make this technique less attractive.

The spouted bed technique, on the other hand, has been successfully used in low temperature carbonisation of a variety of N.S.W. coals. A much coarser particle (usually larger than 1mm) can be used in the bed without agglomeration problems, (13,14). The system was also shown to be a good contacting device for gas and solids. These advantageous characteristics of the technique could, therefore, be used to provide an enviroment for reducing sulphur dioxide with a solid, such as coal.

1.5 REDUCTION OF SULPHUR DIOXIDE CARBON AND COAL

1.5.1 Thermodynamics

The first thorough thermodynamic calculations for the sulphur dioxide carbon systems were given by Lepsoe in 1938 (10). In this study, Lepsoe calculated the equilibrium composition of gases resulting from the passing of pure sulphur dioxide through an incandescent carbon bed. The reactions considered in the computation were:

$$2CO + SO_2 = 2CO_2 + 1/2\ S_2$$
$$C + CO_2 = 2CO$$
$$C + S_2 = CS_2$$
$$C + CO_2 + S_2 = 2COS$$
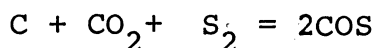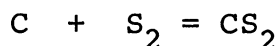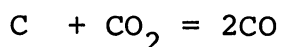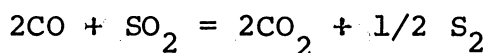
In addition to the above equilibria, equilibria between sulphur polymers S_2, S_6 and S_8 were taken into account at temperature below 800°C. From the results presented, it is also noted that there is an optimum temperature at which COS is at a maximum in the final equilibrium gas mixture over the temperature range of 300-1000°C. At high temperature, the amount of COS was found to be negligible, Further, it was established that the amount of CS_2 in the mixture was also practically nil in comparison to other species present.

Lepsoe also considered sulphur dioxide reduction with methane. It was noted that when methane was used, several side reactions producing hydrogen occurred. The presence of water vapour in the sulphur dioxide-carbon system was shown to reduce the sulphur dioxide conversion by converting sulphur to hydrogen sulphide.

The thermal stability of carbon oxysulphide and carbon di-sulphide was studied by Siller in 1948 (15), over a tempera-ture range of 600-1200°C. The results given indicated that while COS tends to become unstable as the temperature increases, carbon disulphide is stable over the entire range of temperature studied. Siller also noticed the complexity of the carbon-sulphur dioxide system by listing the various

possibilities of chemical equilibria for such a system. No calculation was performed.

In 1951 Owen et al (16) studied the thermodynamics of carbon disulphide synthesis using various systems. The sulphur dioxide-carbon system was one of those. They found that considerable quantities of carbon disulphide were formed. The results differ a great deal from those of Lepsoe (10). They attributed this discrepancy to the fact that more recent and reliable thermodynamic data was used in their calculations.

Results from this earlier work on sulphur dioxide reduction with carbon discussed above are unreliable. This is because complete thermodynamic data regarding the sulphur vapour equilibria was not available and also, because the problem could not be tackled in its full complexity without the aid of a computer.

Recently, Kellogg(17) investigated the equilibria in the systems C-O-S and C-O-S-H with reference to sulphur recovery from sulphur dioxide over a temperature range of 400-800°K. This is by far the most comprehensive themodynamic study attempted. In the study of the C-O-S system, Kellogg took into account all the possible polymers of sulphur vapour in addition to the following chemical species: CO, CO_2, CS_2, COS, SO_2, SO_3, S_2O and O_2. For the C-O-S-H system, additional species H_2, H_2O, H_2S and CH_4 were included. Many other species were also considered but found to be present in negligible concentration. According to this analysis, for

optimum recovery of elemental sulphur in a C-O-S system the
ratio of carbon atoms to oxygen atoms should be kept at 0.5
since at this ratio the amount of combined sulphur is at a
minimum and elemental sulphur is at a maximum. In line with
this finding a scheme for producing elemental sulphur from
sulphur dioxide reduction with carbon was discussed. It was
suggested that a good yield of elemental sulphur is possible
by firstly reacting sulphur dioxide with excess carbon at
high temperature (at 1100°K or higher) to give a C/O larger
than 0.5 and then metering a small amount of sulphur dioxide
into the reacted gas to achieve the necessary stoichiometry.
It was also noted that the gaseous equilibria involved in the
systems C-O-S and C-O-S-H were sensitive to total pressure
or to the presence of inert gas at constant total pressure.
Any inert gas in the system reduces the effective pressure
to a level which is equal to the difference between actual
total pressure and the partial pressure of the inert gas.
Based on Kellogg's results, inert gas should be avoided if
maximum sulphur recovery is sought. Unfortunately, nitrogen
is always a predominant specie in flue gases. Although
Kellogg realised the influence of inert gas on sulphur re-
covery, no allowance was made for this in his analysis. The
results given are therefore of limited use for systems such
as flue gas desulphurisation.

1.5.2   Kinetics

The possibility of using carbon to reduce sulphur dioxide to
elemental sulphur was quite well known in 1930. However, it

was not until 1940 that Lepsoe (10,11) investigated and published the chemistry of this process. A series of experiments were conducted using pure sulphur dioxide and metallurgical coke at temperatures between 850-1200°C. According to the results, 99% conversion of sulphur dioxide was obtained, however, considerable quantities of COS were also formed. Since Lepsoe had shown in his thermodynamic calculations that the amount of COS that can be in equilibrium with carbon monoxide and sulphur vapour is very small at temperature above 800°C, most of the COS found was therefore assumed to be the result of the extremely fast reaction, $CO + 1/2 \ S_2 = COS$ which took place homogeneously during the cooling of the gas samples. Further examination of the results led him to postulate that the following sequence of reactions could have occurred in the system:

$$SO_2 + C = CO_2 + 1/2 \ S_2$$
$$CO_2 + C = 2CO$$
$$SO_2 + 2CO = 2CO_2 + 1/2 \ S_2$$
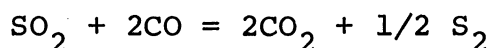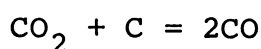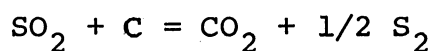
The third reaction takes place at the surface of the coke with ash as catalyst. Other reactions were also assumed to have occurred on the surface being kinetically first order reactions. The controlling steps of the process were also considered. Using published data on the reactions $C + O_2$ and $C + CO_2$ Lepsoe concluded that the reduction of sulphur dioxide is controlled by chemical reaction up to 1200°C, whereas beyond this diffusion becomes controlling.

The operational aspects of a sulphur dioxide reduction

process were compared with those for producer gas operation by Lepsoe (11). He found that the two operations were very similar and both depended on oxygen (air) for heat. As the reaction rate is low at low temperature for the sulphur dioxide reduction with coke, temperatures in the hot zone of the bed should not be less than 1300°C. Because the reaction will produce a gaseous mixture containing SO_2, CO_2, CO and COS (and H_2S, H_2 and H_2O if coal is used) a further reduction step in a catalytic chamber is required. It was found that at temperatures above 800°C the reduction of sulphur dioxide by means of carbon monoxide and carbon oxysulphide was fast with any kind of catalytic surface. At lower temperatures (250° - 500°C) alumina in the slightly hydrated and acid form was an efficient catalyst. The reaction $CO + SO_2$ also appeared to be of the first order.

The reduction of sulphur dioxide with carbon is a complicated system because its mechanism is sensitive to the reacting enviroment and the type of carbon source. Therefore depending on the prevailing conditions different end products can be formed. This characteristic of the system was demonstrated by Siller (15), who investigated means of recovering sulphur dioxide in smelter gases in a useful form. In his experiment, sulphur dioxide was reduced by anthracite and the desired product was carbon disulphide. High carbon disulphide yields were obtained. To achieve this, it was necessary to maintain a temperature gradient in the bed, with the hot zone at the middle. Siller believed that the process could have taken place in three steps. These steps can be

expressed by the following stoichiometric expressions:

Step I   (bed bottom cooler zone - 500°-700°C):

$$3C + 2SO_2 = 2COS + CO_2$$

$$C + CO_2 = 2CO$$
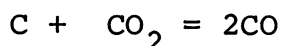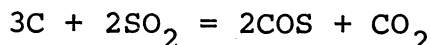
Step II (centre hot zone - temperature > 1000°C):

$$2COS = 2CO + 2S$$

Step III (hot zone - top cooler zone):

$$C + 2S = CS_2$$
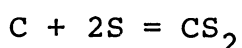
The   overall expression for the process thus becomes

$$5C + 2SO_2 = CS_2 + 4CO$$
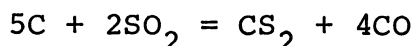
As indicated by the data tabulated, this process depends
quite strongly on the residence time of the gas. To ensure
that equilibrium conditions were reached, Siller had used
gas mean residence time no less than 1.5 minutes. There is
also a suggestion that the reaction rate of this process is
low. Moreover, the chemical reactivity of the carbon used
in the process is important. It was found that when metallur-
gical coke was substituted for anthracite coal very little
carbon disulphide was formed.

The use of carbon or coal as a means for reducing sulphur
dioxide emission from stationary source gained renewed
attention recently.

In 1968 Biswas et al (18) looked at the prospect of recover-
ing sulphur dioxide from smelter gas in the form of elemental
sulphur and carbon disulphide. They used a fixed bed of
charcoal or coke or coke soaked with 2% Na_2CO_3 as a catalyst.

The bed was heated uniformly between 900°C and 1200°C. The overall conversion of sulphur dioxide to carbon disulphide was about 10% and to elemental sulphur about 3%. The mean residence time in this case was about 15 seconds.

Giberson and Tingey (19) studied the reaction of sulphur dioxide and graphite in the temperature range 700°-1040°C. The kinetic data obtained was found to be satisfactorily correlated by the Langmuir type equation:

$$R = \frac{K_1 \, P_{SO_2}}{1 + K_2 P_{SO_2}} \qquad \ldots\ldots\ldots 1.1$$

where

$$K_1 = 4.39 \times 10^{-2} \, Exp \, (-5.12 \times 10^3/RT)$$
$$(hr. \, mm. \, Hg)^{-1}$$
$$K_2 = 4.28 \times 10^{-5} \, Exp \, (2.87 \times 10^4/RT)$$

The expression implies that absorption of sulphur dioxide inhibits the reaction rate of this process. The data also reveals the slow reaction rate between graphite and sulphur dioxide, since at temperatures as high as 1040°C the conversion of sulphur dioxide was only 10%. The effect of the presence of carbon monoxide and carbon dioxide in the gas stream was also studied. The addition of carbon monoxide to the sulphur dioxide inlet gas was found to enhance the rate of formation of carbon oxysulphide, carbon dioxide and elemental sulphur. The addition of carbon dioxide, on the other hand, slightly retarded the formation of the above products.

The mechanism of the C-SO$_2$ reaction was recently reviewed by Stacey et al (20). Based on their observations, they concluded that the reactions do not proceed in the way suggested by Lepsoe (11). Rather, it was believed that an oxygen-transfer reaction takes place between sulphur dioxide and carbon, analogous to the well known reaction in the case of carbon dioxide and carbon (21). An intermediate reactive oxygen complex is formed which can either desorb as an oxide of carbon or convert to a more stable oxygen complex. The process therefore relies on the reactivity of the carbon surface. In order that active sites of the carbon surface can be produced continuously the absorbed sulphur dioxide should be removed. One means of removal is to operate at temperatures sufficiently high for sulphur dioxide to dissociate at the carbon surface and further-more for most of the products formed to either leave the carbon bed or at least migrate to less active sites. The minimum temperature required for this phenomenon was found to be about 500°C.

Flue gas desulphurisation using active charcoal and bituminous coal char was the subject matter of the paper given by Sappok and Walker (22). The simulated flue gas had the following composition: 0.35% SO$_2$, 2.3% H$_2$O, 3.2% O$_2$ and 15.8% CO$_2$ in helium. The reaction temperature was 600°-800°C and the mean residence time of the gas was about 1.5 seconds. It was found that sulphur dioxide in the flue gas interacted with the carbon to form primarily hydrogen sulphide, carbon oxysulphide and a carbon-surface complex. Active charcoal was found to be very reactive in reducing sulphur dioxide and retaining the sulphur as carbon-surface complex. Hydrogen sulphide and carbon oxysulphide were emitted   from

the bed only when all the carbon was saturated with sulphur.
Char was also shown to be reactive for reducing sulphur
dioxide but the capacity for capturing sulphur was less
compared to that of active charcoal. The production of
hydrogen sulphide and carbon oxysulphide are, of course, by
no means desirable. Therefore a catalytic oxidation step
was proposed. By connecting an active carbon bed maintained
at 100°C to the outlet of the reduction reactor tube and then
by introducing a slight excess of oxygen to the converted
flue gas, they found that complete oxidation of the sulphur
compounds to elemental sulphur was possible.

The success of reducing sulphur dioxide with carbon and then
oxidising the sulphur compounds to elemental sulphur for
later recovery prompted Sappok and Walker to outline a new
process for removal of sulphur dioxide from stack gases.
Basically, two steps are required: (1) The sulphur dioxide in
the flue gas is converted in the first reactor to hydrogen
sulphide and carbon oxysulphide through reduction by carbon-
aceous materials. (2) The gas coming from the first unit
is then cooled down, air is added, and hydrogen sulphide and
carbon oxysulphide are oxidized in a second reactor to ele-
mental sulphur, possibly using active carbon as a catalyst.

As a follow-up to this work, Walker and Sinha (23) studied
the interactions of calcined anthracite with flue gas in a
fluidised bed reactor. The temperatures used were between
700° and 900°C. Simulated dry and wet flue gases were
employed. The anthracite was ground to a size less than
60 U.S. mesh in order to achieve fluidisation at a flow rate

of 1.2 1/min (N.T.P.) of flue gas. It was found that the reaction mechanism was similar to that of the sulphur dioxide-active carbon system. At 800°C anthracite reacted with sulphur dioxide to form elemental sulphur, hydrogen sulphide and carbon oxysulphide. Fresh anthracite was found to be rather unreactive. However, after an activation period, due probably to the $C-CO_2$ and $C-O_2$ gasification process, satisfactory sulphur dioxide removal was achieved. Complete removal of sulphur dioxide on a continuous basis was shown to be feasible by charging fresh anthracite into the reactor at a rate at which it was removed from the bed by gasification.

In 1971, Malmsron and Tuominen (24) reported the development of a pilot plant using pulverized coal to reduce sulphur dioxide produced from a flash smelter. In this method, predried pulverized coal was injected at the flash furnace uptake at 1300°-1350°C. The coal then reacted with sulphur dioxide in a suspended state. As coal contains quite a substantial amount of hydrocarbon, the reaction process thus becomes rather complicated. They believe that sulphur dioxide reacts with carbon and gaseous hydrocarbons as proposed by Lepsoe (10,11). The reaction of sulphur dioxide with gaseous hydrocarbons produces carbon monoxide, hydrogen, hydrogen sulphide and water vapour. Despite this, they found that good recovery of sulphur in elemental form could be realised by controlling the coal feed rate to produce a gas mixture which could be effectively used in a subsequent stage to recover more sulphur. Since it was noted that the

following reactions:

$$2CO + SO_2 = 1/2S_2 + 2CO_2$$
$$2COS + SO_2 = 3/2S_2 + 2CO_2$$
$$2H_2 + SO_2 = 1/2S_2 + 2H_2O$$
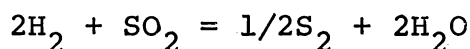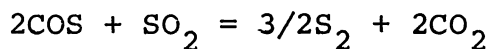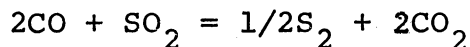
could be effected catalytically, an optimum gas mixture there-
fore should contain the reducing components i.e. CO, COS, H_2
H_2S at twice the concentration of sulphur dioxide. Under
such operational conditions, they found that 85-90% of the
sulphur was converted into elemental form.

1.6 THE SPOUTED BED TECHNIQUE

1.6.1 General Description of a Spouted Bed

Spouting was the name given by Mathur and Gishler (38) to a
fluid-solid contacting process somewhat similar to fluidiza-
tion. Application of the fluidized bed has been limited to
relatively fine solids because coarse materials when sub-
jected to fluidization show a marked tendency towards slug-
ging. Spouting appears not to be just a special form of
fluidizing; it can be used to materials that are too coarse
or too uniform a particle size for good fluidization. In
spouting, the upward motion is very rapid and is restricted
to a well defined central core. In the remainder of the bed,
there is never any upward motion of particles, rather, a
packed bed moving steadily downward and to some extent in-
ward. This steady motion eliminates backmixing of particles
in the annulus. At the same time, the fairly rapid bed turn-
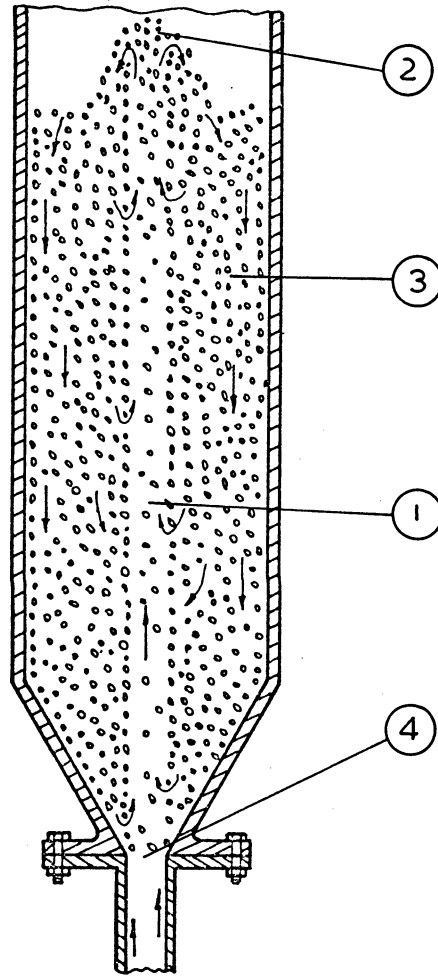
Fig. 1.1 A half-sectional Diagram
of a Single Spouted Bed

over tends to reduce the temperature differences usually
associated with conventional packed bed systems.

Qualitative studies using sectional models have shown that a
spouted bed is a combination of a dilute fluidized or en-
trained phase and a coexistent moving bed of solids. This
is readily seen from Fig. 1.1, which is a schematic diagram
of a spouted bed. The spouting medium enters the apparatus
through an opening in the apex of a conical inlet. Particles
are lifted as a dilute suspension through the central core,
1, by the high velocity gas stream. At the top of the bed,
2, where the central stream velocity is suddenly reduced,
particles fall back onto the bed. These particles then flow
as a slowly moving packed bed, 3, downward and towards the
spout. The gas enters the column through an orifice, 4,
and flows up the spout and up through the void space in the
moving packed bed.

Detaileddiscussion of the special characteristics of spouted
beds is available in the literature (45,60).

1.6.2. Previous Work

Extensive reviews of this topic have been published (45,60)
and so only a brief summary of the major hydrodynamic features
is given in the following section.

1.6.2.1 Hydrodynamic Features

Since the introduction of the spouted bed technique by
Mathur and Gishler some twenty years ago, quite a lot of

research has contributed to a better fundamental understanding. Most of this work has been devoted to the study of the hydrodynamics of the system. Hydrodynamic features which have received attention are as follows:

(i)   spouting pressure drop, ΔP_s (39,47,75,77,89),

(ii) maximum spouting pressure drop, ΔP_{ms} (74,75,77),

(iii) minimum spouting velocity, v_s (38,46,59,77,80,89),

(iv) maximum spoutable bed depth, H_m (39,46,59,77,75),

(v)   flow pattern of solids and fluid (44,59,46,73,75, 81,90),

(vi) void fraction (38,46,90) and

(vii) spout diameter, D_s (38,46,75,76,91).

1.6.2.2 Heat Transfer

Heat transfer studies include the following:

(i)   between wall and bed (92,93,94,95),

(ii) between submerged heater and bed (93) and

(iii) between particles and gas (96,97).

1.6.2.3 Mass Transfer

Mass transfer studies include the following:

(i)   between particles and fluid (100,101) and,

(ii) intra-particle mass transfer (81,102,83,103).

1.6.2.4. Application

Because of its unique gas-solids flow characteristics, the spouted bed has been used for the drying of wheat (61,81, 98), wood chips (62), and peas, lentils and flax (64).

Application of the technique for drying of chemicals such
as activated carbon, superphosphate, gelatine and pharma-
ceuticals has also found to be an advantage (63). It has
also been found useful for a variety of seemingly unrelated
processes such as cooling (65), bleeding (66) and coating
of various materials (67,68), granulation of fertilizers and
other products (69,70), pyrolysis of shale (71) and low
temperature carbonization of coal (13,14,72,73). More re-
cently, the techniques has been found useful in the direct
reduction of iron ore (107). It was also used for thermal
cracking of petroleum such as heavy oil, kerosine and crude
oil by Uemaki et al (105,106). The temperature range used was
600° to 850°C and heat carriers employed were Al_2O_3, Cr/Al_2O_3
and coke. Steam was employed as carrier gas for oil.
Satisfactory yields of ethylene and propylene were obtained.
These results were found to compare more favourably than
those obtained by using fluidised beds. The operability of
the spouted bed was found to be higher than those of fluidised
beds.

1.6.2.5. Flow Model for Theoretical Analysis

Recently Mathur and Lim (47) theoretically formulated a flow
model of a spouted bed involving vapour phase chemical reac-
tion in the presence of catalyst or heat carrier particles.
The hydrodynamic characteristics of the spouted bed relevant
to the model are described by the available information. The
model as it stands is rather general but its usefulness is
restricted by the incomplete information on certain hydro-
dynamic features, such as the voidage profile of the bed and
the longitudinal profile of the gas velocity in the annulus

region. Nevertheless, the application of the model is
demonstrated by making certain predictions concerning the
effect of the important variables such as spouting gas
velocity, column size, bed depth, particle size and spout
voidage, on the gas conversion of a first order reaction.
The relative performance of spouted, fixed and fluidised beds
was also compared using two types of catalysts, viz. ideal-
ised porous and non-porous catalysts. The results indicated
that with the idealised porous catalyst where the reaction
rate is independent of particle size, the spouted bed is seen
to give higher conversions than the fluidised bed, the differ-
ence being substantial for the faster reaction considered.
This behaviour follows from the fact that in order to match
the high gas flow rates permitted by the use of coarse parti-
cles in a spouted bed, an equivalent fluidised bed with its
finer particles must be operated at high multiples of mini-
mum fluidization velocity. Under such condition, gas con-
version in a fluidised bed becomes poor because of excess-
ive by-passing of gas in the form of bubbles and the spouted bed
becomes the more attractive method.

1.7 CONCLUSION FROM LITERATURE SURVEY

The preceding survey shows that atmospheric pollution by
sulphur dioxide has rapidly become a major problem. In
Australia, the major sulphur dioxide emitters are coal and
oil fired power plants and sulphide ore smelters.

The potential hazard of uncontrolled emission of sulphur
dioxide into the atmosphere is recognised at government

level by leading industrialised countries such as the
United States. The involvement of government has resulted
in a lot of research activity. Most of these research
efforts have been centred on ways and means of reducing
sulphur dioxide in the flue gases. There are two general
approaches to the problem:

(1)   Recover sulphur dioxide as useful products.

(2)   Capture sulphur dioxide in a form that is
        harmless and can be disposed as waste.

Recovering sulphur dioxide as elemental sulphur has some
attraction since elemental sulphur is valuable raw material
which can be handled with ease.

Since detailed thermodynamic analysis of the C-O-S and
C-O-S-H systems is not possible without the aid of a computer,
early work has been oversimplified. This work invariably used
idealised systems such as pure carbon and pure sulphur dioxide
or pure methane and pure sulphur dioxide for analysis (10,15,
16,26,27).

From the survey, it is also clear that the technology of
using a fixed bed of coke to reduce sulphur dioxide produced
from ore smelting to elemental sulphur is rather well devel-
oped. The cost of producing elemental sulphur using these
processes, however, is not economical. This cost can be re-
duced in part if cheap reductants such as high sulphur coal,
brown coal, anthracite or char produced from gasification
processes are used. Further cost reduction may be possible

if a flow system could be used in place of a fixed bed system.
Some recent researches have directed their efforts along this
line (22,23,24) and have shown promising results in employ-
ing anthracite and char for controlling sulphur dioxide
emission. Unfortunately, these studies are very fundamental
in nature and offer only limited design information.

The actual application of pulverised coal in the entrained
state to reduce sulphur dioxide in flash smelter gas (24) is
indeed an interesting development in this area. The techni-
que is only suitable for processes which give flue gases with
temperatures higher than 1300°C. Flow processes other than
this have not been investigated in detail.

The spouted bed technique is relatively new compared to the
well known fluidized bed method. Since its inception in 1955,
the technique has attracted a certain degree of attention,
although it has not gained general acceptance. This is pro-
bably due to the novel characteristics of the method which
only allow it to be used in specific circumstances. The
technique has been used in processes such as drying, blend-
ing and coating of coarse particles (45). It is reported
that it has been used as a reactor to promote gas-solids
reactions such as direct reduction of iron ore (107) and
thermal cracking of petroleum (105,106). The successful
application of the technique in low temperature carboniza-
tion (13,14) is particularly interesting since this indicates
a potential for its use in sulphur dioxide reduction with
coals. The operation of a spouted bed at elevated

temperatures, however, has not been studied extensively. Since most of the design correlations have been developed from data collected at room conditions (45), the validity of these correlations at elevated temperatures is not known. Furthermore, it is noticed that very little attempt has been given to use the spouted bed for gas-solids reactions despite the fact that it possesses several of the same properties which have been responsible for the wide spread application of fluidized beds in this area, viz. intimate gas-solids contact, ease of addition and withdrawal of solids and good agitation. Recent work (47) on theoretical analysis of a spouted bed process involving gas-solids reaction indicated that performance of the spouted bed is better than those of the fixed and fluidized beds when idealised porous solids are used.

CHAPTER TWO

THERMODYNAMIC ANALYSIS

2.1 <u>INTRODUCTION</u>

Before experimenting on a chemical reaction system, it is desirable to know the most favourable conditions of temperature, pressure, composition and ratios of reactants to obtain the greatest conversion and the highest yield of desired products. In this regard, the thermodynamics of the reaction is as important as the kinetics, since it furnishes such fundamental information.

In the following thermodynamic analysis, gases similar to those emitted either from smelters or power generation plants were considered. The effects of temperature, type of reactant and air dilution were studied.

For thermodynamic calculations, two methods are available. These are:

(1) Solution of simultaneous equations,

(2) Free energy minimization.

Since mathematically there can be only one equilibrium composition for a particular chemical system, it is immaterial which method is used, except that the latter approach is more general (37). In this calculation the former method is employed.

2.2 REACTION SYSTEM

When sulphur dioxide is passed over carbon or coal quite a number of chemical species can coexist. For a carbon-sulphur dioxide (C-O-S system CO, CO_2, COS, S_2, SO_2, SO_3 can exist in the equilibrium gas phase between 1000-1600°K. For a coal-sulphur dioxide (C-O-S-H) system, additional species viz. H_2, H_2O, H_2S and CH_4 would have to be considered. Monoatomic sulphur, polyatomic sulphur molecules, SO molecules and HS radicals cannot be present in appreciable amounts over the temperature range quoted above (10,17,25,26,27).

In the present analysis the temperature range selected was 800°-1600°K. Between 800° and 1000°K sulphur vapour exists in a complicated equilibrium among S_2, S_3, S_4, S_5, S_6, S_7 and S_8, whose distribution is a function of temperature and total sulphur partical pressure (17,29,30,31). However, the species S_3, S_4 and S_5 are not present in significant amounts in this temperature range. It has been found that the discrepancy between experimental results and thermodynamic predictions caused by considering only S_2-S_6-S_8 equilibria is about 4% (32,33).

2.2.1 System C-O-S

This is an idealised situation where pure carbon reacts with pure sulphur dioxide. In reality, nitrogen is present in all flue gases, and has been included in the analysis.

The important reaction equilibria of this system in the temperature range 1000°-1600°K are:

$$C \quad + \quad SO_2 \quad = \quad CO_2 \quad + \quad 1/2S_2 \qquad (1)$$

$$C \quad + \quad CO_2 \quad = \quad 2CO \qquad (2)$$

$$2CO \quad + \quad S_2 \quad = \quad 2COS \qquad (3)$$

$$2COS \quad = \quad CO_2 \quad + \quad CS_2 \qquad (4)$$

$$1/6S_2 \quad + \quad 2/3SO_3 \quad = \quad SO_2 \qquad (5)$$
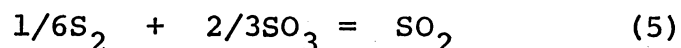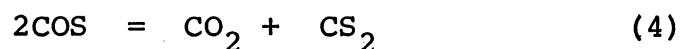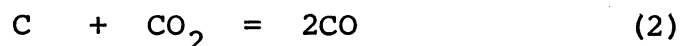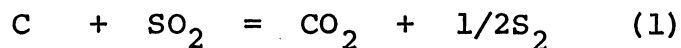
In the temperature range $800°-1000°K$ S_2-S_6-S_8 equilibria were included:

$$3S_2 \quad = \quad S_6 \qquad (6)$$

$$4S_2 \quad = \quad S_8 \qquad (7)$$

There are other possible reactions between the co-existing chemical species (15,36), but many of these are interrelated and therefore need not be included in the equilibrium composition calculation (37). The seven chemical equilibria given above are independent and express the interrelations of the nine important gaseous species adequately. Since not all the possible chemical species in the final equilibrium gas mixture are considered the above equilibria constitutes a valid, but not a unique set of equilibria.

2.2.2 System C-O-S-H

There are two types of flue gas which are of particular interest, namely power plant stack gases and gases generated by sulphide ore smelters. The concentration of gases in the power plant effluent varies with the fuel burned, operating conditions and boiler efficiency. The flue gas composition given in Table 2.1 is that resulting from a coal feed with a

sulphur content of 3.2% by weight. For a conventional smelter, the following three major steps are usually used for ore processing:

(i)   ore roasting,

(ii) ore smelting in a reverberatory furnace, and

(iii) oxidation in a converter.

All these ore treating steps emit sulphur dioxide. The concentration of sulphur varies from one step to another because the conditions employed are different in each step. In Table 2.2, cases of flue gas compositions that could exit from these steps are listed. It should be pointed out, however, that these flue gases are only reasonable representations of gases that emit from smelters (34).

The important chemical equilibria that could be produced from the reaction of the smelter flue gases with carbon are essentially the same as those proposed for the C-O-S system except for the addition of the following equilibria:

$$H_2O + CO = CO_2 + H_2 \qquad (8)$$
$$H_2 + 1/2S_2 = H_2S \qquad (9)$$
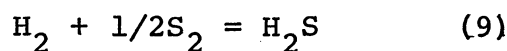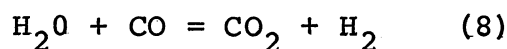
Oxygen present in the gases is assumed to be converted to CO_2 according to the reaction $C + O_2 = CO_2$

When coal is the reductant, gaseous hydrocarbons evolved from the coal make the reaction more complicated to analyse. For ease of analysis, these hydrocarbons are taken as methane only. The overall reaction of sulphur dioxide with methane can be written as:

$$2SO_2 + CH_4 = S_2 + CO_2 + 2H_2O \quad (10)$$
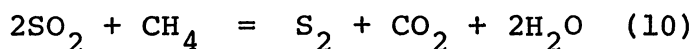
As in the case of the C-O-S system the equations given above again constitute a valid set of equilibria.

Since there are more variables than independent equations in the above two cases, more equations are required to make the system determinate. The method of solving these simultaneous equations is given in the following section.

2.3 METHOD OF CALCULATION

When an ideal gaseous reaction is at equilibrium the partial pressures of the chemical species in this system are related in the following manner:

$$aA + bB = cC + dD$$
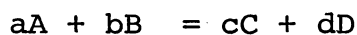
$$K_e = \frac{p_C^c p_D^d}{p_A^a p_B^b}$$

Where K_e is the equilibrium constant. For the C-O-S system seven similar expressions and for the C-O-S-H system either nine or ten similar expressions can be written. Simultaneous solution of these equations and the relevant equations that specify the total pressure and composition of the system in question will then give the equilibrium composition of the system. For example, for the coal-SO_2 system there are thirteen gaseous species (including nitrogen), so thirteen independent equations must be solved in order to calculate the composition of the equilibrium mixture. Therefore three additional equations are required: one equation relates

total pressure to the sum of the partial pressures and two

equations which specify the composition of the system in

question. The latter three equations are expressed below:

$$P_T = P_{co} + P_{co_2} + P_{cos} + P_{cs_2} + P_{s_2} + P_{N_2} + \cdots$$

$$Q = \frac{P_{cos} + 2P_{cs_2} + P_{so_2} + 2P_{s_2} + 6P_{s_6} + 8P_{s_8}}{2P_{so_2} + P_{co_2} + P_{co} + 2P_{co_2} + 3P_{so_3}}$$

$$= \text{atom ratio sulphur/oxygen in the gas}$$

$$R = \text{atom ratio nitrogen/oxygen in the gas}$$

$$= \frac{2P_{N_2}}{2P_{so_2} + P_{cos} + P_{co} + 2P_{co_2} + 3P_{so_3}}$$

From the foregoing, it is clear that the basic information

required for performing the analysis is a knowledge of the

equilibrium constants. These constants can be computed with

the expression given below if the standard free energy

changes of the reactions are known:

$$\ln K_e = - \frac{F_f^o}{RT}$$

where F_f^o is the change of the standard free energy, R the

gas constant and T the temperature. A convenient method of

calculating the changes of standard free energies, F_f^o, at

various temperatures is the use of the standard free energies

of formation. This information is available in the literature

(17,28). A simple computer programme was written for calcula-

ting the equilibrium constants for all the reactions under

consideration. The programme is given in Appendix A. The

calculated equilibrium constants are shown in Table 2.3.

To solve the simultaneous equations describing the various chemical systems the service of a computer was again sought. A general "hill climbing" programme was used in an I.B.M. 360/50 computer. The standard programme was written for the purposes of maximization but was adapted for minimization using a subprogramme. Description of this programme and a sample set of print out is given in Appendix B.

2.4 RESULTS

In this thermodynamic analysis equilibrium gas compositions were computed for SO_2-C, SO_2-C-H_2O and SO_2-C-H_2O-CH_4 systems using four different types of flue gas tabulated in Table 2.1 and 2.2. The effects of temperature, air dilution, water vapour and the concentration of methane on equilibrium gas compositions and sulphur recovery were studied.

The complete results of these calculations are given in Tables 2.4 to 2.7 and typical results are shown in Figures 2.1 to 2.9:

Fig. 2.1, 2.2 and 2.3:

These figures show the temperature dependence of the distribution of sulphur between components in the equilibrium gas mixture for the reduction of SO_2 in the smelter gas produced from an ore converter (Table 2.2-case 2), in the smelter gas produced from an ore converter and reverberatory furnace (Table 2.2-case 3) and in power plant flue gas (Table 2.1) respectively with carbon.

Fig. 2.4:

This shows the temperature dependence of the distribution

of sulphur between components in the equilibrium gas
mixture for the reduction of SO_2 in the smelter gas pro-
duced from ore converter and reverberatory furnace
(Table 2.2-case 3) with 2% methane added to it.

Fig. 2.5a and 2.5b:

The typical effects of air dilution on sulphur recovery
at different temperatures are given in these figures.
The gases used for analysis were the smelter gas gener-
ated by the ore converter (Table 2.2-case 1) and that
produced from the ore converter and reverberatory fur-
nace (Table 2.2-case 3).

Fig. 2.6:

This gives the effect of air dilution on the formation
of COS at different temperatures in the reduction of
SO_2 with carbon in the smelter gas production from an ore
converter (Table 2.2-case 1).

Fig. 2.7:

This shows the effect of air dilution on the formation of
CS_2 in the reduction of SO_2 with carbon in the smelter gas
generated from an ore converter (Table 2.2-case 1).

Fig. 2.8:

This shows the effect of CH_4 on sulphur recovery at diff-
erent temperatures. The flue gas generated by an ore
converter and a reverberatory furnace (Table 2.2-case 3)
was used.

<u>Fig. 2.9</u>:

This figure compares the sulphur recovery using carbon and carbon + 2% methane. The flue gas used was smelter gas produced from ~~an~~ ore converter and reverberatory furnace (Table 2.2-case 3).

2.5 DISCUSSION OF RESULTS

2.5.1 Effect of Temperature

(a) On Sulphur Recovery

From the results obtained, it may seem that if elemental sulphur is the prime product, then sulphur dioxide reduction should be carried out at a temperature as low as possible. The lowest operational temperature, however, is dictated by the reaction rate of the reacting system which can not be indicated in the thermodynamic analysis. It has been shown that for a C-O-S system, temperatures well above 800°K are needed to give a satisfactory sulphur dioxide conversion (20,21,22,24).

In all cases studied, temperature was shown to have a marked effect on the recovery of sulphur. In Fig. 2.1 to 2.4, it can be seen that for temperatures above 900°K sulphur concentration drops rapidly to a negligible level. Thus S_2 appears as other chemical species such as COS, CS_2 and H_2S.

(b)   On COS, CS_2 and H_2S Formation

    In Fig. 2.1 to 2.4, the concentration of COS
is shown to be low at 800°K, rising quickly to
a maximum at about 1000° - 1100°K. At higher
temperatures, COS is found to be unstable and
the predominating chemical specie becomes CS_2.

    With the presence of methane and/or water
vapour in the reaction system most of the
sulphur is converted to H_2S at the lower end of
the temperature range studied. Like COS, H_2S
is also found to be unstable at high temperatures.
The maxima of H_2S formation is at about 900°K.

(c)   On SO_2 Conversion

    The effect of temperature on SO_2 conversion is
shown to be negligible over the temperature
range studied. This is because conversion of
SO_2 is close to 100% at all temperature levels.

2.5.2 Effect of Air Dilution

The presence of oxygen from air dilution of flue gases is
found to reduce the recovery of elemental sulphur (Fig. 2.5a
and 2.5b). The formation of COS and CS_2 are also affected
(Fig. 2.6 and 2.7): the concentration of COS increases with
air dilution, while CS_2 decreases. This is due to the
greater availability of carbon monoxide resulting from the
introduction of oxygen. Carbon monoxide is produced from
the carbon gasification reaction $C + CO_2 = 2CO$.

2.5.3. Effect of Methane

The yield of elemental sulphur is seen to increase with decrease in methane concentration at different temperatures (Fig. 2.8 and 2.9). In the presence of methane, sulphur in the system is mainly converted to H_2S and CS_2. A significant amount of H_2 is also formed as a result of the water-gas shift reaction, which is favoured at high temperatures.

2.5.4. General Discussion

The concentration of sulphur polymers S_6 and S_8 and SO_3 relative to initial sulphur content are found to be significant only at temperatures below 1000°K. Their influence on equilibrium compositions are only marginal. Hence, for part of the calculations only S_2 was considered.

The general pattern of the results for this analysis shows a close resemblance to that of Averbukh et al (26,27) except that while their results for sulphur vapour increased slightly with temperature, the results for this study showed a downward trend as temperature increased. This is probably because Averbukh et al used a pure system of carbon-methane for their calculations. Furthermore, thermodynamic data also differed to a certain extent because they were derived from different sources.

2.6 CONCLUSION

The reduction of sulphur dioxide in flue gas produced from smelters and power generation plants has been proved theoretically feasible. The question of whether or not it is

economically feasible, however, depends on factors such as fixed and operating costs, cost of reductant and credit from sale of sulphur recovered etc. From the thermodynamic point of view, it follows that a process using carbon/coal to reduce sulphur dioxide should be operated at high temperatures (above 1400°K) because of low COS and H_2S formations. At high temperatures CS_2 is the predominating chemical specie. It is valuable and can be recovered easily. At moderate temperatures COS, CS_2 and H_2S are present in significant proportions.

The formation of COS and H_2S are most undesirable from the view point of air pollution. Therefore, reduction of sulphur dioxide with carbon/coal can only be an initial step in reducing sulphur dioxide in flue gases. Further steps such as those proposed in Ref. (12,24) to yield elemental sulphur as a product, is probably required.

In the following chapter the use of the spouted bed technique for providing an enviroment for reducing sulphur dioxide is presented.

TABLE 2.1

POWER PLANT STACK GAS COMPOSITION

CHEMICAL SPECIE	v/v %
CO_2	15.8
NO_x	0
CO	0
O_2	3.2
SO_2	0.35
H_2O	2.3
N_2	78.35
TOTAL	100.0
EXCESS AIR	18

TABLE 2.2

SMELTER   GAS   COMPOSITIONS

Chemical Specie	Case 1 Converter Only no Air Dilution, %	Case 2 Converter Only Air Diluted , %	Case 3 Converter + Reverberator Air Diluted., %
SO_2	15.8	4.5	2.9
O_2	1.2	16.5	14.3
CO_2	-	-	1.7
CO	-	-	0.6
H_2O	-	-	0.1
N_2	83.0	79.0	80.4
TOTAL	100.0	100.0	100.0
S/O ratio	0.465	0.107	0.753
S/H ratio	-	-	14.5

TABLE 2.3

VALUES OF $Ln K_e$

Reaction	Values of $Ln K_e$ at Temperatures (K^o)					
	800	900	1000	1200	1400	1600
1	13.8286	13.2942	12.8621	12.2039	11.7241	11.3563
2	-4.6125	-1.7380	0.5486	3.9494	6.3491	8.1244
3	8.5003	5.4476	3.01962	-0.5905	-3.1375	-5.0201
4	-1.4677	-1.4701	-1.4731	-1.4792	-1.4875	-1.4960
5	10.3115	10.2543	9.4904	8.2411	7.3201	6.6038
6	4.2407	-0.2589	-3.8250	-	-	-
7	5.7674	-0.8167	-6.0392	-	-	-
8	1.4456	0.8388	0.3669	-0.3099	-0.7678	-1.0921
9	9.3888	6.1550	4.9527	3.1413	1.8438	0.8713
10	29.0432	27.7834	26.7695	25.2247	24.0970	23.2269

TABLE 2.4a COMPOSITION OF EQUILIBRIUM MIXTURES IN THE SYSTEM SULPHUR DIOXIDE - CARBON (SMELTER GAS CASE 1, TABLE 2.2)

S : O Ratio	EQUILIBRIUM COMPOSITION							
	S_2	SO_2	CO_2	CO	COS	CS_2	SO_3	N_2
	Temperature 800°k							
0.465	0.075	3.576×10^{-8}	0.1608	1.585×10^{-5}	2.503×10^{-4}	8.981×10^{-8}	3.352×10^{-4}	0.787
0.267	0.048	3.522×10^{-8}	0.1818	1.792×10^{-5}	2.487×10^{-4}	7.838×10^{-8}	3.541×10^{-4}	.783
0.107	0.022	2.933×10^{-8}	0.2057	2.028×10^{-5}	$2.053.10^{-4}$	4.727×10^{-8}	3.109×10^{-4}	0.772
	Temperature 900°K							
0.465	0.064	6.212×10^{-8}	0.1461	4.520×10^{-3}	1.735×10^{-2}	4.755×10^{-4}	1.595×10^{-4}	0.767
0.267	0.039	5.692×10^{-8}	0.1695	5.243×10^{-3}	1.593×10^{-2}	3.442×10^{-4}	1.575×10^{-4}	0.769
0.107	0.0160	4.173×10^{-8}	0.1962	6.070×10^{-3}	1.168×10^{-2}	1.598×10^{-4}	1.242×10^{-4}	0.770
	Temperature 1000°K							
0.465	1.193×10^{-2}	1.285×10^{-8}	4.536×10^{-2}	0.1359	6.717×10^{-2}	2.280×10^{-2}	–	0.717
0.267	5.163×10^{-3}	1.035×10^{-8}	5.553×10^{-2}	0.1663	5.408×10^{-2}	1.208×10^{-2}	–	0.707
0.107	1.129×10^{-3}	5.834×10^{-9}	6.693×10^{-2}	0.2005	3.049×10^{-2}	3.183×10^{-3}	–	0.698
	Temperature 1200°K							
0.465	6.618×10^{-4}	–	9.936×10^{-5}	0.2677	5.126×10^{-3}	6.035×10^{-2}	–	0.666
0.267	4.099×10^{-4}	–	1.117×10^{-4}	0.3010	4.536×10^{-3}	4.046×10^{-2}	–	0.652
0.107	1.447×10^{-4}	–	1.257×10^{-4}	0.3387	3.033×10^{-3}	1.667×10^{-2}	–	0.641

TABLE 2.4a cont.

S : O Ratio	EQUILIBRIUM COMPOSITION							
	S_2	SO_2	CO_2	CO	COS	CS_2	SO_3	N_2
Temperature 1400°K								
0.465	7.226×10^{-5}	–	8.310×10^{-7}	0.2719	4.814×10^{-4}	6.301×10^{-2}	–	0.665
0.267	4.146×10^{-5}	–	9.347×10^{-7}	0.3058	4.102×10^{-4}	4.067×10^{-2}	–	0.653
0.107	1.658×10^{-5}	–	1.043×10^{-6}	0.3412	2.894×10^{-4}	1.814×10^{-2}	–	0.640
Temperature 1600°K								
0.465	1.375×10^{-5}	–	2.389×10^{-8}	0.2722	8.213×10^{-5}	6.326×10^{-2}	–	0.664
0.267	7.918×10^{-6}	–	2.686×10^{-8}	0.3061	7.000×10^{-5}	4.087×10^{-2}	–	0.653
0.107	3.175×10^{-6}	–	2.996×10^{-8}	0.3414	4.944×10^{-5}	1.827×10^{-2}	–	0.640

* SULPHUR POLYMERS S_6 and S_8 ARE REGARDED AS S_2.

TABLE 2.4b   SULPHUR DISTRIBUTION IN THE SYSTEM
SO_2 - CARBON (SMELTER GAS CASE 1 & 2
TABLE 2.2)

S/O	S DISTRIBUTION (%)			
Ratio	S_2	COS	CS_2	SO_3
Temperature 800°K				
0.465	98.99	0.43	–	0.58
0.267	98.50	0.58	–	0.84
0.107	97.61	0.95	–	1.44
Temperature 900°K				
0.465	77.97	21.28	0.58	0.17
0.267	70.79	28,37	0.61	0.23
0.107	56.99	41.86	0.57	0.58
Temperature 1000°K				
0.465	11.70	65.92	22.37	0.01
0.267	7.24	75.83	16.93	–
0.107	3.24	87.61	9.15	–
Temperature 1200°K				
0.465	1.00	7.77	91.23	–
0.267	0.88	9.67	59.45	–
0.107	0.73	15.28	83.99	–
Temperature 1400°K				
0.465	0.11	0.76	99.3	–
0.267	0.09	0.10	98.91	–
0.107	0.08	1.57	98.35	–
Temperature 1600°K				
0.465	0.02	0.13	99.85	–
0.267	–	0.04	99.96	–
0.107	–	0.25	99.75	–

TABLE 2.5a COMPOSITION OF EQUILIBRIUM MIXTURES IN THE SYSTEM SO_2 - CARBON - METHANE - H_2O (SMELTER GAS CASE 3 TABLE 2.2)

S:O Ratio	S:H Ratio	EQUILIBRIUM COMPOSITION									
		S_2^+	SO_2	CO_2	CO	COS	CS_2	H_2S	H_2	CH_4	N_2
		Temperature 800°K									
.753	0.348*	8.041×10^{-3}	1.529×10^{-8}	0.1728	1.703×10^{-5}	1.071×10^{-4}	1.529×10^{-8}	1.184×10^{-2}	1.104×10^{-5}	1.01×10^{-3}	0.780
	0.683*	1.064×10^{-2}	1.845×10^{-8}	0.1812	1.786×10^{-5}	1.292×10^{-4}	2.123×10^{-8}	6.884×10^{-3}	5.581×10^{-6}	2.456×10^{-4}	0.787
	1.376*	1.233×10^{-2}	2.034×10^{-8}	0.1856	1.829×10^{-5}	1.433×10^{-4}	2.518×10^{-8}	2.749×10^{-3}	2.749×10^{-6}	1.317×10^{-6}	0.792
		Temperature 900°k									
	0.345	1.535×10^{-3}	1.142×10^{-8}	0.1730	5.352×10^{-3}	3.196×10^{-3}	1.357×10^{-5}	2.164×10^{-2}	1.172×10^{-4}	4.695×10^{-4}	0.777
	0.683	4.360×10^{-3}	1.988×10^{-8}	0.1787	5.529×10^{-3}	5.563×10^{-3}	1.386×10^{-5}	1.386×10^{-2}	4.455×10^{-4}	6.563×10^{-5}	0.785
	1.376	6.873×10^{-3}	2.524×10^{-8}	0.1810	5.591×10^{-3}	7.063×10^{-3}	6.346×10^{-5}	7.435×10^{-3}	1.904×10^{-4}	1.185×10^{-5}	0.789
		Temperature 1000°K									
	0.348	6.710×10^{-4}	1.373×10^{-9}	6.456×10^{-2}	0.1935	7.175×10^{-3}	1.827×10^{-4}	1.743×10^{-2}	1.503×10^{-2}	6.578×10^{-5}	0.698
	0.683	2.000×10^{-4}	2.382×10^{-9}	6.495×10^{-2}	0.1946	1.245×10^{-2}	5.467×10^{-4}	1.153×10^{-2}	5.763×10^{-3}	9.619×10^{-6}	0.709
	1.376	3.576×10^{-4}	3.178×10^{-9}	6.478×10^{-2}	0.1941	1.661×10^{-2}	9.760×10^{-4}	6.384×10^{-3}	2.384×10^{-3}	1.652×10^{-6}	0.714
		Temperature 1200°K									
	0.345	7.611×10^{-5}	$-$	1.141×10^{-4}	0.3075	1.997×10^{-3}	9.959×10^{-3}	5.255×10^{-3}	2.824×10^{-2}	7.903×10^{-8}	0.649
	0.683	8.699×10^{-5}	$-$	1.159×10^{-4}	0.3121	2.167×10^{-3}	9.234×10^{-3}	2.876×10^{-3}	1.445×10^{-2}	2.040×10^{-7}	0.659
	1.376	9.323×10^{-5}	$-$	1.168×10^{-4}	0.3146	2.261×10^{-3}	9.974×10^{-3}	1.481×10^{-3}	7.191×10^{-3}	5.009×10^{-8}	0.664

TABLE 2.5a cont.

- 4 9 -

S:O Ratio	S:H Ratio	EQUILIBRIUM COMPOSITION									
		S_2^+	SO_2	CO_2	CO	COS	CS_2	H_2S	H_2	CH_4	N_2
					Temperature 1400°K						
0.753	0.348	1.128×10^{-5}	-	9.429×10^{-7}	0.3085	2.158×10^{-4}	1.116×10^{-2}	6.941×10^{-4}	3.270×10^{-2}	2.572×10^{-8}	0.647
	0.683	1.145×10^{-5}	-	9.584×10^{-7}	0.3136	2.210×10^{-4}	1.151×10^{-2}	3.621×10^{-4}	1.694×10^{-2}	6.787×10^{-9}	0.657
	1.376	1.1536×10^{-5}	-	9.667×10^{-7}	0.3163	2.238×10^{-4}	1.170×10^{-2}	1.820×10^{-4}	8.478×10^{-3}	1.689×10^{-9}	0.663
					Temperature 1600°K						
	0.348	2.218×10^{-6}	-	2.708×10^{-8}	0.3086	3.734×10^{-5}	1.154×10^{-2}	1.184×10^{-4}	3.327×10^{-2}	1.672×10^{-9}	0.646
	0.683	2.223×10^{-6}	-	2.752×10^{-8}	0.3137	3.801×10^{-5}	1.176×10^{-2}	6.141×10^{-5}	1.723×10^{-2}	4.413×10^{-10}	0.657
	1.376	2.227×10^{-6}	-	2.777×10^{-8}	0.3164	3.837×10^{-5}	1.188×10^{-2}	3.077×10^{-5}	8.628×10^{-3}	1.097×10^{-10}	0.663

* Equivalent to 2.0, 1.0 and 0.5 volume % of CH_4 respectively
\+ Sulphur polymers S_6 and S_8 are regarded as S_2.

TABLE 2.5b SULPHUR DISTRIBUTION IN THE SYSTEM
SO_2 - C - CH_4 - H_2O (SMELTER GAS
CASE 3, TABLE 2.2)

S/O Ratio	S/H Ratio	S DISTRIBUTION (%)			
		S_2	H_2S	COS	CS_2
		Temperature 800°K			
0.753	0.348	40.23	59.23	0.54	–
	0.683	60.28	38.99	0.73	–
	1.376	76.49	22.63	1.88	–
		Temperature 900°K			
	0.348	5.82	82.02	12.11	0.05
	0.683	18.31	58.18	23.36	0.15
	1.376	32.07	34.70	32.96	0.27
		Temperature 1000°K			
	0.348	0.38	70.05	28.84	0.73
	0.683	0.79	46.65	50.35	2.21
	1.376	1.48	26.24	68.27	4.01
		Temperature 1200°K			
	0.348	0.72	30.40	11.26	57.62
	0.683	0.58	20.03	15.09	64.30
	1.376	0.63	10.73	16.35	72.28
		Temperature 1400°K			
	0.348	0.08	5.75	1.79	92.38
	0.683	0.1	2.99	1.83	95.08
	1.376	0.14	1.48	1.85	96.53
		Temperature 1600°K			
	0.348	–	1.01	0.29	98.70
	0.683	–	0.53	0.32	99.15
	1.376	–	0.28	0.32	99.40

TABLE 2.6a COMPOSITION OF EQUILIBRIUM MIXTURES IN THE SYSTEM SO_2-C-H_2O (SMELTER GAS CASE 3 Table 2.2)

Temp. °K					EQUILIBRIUM COMPOSITION					
	S_2	SO_2	CO_2	CO	COS	CS_2	H_2	H_2S	H_2O	N_2
800	1.423×10^{-2}	2.232×10^{-8}	1.896×10^{-1}	1.269×10^{-5}	1.563×10^{-4}	2.968×10^{-8}	2.220×10^{-8}	3.165×10^{-6}	9.560×10^{-4}	0.7950
900	9.756×10^{-3}	3.032×10^{-8}	1.823×10^{-1}	5.639×10^{-3}	8.487×10^{-3}	9.084×10^{-5}	8.185×10^{-6}	3.808×10^{-4}	6.122×10^{-4}	0.7927
1000	5.729×10^{-4}	4.010×10^{-9}	6.457×10^{-2}	1.934×10^{-1}	2.095×10^{-2}	1.558×10^{-3}	1.931×10^{-4}	6.543×10^{-4}	4.467×10^{-5}	0.7180
1100	2.906×10^{-4}	–	2.487×10^{-3}	3.173×10^{-1}	2.850×10^{-3}	7.201×10^{-3}	4.375×10^{-4}	3.939×10^{-4}	3.564×10^{-6}	0.6724
1200	9.913×10^{-5}	–	1.178×10^{-4}	3.193×10^{-1}	2.357×10^{-4}	1.070×10^{-2}	6.848×10^{-4}	1.454×10^{-4}	3.465×10^{-7}	0.6686
1400	1.162×10^{-5}	–	9.758×10^{-7}	3.194×10^{-1}	2.266×10^{-5}	1.189×10^{-2}	8.121×10^{-4}	1.749×10^{-5}	5.349×10^{-9}	0.6678
1600	2.229×10^{-6}	–	2.803×10^{-8}	3.194×10^{-1}	3.876×10^{-6}	1.200×10^{-2}	8.265×10^{-4}	2.949×10^{-6}	2.162×10^{-10}	0.6677

TABLE 2.6b SULPHUR DISTRIBUTION IN THE SYSTEM
SO_2-C-H_2O (SMELTER GAS CASE 3, TABLE 2.2)

Temp. °K	S DISTRIBUTION (%)			
	S_2	COS	CS_2	H_2S
800	98.94	1.06	–	–
900	52.14	45.36	0.46	2.04
1000	2.41	88.26	6.56	2.76
1100	1.73	52.90	43.04	2.33
1200	0.73	17.69	80.49	1.09
1400	0.10	1.86	97.9	0.14
1600	–	–	100.0	–

TABLE 2.7a COMPOSITION OF EQUILIBRIUM MIXTURES IN THE SYSTEM SO_2–C–H_2O (POWER PLANT FLUE GAS, TABLE 2.1)

Temp. °K				EQUILIBRIUM COMPOSITION						
	S_2	SO_2	CO_2	CO	COS	CS_2	H_2	H_2S	H_2O	N_2
800	5.381×10^{-4}	4.446×10^{-9}	1.942×10^{-1}	1.914×10^{-5}	3.113×10^{-5}	1.149×10^{-9}	8.589×10^{-6}	2.382×10^{-3}	2.053×10^{-2}	0.7822
900	2.304×10^{-5}	1.547×10^{-9}	1.913×10^{-1}	5.919×10^{-3}	4.329×10^{-4}	2.252×10^{-7}	1.325×10^{-3}	2.997×10^{-3}	1.852×10^{-2}	0.7794
1000	1.012×10^{-6}	1.869×10^{-10}	7.161×10^{-2}	2.145×10^{-1}	9.768×10^{-4}	3.054×10^{-6}	1.477×10^{-2}	2.104×10^{-3}	3.417×10^{-3}	0.6926
1200	5.833×10^{-6}	1.508×10^{-12}	1.246×10^{-4}	3.358×10^{-1}	6.037×10^{-4}	6.662×10^{-4}	1.794×10^{-2}	9.241×10^{-4}	9.076×10^{-6}	0.6440
1400	9.323×10^{-7}	–	1.033×10^{-6}	3.380×10^{-1}	6.799×10^{-5}	1.011×10^{-3}	1.882×10^{-2}	8.680×10^{-4}	9.369×10^{-8}	0.6436
1600	2.498×10^{-7}	–	2.952×10^{-8}	3.364×10^{-1}	1.366×10^{-5}	1.416×10^{-3}	1.883×10^{-2}	2.249×10^{-5}	4.925×10^{-9}	0.6433

TABLE 2.7b   SULPHUR DISTRIBUTION IN THE SYSTEM

SO_2-C-H_2O (POWER PLANT FLUE GAS, TABLE 2.1)

Temp. °K	SULPHUR DISTRIBUTION (%)			
	S_2	COS	CS_2	H_2S
800	18.24	1.08	–	80.68
900	0.67	12.54	–	86.79
1000	0.04	31.66	0.1	68.20
1200	–	27.50	30.39	42.11
1400	–	5.85	86.71	7.44
1600	–	0.91·	97.54	1.55
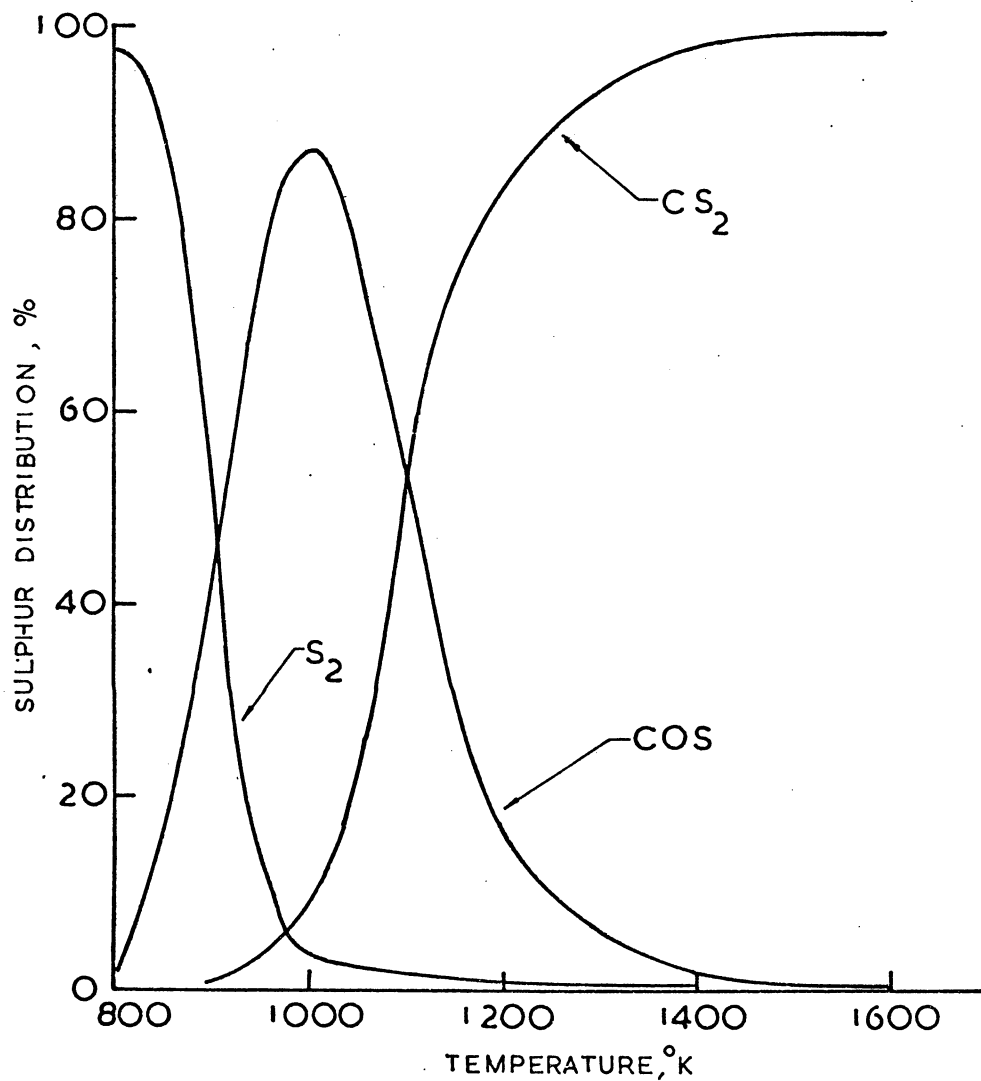
Fig. 2.1   Dependence of the Equilibrium Distribution

of Sulphur between the components on

Temperature in the Reduction of SO_2 with

Carbon (Table 2.4b).

(Gas type: Table 2.2, case 2 - Smelter Gas

given by ore converter) S/O = 0.107
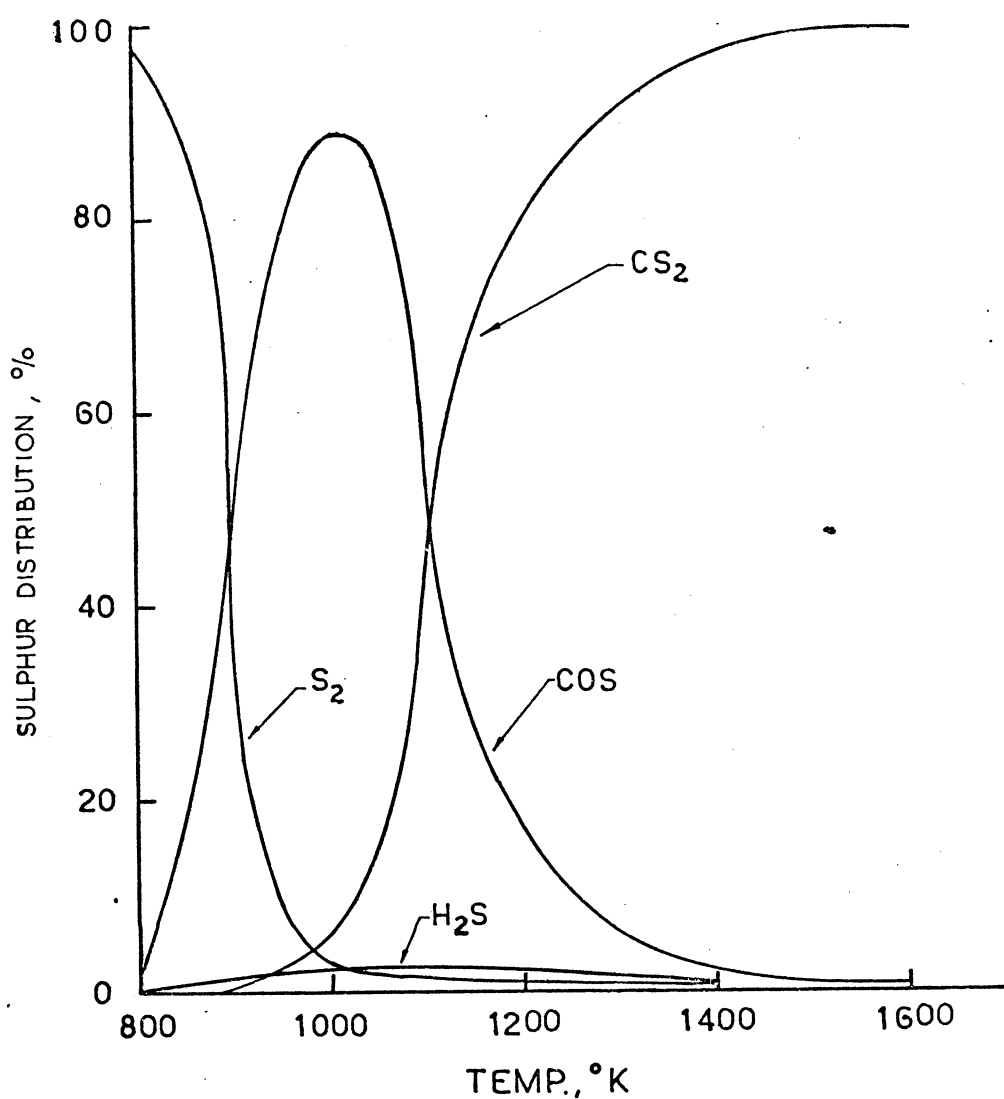
Fig. 2.2 Dependence of the Equilibrium Distribution of sulphur between the components on Temperature in the Reduction of SO_2 with Carbon (Table 2.6b)

(Gas type: Table 2.2, case 3 - Smelter Gas given by ore Converter and Reverberatory Furnace, S/O ratio = 0.753

S/H ratio = 14.50)
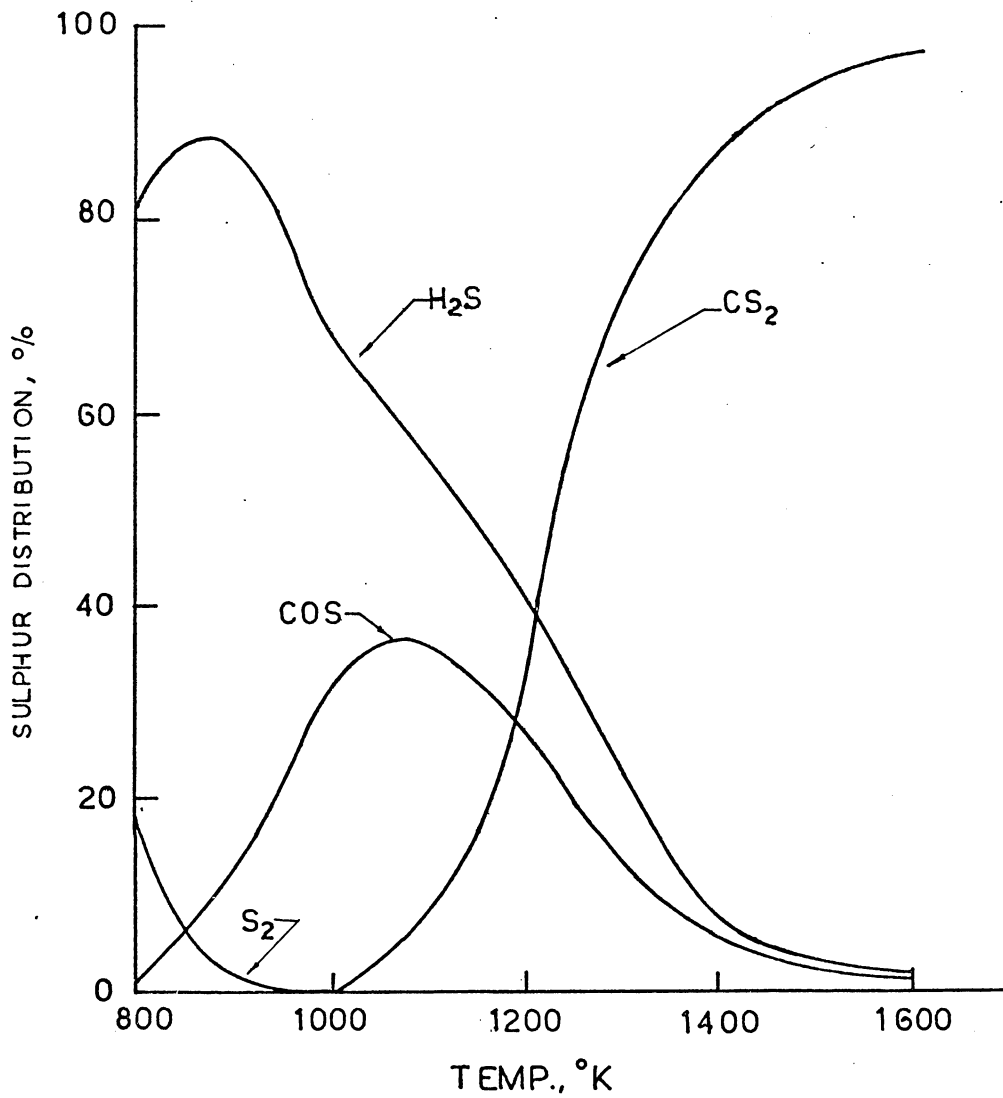
Fig. 2.3 Dependence of Equilibrium Distribution of
Sulphur between Components on Temperature in
the Reduction of SO_2 with Carbon (Table 2.7b)
(gas type: Table 2.1 - power plant flue gas)
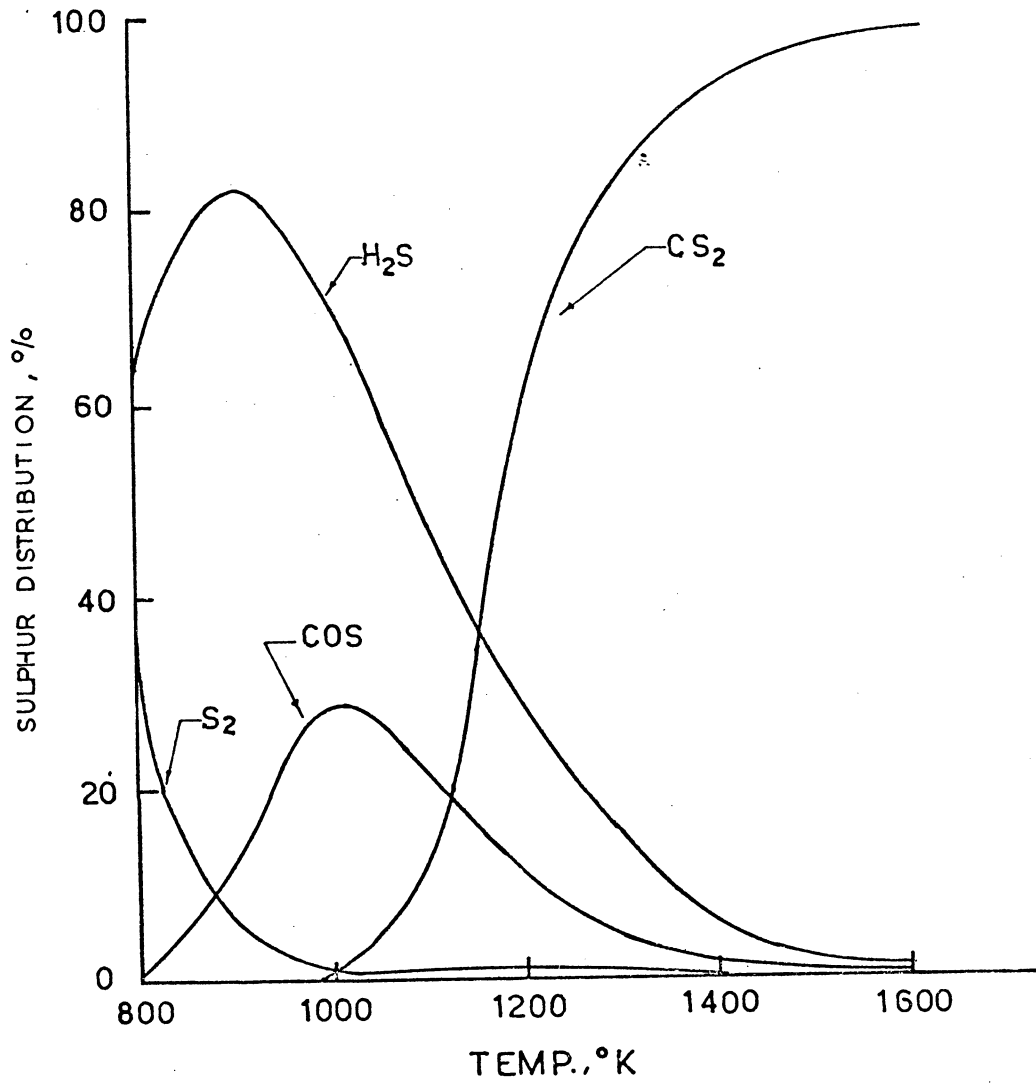
Fig. 2.4 Dependence of Equilibrium Distribution of

Sulphur between components on Temperature in

the Reduction of SO_2 in Smelter Gas given by

ore converter and Reberveratory Furnace with

carbon and 2.0% methane. (Table 2.5b,

S/O ratio = 0.753, S/H ratio = 0.348)
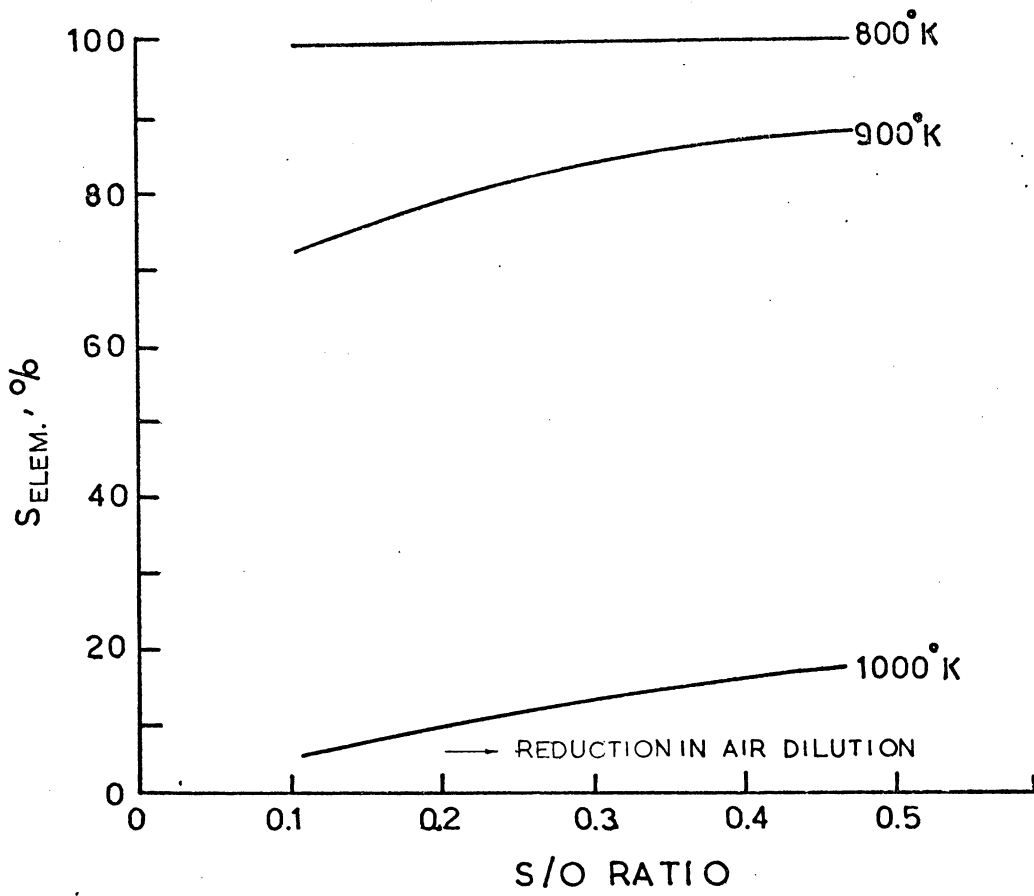
Fig. 2.5a   Effect of Air Dilution on Sulfur Recovery in
the Reduction of SO_2 with Carbon (Gas type;
Table 2.2, Case 1 - Smelter Gas given by ore
converter furnace)
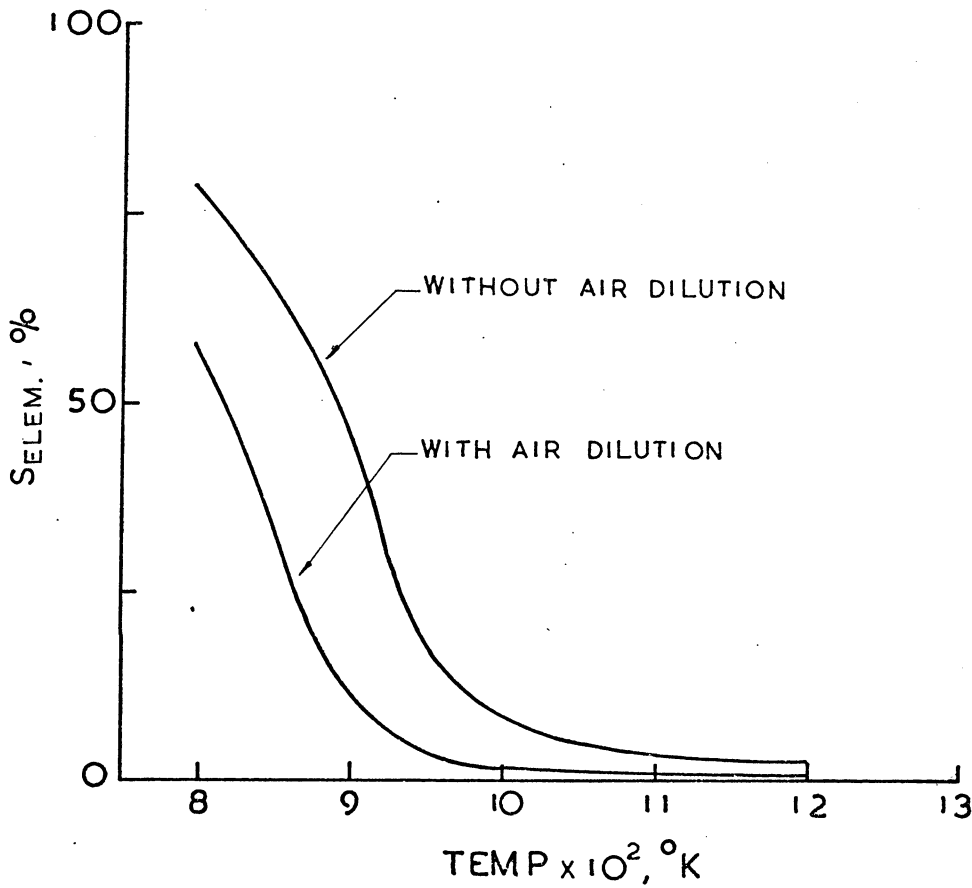
Fig. 2.5 b Effect of Air Dilution on Sulfur recovery in SO_2

Reduction with Carbon and Methane (2.0%)

(Type of gas: Table 2.2, case 3 - Smelter gas

produced by ore converter and Reverberatory

Furnace)
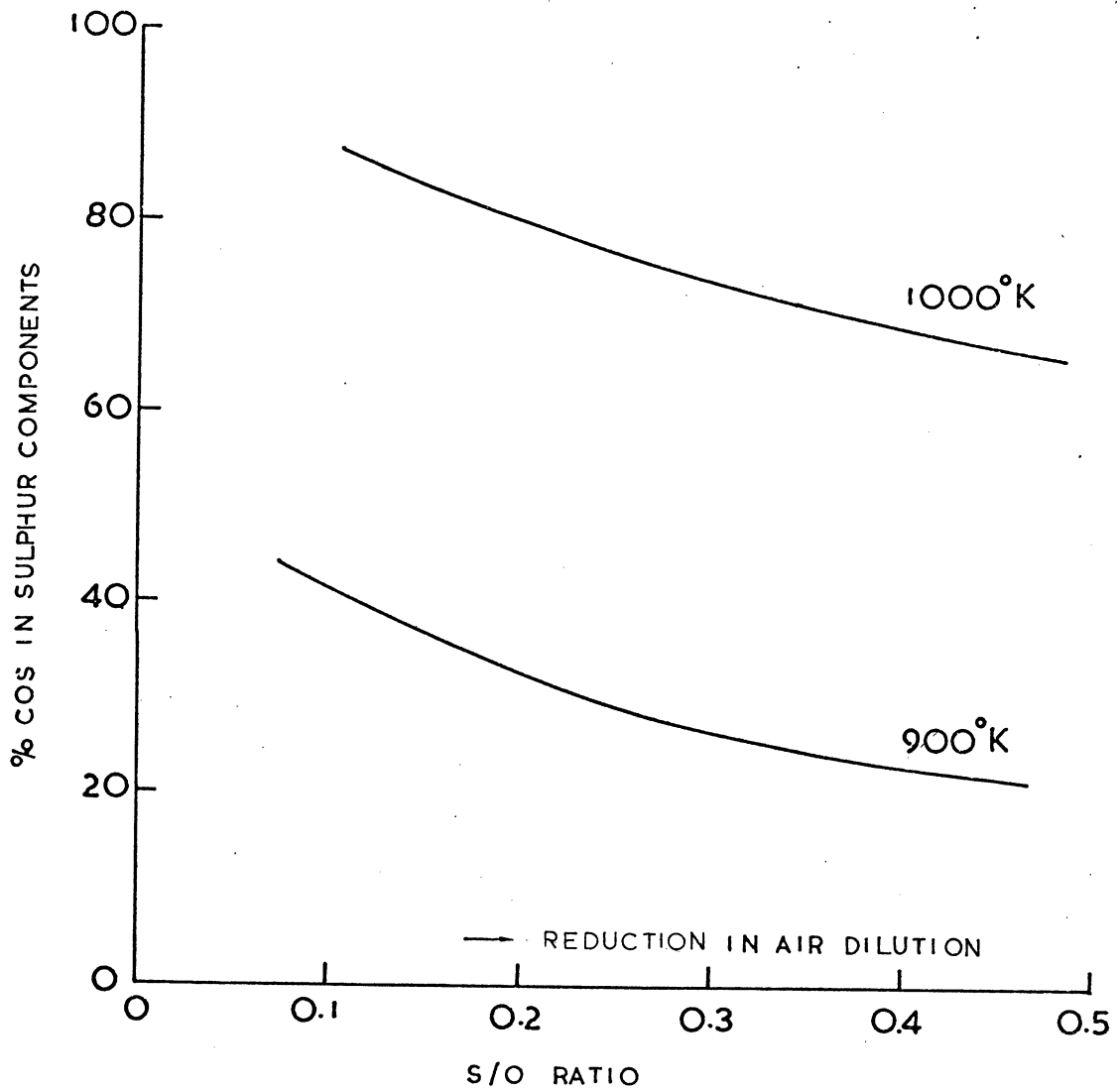
Fig. 2.6 Effect of Air Dilution on the Formation of COS

at Different Temperatures in SO_2 Reduction

with Carbon (Type of gas: Table 2.2, case 1 -

smelter gas produced by ore converter)
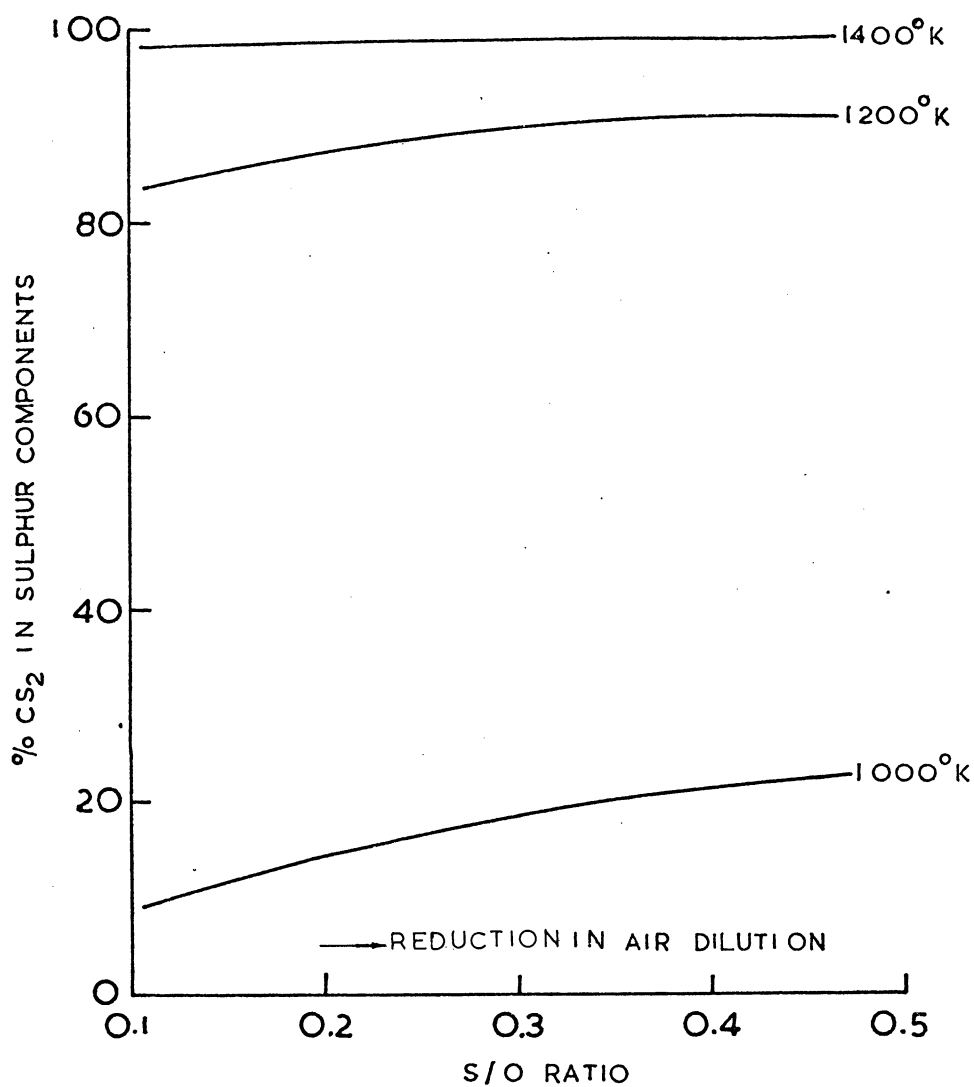
Fig. 2.7 Effect of Air Dilution on the Formation of CS_2 at Different Temperatures in SO_2 Reduction with Carbon. (Type of gas: Table 2.2, case 1 smelter gas produced by ore converter)
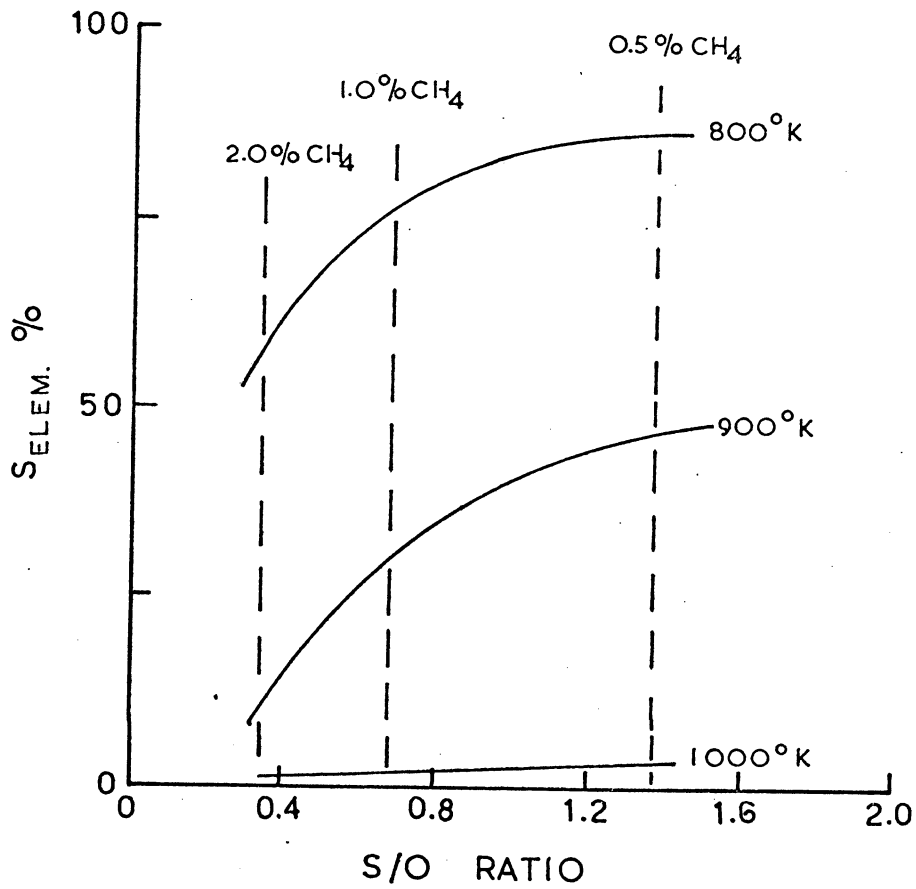
Fig. 2.8 Effect of CH_4 Conc. on Sulfur recovery. (Gas Type: Table 2.2, case 3 - smelter gas produced by ore converter and Reverberatory furnace)
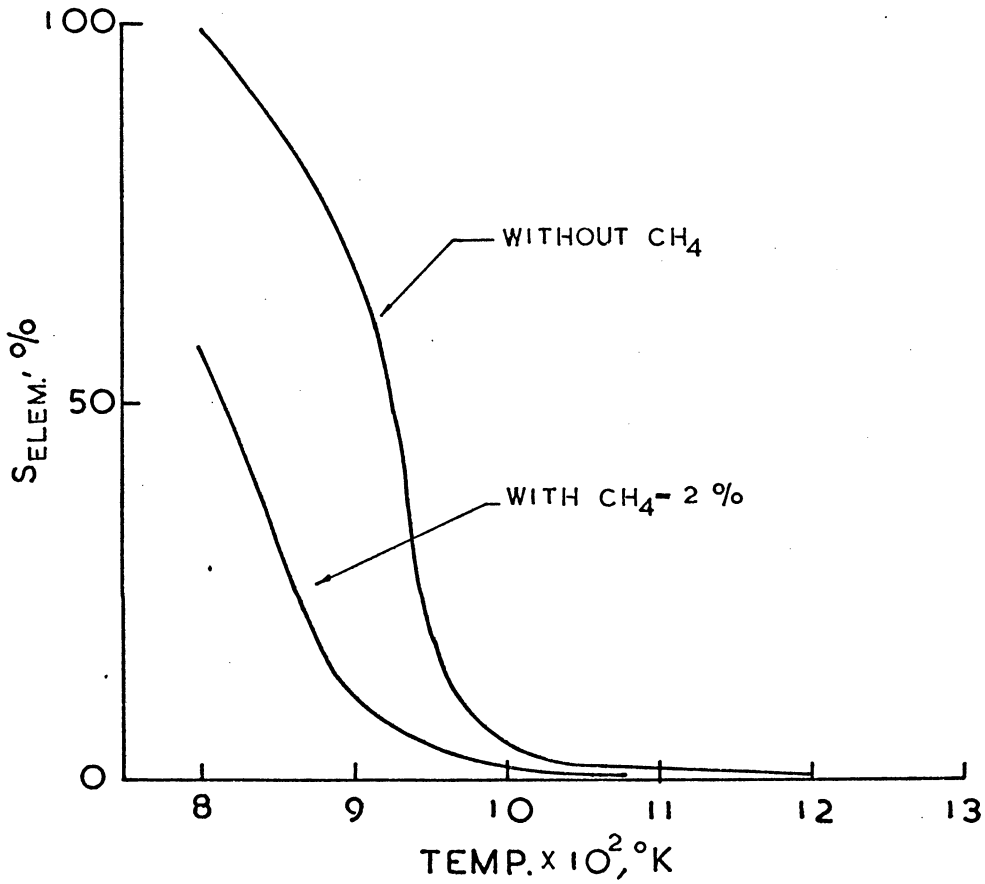
Fig. 2.9 Comparison of Sulfur recovery between SO_2

Reduction with Carbon and Carbon + Methane (2.0%)

(Gas Type: Smelter gas produced by ore converter

and Reverberatory furnace - Table 2.2, case 3)

CHAPTER   THREE

REDUCTION OF SULPHUR DIOXIDE IN A SPOUTED BED

CONTENTS

CONTENTS CONT.

3.1 INTRODUCTION

In the foregoing chapters the reduction of sulphur dioxide with carbon/coal has been studied theoretically. The possible use of the spouted bed technique to provide the necessary reaction environment has been suggested. It was necessary to test this idea experimentally. The following objectives were set:

(1)   Establishment of the spouted bed conditions necessary to significantly reduce inlet SO_2 concentration.

The reduction of SO_2 in a spouted bed has not been studied. Theoretically, SO_2 would react with carbon/coal at all temperatures, the reaction rate being dependent on the temperature used. It was therefore necessary to conduct preliminary studies to establish the spouted conditions needed for significant SO_2 reduction. The important parameters are the reaction temperature, the initial SO_2 concentration, the flow rate of the spouting gas, the particle size and the type of reductant. Among these variables, the reaction temperature and the reductant were thought to be the most important. Spouting gas flow rate and particle size are not truly independent variables. For satisfactory operation

of a spouted bed these variables have to be set within fairly strict limits. The inlet SO_2 concentration is of course determined by the type of waste gas being treated. For these reasons only reaction temperature and reductant type were varied. Reaction temperature was varied between 700 and 900°C using three reductants, viz. activated carbon, brown coal and anthracite. The reductants chosen cover the range from a highly reactive carbon source (activated carbon) to the more practical brown coal.

The choice of the above temperature range was based on previous experience using packed beds and fluidised beds for the reduction process (20,21,22,24). Satisfactory conversion of SO_2 had been achieved in this temperature range, and although gas-solids contact time in a spouted bed is usually shorter than that in packed and fluidised beds this temperature range appeared to be a satisfactory starting point.

Activated carbon, brown coal and anthracite was used for the following reasons:

(i) Activated carbon -

Sulphur dioxide can be reduced by carbon or coal - a combination mainly of carbon and hydrocarbons. Therefore, it is logical to conduct these reactions separately starting from the simple one. Activated carbon is expensive, so it is unlikely that it would be used commercially as a reductant. It was employed here because of its availability as a carbon source.

(ii) Coals -

For a gas-solids reduction process, the viability weighs rather heavily on the cost of the reductant used (49,50,51). A literature survey has revealed that in recent years there were numerous papers published on SO_2 reduction with carbon and treated coals (20,22,23,36,52). Raw coal is obviously a cheaper source of reductant. This is particularly so when coals such as high sulphur content coal, brown coal or anthracite could be used as reductants. Therefore, brown coal and anthracite were chosen. The primary objective in this study was to assess the reactivity of these reductants.

(2) Determination of the relative significance of the variables affecting the reduction process:

The relative significance of the process variables influencing the conversion of the reactants and the yield of the desired product is of particular interest to process development and optimization. Activated carbon was chosen as the reductant to study the effect of reaction temperature, initial SO_2 concentration, bed particle size and gas-solids contact time on SO_2 conversion.

The relative significance of the above four parameters was studied using a Plakett-Burman statistical experimental design.

(3) Establishment of the validity of the Mathur and Lim's gas flow model for the spouting system:

In process design it is essential that a gas or solids flow model of the system concerned is available for performance prediction. The aim of this work was to find a gas phase flow model for the reacting system in the spouted bed.

The general flow patterns of the gas and the solids in a spouted bed are well established (38,44,46). Quantitative studies of the gas flow pattern have been carried out by a number of researchers (14,38,44, 46). Gas distribution studies conducted by Mathur and Gishler (38) and Rigby (14) have shown that the spouting gas is distributed between the annulus and the spout at a ratio of about 3 to 2. Therefore, both regions contribute significantly to the efficiency of the gas-solids reaction. Because of this, a two-region model proposed by Mathur and Lim for the gas phase reaction in a spouted bed of catalyst of heat carrier, appeared promising. The validity of this model has been tested for the SO_2/C reaction in a spouted bed.

3.2 EXPERIMENTAL

3.2.1 Equipment Design

3.2.1.1 Design Considerations

Success of this experimental work depended largely on the
design of a high temperature spouted bed. The problems
were:

(i) Lack of design data.

(ii) Problems of heating and maintaining high,
stable temperatures over extended periods.

(iii) Materials of construction to handle

(a) high temperatures,

(b) corrosive gases, i.e.

SO_2 and S_2.

Given a specific column diameter and particle size, a gas
inlet orifice size may be chosen using several rules of
thumb. The dependent variables, minimum spouting velocity,
maximum spoutable bed depth and spouting pressure drop can
then be calculated with some degree of confidence provided
temperatures are low.

A literature survey has indicated a complete lack of under-
standing in regard to the spouting behaviour (particularly
bed stability) at elevated temperatures. In fact, all
available design correlations were developed at low tempera-
tures. At high temperatures, changes in the system's char-
acteristics such as the gas viscosity are likely to render
existing correlations invalid.

In this work, the high temperature bed was designed accord-
ing to normal practice but the actual parameters were

determined by experiments over the operating temperature range.

3.2.1.2 Design of the High Temperature Spouted Bed System

Fig. 3.1 and 3.2 show a half-section drawing of the high temperature spouted bed and a flow sheet of the ancillary equipment respectively. A photograph of the equipment is shown in Fig. 3.3.

The equipment consists essentially of a spouted bed reactor bed heater, spouting gas supply and sampling system. These items are described below:

Spouted Bed Reactor :

> The reactor was made from a high chromium steel
> pipe 61cm long by 3.913 cm I.D. The conical
> section of the bed was formed by a ceramic in-
> sert. The cone angle was 60° and the gas inlet
> orifice had a diameter of 0.633 cm. A bed
> charging port was provided at the top of the
> bed as shown. A gas sampling point was located
> at the reactor's inlet to allow determination
> of the inlet gas composition. A 0.633 cm O.D.
> crusilite alumina thermocouple well extended
> from the top of the reactor to a position about
> 1.5 cm below the bed surface. Pressure tappings
> were provided at the inlet and outlet of the
> reactor.

BED MATERIAL
INLET

THERMOCOUPLE
WELL

GAS OUTLET

ST. STEEL
REACTOR

ELECTRIC
FURNACE

PRESSURE
&
SAMPLING POINT

ZIRCON
INSERT

GAS INLET

Fig. 3.1   High Temperature Spouted Bed

Fig. 3.2 Flow Diagram of the Experimental Equipment
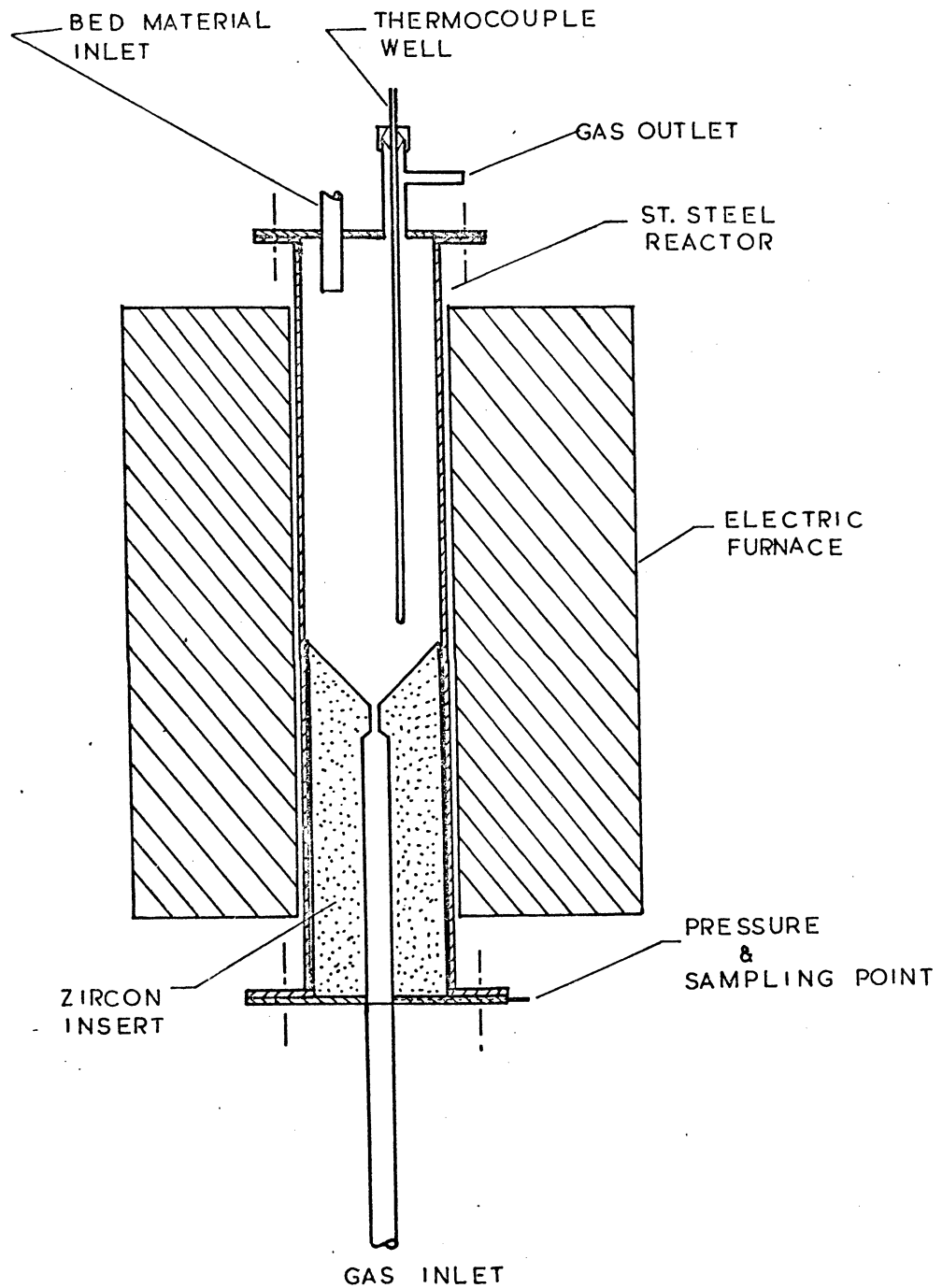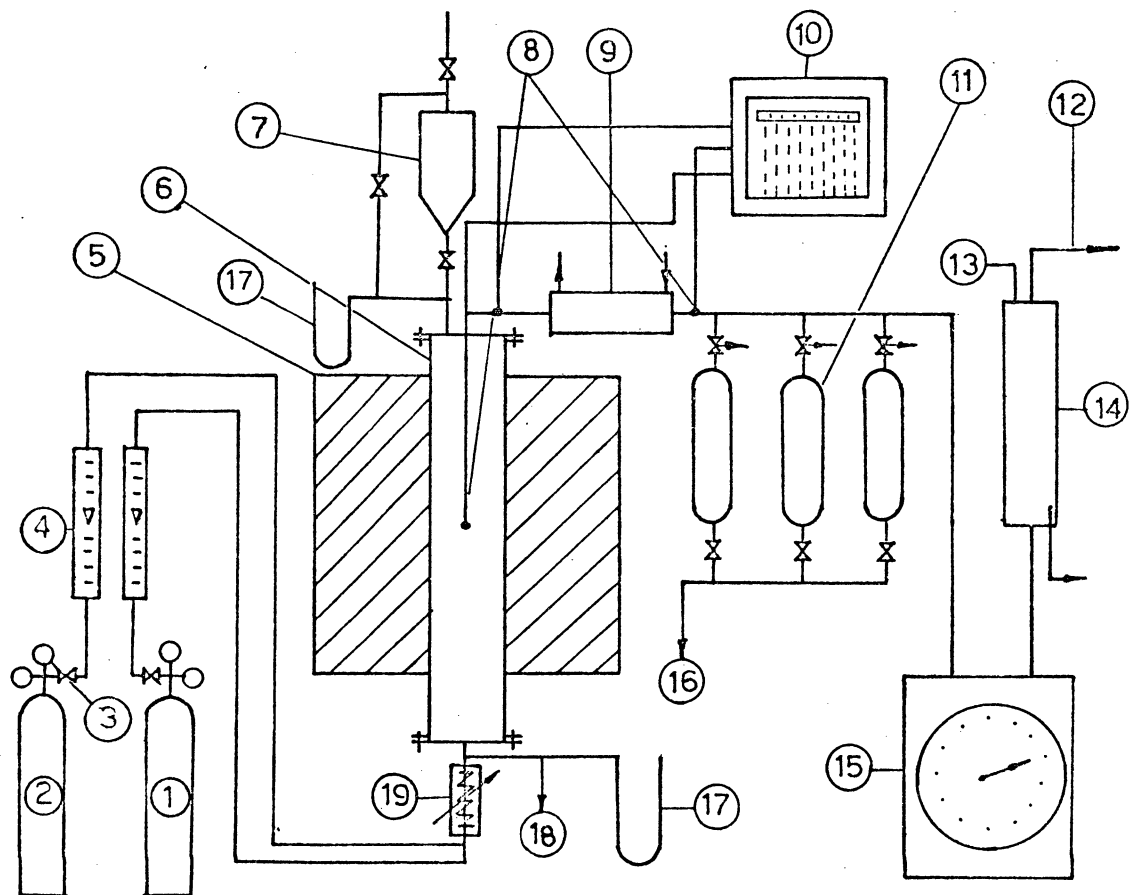
(1)	SO$_2$ Cylinder	(11)	Sampling Bottle
(2)	N$_2$ Cylinder	(12)	Gas Exhaust
(3)	Needle valves	(13)	Water Inlet
(4)	Rotameters	(14)	Gas Wash Tower
(5)	Electrical Furnace	(15)	Dry Gas Meter
(6)	The Spouted Bed	(16)	To Vacuum
(7)	Bed Material Feeder	(17)	Hg Manometer
(8)	Thermocouples (Ch-Al)	(18)	Gas Sampling Point
(9)	Water Cooled Condenser	(19)	Gas Preheater
(10)	Temperature Recorder		
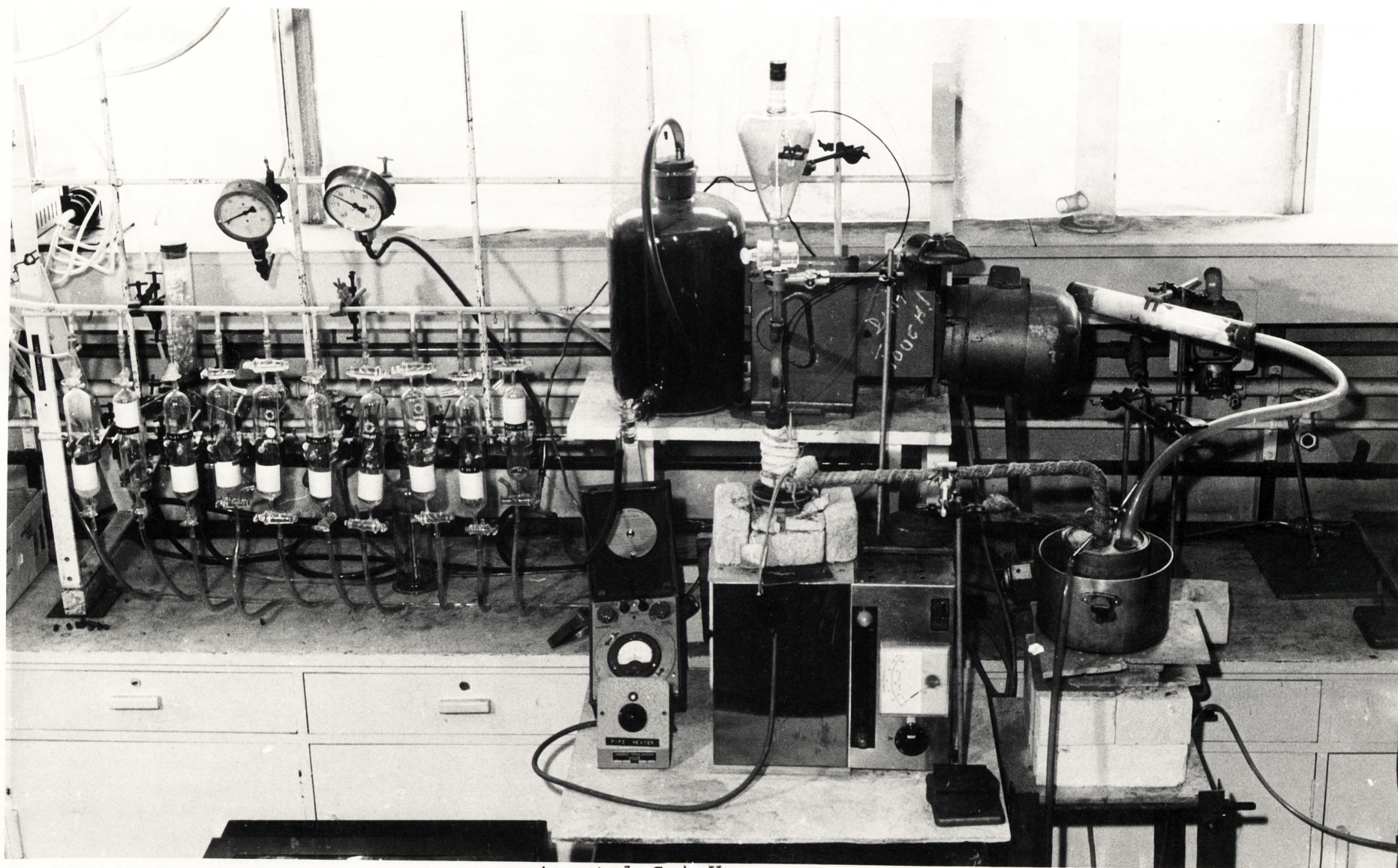
Fig. 3.3 Photograph of the Experimental Set-Up

Heating System:

Heating of the reactor was provided by a tubular
furnace. It was capable of raising the bed tempera-
ture to 1200°C. The power supply to the furnace
was manually controlled by variable transformers.
A 1.3 kw flexible pipe heating tape was wound
over the N_2-SO_2 mixing tube to serve as a pre-
heater. This was found necessary when gas flow
rates were high. The lower section of the cera-
mic insert served well as a preheater,and as
insulation.

Spouting Gas System:

Compressed nitrogen was the spouting medium for
this system. The gas was regulated and metered before
delivery to the bottom of the bed. Sulphur dioxide
was also regulated, metered and then injected
before a mixing tube to give various concentrations
of SO_2 in the spouting gas.

Sampling System:

Exit gas from the reactor was first cooled with a
water condenser and then water scrubbed before ex-
haust to atmosphere. Ten sampling points were pro-
vided after the water condenser. Gaseous products
were sampled in sampling bottles. Each bottle was

250 ml in volume and fitted with stop cocks on
both ends. These bottles were purged and evacu-
ated before sampling. A water ejector was used
for the evacuation. A vacuum gauge was used to
measure the degree of evacuation which then
allowed a correction to be applied to the gas
sample for obtaining a true analysis. The
method was found more convenient and reliable
than those using confining liquids because of the
reactivity and solubility of SO_2.

Ancillary Equipment:

All pressures were indicated by water manometers.
18 G. chromel-alumel themocouple junctions were
used throughout for temperature measurement.
These temperatures were recorded on a multi-
channel potentiometric recorder. Two temperature
indicators were employed for continuous indication
of the bed temperature and spouting gas mixture
preheat temperature. A screw feeder fitted with
a variable speed motor was used for bed charging.

3.2.1.3 Calibration of Equipment

1. Furnace Control

The power supply to the furnace was regulated by
variable transformers. The scales were calibrated
to indicate approximate steady state furnace
temperatures.

2. Rotameters

The rotameter for metering nitrogen was calibra-
ted with a standard dry gas meter. The sulphur
dioxide rotameter was calibrated using nitrogen
and a wet gas meter (because of the low flows).
Conversion from nitrogen to sulphur dioxide was
then carried out using the usual theoretical
correlation.

3. Temperature Recorder

The potentiometric recorder was calibrated with a
standard potentiometer. Chromel-alumel thermo-
couples in protective sheaths were used for temper-
ature measurement.

4. Vacuum Gauge

This was calibrated with a mercury manometer.

5. Gas Meter

The dry gas meter for measuring total gas flow at
the outlet was checked against a standard gas meter

3.2.2 Analyses of Reductants Used

As stated in the introduction, activated carbon, brown
coal and anthracite were used in the work.

(a) Activated Carbon

The activated carbon was made from peat. Its physical properties which were supplied by the manufacturer are given in the following table.

Table 3.1a

Physical Properties of Activated Carbon

Total B.E.T. internal pore surface, m^3/gm carbon	1100
Open pore volume, cm^3/gm carbon	0.55
Apparent density, gm/cm^3	0.504
Apparent bed voidage	0.454 (-14+18#B.S.)
	0.430 (-18+25#B.S.)

(b) Brown Coal and Anthracite

Proximate analysis of the brown coal and anthracite were carried out in accordance with B.S. 1016 Part 3: 1973. The results are given in the following table.

Table 3.1b

Proximate Analysis of Brown Coal and Anthracite
(Water free basis[+])

Coal Composition	Brown Coal	Anthracite
V.M.	20.9	7.8
Ash	9.4	10.4
Fixed Carbon	69.7	81.8

+ For actual experimental runs the coals were

predried using a low temperature (100°C)

vacuum oven.

3.3 REDUCTION OF SO_2 IN A SPOUTED BED

3.3.1 Determination of Operational Conditions

As shown in the literature survey a spouted bed will be

formed only when it is operated in a certain hydrodynamic

regime. This regime is governed by bed geometry and the

physical properties of the bed material and the spouting

medium. Therefore, before the system can be used for ex-

perimentation, it is necessary to determine its operational

regime. There are three important design parameters which

need predetermination. These are the particle size, the

spouting velocity and the maximum spoutable bed height.

(1)   Particle size:

Since the bed used for the present study was only

3.913 cm in diameter the particle size of the bed

material was restricted. Thus in this preliminary

work, carbon particles with sizes of -10+14, -14+18,

-18+25 and -25+30 B.S. mesh were tested at tempera-

tures between 600°C and 1000°C. Pure nitrogen was

used as the spouting gas.

From a series of observations, it was found that the

larger particles (i.e. -10+14 B.S. mesh) were diffi-

cult to spout. On the other hand, the smallest

particles (i.e. -25+30 B.S. mesh) tend to fluidise quite easily. Good spouting was possible for the -14+18 and -18+25 B.S. mesh particles.

(2)   Spouting Velocity:

Using the above selected particle size gas flow rates for achieving spouting were determined. Minimum spouting velocities obtained from this series of runs were compared with those calculated from the correlation proposed by Mathur and Gishler (38). This comparison is shown in Fig. 3.4. As can be seen from the figure, the calculated minimum spouting velocity is invariably higher than the experimental one. The inadequacy of this correlation for spouting gas flow rate prediction at elevated temperatures is clearly demonstrated.

(3)   Maximum Spoutable Bed Height:

For these two particle sizes, -14+18 and -18+25 B.S. mesh, the maximum spoutable bed heights were found to be 7.5 and 7.2 cm respectively. These values are comparable to those calculated from Malek and Lu's correlation (39).

As a result of this series of experiments the following limiting conditions were used for planning the subsequent SO_2 reduction experiment in the spouted bed.
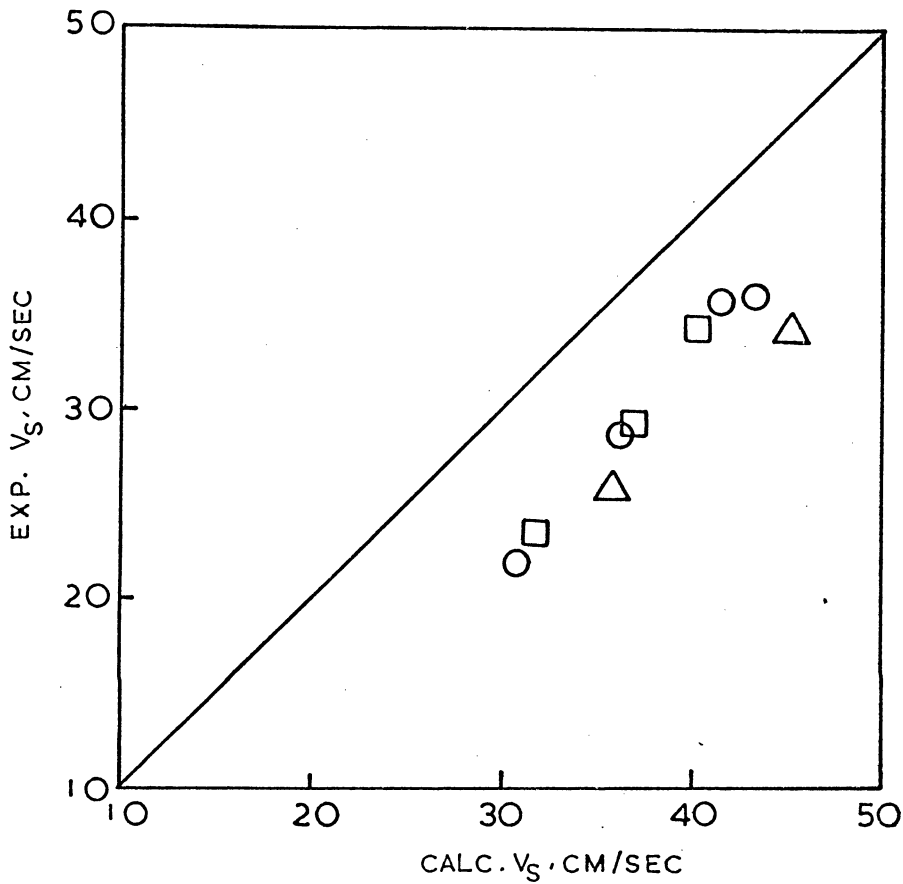
Fig. 3.4 Comparison of Calc. and Exp. minimum Spouting

Velocity at Elevated Temperature.

☐   Charcoal   Size = 0.103 cm (-14+18B.S. mesh)
              Temp. = 780°C

△   Charcoal   Size = 0.103 cm
              Temp. = 1040°C

◯   Charcoal   Size = 0.0726 cm (-18+25 B.S. mesh)
              Temp. = 730°C

      Particle size: -14+18 and -18+25
      (B.S. mesh)

      Spouting gas flow

      rate (at bed temperature): Min. 25 l/min

      Bed charge: 18 gm (This gave an

                                    unexpanded bed height

                                    of about 7 cm)

3.3.2 Experimental Procedure

(1) SO_2 Reduction with Activated Carbon

The furnace was switched on and the power supply
adjusted according to the temperature required.
Initial heating up was allowed to proceed (with the
bed in a static condition) until the reactor had
reached a temperature higher than that desired.
Nitrogen was then introduced at a predetermined flow
rate. The exhaust suction pump was switched on and
water for the SO_2 scrubber and sulphur vapour con-
denser started.

Under this start-up procedure, the reactor would
reach steady state in 2-3 hours. Meanwhile, the
whole system was purged thoroughly with pure nitro-
gen. The sampling bottles were also purged with
this stream of nitrogen.

When the reactor temperature had reached steady

state, a known amount of carbon was charged from the top using a solids feeder. At this stage the water ejector for evacuating the sampling bottles was in operation.

As the carbon particles were charged at room temperature the reactor temperature fell 50°C or so. Regaining the original steady state temperature was rapid as the bed was in a spouting state. When this had been achieved, pure SO_2 was turned on and vented to atmosphere while the desired flow rate was set.

At zero time this SO_2 gas stream was diverted to the bed by means of a three-way valve. Gaseous product was then sampled at convenient intervals. Usually, ten samples were taken for each run.

At the completion of a run, the flow of SO_2 was first stopped, and the furnace switched off after a few minutes of nitrogen purging. When the reactor was sufficiently cool, the remaining bed material was withdrawn and weighed. The length of time for the run was recorded and the total gas flow noted from the register of the dry gas meter. Finally, the gas samples were analysed using gas chromatography.

(2) SO_2 Reduction with Brown Coal and Anthracite

The procedure for this set of experiments was modified to cope with the evolution of volatile matter

from the coal. Since the SO_2/coal reaction is best followed in a system with continuous gas and solids flow and the present reactor was semi-batch, i.e. batchwise with respect to solids, the following alterations were made to the two previous experimental procedures:

(1) Weigh and keep brown coal/anthracite in a solids feed hopper.

(2) When the reactor had reached a steady state, SO_2 was allowed to flow in and mix with nitrogen. The resultant gas mixture contained about 4% SO_2 and gave a flow rate of about 25 l/min at bed temperature.

(3) Start feeding coal at a fixed rate of about 0.6 gm/min using a screw feeder. This feeding rate was used because it was found that it caused only very slight disturbance to the bed temperature.

(4) Collect gas samples at convenient time intervals. Samples were collected more frequently during the coal feeding period.

Experiment time for most runs was as long as five hours.

3.3.3 Method for Gas Analysis

Gas analysis was carried out using gas chromatography.

Thermal conductivity detectors were used. Details of the gas sampling and analytical methods are given in Appendix D.

3.4 SO$_2$ REDUCTION RESULTS AND DISCUSSION

3.4.1 Preliminary and Feasibility Study

3.4.1.1 SO$_2$ Reduction with Activated Carbon

In this section, results obtained from four sulphur dioxide reduction runs under spouting conditions are reported. These runs were conducted at 712°, 801° and 917°C using the operational conditions determined in Section 3.3.1. The results of these runs are shown in Fig. 3.5 to 3.8 and are tabulated in Appendix E. Figs. 3.5 to 3.7 show the compositions of outlet gases for various runs. The distribution of sulphur in the reaction products is given in Fig. 3.8.

Although these experiments were of an exploratory nature a number of useful observations were made.

(1)   Reliability of Results

Indication of the accuracy and reliability of the gas analysis results were obtained by mass balancing the inlet and outlet oxygen. Oxygen entered the system as SO$_2$ in known quantity and left as CO$_2$, CO, COS and SO$_2$. The results given in Table E.1 (Appendix E) shows that this mass balance is quite accurate
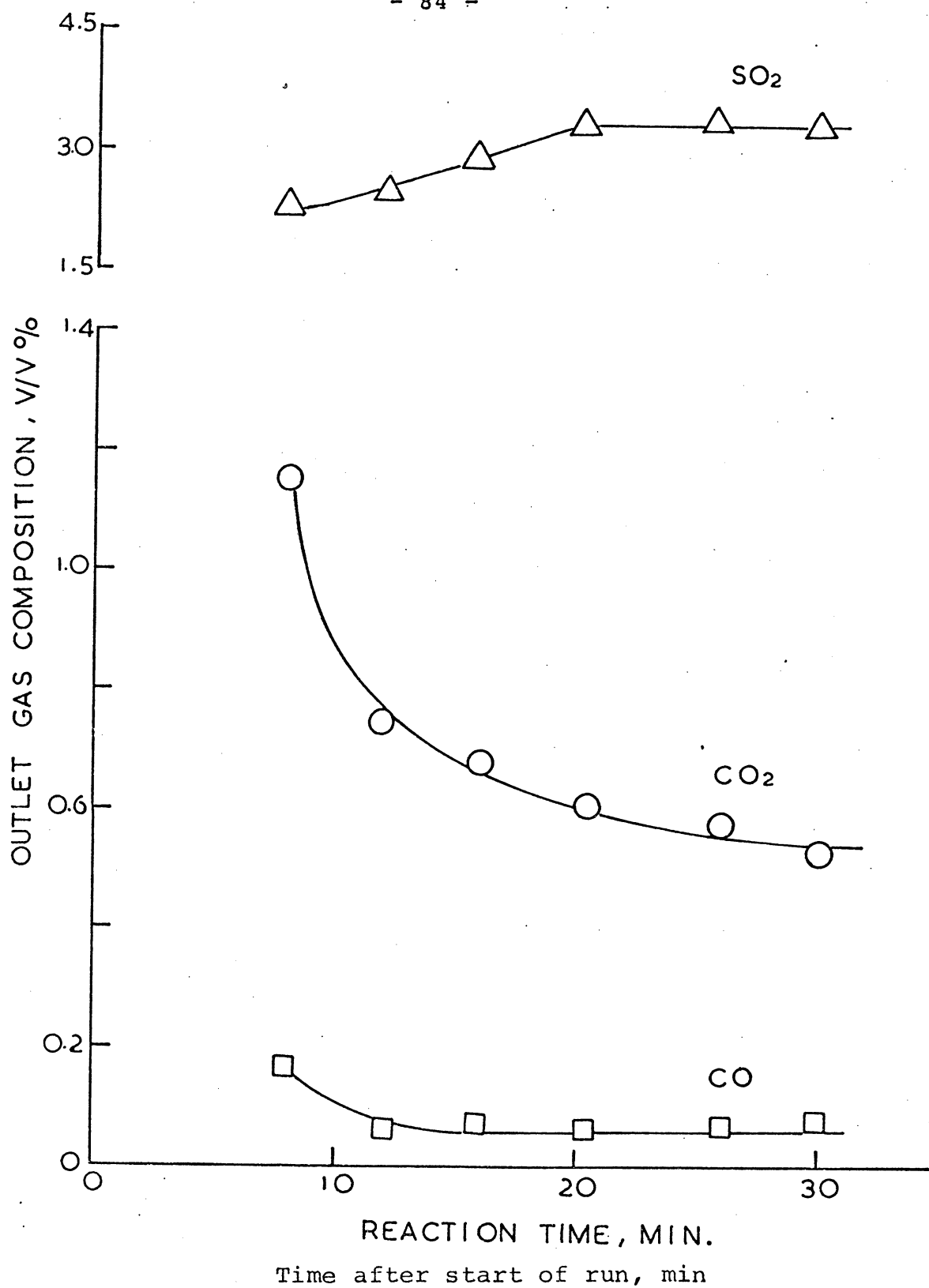
Fig. 3.5 Sulphur Dioxide Reduction with Activated Carbon

in a Spouted Bed at 712°C
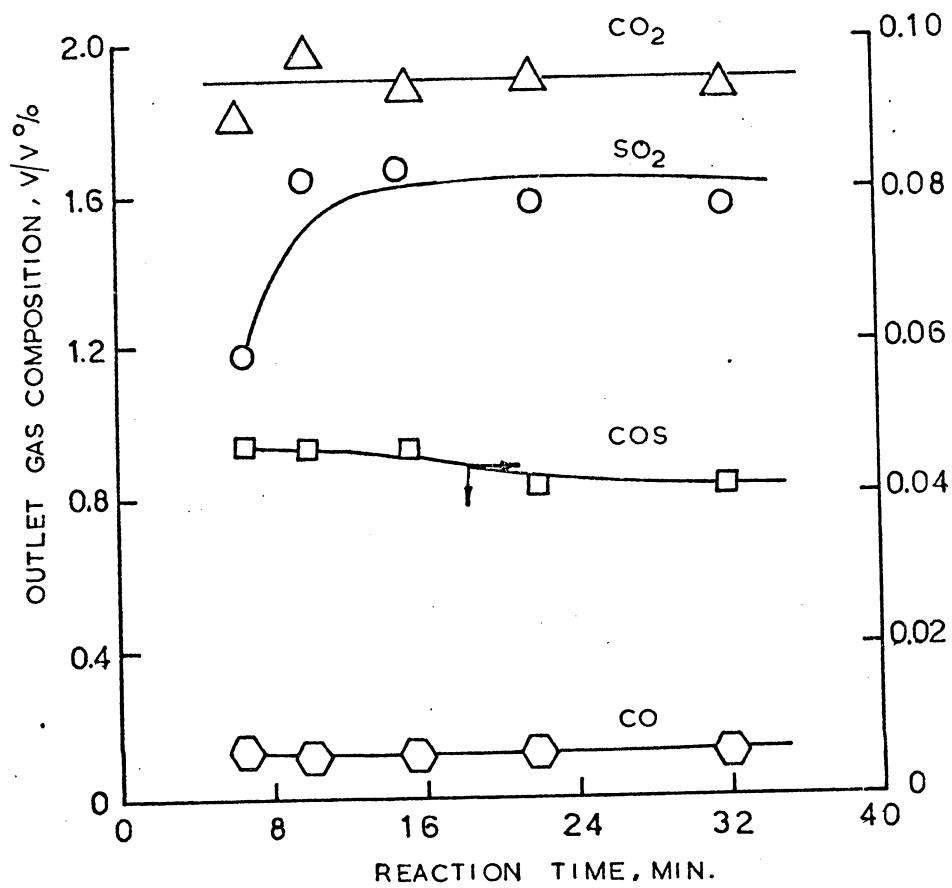
Fig. 3.6 SO_2 Reduction with Activated Carbon
in a Spouted Bed at 801°C
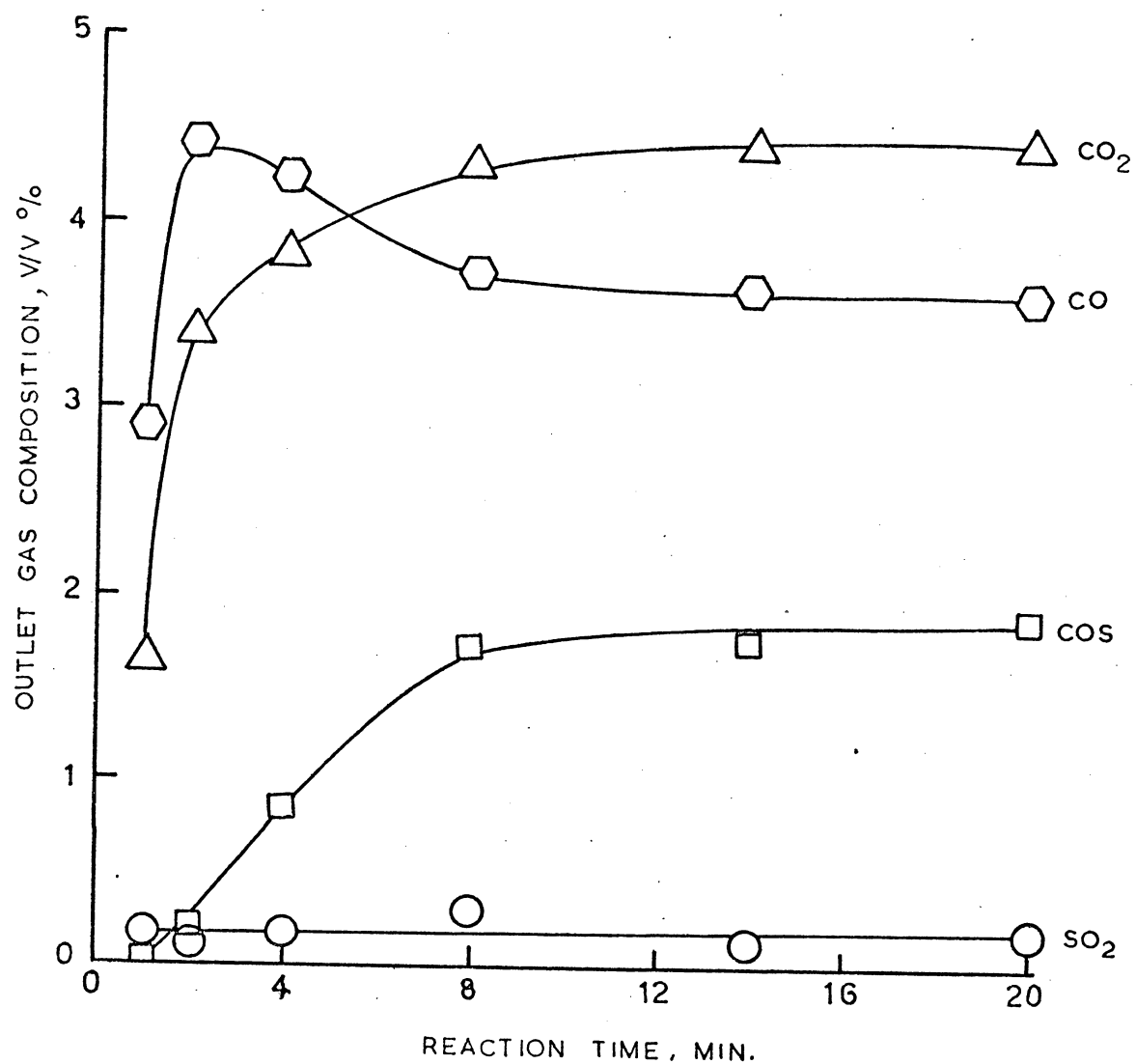
Fig. 3.7   Sulphur Dioxide Reduction with Activated Carbon
at 917°C in a Spouted Bed

except in the unsteady-state period during which

the oxygen leaving the system was found to be less

than that supplied to the system. This was due to

the initial adsorption of sulphur dioxide by the

activated carbon (20,36) and thus caused a signifi-

cant disappearance of SO_2.

(2)　Approach to Steady State

The reaction approached a steady state quite rapidly.

At 712°C a steady state was established in about 20

minutes. At 917°C this was reached in less than one

minute.

(3)　Effect of temperature

The reaction rate was seen to be very sensitive to

temperature. At 712°C the conversion of SO_2 was

about 16% but at 917°C the conversion was as high

as 97%. The time required in attaining steady

state was significantly affected by temperature as

indicated in (2) above.

(4)　Selection of Inlet SO_2 Concentration

Two levels of inlet SO_2 concentration were used (3.84

and 7.12%). These levels of SO_2 could be present in

smelter gases but lower concentrations of SO_2 are

present in the flue gases produced from power genera-

tion plants using coal as fuel. Since accurate

determination of gases with only minute quantities
of SO_2 is a problem (see Appendix D). This simu-
lation was not attempted.

Using the above two levels of SO_2 inlet concentra-
tion, product gases obtained from experiments were
shown to be satisfactorily analysed.

(5)   Effect of Gas Flow Rate

The effect of gas flow rate on SO_2 conversion was
found to be quite significant. At 712°C, the con-
version of SO_2 was seen to drop from about 16% to
about 10% when the gas-solids contact time was de-
creased from 0.079 sec. to 0.065 sec.

(6)   Product Distribution

The products of reaction were found to consist of
SO_2, CO_2, CO and COS. At 917°C CO_2 and CO were the
predominant species. COS was found to increase with
reaction temperature. At 712°C the concentration of
COS was only 0.02% but at 917°C it was in excess of
1%. CS_2 was not detected in these runs but was ob-
served in comparable research work (20,21,22,36,52)
conducted with much longer gas residence times
(about 1 sec. and longer). In addition, the reaction
temperatures used in the work were not high enough to
produce significant quantities of CS_2. The thermo-
dynamic analysis given in Chapter Two indicates that

high temperatures strongly favour the formation of CS_2 and noticeable amount of CS_2 forms only at temperatures higher than 1100°C. Therefore it is reasonable to accept that CS_2 would not form in appreciable amounts under the conditions of the experiments.

(7)   Elemental Sulphur Recovery

Sulphur fed into the system was found to appear in the effluent as COS, elemental sulphur and SO_2. Because of the practical difficulties of condensing and collecting the finely divided elemental sulphur completely, exit gas S_2 con-cen-trations were calculated from mass balance. The results are shown in Fig. 3.8.

Sulphur recovery appeared to be more favourable with increase in temperature. It is seen that a recovery of 66% of sulphur fed into the system was achieved at 917°C. This degree of recovery is rather high and seems probable only when the system is operated far from a state of thermodynamic equilibrium. In Chapter Two it has been shown that at 900°C the equi- librium concentration of sulphur vapour is only of the order of several percent. The rest of the sul- phur is in the form of COS.

3.4.1.2.   Sulphur Dioxide Reduction with Coals

Six runs were conducted in this set of experiments. Results
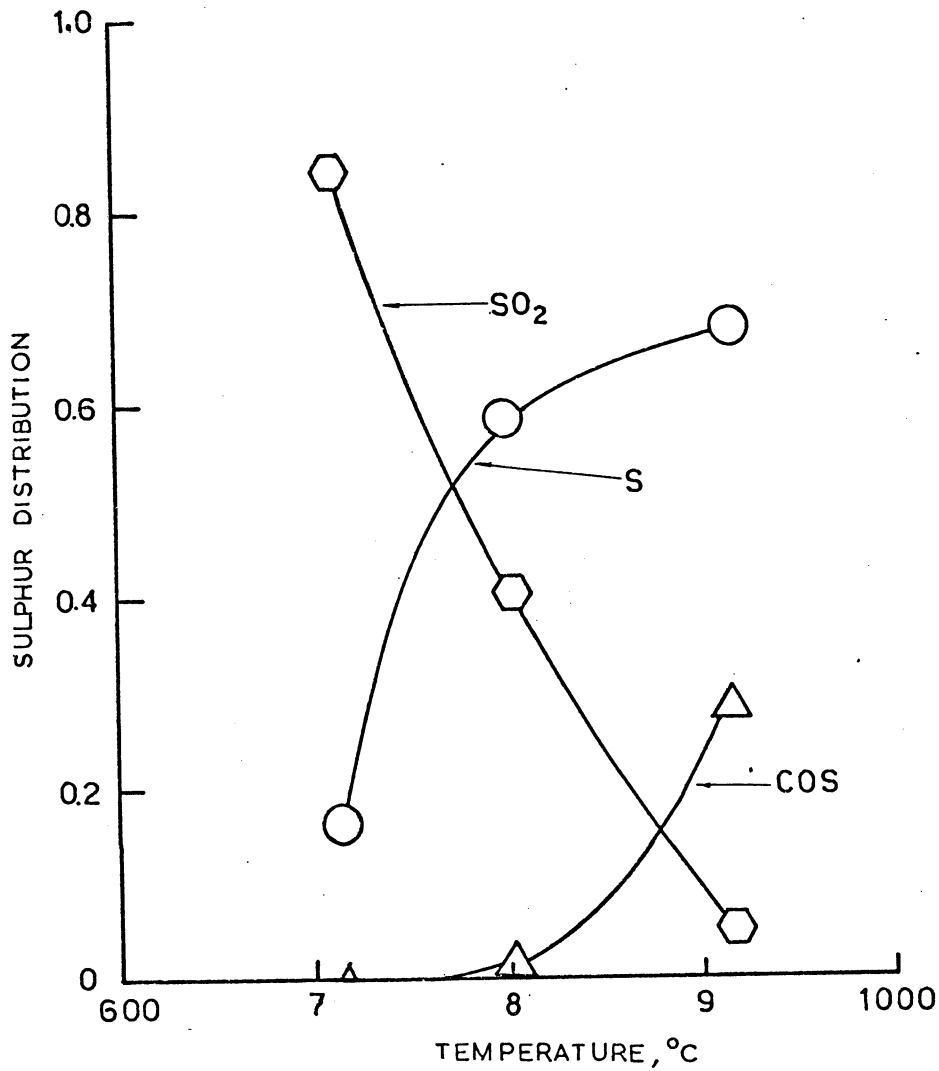
Fig. 3.8   Sulphur selectivity at different temperature
level for the SO_2 Reduction with Activated
Carbon in a Spouted Bed

are presented in Fig. 3.9 to 3.12 and tabulated in Appendix
E. In Fig. 3.13, the effect of temperature on the reacti-
vity of brown coal and anthracite is given. The effect of
temperature on H_2S and COS formation is shown in Fig. 3.14.
The following features are observed in these results:

(1)   Reactivity of Coals

The reactivity of anthracite and brown coal in

sulphur dioxide reduction is shown in Fig. 3.9 to

3.12. The difference in reactivity of the two

types of coals is indeed very distinctive.

Anthracite is seen to be unreactive under all con-

ditions. In contrast to this, brown coal was

rather reactive even at 700°C.

The reactivity of coal appears to be controlled by

the porosity of the coal and the volatile matter

in the coal. Anthracite is not porous and contains

low volatile matter. Therefore it could reduce SO_2

only marginally.

Sinha and Walker (23) reported an increase in surface

area by carbon gasification. They suggested that

the creation of surface area was the result of the

interaction of carbon and carbon dioxide. In their

experiments 16.8% CO_2 was used in the initial gas

mixture and a noticeable change in the coal's reac-

tivity was observed. No similar affect was observed
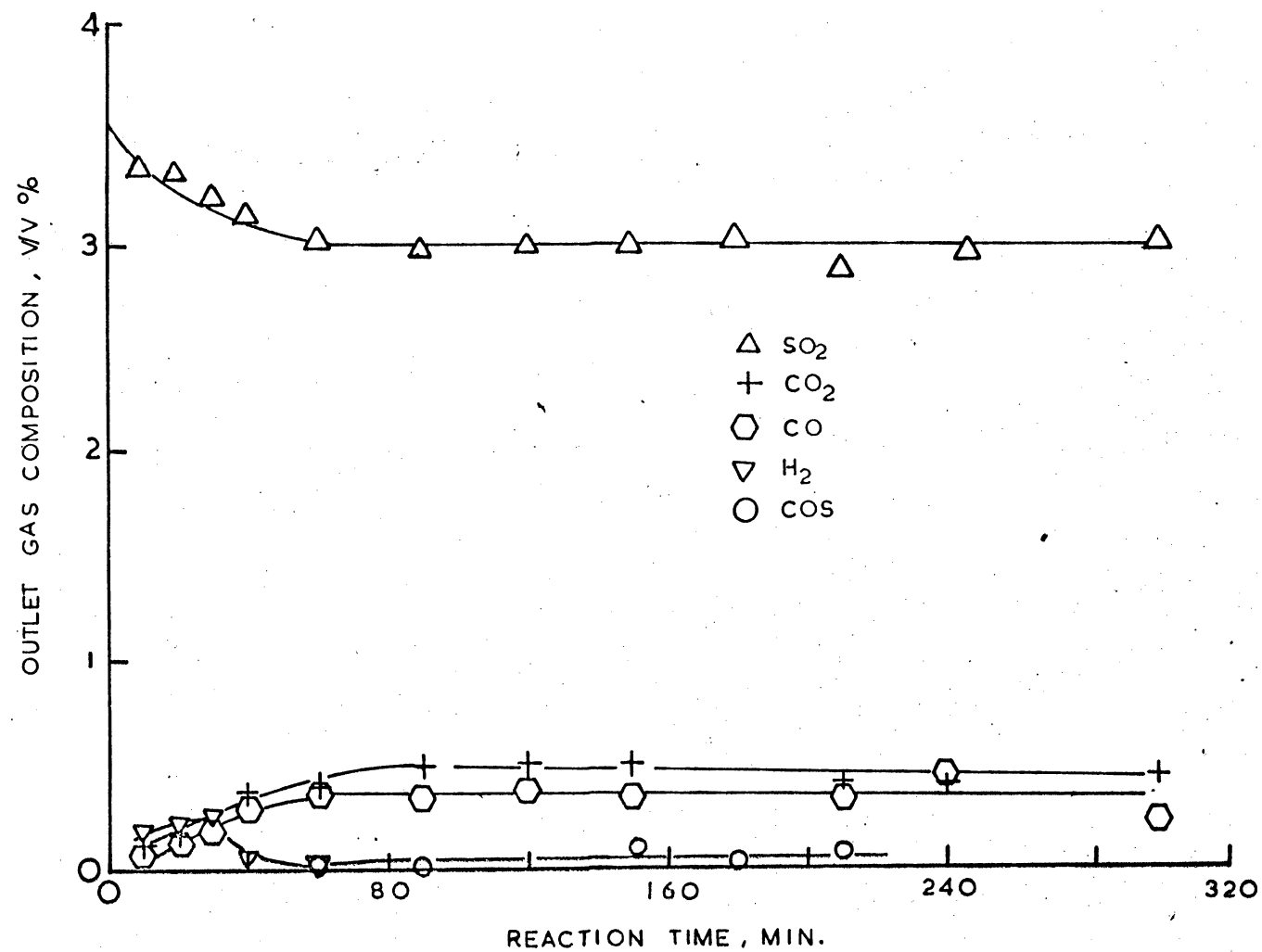
Fig. 3.9 SO$_2$ REDUCTION WITH ANTHRACITE AT 900°C
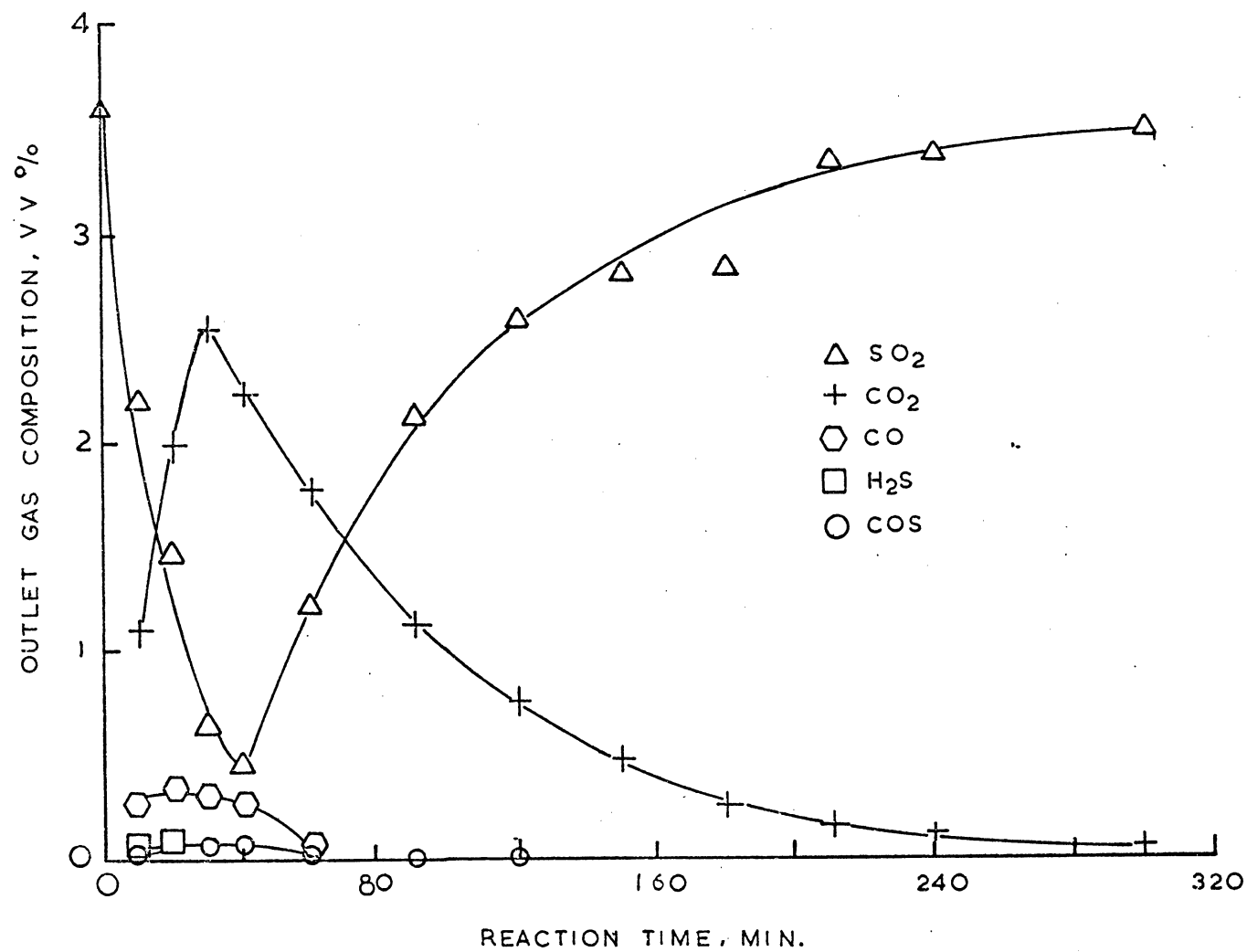
Fig. 3.10 SO$_2$ Reduction with Brown Coal at 700°C
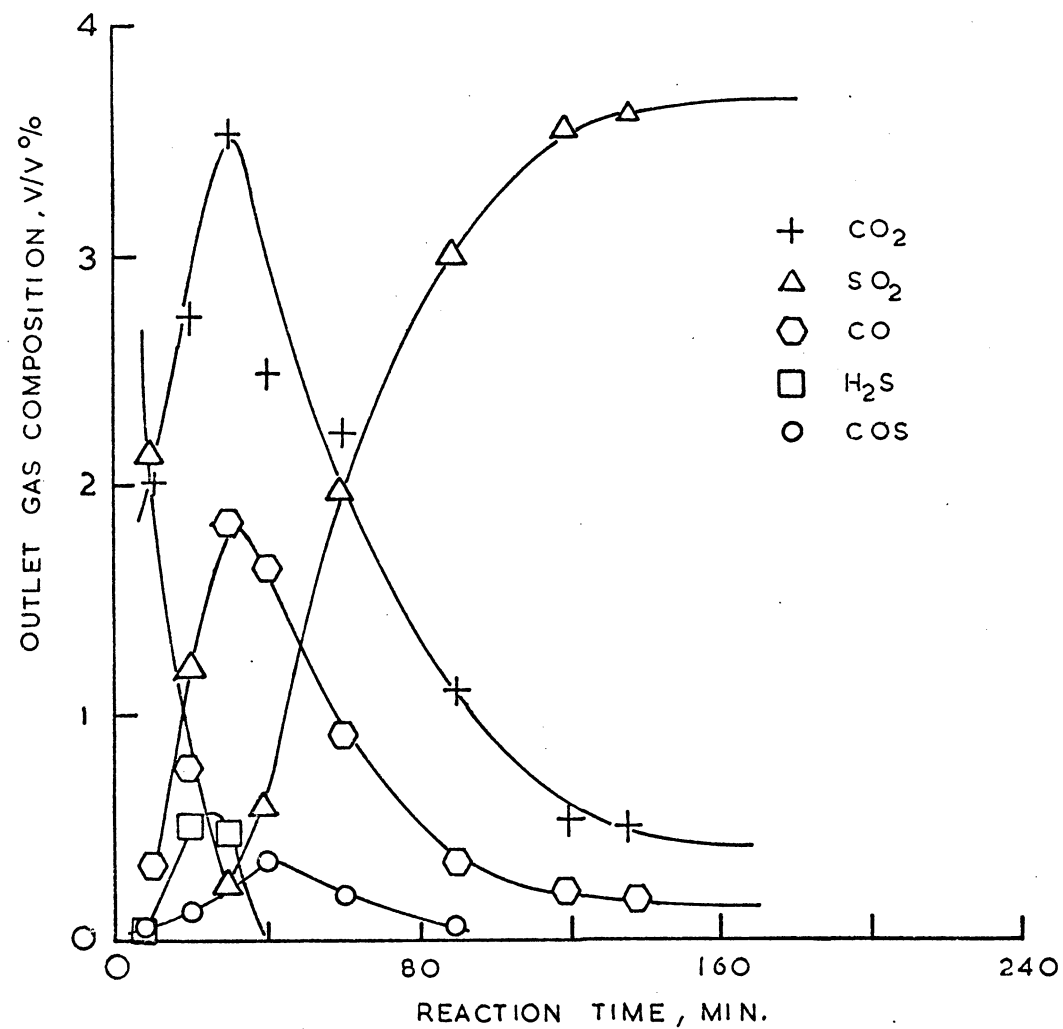
Fig. 3.11 SO$_2$ Reduction with Brown Coal in a Spouted Bed at 810°C
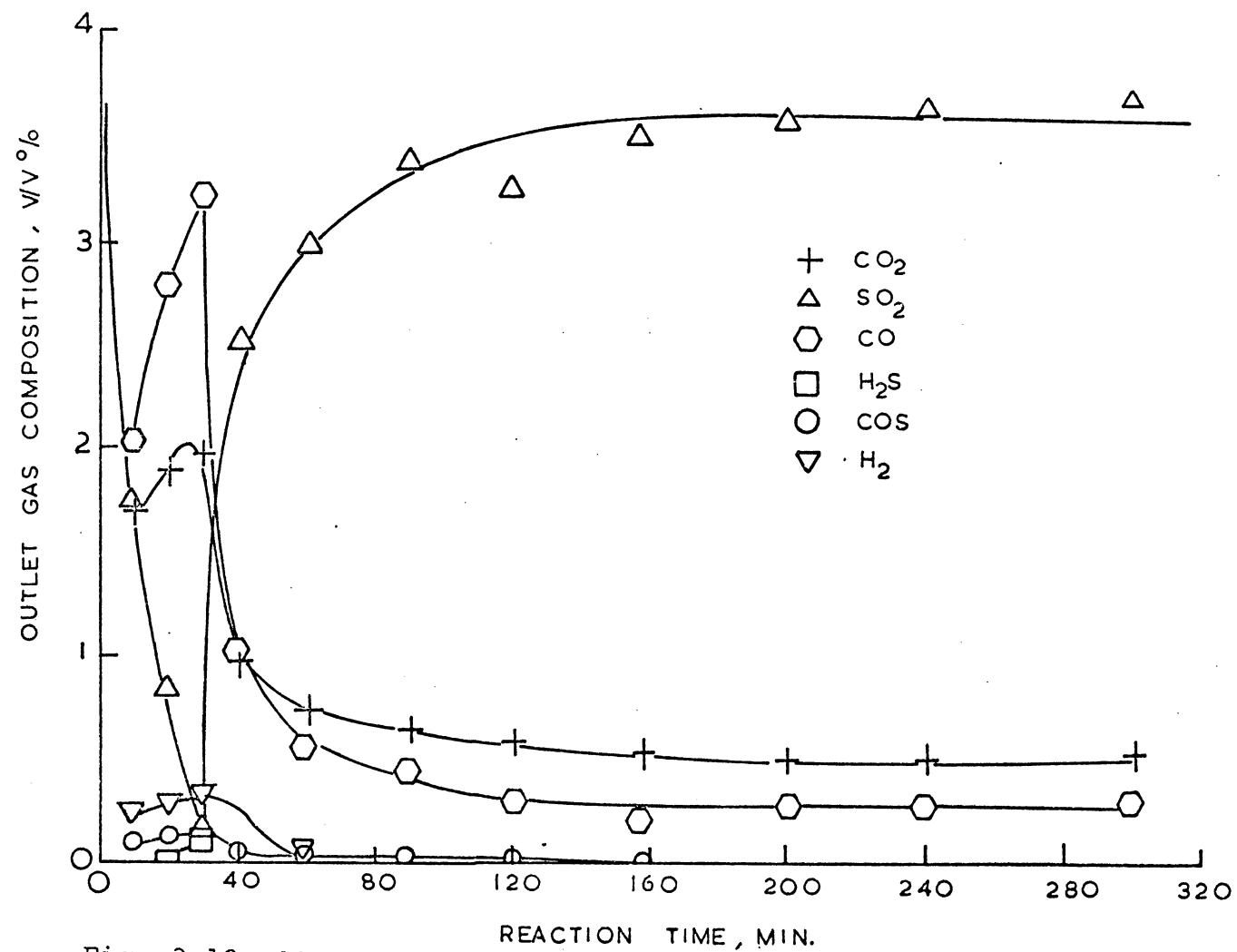
Fig. 3.12   SO$_2$ Reduction with Brown Coal at 900°C
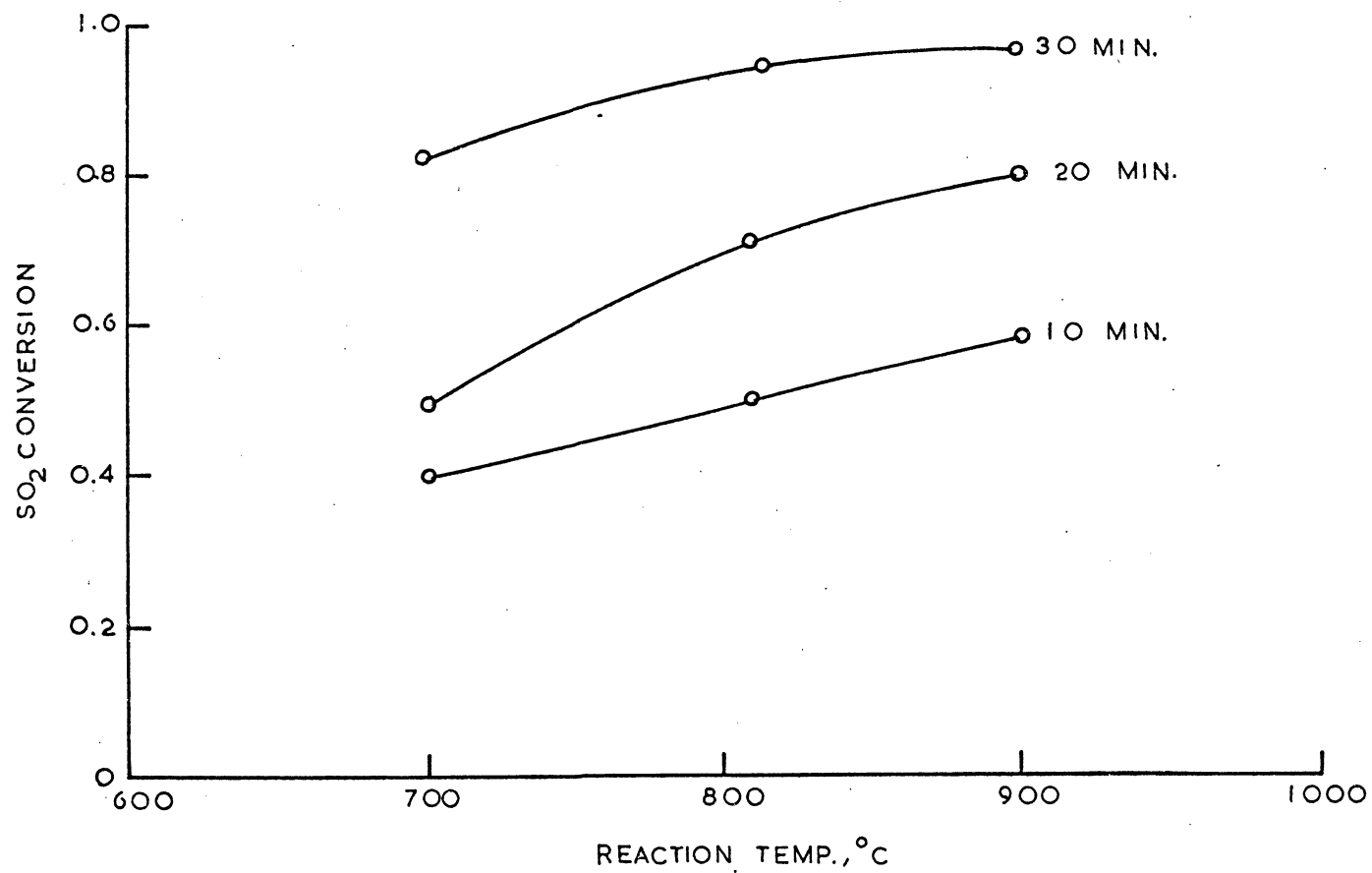
Fig. 3.13 Comparison of Brown Coal's Reactivity during Coal
charging period
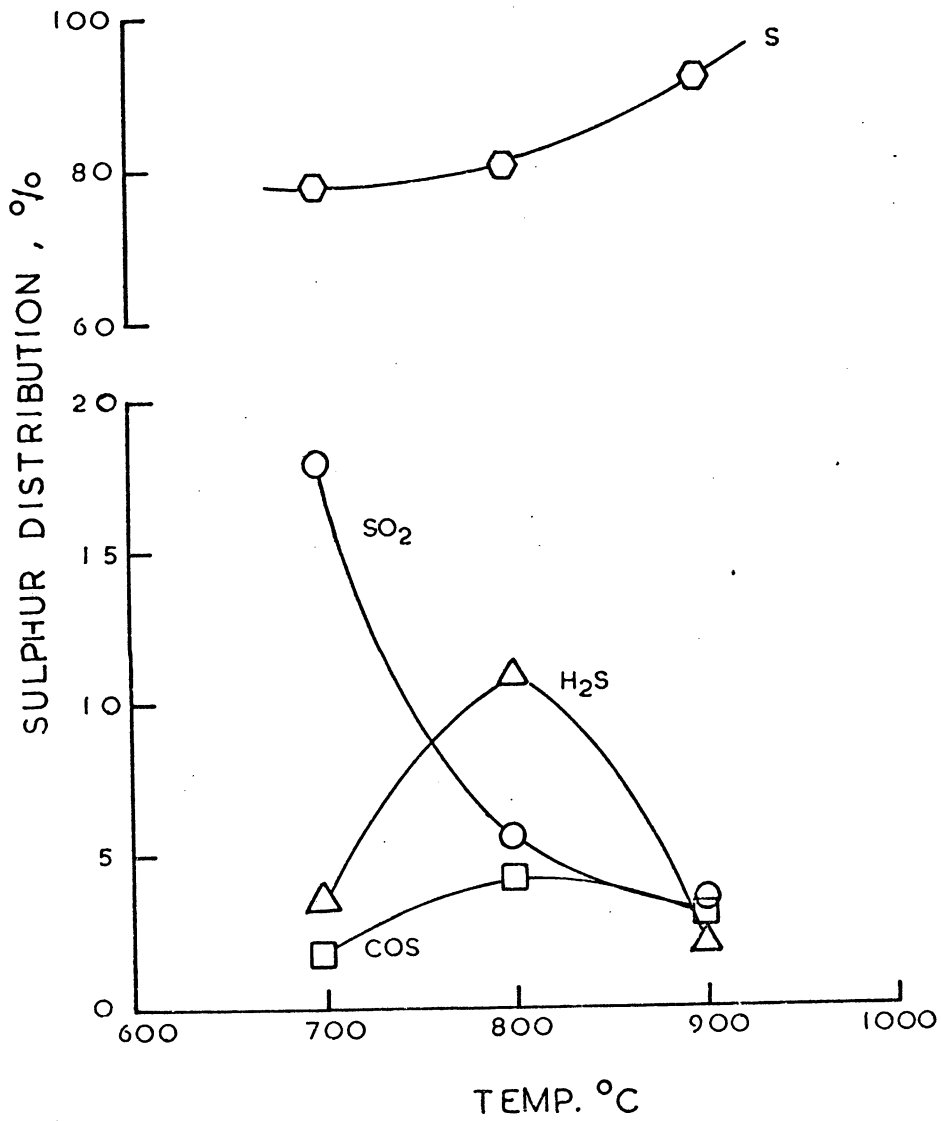
Fig. 3.14 Sulphur selectivity at Different Temperature Level for SO_2 Reduction with Brown Coal in a Spouted Bed

in the present work.

The porosity of coal other than anthracite would
be increased during the carbonization process.
The brown coal used for the experiment had 20.9%
volatile matter. Considerable surface area would
be created when the coal is devolatilized. The com-
bination of high surface area and volatile matter
makes brown coal a good reductant. The contribu-
tion of volatile matter in SO_2 reduction is evident
by the fact that during the coal charging period
SO_2 conversion was high and then reduced after all
the coal had been fed in (see Fig. 3.10 to 3.12).
After the coal charging period SO_2 in the effluent
was found to rise rather sharply. Two factors con-
tribute to this phenomenon: (1) depletion of vola-
tile matter in the coal and (2) reduction in car-
bon for reaction due to carbon burn-off.

The volatile matter in the brown coal if evolved com-
pletely would give a concentration of about 1.7% of
gaseous material, assumed to be in form of CH_4, in
the spouting gas stream at 700°C and 1.9% at 900°C.
Residual CH_4 in the reactor effluent was found to
be in the order of 0.3%. This again indicates a
high degree of reaction between SO_2 and hydrocarbon
material evolved from the brown coal.

(2) H$_2$S, COS and CO Formation

The experimental results show that no H$_2$S was de-
tected in the effluent when anthracite was used as
reductant. Some H$_2$S was formed when brown coal was
employed as reductant.

Formation of H$_2$S is attributed to the interaction
of SO$_2$ with volatile matter present in the coal.
The actual path for H$_2$S formation, however, is not
clear. In any case it is most probably a product
of a consecutive reaction as depicted in Chapter
Two. The principle reason that H$_2$S could not be
detected in the effluent when anthracite was used
as reductant perhaps, because the overall extent of
the reaction was low in the temperature range in-
vestigated. With brown coal the extent of the
reaction was high and thus there was more hydrogen
and sulphur for H$_2$S formation. In Fig. 3.14 the
effect of reaction temperature on H$_2$S formation is
shown. Brown coal was the reductant. More H$_2$S is
seen to form at 810°C. This is probably because
H$_2$S is unstable at high temperatures (see Chapter
Two).

Like H$_2$S formation, the production of COS relied
largely on the extent of the interaction between
SO$_2$ and the coal. Again in Fig. 3.14, COS concen-
tration is seen to be highest at 810°C. This is
because COS is also thermally unstable at high

temperatures and the dissociation could be catalysed by bed material at temperatures higher than 800°C. (15).

The production of CO is the result of the $C-CO_2$ reaction (23). This reaction is sensitive to the increase in reaction temperature. At 810°C it is seen to become quite significant in the interaction of SO_2 with brown coal. The reaction would produce active surface area for reducing SO_2 (22,23), however, a high concentration of CO in the effluent is undesirable from an atmospheric pollution point of view.

(3)   Sulphur Recovery

Sulphur fed into the system was found to appear in the effluent as H_2S, COS, S_2, elemental sulphur and SO_2. The experimental results of the interaction of SO_2 with brown coal suggest a high recovery of elemental sulphur, since H_2S and COS were found in small amounts. Interaction of SO_2 with activated carbon in the spouted bed also gave high elemental sulphur recovery. This finding appears to suggest that the special characteristics of a spouted bed favours high sulphur recovery (see Section 3.4.1.1 (7)).

3.4.2.   Determination of the Relative Significance of

Some of the Basic Design Variables

The relative significance of some of the basic variables, i.e. reaction temperature, initial SO_2 concentration, particle size and gas-solids contact time, was studied using a Plackett-Burman statistical method. The explanation of this method is given in Appendix C.

In this series of experiments eight runs were conducted. The results are summarised in Table 3.2. Complete experimental results and detailed calculations of these runs are given in Appendix C. It can be seen that only two variables can be regarded as significant, i.e. the reaction temperature and the flow rate of the spouting gas.

This finding is not unexpected. If the rate of reaction is first order with respect to the concentration of SO_2 then the extent of conversion of SO_2 is independent of the initial SO_2 concentration. Also if the particle used is highly porous then the effect of particle size will be negligible. This is particularly true when the high and low levels of the particle size do not differ very much as in the present case. Activated carbon is very porous (see Table 3.1) so the total surface area contributed from the outer surface is comparatively small.

In Table 3.2 it is also noted that the effect of the dummy variable F is as high as that of the gas flow rate. As explained in Appendix C, Section C.1, the high significance of the dummy variables may be due either to interaction between variables and/or to experimental error. As

precautions have been taken to avoid experimental error, it is suspected that this large value of F is probably caused by interaction between variables. According to Stowe and Mayer (41), this value could be due to one of the possible two-factor interactions with which F is confounded. To see if this could be the case, a table of primary and two-factor effect confounding was constructed (Table 3.3). The construction of this table is simple. Taking variable A, for example, it is noted that A equals BF. The matrix in Fig. C.1 shows that algebraic multiplication of B and F gives a minus sign in the first row. Similarly, the operation gives minus in 2nd, 3rd row and a plus in the 4th row. In each of these cases, the resulting sign is opposite to the sign in the column headed by A, i.e. equal to -A. This equality holds true throughout the remaining rows of B and F. Table 3.3 is constructed in this manner for each variable by finding the two different sets of column, which when multiplied together, produce a sign opposite to the sign of the variable.

From Table 3.3, it is seen that dummy variable F is confounded with AB and BG. The confounding effect of AB could be large. This is because of the very large value of the variable B despite the insignificance of variable A. Unfortunately, verification of this theory is impossible without further experimental work.

Table 3.2 <u>Effects of Variables</u>

	Variable	Effect	Relative Significance	
<u>Code</u>	<u>Name</u>	<u>(-) to (+)</u>	<u>(t - test)</u>	
A	SO_2 Conc.	-0.4	-0.16	57%
B	Temperature	55.3	22.20	99%
C	Dummy	0.2	0.08	50%
D	Part. Size	-0.02	-0.01	50%
E	Flow Rate	5.1	2.1	94%
F	Dummy	4.3	1.7	90%
G	Dummy	0.6	0.24	57%

Note: (+) denotes high level of variable.

(-) denotes low level of variable.

Table 3.3 <u>Primary and Two-Factor Confounding</u>

<u>Variable</u>

Initial SO_2 Conc.	-A	BF	CD
Temperature	-B	AF	CG
Dummy	-C	AD	EF
Particle Size	-D	AC	BE
Flow Rate	-E	AG	BD
Dummy	-F	AB	BG
Dummy	-G	AE	BC

3.5 FLOW MODEL FOR THE GAS-SOLIDS REACTION IN A SPOUTED BED

3.5.1 Formulation of Mathur and Lim's Flow Model

Mathur and Lim's flow model is a two-region model analogous to the bubble-bed model in fluidization (43). A schematic diagram of the model is shown in Fig. 3.15. It is seen that the two regions mentioned above are the spout and the annulus regions. Since the extent of the reaction in the two regions will be unequal due to difference in gas-solids contact time, they must be treated separately. The basic strategy for this is to formulate material balances (and energy balances if the system is non-isothermal) that relate all the system variables. As such, the system equations are in their most general form. Often some simplifying assumptions can be made. For the present work, the following assumptions were used:

(1)   The reactor is isothermal.

(2)   Changes in volumetric flux due to changes

in molar flux arising from chemical reactions

and pressure changes (if any) are ignored.

(3)   Plug flow of gas prevails in the two regions.

As shown in Fig. 3.15, the parameters used in the model are $\bar{V}_a$, $\bar{V}_s$, C_a and C_s (see list of symbols for physical meanings). Since these parameters are functions of bed level, z , it is convenient to write material balance over a differential height dz for each region of the bed.

The Spout Region

Under steady state conditions, the material balance for the
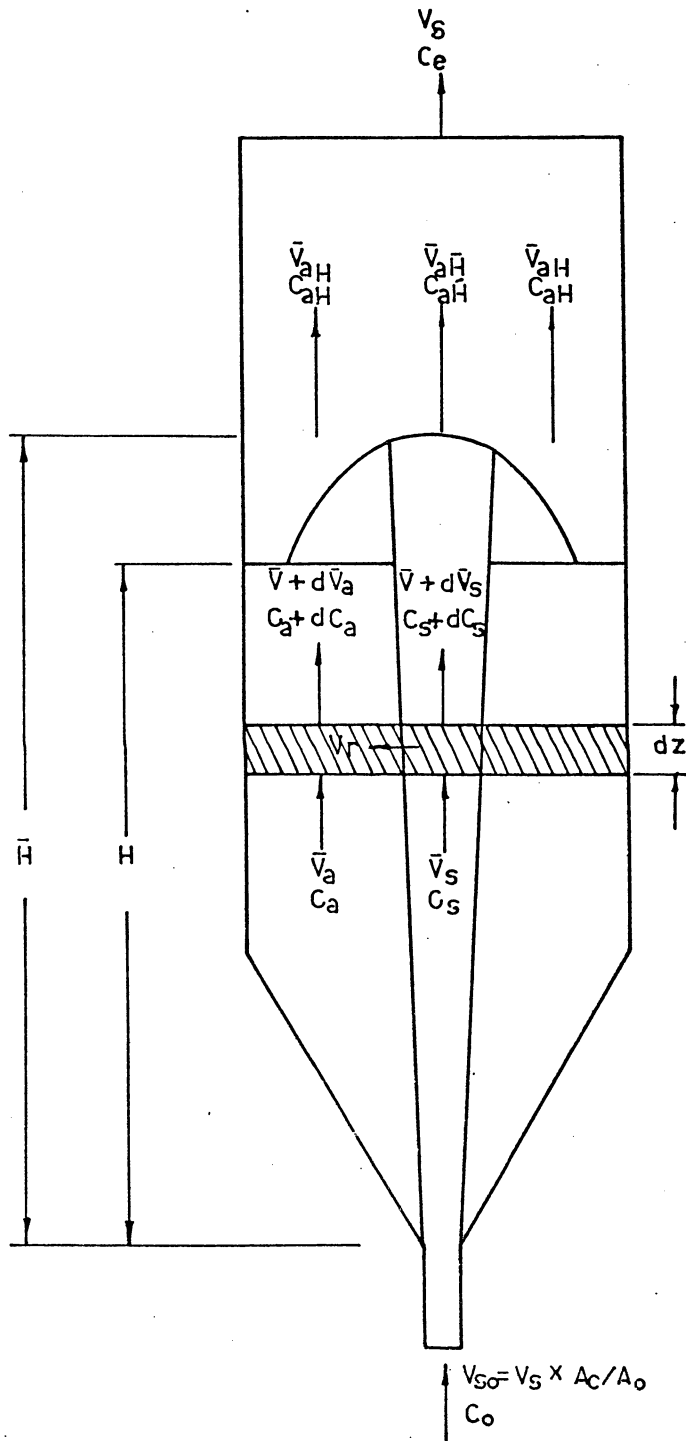
Fig. 3.15 Flow Model of a Spouted Bed

(see page 105a for notations)

NOTATIONS FOR FIG. 3.15

A_c Cross-sectional area of column

A_o Cross-sectional area of inlet

C_a Gaseous reactant conc. in annulus

C_{aH} Gaseous reactant conc. above annulus

C_o Gaseous reactant conc. at inlet

C_s Gaseous reactant conc. in spout

$C_{s\bar{H}}$ Gaseous reactant conc. above spout

C_e Gaseous reactant conc. at outlet

H Bed height

$\bar{H}$ Spout height

dC_a Differential gaseous reactant conc. in annulus

dC_s Differential gaseous reactant conc. in spout

$\bar{V}_a$ Superficial gas velocity in the annulus

$\bar{V}_{aH}$ $\bar{V}_a$ at $z = H$

$\bar{V}_s$ Superficial gas velocity in the spout

$\bar{V}_{s\bar{H}}$ $\bar{V}_s$ at $z = H$

V_{so} Spouting gas velocity at the inlet

V_s Spouting gas velocity

V_r Radial gas percolation velocity

dz Diff. vertical distance from gas inlet

z Vertical distance from gas inlet

spout section dz is given below:

Reactant entering section from below per unit time

= Reactant leaving from above + Reactant cross

flowing into annulus + Reactant consumed by

reaction

.... 3.5.1

In symbols, equation 3.5.1 can be written as follows:
(see List of Symbols for physical meanings of symbols
used in the equation.)

$$\bar{v}_s A_s C_s = [\bar{v}_s A_s + d(\bar{v}_s A_s)] [C_s + dC_s] + (\pi D_s dz) v_r C_s$$

$$+ A_s (1 - \varepsilon_s) dz (-r) \qquad ......3.5.2$$

Consider the simple case of a first order reaction if the

particles are porous and mass transfer and diffusional

effects are absent, then the kinetics of the reaction is

described by (43):

$$-r = - \frac{1}{V_r} \frac{dN}{dt} = K_r C \qquad .....3.5.3$$

From a gas material balance over the section dz

$$v_r = -\frac{1}{\pi D_s} \frac{d(\bar{v}_s A_s)}{dz} \qquad ......3.5.4$$

Substituting Eqs. (3.5.3) and (3.5.4) into Eq. (3.5.2) and

rearranging, we get

$$\bar{v}_s \frac{dc_s}{dz} + K_r (1 - \varepsilon_s) C_s = 0 \qquad ......3.5.5$$

The Annulus Region

The material balance for the annulus section dZ is simi-

larly given as follows:

Reactant entering section from below per unit time

+Reactant entering from spout = Reactant leaving above

+Reactant consumed by reaction

or in symbols:

$$\bar{v}_a A_a C_a + v_r \pi D_s dz C_s = [\bar{v}_a A_a + d(\bar{v}_a A_a)] \cdot$$
$$(C_a + dC_a) + K_r(1 - \varepsilon_o) x A_a dz C_a$$
$$\dots\dots\dots 3.5.6$$

From a gas material balance,

$$v_r = \frac{1}{\pi D_s} \cdot \frac{d(\bar{v}_a A_a)}{dz} \qquad \dots\dots\dots 3.5.7$$

substituting Eq. (3.5.7) into Eq. (3.5.6) and rearranging

yields,

$$\bar{v}_a \frac{dC_a}{dz} + \frac{1}{A_a} \frac{d(\bar{v}_a A_a)}{dz} \cdot (C_a - C_s)$$
$$+ K_r(1 - \varepsilon_o) C_a = 0 \qquad \dots\dots\dots 3.5.8$$

Equations (3.5.5) and (3.5.8) can be solved numerically

with the boundary conditions $C_s = C_a = C_o$ at $z=0$ to

yield $C_{s\bar{H}}$ and $C_{a\bar{H}}$ provided that $\bar{v}_a$, $\bar{v}_s$ and ε_s can be

quantitatively described as functions of z. The concen-

tration of unconverted reactant leaving the reactor is

obtained by combining the gas leaving each region. Thus,

$$C_e = \frac{\bar{v}_{aH} A_a C_{aH} + \bar{v}_{sH} A_s C_{sH}}{v_s A_c} \qquad \dots\dots\dots 3.5.9$$

The overall fractional conversion, X, can then be calcula-

ted from Eq. (3.5.10),

$$X = 1 - C_e / C_o \qquad \dots\dots 3.5.10$$

3.5.2 <u>Description of Hydrodynamic Features</u>

As mentioned above the hydrodynamic features $\bar{v}_a$, $\bar{v}_s$ and

ε_s used need quantifying with respect to bed height z.

The following relationships have been selected to describe them.

(1) $\bar{v}_a$ as a Function of z

The Mamuro and Hattori equation (44) given below is used to relate $\bar{v}_a$ to z.

$$\bar{v}_a/\bar{v}_{aH} = 1 - (1 - {}^z/H)^3 \qquad \ldots\ldots 3.5.11$$

Although this relationship has been shown to be somewhat simplified (45) it is a good first approximation. The parameter $\bar{v}_{aH}$ is not known and therefore has to be related to the independent variables of the system, viz. solid properties and bed geometry. While the effect of the solid properties on the gas flow pattern has not been studied in detail, considerable data on $\bar{v}_{aH}$ based on measurement of static pressure gradients along the column wall are available for wheat beds of 15 cm, 30.5 cm and 61 cm columns (38,46). The data for the 61 cm column (46) also cover varying bed heights (91.5-183 cm), air inlet diameters (5.1-10.2 cm) and air flow rates (1.1v_{ms}-1.3v_{ms}). Mathur and Lim (47) have shown that all the above data could be brought together if $\bar{v}_{aH}/v_{mf}$ was plotted against H/H_m (see Fig. 3.16). This plot shows that the relationship between the two ratios is roughly parabolic, i.e. $\bar{v}_{aH}/v_{mf} = \sqrt{H/H_m}$. The H_m values used for the 15.2 cm and 30.5 cm columns in this plot were those reported by Mathur and Gishler (38). H_m values for the 61 cm
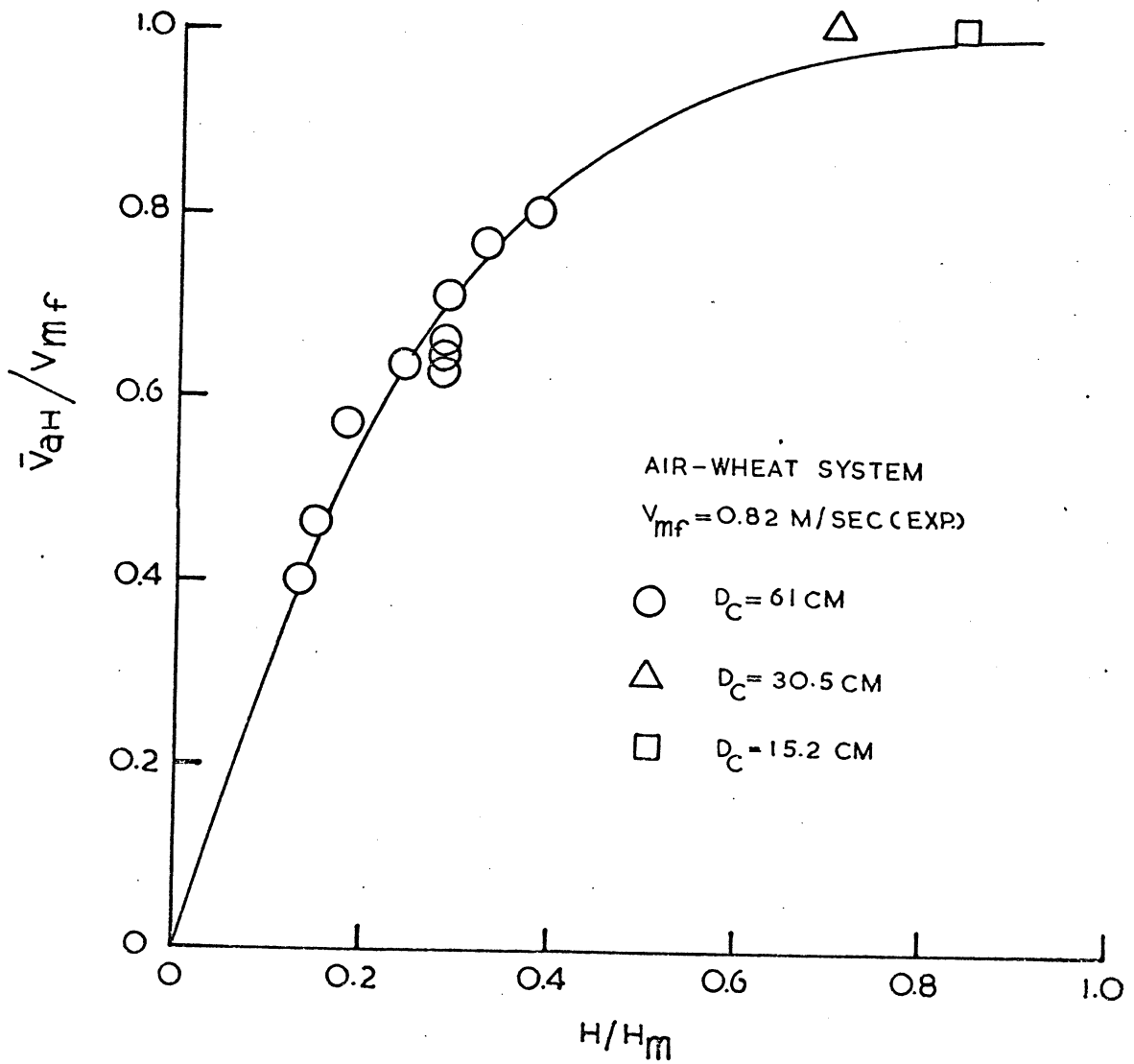
Fig. 3.16 Variation of $\bar{v}_{aH}/v_{mf}$ with H/H_m

column were estimated using the following empirical

equation (39):

$$H_m/D_c = 0.105 \left(D_c/D_p \right)^{0.75} \cdot \left(D_c/D_i \right)^{0.4} \cdot \lambda^2 / \rho_s^{1.2} \qquad \ldots 3.5.12$$

where H_m is in cm and ρ_s in gm/cm^3, λ being a

particle shape factor (see List of Symbols).

In calculating v_{mf} the following expression which is

based on the Ergun's fixed bed pressure drop equa-

tion (48) was used:

$$\left(\frac{1.75}{\phi_s \varepsilon^3_{mf}} \right)\left(\frac{D_p (v_{mf} \rho_p)^3}{\mu} \right) + \left(\frac{150(1-\varepsilon_{mf})}{\phi_s^2 \varepsilon^3_{mf}} \right) \cdot \left(\frac{D_p v_{mf} \rho_p}{\mu} \right)$$
$$= \frac{D_p^3 \rho_p (\rho_s - \rho_p) g}{\mu^2} \qquad \ldots \ldots 3.5.13$$

where all symbols used are defined in the List of

Symbols.

Thus Eq. (3.5.11) - (3.5.13) and the empirical

generalization respresented in Fig. 3.16 all to-

gether provide a method for predicting $\bar{v}_a$ as a

function of z for any given material and bed geo-

metry.

(2) $\underline{\bar{v}_s \text{ as a Function of } z}$

$\bar{v}_s$ is related to z with the following gas material

balance:

$$\bar{v}_s A_s + \bar{v}_a (A_c - A_s) = v_s A_s \qquad \ldots \ldots 3.5.14$$

A_s is assumed to be independent of z. The conical

base of the bed is taken into account by allowing the

cross-sectional area of the annulus, $A_c - A_s$, to in-

crease with z until the top of the conical section

is reached.

(3) ε_s as a Function of z

There is no generalized expression that correlates ε_s with z (45) nor is there published spout voidage distribution data obtained under conditions comparable to the present work. If precise analysis is required it is necessary to measure the actual profile of voidage. Because of the experimental difficulties of determining voidage under conditions of high temperature this voidage was left as an unknown and assumed values used in the calculation of the flow model.

(4) Mean Spout Diameter, D_s

Mean spout diameter, D_s, used in the analysis was measured using a clear front half-sectional bed at room conditions. The dimension, bed geometry and spouting material were the same as those in the actual hot experiment. This was found more reliable since for a small reactor such as the one employed here (dia.=3.913 cm) overall conversion is sensitive to variations in D_s.

(5) Others

In this calculation it was assumed that the spout height, $\bar{H}$ was equal to 1.25 H.

The annulus voidage was determined at static and random packed bed conditions. This was found to

average 0.454.

3.5.3 Development of a Kinetic Expression for the SO_2/ Activated Carbon Reaction

3.5.3.1 Introduction

In Section 3.5.1 the flow model of a spouted bed was presented. In order to use the model it is necessary to have a chemical rate equation. For reasons of simplicity the chemical reaction chosen was SO_2/C. The kinetics of the SO_2/C reaction is much less complicated than that of the SO_2/coal reaction and a simple overall kinetic expression could be anticipated. There are two methods generally employed in the kinetics study of gas-solids reactions in flow systems viz. differential analysis and integral analysis. The former is more suitable for mechanism study while the latter is comparatively simpler and generally used for obtaining a working rate equation. The integral method was therefore selected for the present work. The integral reactor was a packed bed of activated carbon with a depth of about 3 cm through which flowed a SO_2 nitrogen gas mixture.

3.5.3.2 Selection of Experimental Parameters

Two parameters were thought to be most relevant in the study. These were reaction temperature and gas flow rate. Other variables such as SO_2 concentration, particle size etc. were excluded because the study was not intended for detailed mechanism investigation.

The important points considered in this series of runs
were as follows:

(i)   Reaction Time

       Earlier experiments in the spouted bed had es-

       tablished that a steady state was reached

       within 20 minutes for all SO_2-C reactions con-

       ducted between 700-900°C. It was necessary to

       conduct some exploratory runs to determine the

       situation in a packed bed.

(ii)   Temperature Range and Gas Flow Rates

       Temperature and gas residence times were chosen

       to be comparable to those used in the spouted

       bed work.

3.5.3.3 Equipment Design

The equipment used in this series of experiments was

essentially the same as that described in Section 3.2.1

except that the reactor was different. This reactor was

made of a 4 cm I.D. alumina tube. The carbon bed for

sulphur dioxide reduction was supported by a ceramic disc

made of firebrick. A thermowell was inserted from the gas

inlet and into the centre of the reaction zone. As the

gas emmitted from the reactor was several hundred degrees

Celcius a gas cooler was located at the gas outlet end of

the reaction tube in order to protect the less heat resis-

tant fittings. Like the spouted bed, the reaction tube was

kept vertical but the sulphur dioxide mixture was allowed to flow in from the top. This was designed to prevent fluidization of the carbon bed.

3.5.3.4 Experimental Procedure

The experimental procedures were essentially the same as those in the spouted bed runs. These were described in Section 3.3.2 and in Appendix C.

3.5.3.5 Results and Discussion

(1) Approach to Steady State

The time required for the system to reach a steady state was found to be rather rapid. This is shown in Fig. 3.17. It shows that at 660°C and 0.35 sec. superficial mean residence time the system established a steady state in about 10 minutes. Therefore at higher temperatures and gas flow rates it is probable that steady state would be reached somewhat faster. This information was used subsequently for other runs in deriving steady state SO_2 conversion.

(2) Kinetic Data

In Table 3.4 gas analysis of the reaction products from the kinetic study of SO_2 reduction with activated carbon are given. Four gas samples were taken for every run at intervals of about 3 minutes. From this Table it is obvious that
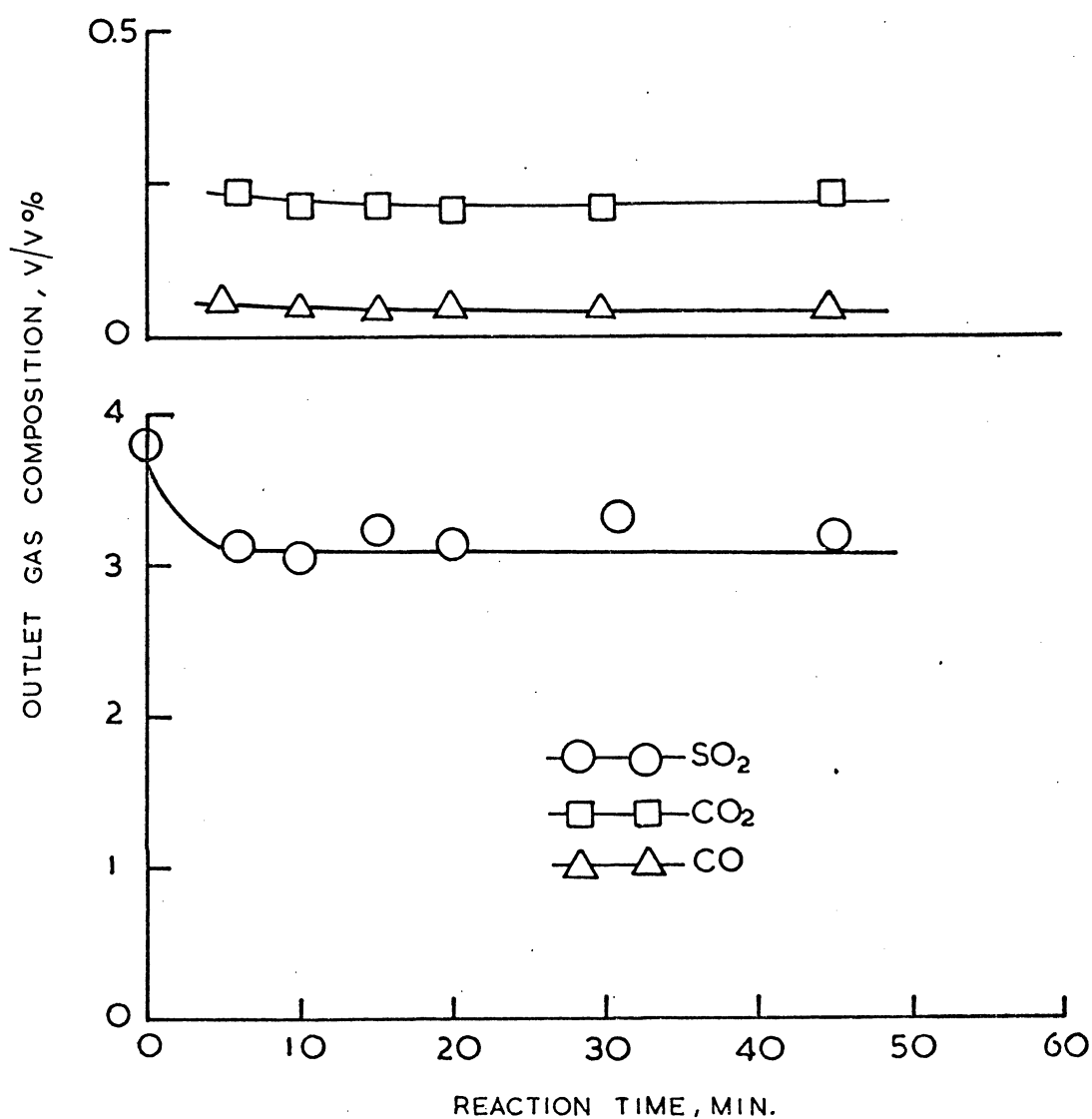
Fig. 3.17 Reduction of SO_2 with Activated Carbon in a Packed Bed at 660°C, 0.25 sec mean superficial residence time

TABLE 3.4 Gas Analysis for Kinetic Study of SO_2
Reduction with Activated Carbon

RUN NO.		1	2	3	4	5	6
Temp. °C		660	660	660	710	710	710
Mean Gas Residence Time, sec.		0.203	0.257	0.325	0.153	0.183	0.264
Conc. %		3.76	3.76	3.76	3.64	3.64	3.64
p. size, cm		0.103	0.103	0.103	0.103	0.103	0.103
Vol. %	SO_2	3.41	3.15	3.11	2.88	2.57	2.23
	CO_2	0.32	0.38	0.37	0.67	0.76	1.24
(1)	CO	0.16	0.17	0.10	0.18	0.09	0.07
	COS	–	–	–	–	–	–
	X	9.31	16.22	17.29	20.88	29.40	38.74
Vol. %	SO_2	3.22	3.23	3.03	2.87	2.61	2.28
	CO_2	0.21	0.25	0.32	0.50	0.75	1.21
(2)	CO	0.14	0.123	0.09	0.15	0.08	0.08
	COS	–	–	–	–	–	–
	X	14.30	14.10	19.42	21.15	28.30	37.36
Vol. %	SO_2	3.30	3.32	3.24	2.87	2.54	2.17
	CO_2	0.24	0.25	0.31	0.42	0.80	1.30
(3)	CO	0.07	0.13	0.09	0.08	0.08	0.07
	COS	–	–	–	–	–	–
	X	12.23	11.70	13.83	21.15	30.22	40.39
Vol. %	SO_2	3.31	3.26	3.11	2.56	2.58	2.22
	CO_2	0.27	0.28	0.31	0.41	0.81	1.32
(4)	CO	0.13	0.10	0.09	0.08	0.08	0.07
	COS	–	–	–	–	–	–
	X	11.97	13.30	17.25	21.43	29.12	39.01
AVERAGE X, %		11.97	13.83	16.96	21.15	29.26	38.88

Table 3.4 (Cont.) Gas Analysis for Kinetic Study of
SO$_2$ Reduction with Activated Carbon

RUN NO:	7	8	9	10	11	12
Temp. °C	710	760	760	760	760	810
Mean Gas Residence Time, sec.	0.349	0.136	0.152	0.183	0.260	0.152
Conc. %	3.64	3.74	3.74	3.74	3.74	3.46
p. size, cm	0.103	0.103	0.103	0.103	0.103	0.103
Vol. % SO$_2$	1.79	0.96	0.81	0.51	0.38	0.41
CO$_2$	1.51	2.31	2.73	3.18	2.79	2.32
(1) CO	0.06	0.15	0.14	0.14	1.21	1.01
COS	0.013	0.04	0.05	0.07	0.09	0.53
X	50.83	74.33	78.34	86.63	89.84	88.15
Vol. % SO$_2$	1.83	1.03	0.79	0.53	0.45	0.45
CO$_2$	1.48	2.32	2.78	3.75	2.93	2.37
(2) CO	0.05	0.14	0.11	0.11	1.05	1.12
COS	0.012	0.04	0.05	0.07	0.08	0.53
X	49.73	72.46	78.88	55.83	87.97	86.99
Vol. % SO$_2$	1.78	0.92	0.83	0.48	0.33	0.43
CO$_2$	1.57	2.29	2.68	3.20	2.87	2.33
(3) CO	0.06	0.16	0.15	0.11	1.15	1.08
COS	0.012	0.04	0.05	0.08	0.08	0.51
X	51.10	75.40	77.81	87.17	91.18	87.57
Vol. % SO$_2$	1.81	1.01	0.88	0.51	0.35	0.42
CO$_2$	1.50	2.25	2.80	3.22	2.84	2.38
(4) CO	0.06	0.13	0.10	0.10	1.20	1.00
COS	0.01	0.05	0.05	0.08	0.08	0.55
X	50.28	73.00	76.47	83.69	90.64	87.86
AVERAGE X, %	50.49	73.80	77.88	85.83	89.91	87.65

Table 3.4 (Cont.)   Gas Analysis for Kinetic Study of SO_2
Reduction with Activated Carbon

RUN NO.		13	14
Temp. °C		810	810
Mean Gas Residence Time, sec.		0.21	0.280
Conc. %		3.64	3.64
P. size, cm		0.103	0.103
Vol. % SO_2		0.13	0.073
	CO_2	1.89	1.73
(1)	CO	2.32	2.58
	COS	0.73	1.15
	X	96.43	97.99
Vol. % SO_2		0.20	0.08
	CO_2	1.92	1.70
(2)	CO	2.18	2.62
	COS	0.81	1.12
	X	94.51	97.80
Vol. % SO_2		0.15	0.07
	CO_2	1.90	1.78
(3)	CO	2.28	2.49
	COS	0.81	1.08
	X	95.88	97.99
Vol. % SO_2		0.16	0.07
	CO_2	1.95	1.69
(4)	CO	2.28	2.52
	COS	0.79	1.10
	X	95.61	97.99
AVERAGE X, %		95.61	97.94

steady state for each run had been established.
Average SO_2 conversions were obtained and are
shown in Fig. 3.18

3.5.3.6. A Kinetic Model for the SO_2-Activated Carbon Reaction

In order to use the integral analysis method, the reactor
volume (i.e. the carbon bed) must remain constant.
Because of the rapid attainment of the steady state, only
a small amount of carbon had been consumed and therefore
only a small change in bed volume could have occurred
before samples were taken. Quantitative support for this
assumption was obtained by measuring the bed height and
bed weight on completion of an experiment. In fact the
changes in bed heights were found to be unnoticeable in
most of the runs. The assumption of constant reactor vol-
ume was therefore justified.

Other assumptions used in this analysis were as follows:

> (1) Film and diffusional resistances in the
> reaction were insignificant.
>
> (2) The gas mixture was in plug flow.
>
> (3) Density change due to reaction was negligible.

The first assumption is reasonable because of the high gas
flow rate and of the high porosity of the activated carbon
(Table 3.1). Theoretical estimation of the mass transfer
effect was carried out (see Appendix F). The calculated
result supported this assumption.
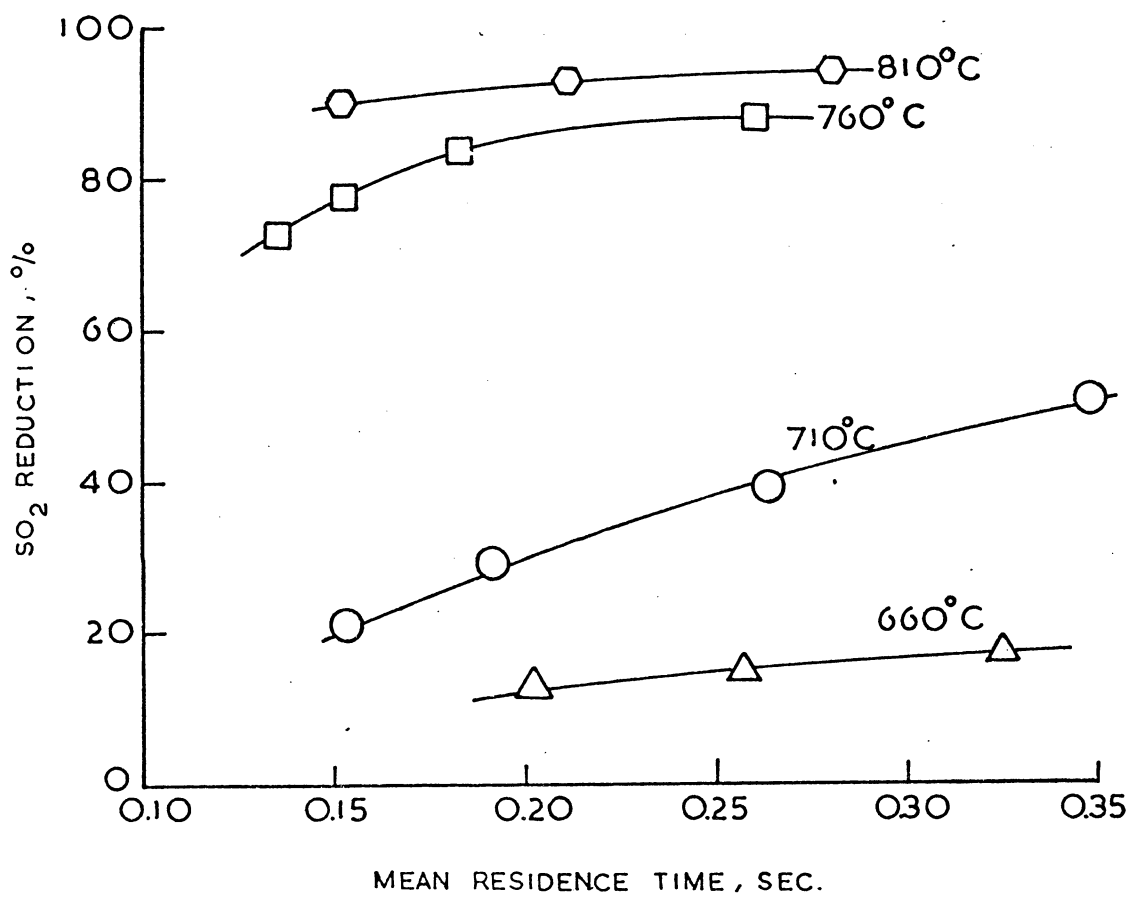
Fig. 3.18 Effect of Gas Flow rate on SO_2 conversion

Since the gas phase is assumed to be in plug flow the reactor design equation is

$$V_r/F_{Ao} = \int_0^{X_A} \frac{dX_A}{-r_A} \qquad \ldots\ldots 3.5.15$$

where $-r_A$, F_{Ao}, X_A etc. are defined in the List of Symbols.

As a first trial, a first order rate expression was assumed. Under the prescribed assumptions as stated above this expression is given as,

$$-r_A = -\frac{1}{V_r} \cdot \frac{dNA}{dt} = K_r C_{Ao}(1-X_A) \qquad \ldots\ldots 3.5.16$$

When Eq. (3.5.16) is substituted in Eq. (3.5.15) and integrated, it gives,

$$\frac{V_r}{F_{Ao}} = \frac{1}{K_r C_{Ao}} \cdot \ln(^1/1 - X_A) \qquad \ldots\ldots 3.4.17$$

If the system is first order kinetically then a plot of $\ln(1/1-X_A)$ against V_r/F_{Ao} should produce a straight line with a slope $1/K_r C_{Ao}$. Fig. 3.19a and 3.19b show plots of the experimental data in terms of Eq. (3.5.17). It can be seen that within the limits of the experiment, the reactor rate is approximately first order with respect to the concentration of sulphur dioxide.

Specific rate constants were determined from the slopes of these plots. These data (see Table 3.5) were then used to give an Arrhenius plot as shown in Fig. 3.20. This figure shows that the specific rate constants are related in a linear manner. This linear relationship is given in the following expression:
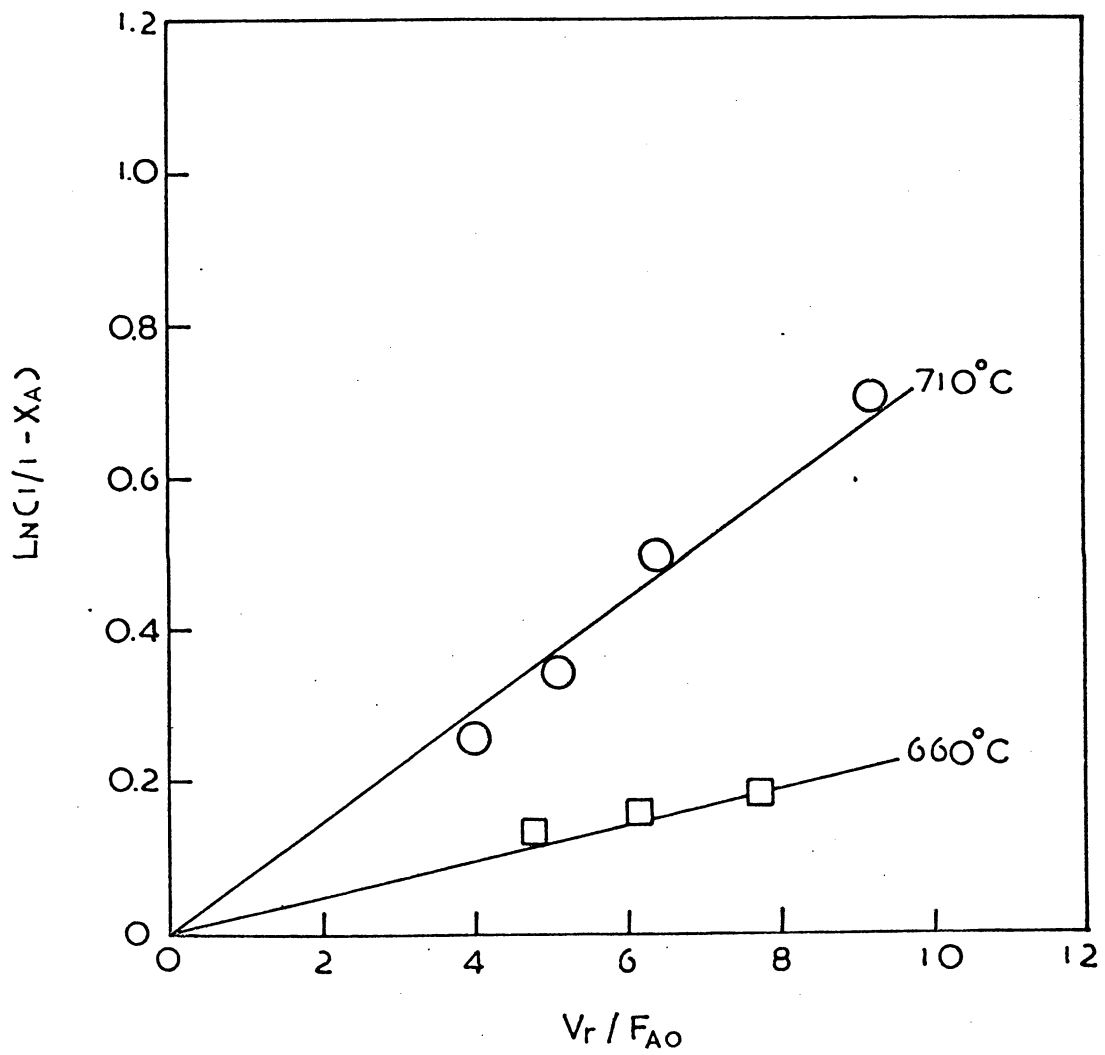
Fig. 3.19 a   Linearity test of the Kinetic data of the

SO_2- activated Carbon reaction
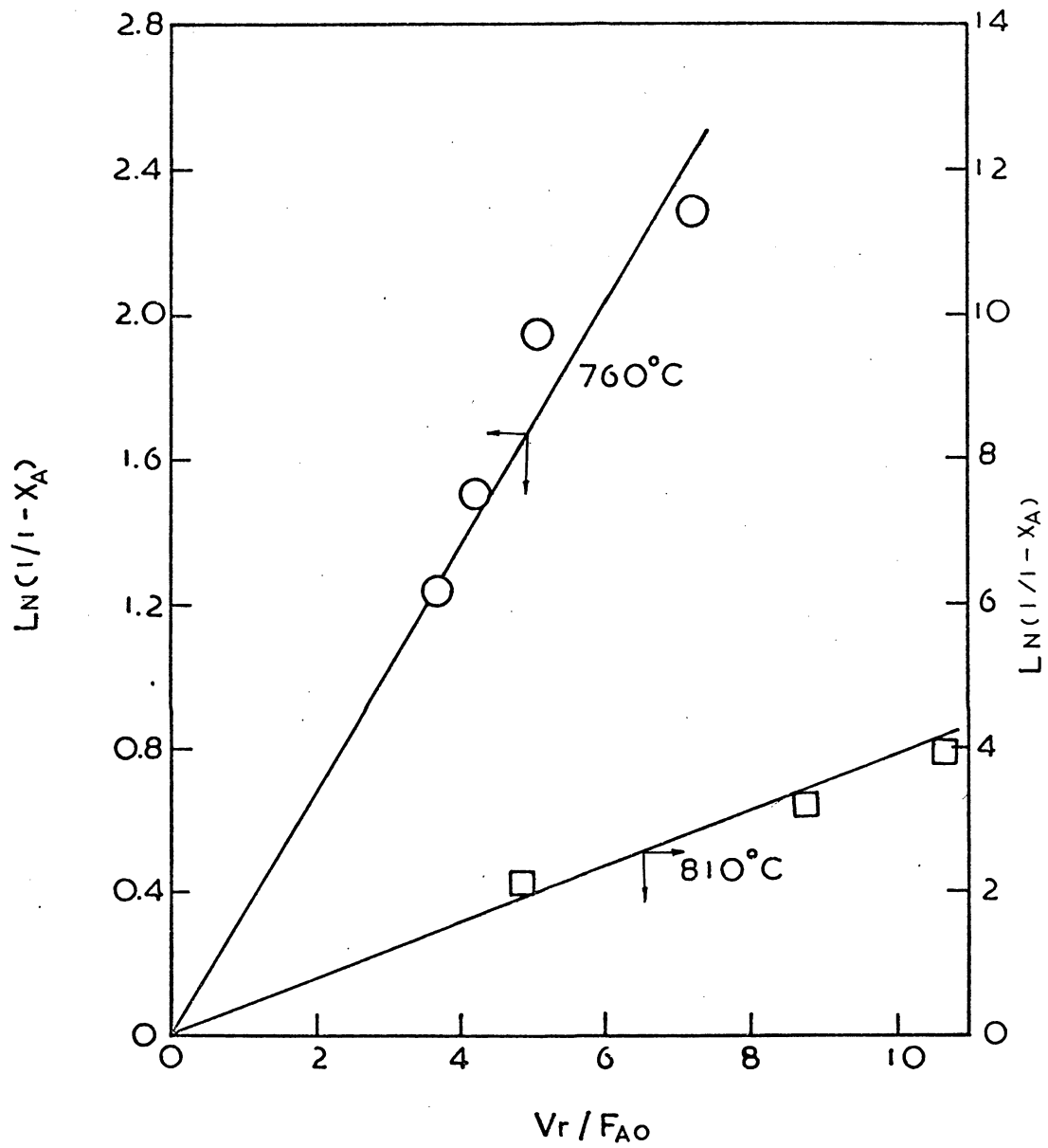
Fig. 3.19 b   Linearity test of the kinetic data of

SO_2- activated Carbon reaction
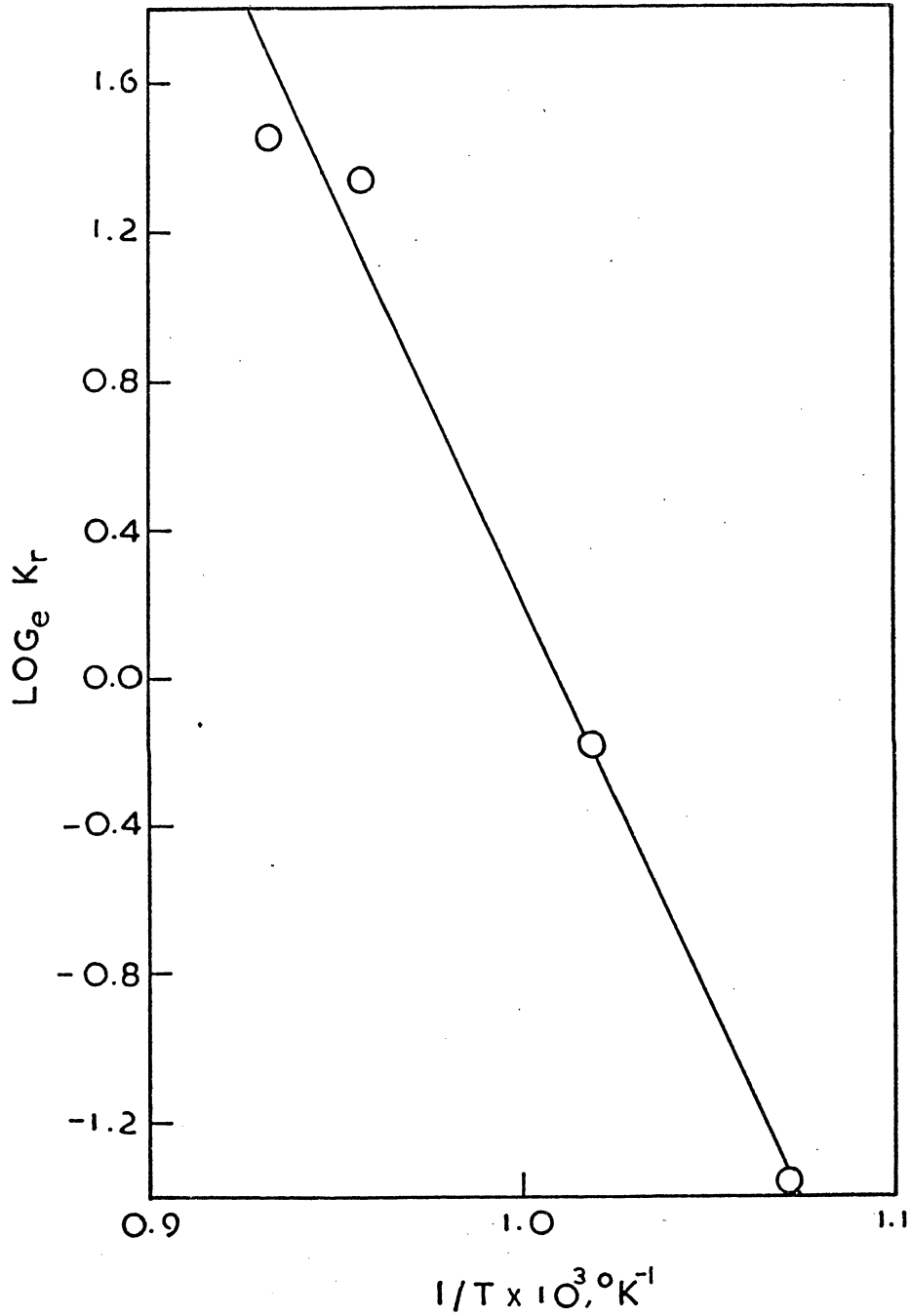
Fig. 3.20   Arrhenius plot for specific rate constants

of the SO_2 and activated Carbon reaction

$$K_r = 5.02 \times 10^9 \text{ Exp}(-2.21 \times 10^4/T) \quad \dots\dots\dots \quad 3.5.18$$
$$(1./\text{sec})$$

The complete kinetic expression is therefore,

$$-r_A = 5.02 \times 10^9 \text{ Exp } (-2.21 \times 10^4/T) \, C_A \quad \dots\dots \quad 3.6.19$$

Eq. (3.5.18) predicts specific rate constants with a standard error of estimate of 0.20. As can be seem from Fig. 3.19 this error of estimate is introduced by data obtained at 770° and 810°C. At these temperatures SO_2 conversions were high, i.e. low SO_2 concentration in gas sample mixtures and as is mentioned in Appendix D, accurate determination of SO_2 in low concentration was difficult.

3.5.4 Comparison of Predicted and Experimental Results

Theoretical prediction of the performance of a spouted bed can be achieved by solving the following equations simultaneously:

$$\bar{v}_s \frac{dC_s}{dz} + K_r(1 - \varepsilon_s)C_s = 0 \qquad \dots\dots 3.5.5$$

$$\bar{v}_a \frac{dC_a}{dz} + \frac{1}{A_a} \frac{d(\bar{v}_a A_a)}{dz} (C_a - C_s)$$

$$+ K_r (1 - \varepsilon_o)C_a = 0 \qquad \dots\dots 3.5.8$$

$$\frac{\bar{v}_a}{\bar{v}_{aH}} = 1 - (1 - z/H)^3 \qquad \dots\dots 3.5.11$$

$$\frac{H_m}{D_c} = 0.105 \, (D_c/D_p)^{0.75} \, (D_c/D_i)^{0.4} \, (\lambda^2/\rho_s^{1.2})$$

$$\dots\dots 3.5.12$$

$$\bar{v}_{aH} = v_{mf} \cdot \sqrt{H/Hm} \qquad \ldots.3.5.20$$

$$V_{mf} = \left(2 \cdot \sqrt{H/Hm} \cdot \rho_f (D_p \varepsilon_o)^3 g \cdot \sqrt{\rho_s} \right) \Big/ \left(\rho_f \cdot D_p \cdot 150 \cdot \mu \cdot (1-\varepsilon_o) \cdot (1- \sqrt{1 + \frac{7g\rho_f (D_p \varepsilon_o)^3}{150 \quad (1-\varepsilon_o)^3}}) \right)$$

$$\ldots..3.5.21$$

$$\bar{v}_s = \frac{1}{A_s}(v_s A_s - \bar{v}_a (A_c - A_s)) \quad \ldots.3.5.14$$

$$-r_A = 5.02 \times 10^9 \text{ Exp. } (-2.21 \times 10^4/_T) C_a$$

$$\ldots..3.5.19$$

A computer programme which utilised the fourth-order Runge-Kutta iteration method was written for this purpose. The initial and terminating conditions were respectively $z=0$, $C_s=C_a=C_o$ and $z=\bar{\bar{H}}=1.25H$, $C_s=C_{sH}$ and $C_a=C_{a\bar{H}}$. The programme was initiated by using the initial conditions and integrated up the bed step by step until $\bar{H}$ was reached. As pointed out in Section 3.5.2 (3) an assumed value was taken for the voidage in the spout, ε_s, (between .7-1.0) was used to find which gave the best fit to the experimental results. This value of ε_s was found to be 0.75. The programme and a typical printout is shown in Appendix G.

The calculated and experimental results are compared in Table 3.5 and Fig. 3.21. The experimental data were collected from experiments of sulphur dioxide reduction with activated carbon in the spouted bed as detailed in Section 3.3 and 3.4. The agreement appears reasonable. The calculated results fit the experimental data with an average Relative absolute error of 8.8 % .

In Table 3.5 it is seen that experimental points 3 and 6 are respectively 20.7% and 25.1% higher than the predicted values. Referring to Table C.2a and C.2b, it can be seen that the experiments that gave these two points are runs 3 and 8. When these runs are compared with runs 5 and 6 (points 4 and 5 in Table 3.5) it is noted that the main differences in experimental conditions are particle size and gas flow rate. Smaller particle size and
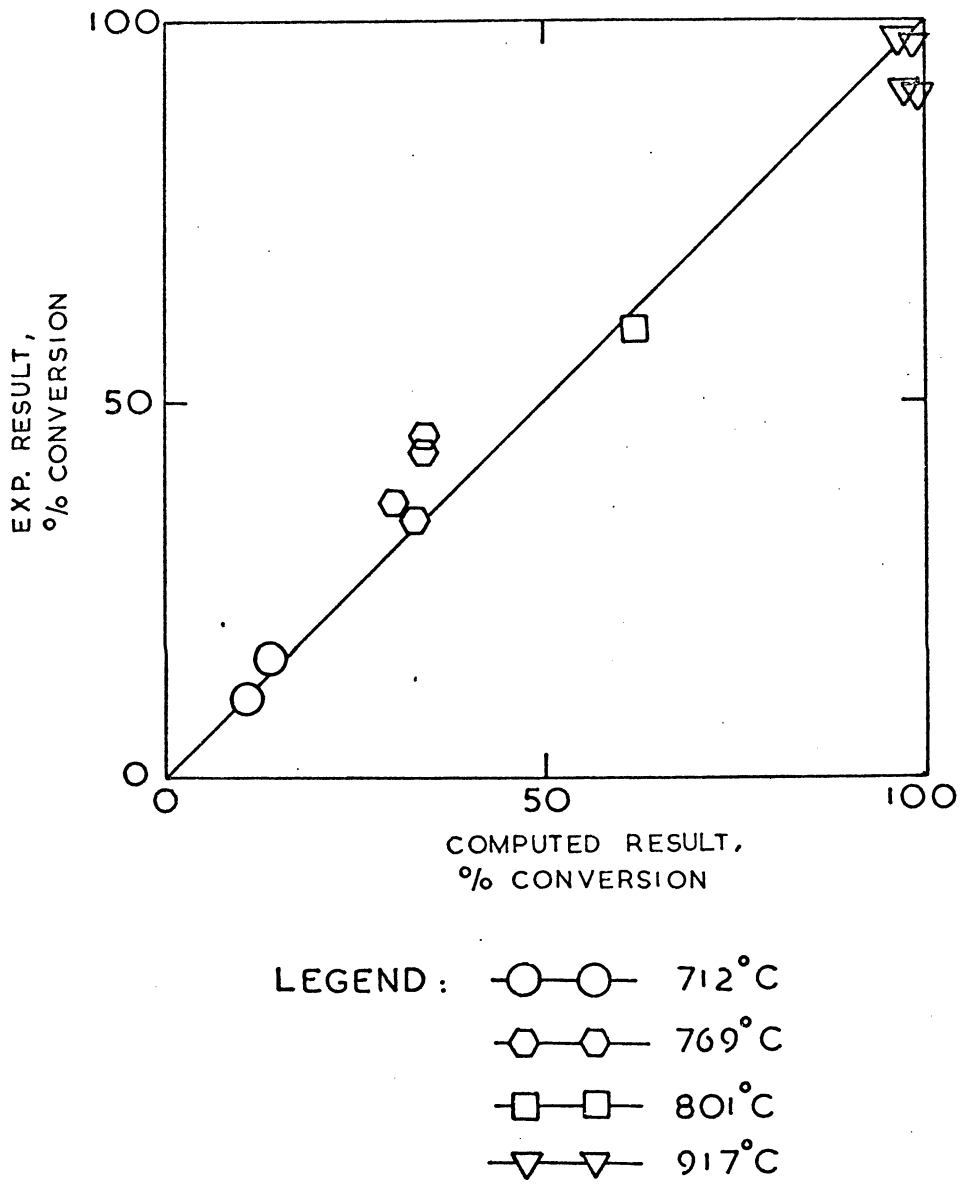
Fig. 3.21 Comparison of computed and experimental results

obtained in a Spouted Bed

$(H_m = 702$ cm, $D_p = 0.103$ cm, $D_i = 0.3913$ cm

$D_i = 0.633$ cm, $\varepsilon_o = 0.454, \varepsilon_s = 0.75)$

lower gas flow rate were used in runs 3 and 8. It appears therefore, that the model does not possess enough sensitivity to account for changes in these parameters, particularly the gas flow rate which has been shown to be significant in affecting the SO_2 conversion in the reduction process (see Section 3.4.2). Improvement in this respect can probably be obtained if the hydrodynamic characteristics of the spouting process are better understood and correlated.

TABLE 3.5 COMPARISON OF EXPERIMENTAL AND CALCULATED RESULTS

General conditions: $H_m = 7.2$ cm
$D_p = 0.103$ cm
$D_s = 1.4$ cm
$\varepsilon_o = 0.454$
$\varepsilon_s = 0.75$

Point No.	*Temp., °C	*Exp. Conv., %	Cal. Conv., %	Percentage+ Disagreement
1	712	15.8	14.51	+8.2
2	712	10.7	11.24	−5.1
3	770	43.5	34.48	+20.7
4	770	32.1	33.51	+4.4
5	767	35.2	30.99	+11.9
6	768	44.6	33.40	+25.1
7	801	59.6	61.67	−3.5
8	916	97.0	97.28	−0.3
9	917	97.7	98.58	−0.9
10	920	90.9	99.39	−9.4
11	916	90.8	97.89	−7.8

Abs, Av. 8.8

* These data were extracted from Tables C.2a, C.2b and E.1. Refer to these Tables for other information.

+ % Disagreement = $\dfrac{Exp.\% - Cal.\%}{Exp.\%} \times 100$

3.6 CONCLUSION

3.6.1 Reduction of SO_2

A spouted bed system has been designed to enable the study of the reduction of sulphur dioxide with activated carbon, brown coal and anthracite. The temperature range for the study was between 650-950°C. Clean simulated flue gases were prepared from pure SO_2 and nitrogen only. The concentration range of the gas mixture used was 1-7 %. From the experimental results it may be concluded that

(1) the spouted bed is suitable for providing an environment for reducing SO_2 in flue gases produced particularly from sulphide ore smelting,

(2) brown coal is found to be most suitable as a reductant and anthracite is found to be inferior as a reductant compared to activated carbon and brown coal, and

(3) satisfactory reduction of SO_2 can be obtained at some intermediate temperature, say about 750°C with high elemental sulphur recovery.

The possible application of brown coal as a reductant has particular significance in the SO_2 process. Brown coal is abundant and is cheap. Its chemical and physical properties makes it unattractive for industrial application. Thus the operating costs can be reduced quite significantly because the cost of reductant constitutes a significant part of the running cost of this process. Further

to this the possibility of reducing SO_2 at about 750°C would considerably lower the operating costs and the process would, therefore, be more acceptable than those reduction processes running at about 1200°C (11,15,24).

Some of the important design variables were evaluted for their relative significance. Activated carbon was used as reductant in the spouted bed. The results showed that reaction temperature and flow rate of the spouting gas were more significant in comparison to particle size and initial SO_2 concentration. In addition particle porosity and volatile matter appeared to have a significant effect in reducing SO_2.

3.6.2 The Flow Model

A mathematical description of the gas phase of a spouted bed reactor was found possible. This model was originally developed for the gas phase reaction in a catalytic bed (47). It is a two-region model analogous to the bubbling bed model of fluidization.

The model was solved numerically to obtain theoretical spouted bed performance of an activated carbon-SO_2 system. Before this could be performed, a kinetic expression was developed for the system. Information regarding the hydrodynamic features of the bed, such as the spout dia-meter, maximum spout height and annulus voidage of the bed were either calculated from existing correlations or direct measurements. It was found that the model gave a

CHARACTERISTICS OF MULTIPLE SPOUTED BEDS

4.1 INTRODUCTION

Fluidization is a well established process for agitating
and contacting particulate solids with fluids. With
coarse and uniform-sized granular solids, however,
fluidized beds show a marked tendency towards slugging
because of the growth of large bubbles. To overcome this
difficulty, Mathur and Gishler (38) developed the spouted-
bed technique in 1954. This process is illustrated in
Fig. 1.1 which is a schematic diagram of a two-dimensional
spouted bed. The phenomenon of spouting as depicted in
the diagram has been exhaustively described elsewhere (38,
45,59,61).

Since its inception, the process has been used for
drying wheat (38,61), wood chips (62) and peas, lentils
and flax (64). This technique has also been successfully
applied to the drying of other materials such as activa-
ted carbon, superphosphate, gelatine and pharmaceuticals
(63). Due ot its unique properties, the spouted bed
has also been found useful for a variety of seemingly-
unrelated processes, such as cooling (65), blending (66)
and coating (67,68) of various materials, granulation of
fertilizers and other products (69,70), pyrolysis of
shale (71) and petroleum (105,105), carbonization of
coal (13,14,72,73) and reduction of iron ore (107).

It appears, therefore, that the method has been quite

widely accepted as a useful means for fluid-solid con-
tacting. Its application to a commercial process, how-
ever, would generally require a larger capacity than can
be handled by a single spouted bed. Also, from the view-
point of plant economics, it is obvious that the fixed
costs of one large bed would be lower than for a number
of smaller beds having a similar thruput. The obvious
solution is scale up, however, scale up of spouted beds
is not straight forward. For example, it has been shown
that for satisfactory operation of spouted bed systems
the column diameter to particle size ratio should be in
the range 25-200 (63). This imposes severe limitations
on the maximum bed diameter. The largest column recorded
in the literature had a diameter of 610 mm (62,64,46).

Although this does not represent an upper limit an order
of magnitude separates the diameters of practical spouted
beds and fluidized beds.

There are two alternatives that could be used for over-
coming this limitation:

    (a)   Staging a number of units and maintaining

          a counter current flow of fluid and solids.

    (b)   Using a multiple spout system.

The former was demonstrated by Madonna et al (74), using
a column of four stages. The latter is not reported in
the literature[*]. The aim of this work, therefore, was to
make a detailed study of the multiple spouted bed system.
The knowledge gained from this can then be used to design

    [*] see addendum at the end of the thesis.

a commercial spouted bed for the treatment of SO_2 in
flue gases.

4.2 EXPERIMENTAL

4.2.1 Preliminary Study

4.2.1.1 Two Dimensional Bed Study

Two dimensional beds have been widely used in the study
of fluidization. The half-sectional bed as shown in
Fig. 1.1 has found equal favour in the study of spouting
(38,46,75,76) where it has been shown to behave as a full
column. Initial work on the multiple spouted bed was,
conducted using a flat bottom, clear front, half-sectional
bed with three 1.27 cm diameter gas inlets. Gas supplied
to the gas inlets was controlled individually. The
materials used in the study were wheat, rape seed and
millet.

The mechanism of obtaining an active multiple spouted
bed was found to resemble that of a single spouted bed.
This bed is shown schematically in Fig. 4.1. Comparison
of Fig. 1.1 and Fig. 4.1 shows that the two processes are
more or less identical except that in the latter there
is a constant exchange of material between spout regions.
This occurance is a result of material being transported
over the bed top and the cross-flow of material through
annular interfaces as the material moves downwards.
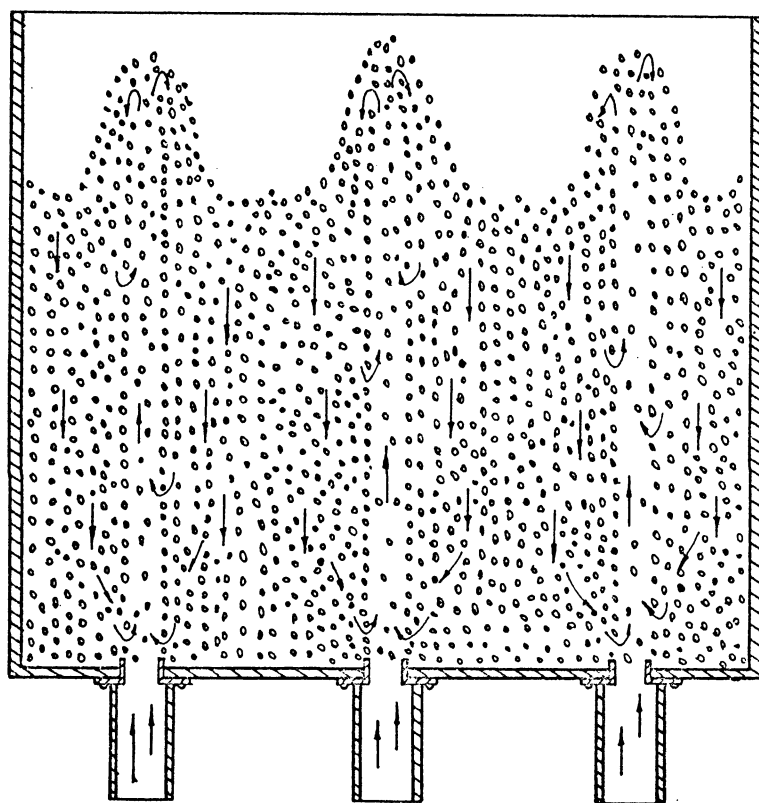
Fig.4.1   Schematic Diagram of a Multiple
           Spouted Bed

The effect of the separation of gas inlets on spout
stability was studied by varying the separation between
gas inlets from 3.81 cm centres to 22.85 cm centres.
With the spouts at 3.81 cm centres the bed became un-
stable as the spouts tended to merge and interfere while
at 22.85 cm centres solids mixing was poor. Satisfactory
solids circulation appeared to be obtainable at a 7.62 cm
separation. However, this is still rather close to the
unstable spout separation.

4.2.1.2   Three Dimensional Bed Study

Further qualitative experiments were carried out in a
column with two gas inlets. This column had a flat bottom
and dimensions of 30.85 cm x 15.24 cm x 152.4 cm. The
gas inlet orifices were placed at 15.24 cm centres and pro-
jected 0.32 cm above the bed floor, a practice which has
been found to improve bed stability (77). Bed behaviour
was observed with various bed materials at various bed
heights. The materials employed were wheat, rape seed ,
millet and polyethylene pellets. (See Table J   for their
physical properties). From these runs, it was found that
in most cases the bed tended to become unstable as the
bed weight was increased. Two combined effects seemed
to be responsible for leading the bed to instability,
namely, spout pulsation and regression. The former
appeared to be associated with spouting all the time and
increased in amplitude and frequency as the bed height

increased. The latter set in at a greater bed depth and seemed to have the same tendency as the former. When the spout started to pulsate and regress, an uneven bed level resulted as each spout possessed its own pulsation and regression frequency. Thus, a slight disturbance in the air flow to the bed usually would cause one of the spouts to collapse. In plate 4.2a and 4.2b, the occurance of spout regression is clearly shown.

The effect of spout pulsation and regression on bed stability was further investigated by operating the bed with a removable baffle inserted vertically between spouts. Under these conditions the bed acted as two single spouted beds. The phenomenon of pulsation and regression was again observed. This finding is in accordance with observations recorded by other workers (74,76, 78). It appears, therefore, that spout instability is inherent with the process. This has been normally overlooked in single spouted beds because of the lack of any apparent ill-effect on the process. In multiple spouted beds, however, the effect of spout pulsation and regression on bed stability is greatly magnified due to spout interaction. This was established by running the bed with and without the baffle. From this study, it was found that at the stage when spout pulsation and regression existed, removal of the baffle usually rendered one of the spouts inoperative.
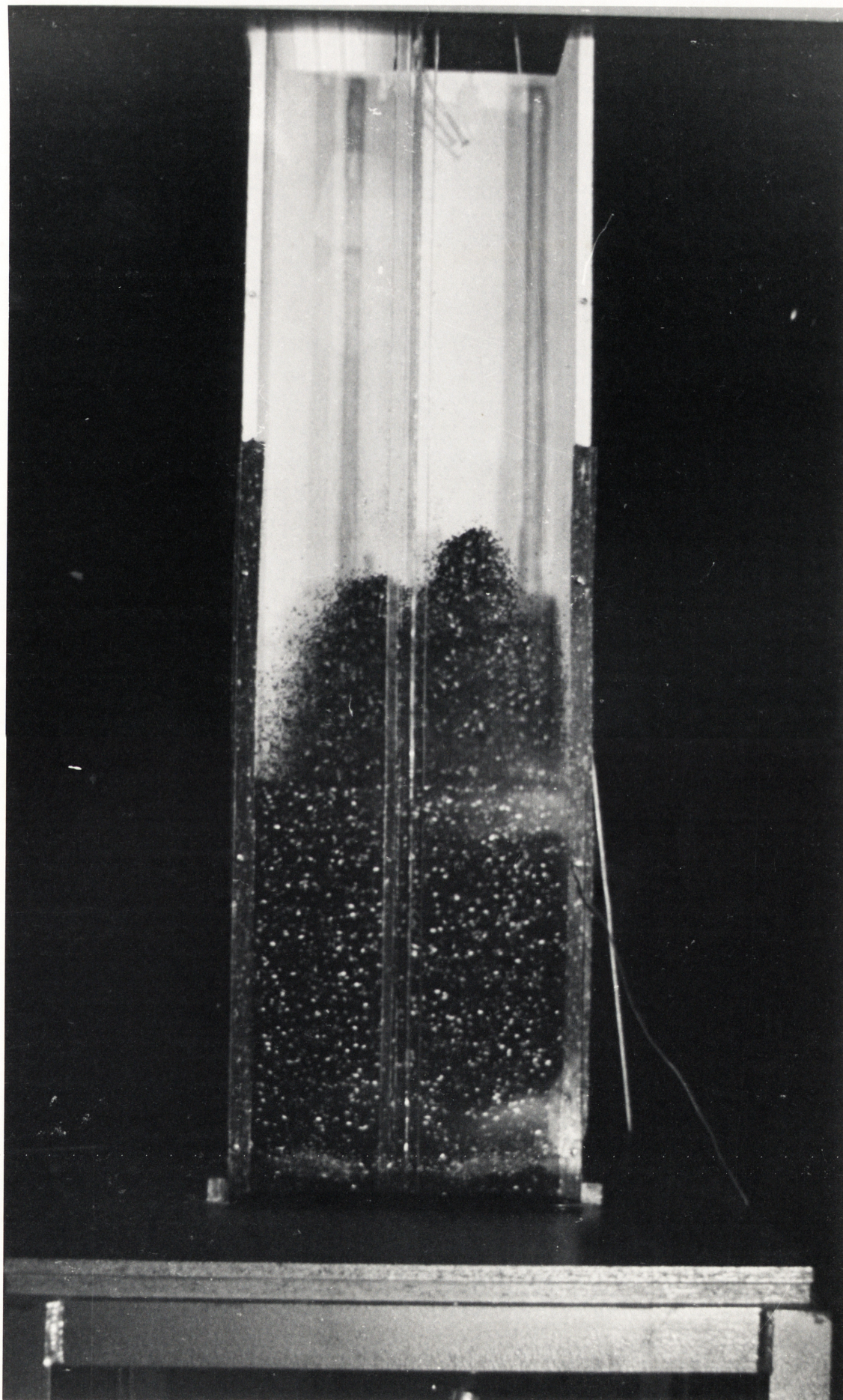
Fig. 4.2a Photograph shows spout Pulsation and Oscillation
(Material: 1:1 Rape Seed and Wheat Mixture, D_i=1.27cm, (D_c)
eq.=16.08cm)
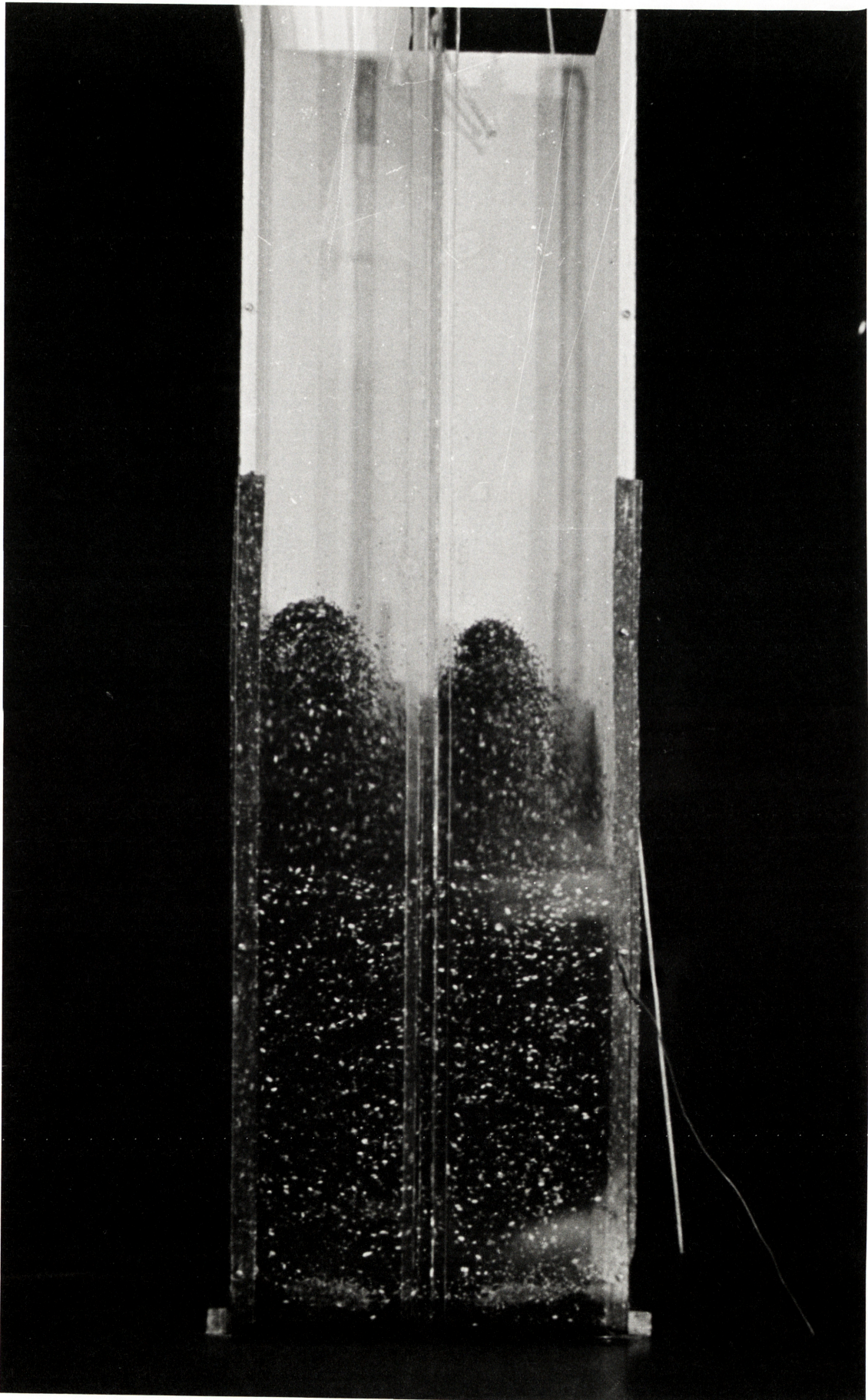
Fig. 4.2b Photograph shows Spout Pulsation and Oscillation (Material: 1:1 Rape Seed and Wheat Mixture, D_i=1.27cm, (D_c) eq.=16.08cm)

An attempt was made to stabilize the bed using baffles to partially isolate neighbouring spouts from one another. These baffles reached to the height of the bed but of course allowed interchange of bed material from one spout region to another over the top of the baffles. However, this was found ineffective in stabilizing the bed because there was still sufficient interaction between spouts due to spout regression and pulsation to cause one of the spouts to collapse. Gas inlet orifice sizes were next varied from 0.635 cm to 2.54 cm diameter. The following observations were made with respect to bed stability:

(a) Wheat

Wheat was the largest bed particle used in the experiment. It had an effective diameter of 0.32 cm. Stable beds were achieved with orifices larger than 2.54 cm diameter.

(b) Rape seed and polythene pellets I and II

For rape seed (1.89 cm), polythene I (0.211 cm) and polythene II (0.249 cm) stable beds were achieved with orifices larger than 1.905 cm.

(c) Millet

For millet (0.119 cm) stable beds were obtained with orifices larger than 1.27 cm diameter.

During these runs it was seen that when suitable orifice sizes were used spout pulsation and regression appeared to

be at a minimum. Also, the spout shape was better de-
fined and spouting could be maintained at flow rates
close to the minimum spouting velocity. Respouting of
the bed after collapse was also found to be easier.
Therefore it appears that bed stability is dependent on
particle size as well as on inlet orifice size. Table
4.1 summarized the results of these runs. From this
Table the optimal effective particle diameter to orifice
diameter ratio, (D_p/D_i), are thus:

Table 4.1 a   Optimum D_p/D_i Ratio

Material	Optimum Ratio, D_p/D_i
Wheat	0.126
Rape seed	0.092
Millet	0.094
Polythene I	0.111
Polythene II	0.131

The range of optimal D_p/D_i ratios (0.092-0.131) is
quite narrow. It is probable that these ratios are not
the true optima   because orifice diameter could only be
varied by discrete values. These results show, however,
that for maximum bed stability this ratio would probably
have to lie within the above stated range. It was neces-
sary to check results obtained in a three dimensional
bed, simulating the real situation.

4.2.2 Design of a Experimental Multiple Spouted Bed System

4.2.2.1 Introduction

The purpose of this work was

TABLE 4.1

EFFECT OF GAS INLET DIAMETER ON BED STABILITY

Material	Orifice Diameter, cm.	Maximum Spoutable Bed ht., cm.	D_p/D_i	Remarks
Wheat	1.270	-	0.252	unstable
	1.905	-	0.168	unstable
	2.540	72.39	0.126	stable
	2.857	60.45	0.112	stable
Rape Seed	1.270	-	0.146	unstable
	1.905	58.42	0.092	stable
	2.540	50.04	0.074	stable
Millet	0.953	-	0.125	unstable
	1.270	142.24	0.094	stable
	1.905	111.76	0.063	stable
	2.540	85.60	0.047	stable
Polythene I	1.270	-	0.176	unstable
	1.905	63.50	0.111	stable
	2.540	55.88	0.832	stable
Polythene II	1.27	-	0.196	unstable
	1.905	64.26	0.131	stable
	2.540	59.94	0.098	stable

(1)   to substantiate the findings

(observed in the two dimensional

model study) using a three di-

mensional bed and

(2)   to study the hydrodynamic

characteristics of a real multiple

spouted bed.

(1)   In the model study it was found that a stable

multiple spouted bed could possibly be achieved

if a suitable D_p/D_i ratio was used. Since inter-

action between spouts contributed greatly to spout

stability there was a need to study behaviour in

a three dimensional bed.

(2)   The hydrodynamic characteristics which are impor-

tant in process design are spouting pressure drop,

minimum spouting velocity, maximum spoutable bed

height, solids and gas mixing patterns and spout

diameter. All these variables (except spout di-

ameter) were studied.

The experimental multiple spouted bed system consisted

essentially of the following parts:

(1)   The experimental multiple spouted bed.

(2)   The spouting air supply system.

(3)   The solids feed system.

(4)   The air flow control and measuring system.

(5)   Pressure measurement.

A complete flow diagram of the experimental system is shown in Fig. 4.3a and Fig. 4.3b.

4.2.2.2   Multiple Spouted Bed Design

The three dimensional bed was constructed such that one spout was completely surrounded by others. This was achieved by arranging seven (7) spouts on a 15.24 cm triangular pitch. The central spout was then free from wall effect and would be typical of the majority of spouts in an industrial size multiple spouted bed. All measurements could then be taken on this spout.

The bed consisted of a 45.72 cm x 41.66 cm x 15.24 cm open topped flat bottom timber box. Like the two-spout bed the spout orifices projected 0.32 cm above the flat bottom. A weir of adjustable height was fitted to one side of the bed to control bed height at any predetermined level. The detailed design of this bed is shown in Fig. 4.4.

4.2.2.3   The Spouting Air Supply

The spouting air was supplied by a positive displacement blower capable of delivering 4.528 m^3/min (N.T.P.) of air at 68.9kPa. An automatic pressure relief valve was employed to regulate pressure in the 0.849 m^3 capacity air receiver. The receiver also acted as a capacitance thus reducing air flow fluctuations.

TO EXHAUST

DISENGAGING
CHAMBER

FEED
DISTRIBUTOR

TO EXHAUST

PRESSURE
RELIEF VALVE

ENTRAINMENT
CHAMBER

FLOW
CONTROL
VALVE

PRODUCT
DISCHAR-
-GE

AIR SUPPLY MANIFOLD

FEED TRANSPORTING AIR

SCALES & FEED HOPPER   BED   ROTAMETERS   AIR RECEIVER   BLOWER
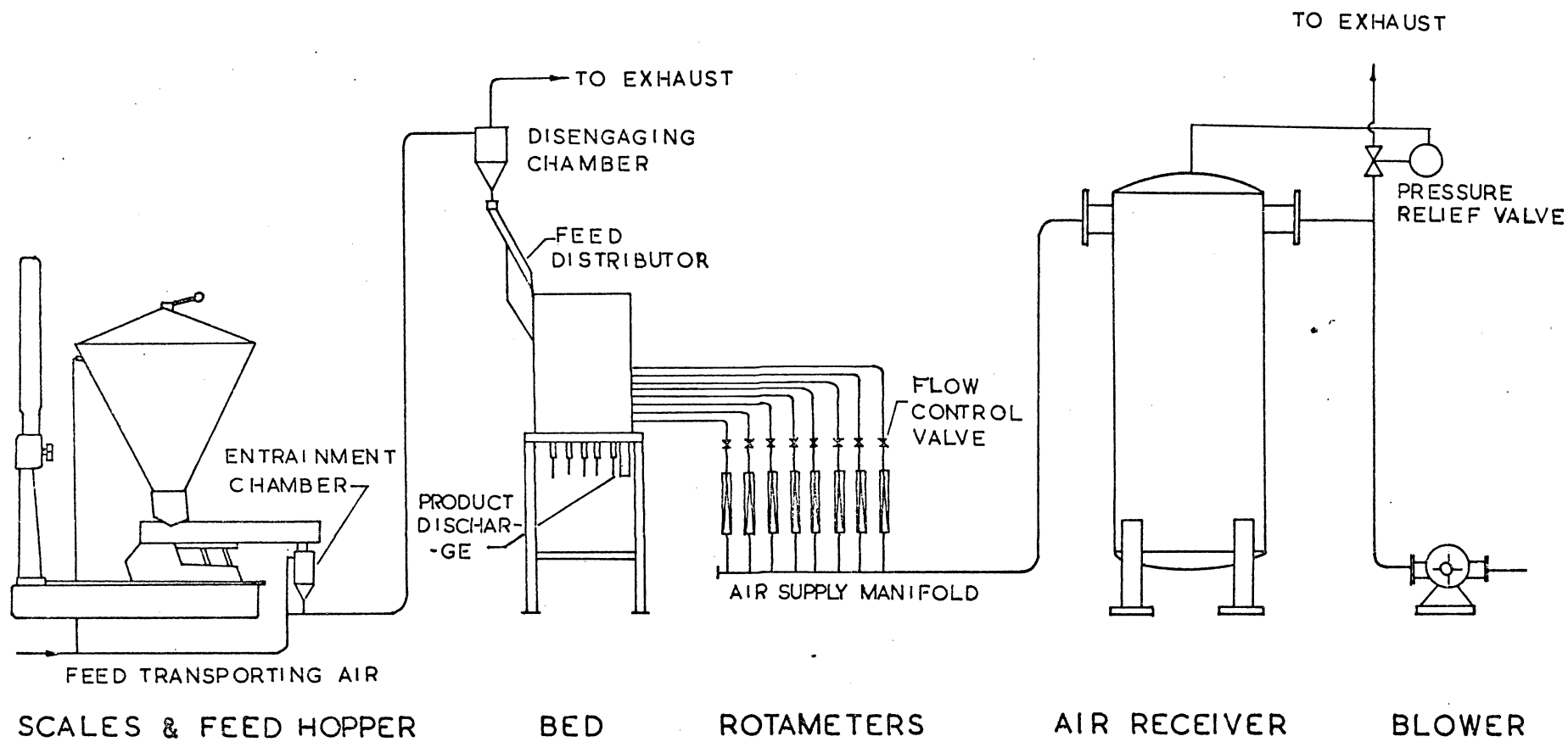
Fig.4.3ª   Flow Diagram of the Experimental Multiple Spouted Bed System

— 146 —
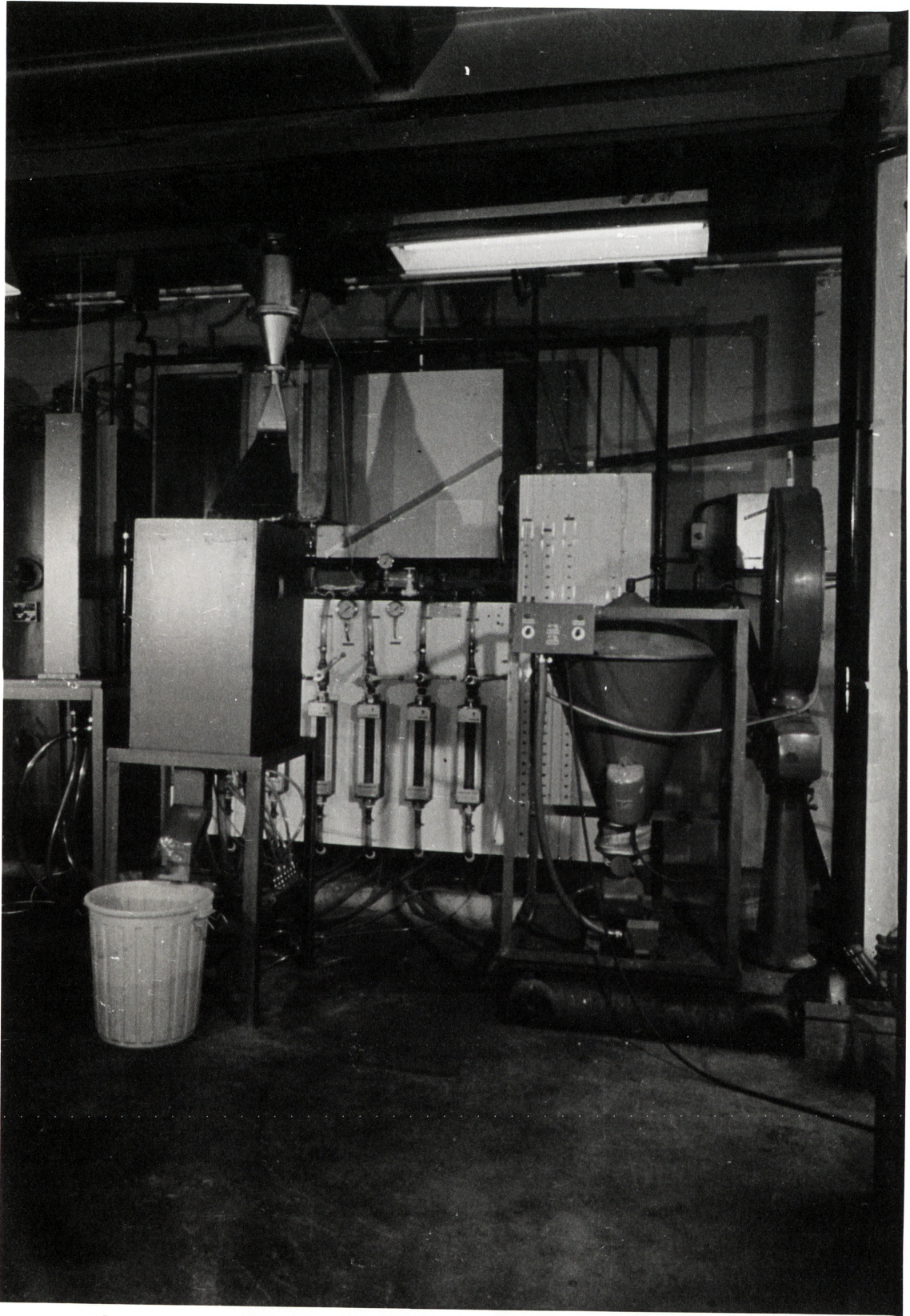
Fig. 4.3b Photograph of the Experimental Arrangement of
the Multiple Spouted Bed System

Fig. 4.4 Detailed Design of the Multiple Spouted Bed
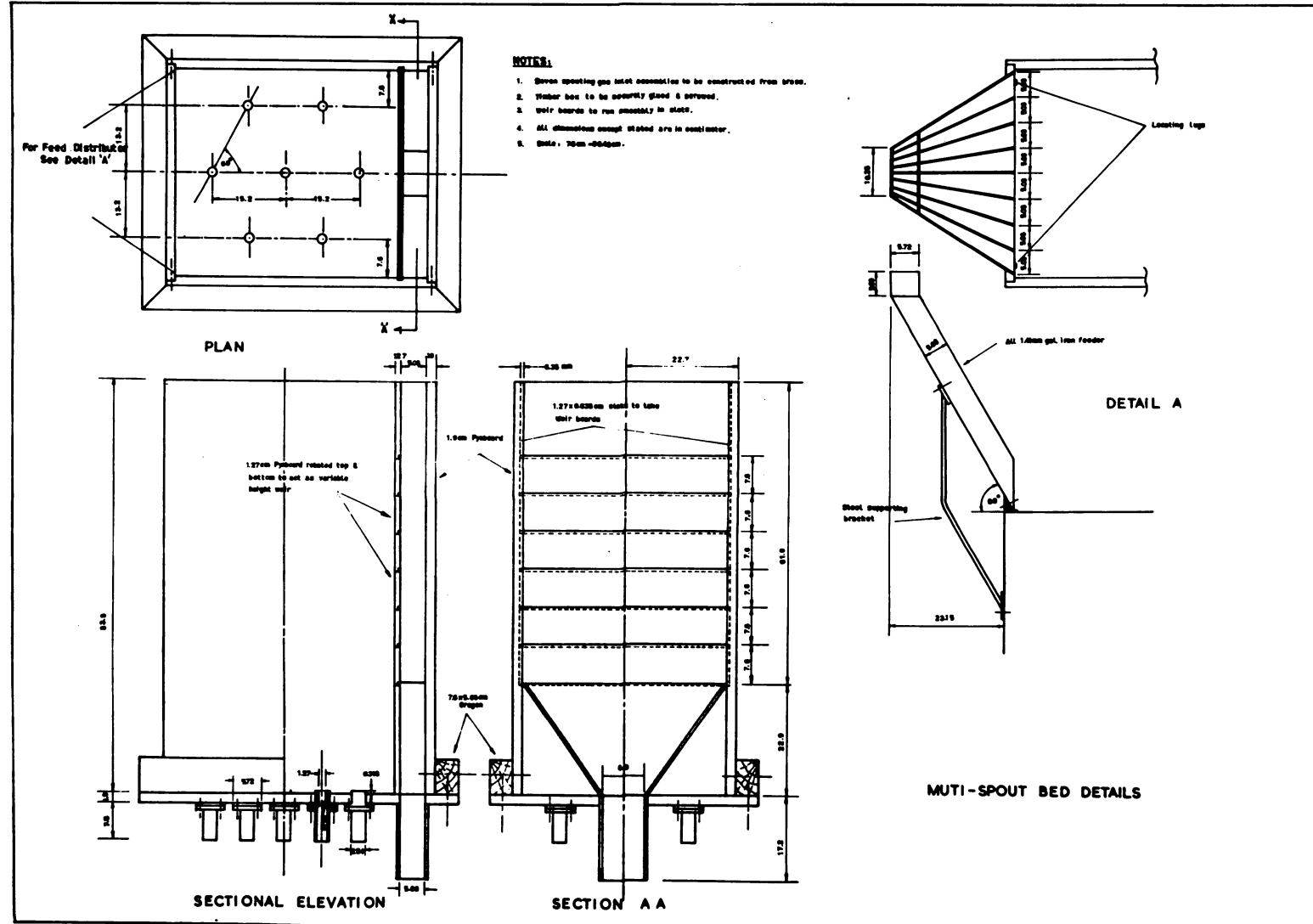
4.2.2.4   The Solids Feed System

A solids feed system was incorporated in the equipment. This consisted of a 0.085 cubic meter vibra-feed hopper, mounted on platform scales, an engaging chamber and a disengaging cyclone. This system was needed for continuous running. In this operation, solids were fed from the hopper and pneumatically transported to one side of the top of the bed.

The feeding rate of the feeder was controlled by a manually-set switch which fixed the vibrating frequency of the feeder. This was calibrated using materials listed in Table J.

4.2.2.5   The Air Flow Control and Measuring System

The flow rate of air to the multiple spouted bed was measured by a set of seven rotameters. These rotameters were supplied with calibration charts. Sample checking of these charts with standardised orifice plates showed that their accuracy was adequate. Hence these rotameters were used without further calibration.

Air flow control valves were fitted to every rotameter. These valves allowed individual control of air flow to each gas inlet. A sufficiently long calming section of pipe was used between the control valve and the orifice to damp out any turbulence in the air flow.

4.2.2.6 Pressure Measurement

Static pressure measuring probes made of 1mm I.D. glass capillaries were located inside each spout region. Water manometers were used for pressure determination. It was found that the pressure probe necessarily be located about 2 cm above the gas inlet orifice to avoid incorrect pressure reading due to venturi effects.

4.2.3 Operation Procedure

The following procedures were used to carry out an experimental run:

(1) Clear the multiple spouted bed.

(2) Load the feed hopper with the required particles.

(3) Switch on the air blower.

(4) Crack control valves to allow a small flow of air to every orifice. This prevented blockages that could happen in the orifices during charging

(5) Switch on the vibra-feeder and set the vibration frequency to give a suitable particle feeding rate. Continue particle feeding until the desired bed height is reached. Determined the weight of bed charge.

(6) Increase air flow at small increments to every orifice. Adjust control valves to achieve approximate equal flow rate to every orifice. Continue doing this until spouting is obtained.

(7) Adjust control valves to give equal spouting height for every spout.

(8)   Determine spouting velocity and spouting
        pressure drop.

(9)   Turn off air blower and measure static bed
        height.

(10)   Switch on air blower and repeat (5) to (9)
        for next bed height.

(11)   Repeat (1) to (10) for next particles.

4.3 RESULTS AND DISCUSSION

4.3.1 Effect of D_p/D_i Ratio on Bed Stability - Qualitative Results

Earlier it was established that in a two-spout bed the
D_p/D_i ratios appeared to have important controlling
effects on bed stability. Experiments were then carried
out in the three dimensional multi-spout bed with the aim
of substantiating the finding. Bed stability was observed
using different D_p/D_i ratios. Bed materials used in the
experiments were the same as those employed in the two-
spout bed experiments. It was found that the bed be-
haved very much the same as the two-spout bed. Again
spout regression and pulsation was observed. The effect
on the stability of this bed appeared to be more severe
than that of the two-spout bed. This is because of the
higher degree of spout interaction between spouts in a
three dimensional bed. D_p/D_i ratios which gave stable
spouting for the two-spout bed were also found to give
stable spouting for this bed.

4.3.2   Quantitative Characterisation of the Bed

System variables usually used in hydrodynamic studies
are the flow rate of the spouting fluid, column diameter,
fluid inlet orifice diameter, particle size, particle
density and shape, fluid density and bed height. In the
present study, column diameter and fluid density were
constant since only one spouted bed was investigated and
air only was used as the spouting fluid. Furthermore,
the inlet orifice diameter was also held constant. The
need for larger inlet orifice diameter for particles with
larger effective diameter as indicated in Table 4.1 pre-
sented problems because of inadequate air supply. Because
of the limited air supply only a 1.27 cm diameter ori-
fice was used. This enabled larger particles to be
spouted at reasonable bed heights but gave less stable
beds when materials larger than millet were spouted.
However, information obtained from the earlier model
studies indicated that the effect of instability on
spouting pressure drop, minimum spouting velocity and
solids mixing pattern was insignificant.

4.3.2.1   Pressure Drop Across the Spouted Bed

The spouting pressure drop of the centre spout was de-
termined using the materials listed in Tables J.
Manurung's equation (ref. 77) for spouting pressure
drop was employed to correlate the spouting pressure
drop data. This correlation was developed by considering
ΔP_s to approach the fluidized pressure drop as the bed

depth increases to infinity.

$$\underset{\frac{H}{D_c} \to \infty}{\text{Lim}} \quad \frac{\Delta P_s}{H \rho_s} = 1$$

The above limit is transformed into the following linear equation

$$\frac{H \rho_b}{\Delta P_s} = 1 + a \left(\frac{D_c}{H}\right) \qquad \ldots\ldots 4.1a$$

By evaluating "a" from experimental data, Manurung obtained the following correlation which was found to fit the data with an average deviation of 12 percent.

$$\Delta P_s = \frac{H \rho_b}{1 + 0.81 \frac{(\tan\beta)^{1.5}}{\phi^2} \left(\frac{D_c D_p}{D_i}\right)^{0.78} \left(\frac{D_c}{H}\right)} \qquad \ldots 4.1b$$

This equation is general for a wide range of particles and column variables in single spout beds and so has been used to correlate the multiple spouted bed data. The only problem is to define D_c (column diameter) for a multiple spouted bed. This has been considered as follows. For a bed with more than one gas inlet, the cross section of each "spout region" generally is non-circular. The effective diameter of each region is thus defined as being equivalent to the diameter of a cylinder having the same cross sectional area as the spout region. For the present case, the spout region under consideration was taken as a 15.24 cm square. The effective diameter of this square is 17.22 cm.

Fig. 4.5 relates the experimental and calculated pressure drops. The agreement is seen to be good.

4.3.2.2 **Minimum Spouting Velocity**

Minimum spouting velocity is one of the most important
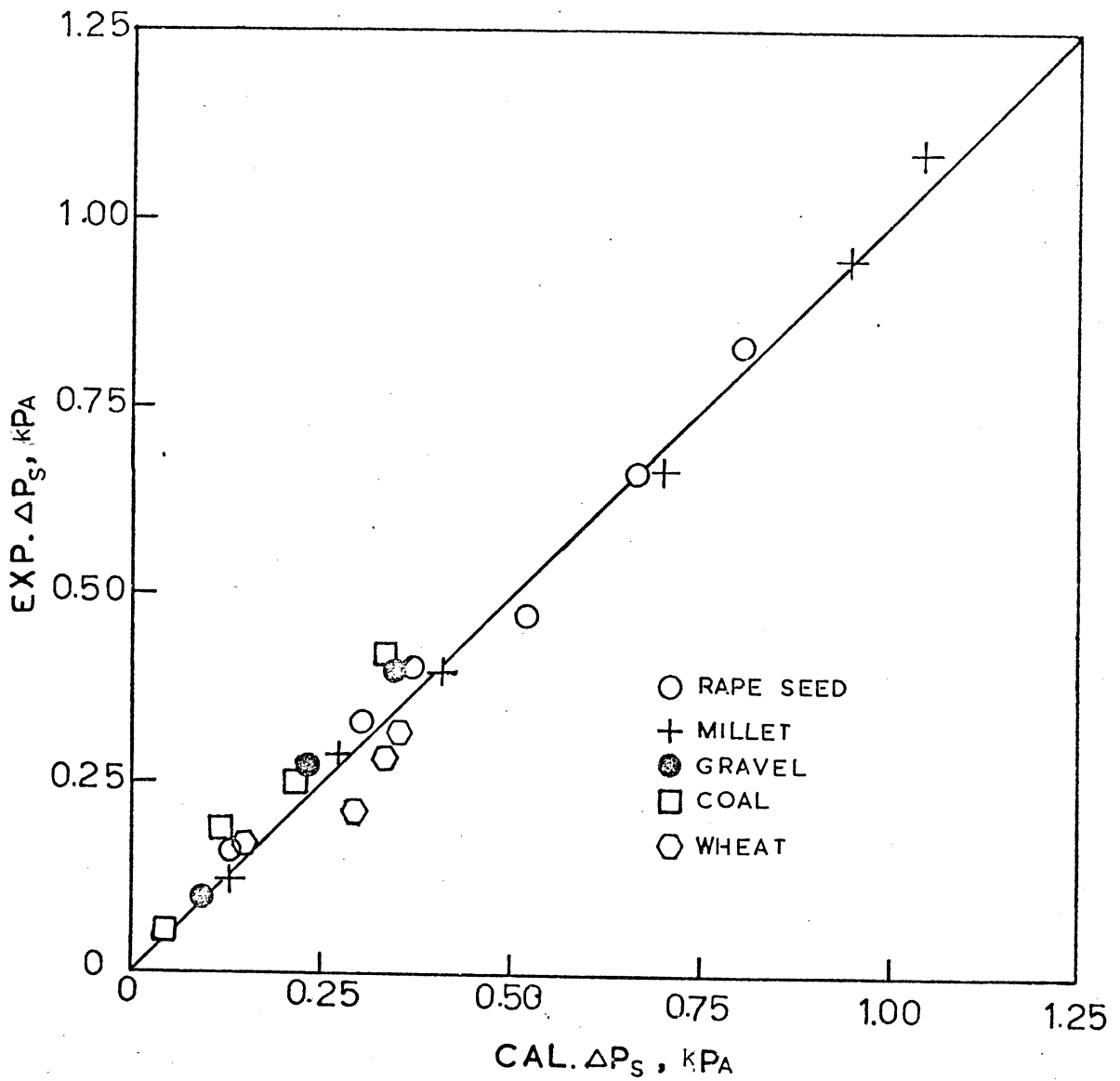
Fig.4.5 Comparison of Experimental and Calculated Spouting Pressure Drop

hydrodynamic variables of the spouting process. Although
it has been the subject of over a dozen investigations, a
satisfactory general correlation for predicting this
variable has not been developed. This is due to the fact
that minimum spouting velocity is dependent on the proper-
ties of solids and fluid as well as bed geometry. The
problem is therefore inherently more complex than in
either fluidization or pneumatic transport, with the
result that most investigators have had to resort to em-
piricism for correlating experimental results. Never-
theless, some of the correlations proposed are sufficiently
general to be of practical value.

Mathur and Epstein (60) compared the validity of correla-
tions proposed by Mathur and Gishler (38), Becker (59),
Manurung (77) and Reddy and Smith (80). The conclusion
was that the first correlation (i.e. Mathur and Gishler's)
although most simple in form gave the most reliable pre-
diction of the minimum spouting velocity for common
material, over a wide range of practical conditions.
This equation is given as follows:

$$v_{ms} = \left(\frac{D_p}{D_c}\right)\left(\frac{D_i}{D_c}\right)^{1/3} \sqrt{2.g.H \frac{(\rho_p - \rho_f)}{\rho_f}} \qquad \ldots\ldots 4.2$$

Comparison of the predicted results and the experimental
data obtained from the centre spout is shown in Fig. 4.6.
From this diagram it appears that most of the experimental
data have a tendency of deviating more from the predicted
as bed height is increased. This is due, to the higher
gas rate required to maintain a spouting bed when D_i does
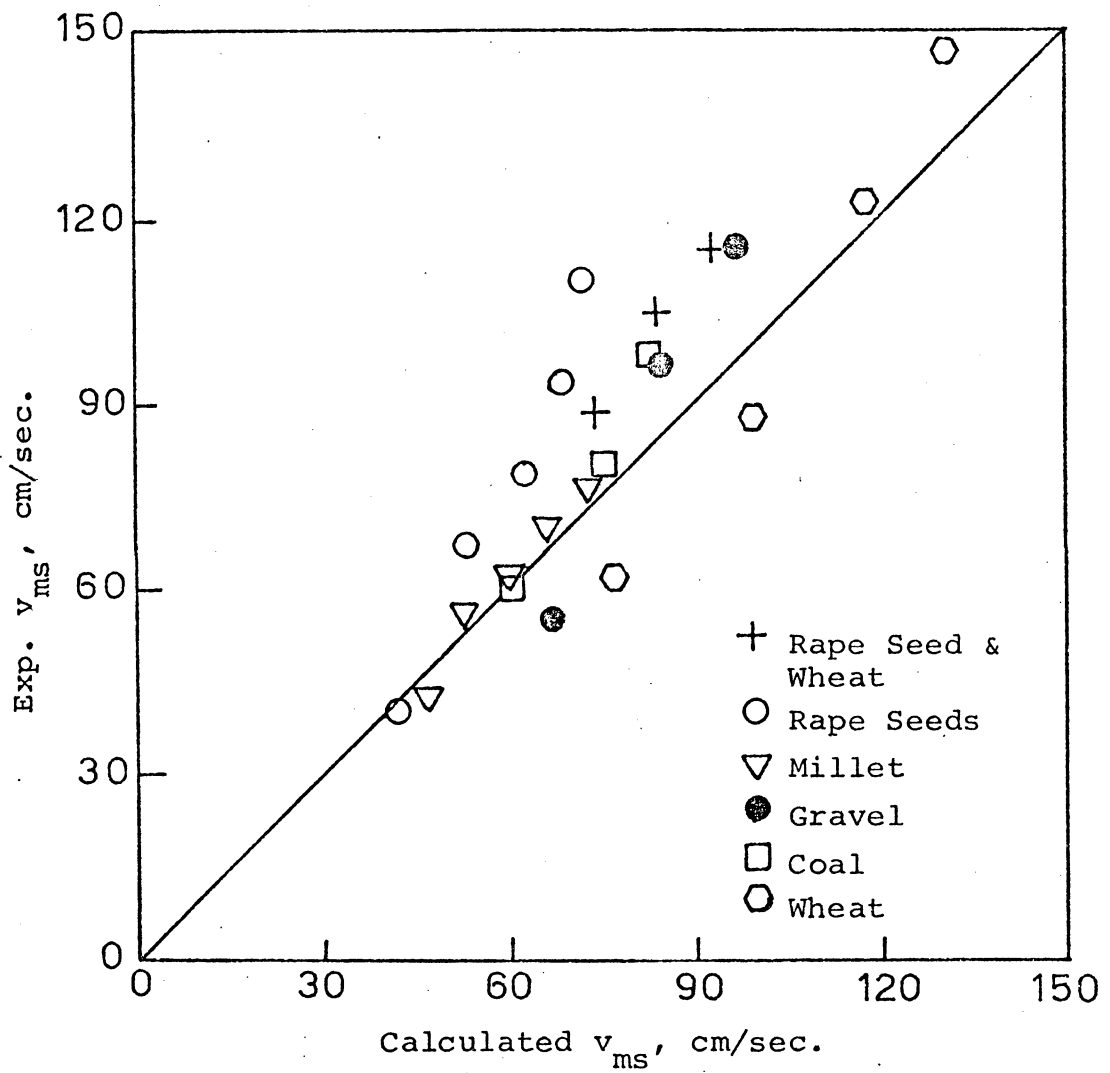
Fig. 4.6 Comparison of Experimental and Calculated Min.

Spouting Velocity

not fall in the optimum region. This is supported by the
fact that for millet with which a stable bed was achieved,
gas requirement could be quite accurately calculated from
the above correlation. Therefore it appears that a correl-
ation which was developed for a single spouted bed may be
used for a stable multispout bed.

4.3.2.3. Maximum Spoutable Bed Height

Maximum spoutable bed height is defined as the height of
a bed above which a spout can not be formed. The maximum
spoutable bed height could not be easily determined in
this system because of the large amount of air required.
However, useful information could be derived from the
results obtained from the two-spout bed.

In Table 4.1 maximum spoutable bed heights for wheat,
rape seed and millet are listed.

Malek and Lu (39) employed a wide range of materials and
different column diameters (i.e. 10.16 cm, 15.24 cm and
22.85 cm) for investigating the maximum spoutable bed
height. The following correlation was proposed:

$$\frac{H_m}{D_c} = K\left(\frac{D_c}{D_p}\right)^{0.75}\left(\frac{D_c}{D_i}\right)^{0.40}\left(\frac{\lambda^2}{\rho_p 1.2}\right) \quad \ldots\ldots 4.3$$

where

$K = 0.105$ for air

$\lambda = 0.205\ S_p/V_p^{2/3}$

By using this correlation, maximum spoutable bed heights
for wheat, rape seed and millet under the "optimal

conditions" are respectively 72.1 cm, 97.4 cm and 135.6

cm. Higher maximum spoutable bed heights for a single

spouted bed is not surprising as spout interaction plays

a very influential role in multiple spouted beds.

4.3.2.4 Solids Mixing Study

For prediction of a spouted bed's solids, fluid contacting

performance, it is essential that the flow pattern of the

gas phase and solids phase are known. In the present

work, this was achieved by the development of a solids flow

model for the multiple spouted bed.

4.3.2.4.1 Experimental Technique

A stimulus response technique was utilised for the study.

This consists of using a tracer which may be introduced

into the system in the form of a step change, a pulse,

a ramp or a sinusoidally varying input and monitoring the

decay or changes which occur at the exit of the vessel.

Several types of tracer have been used in studies of this

type. The choice of the most suitable tracer depends on

the application and the size of the equipment under study.

For solids, methods involving coloured or tagged particles

have been the most popular (81,82). In the present situa-

tion, step function involving a coloured tracer was

employed.

A series of residence time distribution runs was carried

out using wheat and millet as bed materials. 1.27cm gas

orifices were used in both cases and the bed heights were respectively 20.32 cm and 35.56 cm.

Coloured tracers of wheat and millet were prepared by dyeing those materials with water soluble dye. Three colours, red, blue and green were used. The bed material used in the previous run was used as non-tracer for the following run. This conserved bed materials considerably.

4.3.2.4.2 Experimental Procedure

The experimental procedures were essentially the same as those outlined in Section 4.2.3. Briefly, a run was commenced by initially filling the bed with coloured particles to the operating level whilst spouting. The spouting air was then adjusted to about 5% above the minimum spouting gas rate. At time zero, non-tracers were introduced at a predetermined rate and product samples taken at regular intervals for approximately two mean residence times. These samples were then weighed and tracer and non-tracer separated. The weight fraction of the tracer was then determined.

4.3.2.4.3 A Solids-Flow Model

As an aid for developing the solids-flow model some visual observations were conducted using the three-spout half-sectional perspex model. It was found that the feed particles entered the annular region of the bed on the side opposite the product outlet and moved downward to the spout where they were rapidly transported to the fountain region at the top of the bed. Some of the

particles then re-entered the annular section of the bed where the cycle was repeated, and some migrated to the neighbouring spouts as they fell. It was also noted that some degree of cross flow took place at the annular sections between spouts. However, as the circulation of particles in a spouted bed is high (29) the extent of particle mixing would seem to be determined by the random movement of particles travelling from spout to spout over the bed top. The concept of "mixed models" originally proposed by Cholette and Cloutier (84) and Levenspiel (42) has been used to characterize the multispout bed. This model considers the system as consisting of the following kinds of regions: plug flow region, backmix region, dispersed plug flow regions and deadwater regions. In addition to the above regions, "mixed models" may use the following kinds of flow: by-pass flow, recycle flow and cross flow.

From the experimental data an internal age distribution function, I, diagram was constructed and the data correlated statistically by a linear regression method (Fig. 4.7). The method has been written as a subroutine which is given in Appendix H. The following expression was obtained with a standard error of estimate of 0.08.

$$LnI = Ln\ (1-{}^{C}\!/C_o) \qquad \ldots\ldots 4.4$$
$$= 0.02 - 1.17\ \theta$$

After matching the above expression with various mixed models, the model which consists of a relatively large volume of backmix region, a portion of deadwater region,
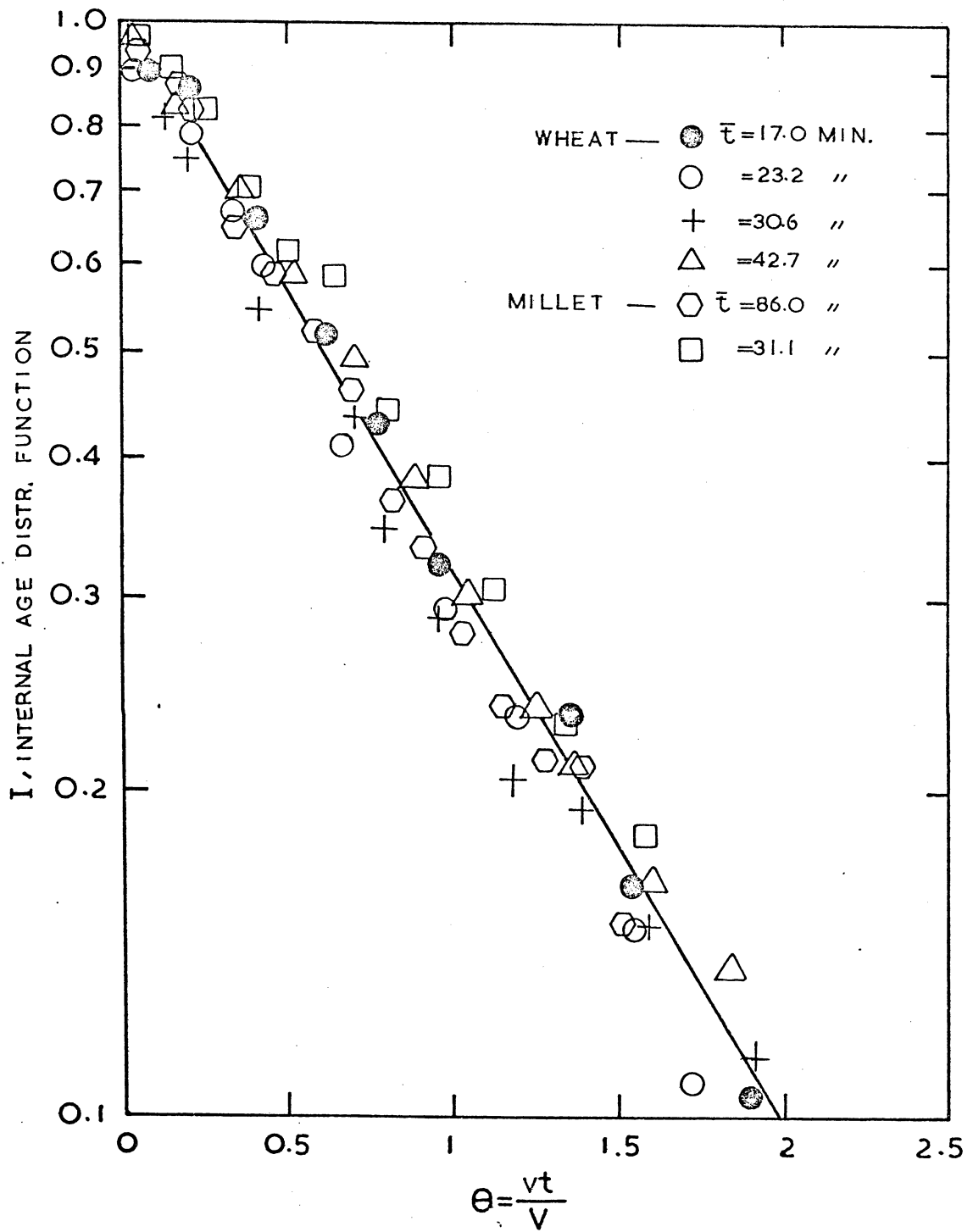
Fig.4.7 Internal Age Distribution Function Diagram

some plug flow region and negligible bypassing appear to give the line of best fit. The model is shown schematically in Fig. 4.8.

Mathematically the model can be shown to be described by the following expression (31):

$$I = \text{Exp} \ [-V/V_b (\theta - V_p/V)] \quad \ldots\ldots\ldots\ldots \quad 4.5$$

From eq. 4.4

$$-V/V_b (\theta - V_p/V) = 0.02 - 1.170$$

and so eq. 4.5 becomes

$$I = \text{Exp} \ [-1/0.855 \ (\theta - 0.017)] \quad \ldots\ldots\ldots \quad 4.6$$

From the above relationship, the total volume of the bed, consists of 85.5 percent completely mixed 1.7 percent in plug flow region and 12.8 percent deadwater region. Cross flow at the annular sections between spouts was also estimated using the method given by Zenz and Othmer (85) (see Appendix H). As expected the rate of cross flow was quite low, being of the order of 4.546 kg/hr. and is too low to account for the rapid mixing of the entire bed material observed in the experiment. It is estimated that if solids cross-flow is the only mode of solids transport, then it would take about one hour to exchange 95% of the bed material between adjacent spout regions. Hence, it is proposed that the bed material in a continuous flow multiple spouted bed is transported as follows:

(a) Overflow of solids at bed surface from one spout region to another.

(b) Internal circulation of each individual spout region due to spouting.
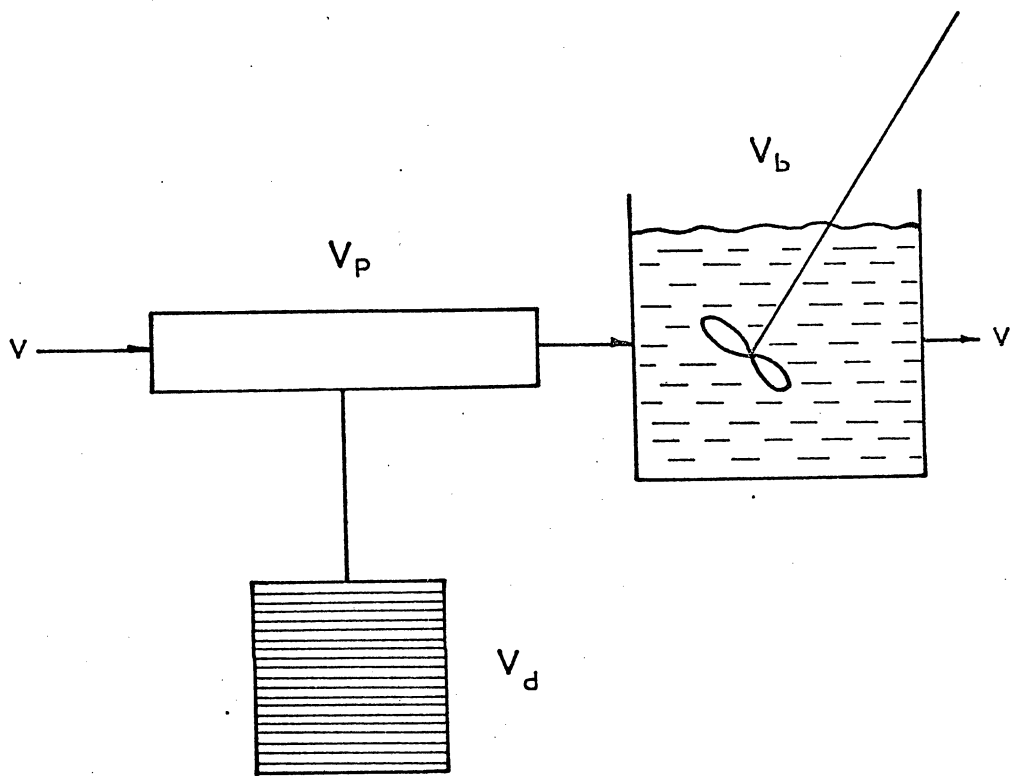
FIG.4.8 SOLIDS-FLOW MODEL

Internal circulation of a spout region is an important contributing factor in forming a well mixed multiple spouted bed. Chaterjee (83) ultilised the same method in studying the internal circulation rate of a single spouted bed. An empirical correlation was thus proposed. Application of the correlation to the present situation gave an internal circulation rate of about 1000 kg/hr.

The general good fit of all the data with expression (5) may be interpreted as an indication of the general application of the model. Kugo et al (81) studied the effects of orifice size, spouting gas velocity, bed height and mean residence time on solids mixing in a 15.24 cm single spouted bed, and concluded that under all conditions investigated the bed was essentially a perfectly mixed system. Although it could be true that for higher bed depths the plug flow element may become larger, as was shown by Barton et al (73), the validity of this model should not be significantly affected.

4.4 CONCLUSION

The experiment-al/work reported in this chapter has shown that the multiple spouted bed is inherently unstable due to the tendency of the spouts towards pulsation and regression. Bed stability was found to be dependent on D_p/D_i ratio as well as bed height. For satisfactory design and operation of a multispout bed the ratio of D_p to D_i would probably have to be in the range of 0.09 - 0.13.

It has also been shown that generally correlations developed
for single spouted beds could be used for the character-
istics of multi-spout beds operated within the stable
regime.

A flow model of solids for this system was developed using
the concept of "mixed models". Comparison of the model
with those of a single spouted bed led to the belief that
this model could be applicable to situations beyond the
present experimental range.

APPENDIX A

Computer Programmes for Calculating Thermodynamic
Properties and Typical Printouts

A.1   Calculations of Standard Free Energy

Changes for Chemical Equilibria in the

C-O-S and C-O-S-H Systems

A.2   Calculations of Standard Free Energy

Changes for the Sulphur Vapour Equilibria

A.3   Typical Printouts

A.1 CALCULATION OF STANDARD FREE ENERGY CHANGES FOR
     CHEMICAL EQUILIBRIA IN THE C-O-S AND C-O-S-H SYSTEMS

```
C       CALCULATION FOR THERMODYNAMIC PROPERTIES FOR C-O-S-H SYSTEM
        DIMENSION COMENT (20), SHNF (20,2) COEFF (20)
        READ, NOFRXN
        KOUNTR=0
 1012 READ 1000, COMENT
 1000 FORMAT (20A4)
        PRINT 1001, COMENT

 1001 FORMAT (1H1,20A4,//)
        T=100.0
        READ,M,NR
        PRINT 1004
 1004 FORMAT (//H, 12H TEMPERATURE, 9X, 16H ENTHALPY CHANGE,
        15X, 19H FREE ENERGY CHANGE,2X,16H LOG EQUILIBRIUM,5X,
        212H EQUILIBRIUM,/,1H ,16H DEGREES KELVINS,5X,9HK
        3CALORIES,12X,9HKCALORIES,12X,9H CONSTANT,12X,9H
        4CONSTANT)
        READ, (COEFF(1), I=1,2), I=1,M)
 1010 READ, ((SHNF(I,J), J=1,2), I=1,M)
        SHRXNR=0.0
        SHRXNP=0.0
        SFEGFR=0.0
        SFEGFP=0.0
        DO 1002 I=1,NR
        SHRXNR=SHRXNR+COEFF (I)*SHNF(I,1)
        SFEGFR=SFEGFR+COEFF(I)*SHNF(I,2)
 1002 CONTINUE
        NP=NR+1
        DO 1003 I=NP,M
        SFEGFP=SFEGFP+COEFF(I)*SHNF(I,2)
        SHRXNP=SHRXNP+COEFF(I)*SHNF(I,1)
 1003 CONTINUE
        HRXNT=SHRXNP-SHRXNR
        FENGT=SFEGFP-SFEGFR
        FENGTC=1000.0*FENGT
        ELNKT=-FENGTC/(1.987*T)
        EQK=EXP (ELNKT)
        PRINT 1005,THRXNT,FENGT,ELNKT,EQK
 1005 FORMAT (/1H,4(F15.5,5X0,E15.5)
        IF(T-1800.0) 1008,1009,1009
 1008 T=T+100.0
        GO TO 1010
 1009 KOUNTR=KOUNTR+1
        IF(NOFRXN-KOUNTR) 1007,1007,1012
 1007 STOP
        END
```

A.2   CALCULATION OF STANDARD FREE ENERGY CHANGES FOR THE

SULPHUR VAPOUR EQUILIBRIA

```
C      STNDARD FREE ENERGY CHANGES FOR THE SULFUR VAPOUR
C      EQUILIBRIUM
       DIMENSION COMENT(20),ABC(3),FENRGT(9),ELNKT(9),EQK(9)
       READ, NOFRXN
       PRINT,NOFRXN
       KOUNTR=0
 1007 READ 1000, COMENT
 1000 FORMAT (20A4)
       PRINT 1001, COMENT
 1001 FORMAT (1H1,20A4)
       PRINT 1006
 1006 FORMAT (1HO,8X,18HTEMPERATURE,KELVIN,5x,18HFREE
      1CHANGE,2X,12HLOG EQUIL. K,8X,12HEQUIL.
      2CONST,/)
 1004 READ, (ABC(I),I=1,3)
       T=400.00
       DO 1002 I=1,7
       FENRGT(I)=ABC(1)+ABC*T*LOG(T)+ABC(3)*T
       ELNKT(I)=-FENRGT(I)/(1.987*T)
       EQK (I)=EXP(ELNKT(I))
       PRINT 1003,T,FENRGT(I),ELNKT(I),EQK(I)
 1003 FORMAT (1H , 12x,F7.1,2(10X,F15,4),10X,E12.5)
       T=T+100.
 1002 CONTINUE
       PRINT, (ABC(I),I=1,3)
       KOUNTR=KOUNTR+1
       IF(NOFRXN-KOUNTR) 1005,1005,1007
 1005 STOP
       END
```

A. 3 TYPICAL PRINTOUTS

REACTION IS $C + SO_2 = CO_2 + 0.5 S_2$

TEMPERATURE DEGREES KELVIN	ENTHALPY CHANGE KCALORIES	FREE ENERGY CHANGE KCALORIES	LOG EQUILIBRIUM CONSTANT	EQUILIBRIUM CONSTANT
100.00000	-7.98950	-9.58200	48.22345	877.36256E+18
200.00000	-7.81900	-11.24600	28.29894	195.01804E+10
300.00000	-7.68600	-12.98800	21.78829	290.09090E+07
400.00000	-7.58950	-14.77150	18.58517	117.88003E+06
500.00000	-7.54250	-16.57300	16.68142	175.65178E+05
600.00000	-7.54100	-18.38050	15.41729	496.18787E+04
700.00000	-7.57350	-20.18550	14.51254	200.77896E+04
800.00000	-7.62500	-21.98200	13.82863	101.32119E+04
900.00000	-7.69300	-23.77400	13.29419	593.73596E+03
1000.00000	-7.76800	-25.55700	12.86210	385.42542E+03
1100.00000	-7.84700	-27.33200	12.50491	269.66021E+03
1200.00000	-7.92900	-29.09900	12.20390	199.56753E+03
1300.00000	-8.01700	-30.86100	11.94727	154.39538E+03
1400.00000	-8.10200	-32.61400	11.72406	123.50822E+03
1500.00000	-8.18900	-34.35900	11.52793	101.51186E+03
1600.00000	-8.27600	-36.10400	11.35631	855.03791E+02
1700.00000	-8.36200	-38.34100	11.35054	850.11600E+02
1800.00000	-8.44800	-39.57200	11.06413	638.40240E+02

A.3 TYPICAL PRINTOUTS CONT.

REACTION IS 3/2 S_2 = S_3

TEMPERATURE,KELVIN	FREE ENERGY CHANGE	LOG EQUIL. K	EQUIL. CONST
400.0	-5748.0920	7.2321	1.38315E+03
500.0	-3819.1520	3.8441	4.67184E+01
600.0	-1900.2780	1.5939	4.92303E-00
700.0	10.2220	-.0073	9.92677E-01
800.0	1913.5560	-1.2037	3.00052E-01
900.0	3810.6230	-2.1308	1.18734E-01
1000.0	5702.1230	-2.8697	5.67151E-02

-1.3687E+04 -5.0000E-01   2.2843E+01

APPENDIX B

GENERAL HILL-CLIMB PROGRAMME

Author : Dr. C. Dixon

School of Chemical Engineering

University of New South Wales

B.1   MAIN PROGRAMME

B.1.1   Programming Method

This programme uses Rosenbrock's method (106) without
constraints to maximise or minimise a function of up to
10 variables:

$$f(x_1, x_2, \ldots\ldots\ldots x_n)$$

In Rosenbrock's method, a set of orthogonal unit vectors
is set up, together with a set of step-sizes (initially
equal). Starting from a given point, a succession of
trial points is obtained by moving along each vector in
turn, by an amount equal to its step size. In each case,
if the value of f at the trial point is greater than or
equal to that at the current point, then the trial point
becomes the current point and the step-size is tripled.
If f is less at the trial point, then the current point
is not moved and the step-size is multiplied by-0.5.
This procedure is continued cyclically through the vectors
until a successful trial followed by an unsuccessful trial
has been obtained in each direction.

The vectors are then rotated so that the first is parallel
with the vector measuring the overall change in the inde-
pendent variables, x, since the last rotation; the second
is parallel to the next best direction which is perpendicu-
lar to this; and so on. This completes one "round". The
procedure then repeats with the new vectors, starting with
each step-size equal to the root-mean-square of the step-
sizes before the rotation.

B.1.2   THE COMPUTER PROGRAMME

```
C       GENERAL HILL-CLIMBING PROGRAM
C       INCLUDES ARRAY FOR CURVE-FITTING DATA, IF REQUIRED
C
C
C       *********************************************
C
C       DATA CARDS
C
C       THE FOLLOWING SET OF CARDS FOR EACH HILL-CLIMBING
C       PROBLEM
C
C....   HEADING CARD
C       NV, NFLOAT, NFIXED, NPTS, NIND
C       X(I), I=1, NV
C       V(I,J), I = 1,NV, J= 1,NV, NEW CARD FOR EACH VECTOR
C       STSIZE
C       NROT, NCRIT
C       RCRIT, CCRIT
C....   FLOAT CONSTANTS, IF ANY
C       FIXED CONSTANTS, IF ANY
C       (DATA(I,J), I=1,NIND), DATA (5,J), J=1,NPTS, NEW -
C       CARD PER POINT   IF APPLICABLE
C       *********************************************
C
C       IFLAG IS SET EQUAL TO -
C            1      BEFORE PRELIMINARY CLIMBF CALL AFTER
C                   READING DATA
C            5      BEFORE START OF EACH ROUND
C            2      BEFORE EXTRA CLIMB CALL AT END OF A
C                   ROUND WHEN STOP CONDITIONS IN THE DATA
C                   ARE SATISFIED
C            3      BEFORE EXTRA CLIMBF CALL AT END OF A
C                   ROUND WHEN STOP CONDITIONS ARE NOT SATIS_
C                   FIED, BUT IFLAG WAS CHANGED TO 4    DURING
C                   THE ROUND
C
C       FOLLOWING A CLIMBF CALL WITH IFLAG = 2 OR 3, HILL
C       CLIMBING WILL CONTINUE IF, AND ONLY IF, IFLAG IS
C       RETURNED = 4
C       *********************************************
C
C       SUBPROGRAMS REQUIRED -
C                             GCLIMB
C                             CLIMBF
C                             DCD210   (DATA INPUT AND CHECKING)
C                             DCD220   (PRINTER AND PUNCH
C                                      OUTPUT)
C
C       *********************************************
C
        DIMENSION X(10), v(10,10), PARAM(50), READ(40),
       1INDEX(15),   DATA(7,20)                              1620
C   **
C       FORMATS
C   **
C
C       NUMERICAL
```

B.1.2. CONT.


```
C
    2 FORMAT ( 1H, 5E15.8 )                              STAND
    8 FORMAT ( 1H, 15X, 5E15.8)
C  **
C     DATA INPUT
C  **
      CALL       DCD210 (NV, NFLOAT, NFIXED, NPTS, NIND,
     1,KEAD x,v, STSIZE, NROT, NCRIT, RCRIT, CCRIT )
C
C     COMPUTE OBJECTIVE FUNCTION  AT STARTING POINT,
C     AND POSSIBLY MODIFY DATA
C
      I = 1
      F = CLIMBF ( NV,X, IFLAG )
C  **
C     PRINT DATA
C  **
      ILINK = 1
      CALL       DCD220 (NV, NFLOAT, NFIXED, NPTS, NIND, KEAD
     1, x, v, STSIZE, NROT, NCRIT, RCRIT, CCRIT, ILINK )
      Al = 0.
      GAMMA = o.
      DIFF = o.
      K = O
      NPEAK = 0
      GO TO201
C  **
C     COMPUTATION (200)
C  **
  209 FOLD = F
      K = K + 1
      IFLAG = 5
      CALL GCLIMBF (NV,X,F,V, STSIZE, Al,GAMMA,IFLAG )
      DIFF = F - FOLD
  201 PRINT 2, GAMMA, Al, F, DIFF
      PRINT 8, (x(I), I=1,NV)
C     TEST FOR STOP CONDITIONS
      IF( Al - CCRIT ) 203,204,202
  202 NPEAK = 0
      GO TO 210
  203 IF( GAMMA -RCRIT ) 202, 204, 204
  204 NPEAK = NPEAK + 1
  206 IF( NPEAK - NCRIT ) 210,207,207
  207 IFLAG = 2
C     EXTRA CLIMBF CALL
  211 FOLD=CLIMBF( NV,X, IFLAG )
C     TEST FOR COMPLETION OF SPECIFIED NUMBER OF ROUNDS
  210 CONTINUE
      IF( K - NROT ) 205,207,207
  205 IF( IFLAG -4 )209,208,209
  208 IFLAG = 3
      GO TO 211
  300 CONTINUE
      ILINK = 2
```

B.1.2 CONT.

```
      CALL        DCD220 (NV, NFLOAT, NFIXED, NPTS, NIND, READ
     1, x,v, STSIZE, NROT, NCRIT, RCRIT, CCRIT, ILINK )
      GO TO 100
      END
      SUBROUTINE DCD210 (NV, NFLOAT, NFIXED, NPTS, NIND, KEAD
     1, x, v, ENORM, NROT, NCRIT, RCRIT, CCRIT )
C
C     READS AND CHECKS HILL-CLIMBING DATA
C
C     LIMITS
C     NFIXED 15
C     NPTS    20 (1620)    -     200 (300)
C     NIND    4
C
      DIMENSION x(1), v(10,1), READ (40),PARAM(50),  INDEX
     1,X(15),DATA(7,20)                                1620
      COMMON PARAM, INDEX, DATA
    1 FORMAT ( 5E15.8 )                               STAND
    3 FORMAT ( 15I5 )                                 STAND
    5 FORMAT (       40A2)                             STAND
      READ 5, READ
C
C     READ NV, x(I), v(I,J), STEPSIZE, STOP CRITERIA
C     PARAMETER AND CURVE-FITTING DATA COUNTERS
C
      READ 3, NV, NFLOAT, NFIXED, NPTS, NIND
      IF( NV - 10   ) 116,116,1000
  116 CONTINUE
      IF( NFLOAT - 50    ) 101,101,1000
  101 CONTINUE
      IF( NFLOAT - 15    ) 102,102,1000
  102 CONTINUE
      IF ( NPTS - 20    ) 113,113,1000              1620
  113 CONTINUE
      IF( NIND - 4      ) 112,112,1000
  112 CONTINUE
      READ 1, (x(I),I=1,NV)
      DO 117 J = 1, NV
  117 READ 1,  ( v(I,J),I=1,NV)
      READ 1,  ENORM
      READ 3, NROT, NCRIT
      READ 1, NCRIT, CCRIT
C
C     READ FIXED AND FLOATING CONSTANTS
C
      IF(  NFLOAT) 108,108,107
  107 READ 1, (PARAM(I),I=1,NFLOAT )
  108 CONTINUE
      IF( NFIXED ) 110,110,109
  109 READ 3, (INDEX(I),I=1,NFIXED)
  110 CONTINUE
      IF( NPTS) 115,115,111
C
C     READ CURVE-FITTING DATA
C
  111 CONTINUE
```

B.1.2 CONT.

```
      DO 114 I = 1, NPTS
  114 READ 1, (DATA(J,I) J=1,NIND), DATA(5,I)
  115 CONTINUE
      RETURN
C  **
C     ERROR (1000)
C  **
 1000 CONTINUE
      PRINT 1001, NV, NFLOAT, NFIXED, NPTS, NIND
 1001 FORMAT (14HOTOO MANY DATA, 15I5 )
      STOP
      END
```

B.1.2   CONT.

```
C       HILL-CLIMBING PROGRAM OUTPUT ROUTINE
C
        DIMENSION x(1), v(10,11), PARAM(50, INDEX(15), READ(4)
       1,   DATA(7,20)                                1620
        COMMON PARAM, INDEX DATA
      1 FORMAT (       5E15.8 )
      2 FORMAT (1H ,   5E15.8 )
      4 FORMAT ( 1H,          15I5)          STAND
      6 FORMAT ( 1H, 40A2)                   STAND
      7 FORMAT ( 1H1 )
      8 FORMAT ( 1H, 15x, 5E15.8)
C
C       HEADING
C
     11 FORMAT (     16HOFLOAT CONSTANTS )
     12 FORMAT (     16HOFIXED CONSTANTS )
     13 FORMAT (     11HO NPTS NIND)
     14 FORMAT (     6HO   NV)
     15 FORMAT (     7HOVALUES)
     16 FORMAT (     10HOSTEP-SIZE )
     17 FORMAT (     11HO NRND NCRIT)
     18 FORMAT (     26HO   RCRIT        CCRIT)
     19 FORMAT (     8HOVECTORS)
     20 FORMAT (     10HOPLOT-BACK )
     21 FORMAT (     1HO, 4x, 8HROTATION, 7x, 8HMOVEMENT, 3x,
       114HFUNCTION VALUE, 1x, 15HFUNCTION CHANGE/
       2 1HO, 21x, 21HINDEPENDENT VARIABLES)
     30 FORMAT (     1H, 21x, 37HHILL-CLIMBING PROGRAM -
       1ORIGINAL DATA)
     32 FORMAT (     1H, 21x, 37HHILL-CLIMBING PROGRAM -
       1FINISHED DATA)
C       PRINT HILL-CLIMBING RESULTS, ACCORDING TO ILINK
C       ILINK = 1 ORIGINAL PRINT-OUT
C       ILINK = 2 FINAL PRINT-OUT
        PRINT 7
        GO TO (100,110), ILINK
    100 PRINT 30
        GO TO 400
    110 PRINT 32
    400 CONTINUE
        PRINT 6
        PRINT 6, KEAD
        GO TO (450,300), ILINK
    450 PRINT 15
        PRINT 2, (x(I),I=1,NV)
        PRINT 19
        DO 440 J = 1, NV
    440 PRINT2, ( V(I,J),I=1,NV)
        PRINT 16
        PRINT 2,ENORM
        PRINT 17
        PRINT 4, NROT, NCRIT
        PRINT 18
        PRINT 2, RCRIT, CCRIT
        IFLAG = 1
C
```

B.1.2 CONT.

```
C     OPEN SUBROUTINE FOR PRINTING FLOATING AND FIXED
C     1PARAMETERS
C
  422 CONTINUE
  410 CONTINUE
      PRINT 11
      PRINT 2, (PARAM(I),I=1,NFLOAT )
  411 CONTINUE
      IF( NFIXED ) 421,421,420
  420 CONTINUE
      PRINT 12,
      PRINT 4, (INDEX(I),I=1,NFIXED)
  421 CONTINUE
      GO TO (431,301), IFLAG
C
C     PRINT CURVE-FITTING COUNTERS IF NON-ZERO
C
  431 CONTINUE
      IF( NPTS) 432,432,430
  430 CONTINUE
      PRINT 13
      PRINT 4, NPTS, NIND
  432 CONTINUE
C
C     OPEN SUBROUTINE FOR PLOT-BACK
C
  600 CONTINUE
      IF( NPTS) 141,141,140
  140 CONTINUE
      PRINT 20
      DO 142 J = I, NPTS
      PRINT 2, (DATA(I,J),I=1,NIND), (DATA(I,J),I=5,7)
  142 CONTINUE
  141 CONTINUE
      GO TO (200,304), IFLAG
  200 CONTINUE
      PRINT 7
      PRINT 6, READ
      PRINT 21
      PRINT 2
  500 RETURN
C  **
C     FINISH (300 )
C  **
  300 CONTINUE
      IFLAG = 2
      PUNCH 1, ( x(I),I=1,NV)
      PRINT 19
      DO 302 J = 1,NV
      PUNCH 1, (V(I,J),I=1,NV)
      PRINT 2, (V(I,J)I=1,NV)
  302 CONTINUE
      PUNCH 1, ENORM
      PRINT 16
      PRINT 2, ENORM
      GO TO 422
```

B.1.2 CONT.

```
  301 CONTINUE
      GO TO 600
  304 CONTINUE
      GO TO 500
      END

      SUBROUTINE GCLIMB   ( NV,X,F, V, STSIZE, TMOVMT,
     1ROTN, IFLAG)                              NOLINK
C
C     ROSENBROCK HILL-CLIMBER, WITHOUT CONSTRAINTS
C     MAXIMUM 10 INDEPENDENT VARIABLES (NO CHECK)
C
      DIMENSION s(10), v(10,10)
     1, XN(10), E(10), IND(10), D(10), A(10,10), B(10),
     2DREAL(10)
      NCONT = NV
      NROUND = O
C
C     INITIALISE PEAK INDICATORS, TOTAL MOVEMENTS, STEP
C     SIZES AND FICTITIOUS MOVEMENTS
C
      DO 10 I = 1,NV
      IND(I) = 2
      DREAL(I) = 0.
      E(I) = STSIZE
      D(I) = o.
   10 CONTINUE
C
C     START NEW ROUND
C
 1001 NROUND = NROUND+ 1
      IF( NROUND - 50 ) 1003,1003,2000
 1003 IMAIN = 1
C
C     TRY NEXT AXIS
C
 1002 CONTINUE
      ICH = 1
      DO 20 1 = 1,NV
      XN(I) = X(I) + E(IMAIN)*V(I,IMAIN)
      IF( XN(I) - x(I) ) 21,20,21
   21 CONTINUE
      ICH = 2
   20 CONTINUE
      GO TO (203,22), ICH
   22 CONTINUE
      Fl = CLIMBF ( NV, XN, IFLAG )
  100 E(IMAIN) = -0.5*E(IMAIN)
      IF( IND(IMAIN) - 1 ) 300,101,300
  101 IND(IMAIN) = 0
      NCONT = NCONT -1
      GO TO 300
  200 CONTINUE
      DREAL(IMAIN) = DREAL(IMAIN) + E(IMAIN)
      F = F1
      DO 202 I = 1,NV
```

B.1.2 CONT.

```
    202 X(I) = XN(I)
    203 CONTINUE
        D(IMAIN) = D(IMAIN) + E(IMAIN)
        E(IMAIN) = 3.*E(IMAIN)
        IF( IND(IMAIN) - 1 ) 300,300,201
    201 IND(IMAIN) = 1
    300 CONTINUE
C
C       TEST FOR END OF STAGE
C
        IF( NCONT ) 500,500,400
    400 IF( IMAIN - NV ) 401,1001,1001
    401 IMAIN = IMAIN + 1
        GO TO 1002
C
C       ROTATE AXES ( PALMER METHOD )
C
    500 CONTINUE
        ROTN = 0.
C
C       ALPHA   VECTORS
C
        DO 510 I = 1,NV
    510 A(I,NV) = D(NV)*v(I,NV)
        B(NV) = D(NV)**2
        IF( 2-NV ) 513,513 533
    513 CONTINUE
        JSUM = 1 + NV
        DO 511 J2 = 2, NV
        J = JSUM - J2
        DO 512 I = 1, NV
    512 A(I,J) = A(I,J+1) + D(J) * v(I,J)
    511 CONTINUE
    514 CONTINUE
C
C       SQUARED MODULI OF ALPHA VECTORS
C
        DO 520 J2 = 2, NV
        J = JSUM - J2
    520 B(J) = B(J+1) + D(J)**2
C
C       NEW ORTHOGONAL UNIT VECTORS
C
        JSUM = 2+ NV
        DO 530 J2 = 2, NV
        J = JSUM - J2
        DIV = SORT( B(J-1)*B(J) )
        IF( DIV ) 531, 530, 531
    531 DO 532 I = 1, NV
        V(I,J) = ( D(J-1)*A(I,J) - v(I,J-1)*B(J) ) / DIV
    532 CONTINUE
    530 CONTINUE
    533 CONTINUE
        DIV = SQRT ( B(1) )
        IF( DIV ) 550,550,542
```

B.1.2   CONT.

```
  542 CONTINUE
      DO 540 I = 1,NV
      V(I,1) = A(I,1) / DIV
  540 CONTINUE
C
C     STAGE STATISTICS
C
      ROTN = SQRT ( B(2) ) / DIV
  550 CONTINUE
      TMOVMT =  0.
      STSIZE =  0.
      DO 551 I = 1,NV
      TMOVMT = TMOVMT + DREAL (I)**2
      STSIZE = STSIZE + E(I)**2
  551 CONTINUE
      TMOVMT = SQRT( TMOVMT )
      XNV = NV
      STSIZE = SQRT ( STSIZE/XNV )
      RETURN
C
C     ERROR
C
 2000 PRINT 2001
 2001 FORMAT ( 19H GCLIMB - 50 CYCLES)
      GO TO 500
      END
```

B.2 SUBPROGRAMME

B.2.1 Programming Method

To use the general hill-climbing programme a FORTRAN
FUNCTION subprogramme to define the function to be maxi-
mised and minimised in the following form:

```
FUNCTION CLIMBF (NV,X,lFLAG)

DIMENSION X (10), FCONT(50), lCONST(20),

DATA (8,200)

COMMON FCONST., ICONST, DATA


CLIMB  =

RETURN

END
```

NV is the number of independent variables in the

function being maximised.

The array X contains a set of trial values of the inde-
pendent variables. The subprogramme must return the value
of the function, for the given values of X, as the value
of CLIMBF.

The array FCONST contains floating-point constants re-
quired in the calculation of CLIMBF, if any. The array
ICONST contains fixed-point constants required in the
calculation of CLIMBF, if any. The array DATA is in-
tended for experimental data, when the programme is being
used for curve-fitting (e.g. by least-squares). Each

column represents one experimental point. Rows 1 to 5 contain values of the independent variables, row 6 the value of the dependent variable. The subprogramme should calculate the values of the dependent variable for the given set of values of the hill-climb variables, X (the parameters in the equation being fitted to the data), and place these in row 7 and the difference between row 7 in row 8.; as well as setting CLIMBF equal to minus the sum of the squares between experimental and calculated values (if the least-squares fitting criterion is being used.) At the end of the run, the main programme gives a 'plot-back' of the DATA array so that the agreement between experimental and predicted values can be seen.

The fixed point variable IFLAG is provided to allow FUNCTION CLIMBS to be used efficiently for carrying out auxiliary calculations, in addition to the normal calculation of the function being maximised. In addition to the normal calls of CLIMBF during the hill-climbing process, CLIMB is also called once after reading the data but before starting the hill-climb and once at the completion of the hill-climb when the stop conditions in the data (see below) are satisfied. The value of IFLAG transmitted indicates the type of call of CLIMBF, as listed below. Also as listed below, an extra call of CLIMBF will be made after a round is complete if IFLAG is changed appropriately by CLIMBF during the round.

IFLAG is set equal to:

1.   Before preliminary CLIMBF call after reading

data. Before start of each round.

2.   Before extra CLIMBF call at end of a round

when stop conditions in the data are satisfied.

3.   Report extra CLIMBF call at end of a round

when stop conditions are not satisfied, but

IFLAG was changed to 4 during the round.

Following a CLIMBF call with IFLAG = 2 or 3, hill climbing

will continue if, and only if, IFLAG is returned = 4.

In simple problems, in which no auxiliary calculations are

required, IFLAG can be ignored.

As shown above, changing IFLAG to A during a round results

in an extra call of CLIMBF on completion of the round.

Note that if IFLAG is changed to 4, it will be transmitted

as 4 for the remainder of the round.

B.2.2 THE SUBPROGRAMME FOR THERMODYNAMIC ANALYSIS

```
C       EQUILIBRIUM COMPOSITION CALCULATION
C       SMELTER AND STACK GASES REDUCED WITH COAL OR CHAR
C
C       INDEPENDENT VARIABLES
C       X(1)#PARTIAL PRESSURE OF CO2
C       X(2)#PARTIAL PRESSURE OF S2
C       X(3)#PARTIAL PRESSURE OF H2O
C
C       DEPENDENT VARIABLES
C
C       FCONST(1)#PARTIAL PRESSURE OF SO2
C       FCONST(2)#PARTIAL PRESSURE OF CO
C       FCONST(3)#PARTIAL PRESSURE OF COS
C       FCONST(4)#PARTIAL PRESSURE OF N2
C       FCONST(5)#PARTIAL PRESSURE OF CS2
C       FCONST(17)#PARTIAL PRESSURE OF H2
C       FCONST(18)#PARTIAL PRESSURE OF H2S
C       FCONST(22)#PARTIAL PRESSURE OF CH4
C
C       FCONST(10)#N TO O RATIO
C       FCONST(11)#S TO O RATIO
C       FCONST(12)#TOTAL PRESSURE
C       FCONST(13)#INITIAL H2O CONCENTRATION
C       FCONST(25)#CALCULATED S/O RATIO
C       FCONST(27)#CALCULATED S/H RATIO
C       FCONST(26)#CALCULATED N/O RATIO
C       FCONST(24)#CALCULATED TOTAL PRESSURE
C       FCONST(28)#SUMMATION OF SULFUR AS ELEMENTAL SULFUR
C       FCONST(29)#SULFUR RECOVERY
C
C       EQUILIBRIUM CONSTANTS
C
C       FCONST(6)#EQUILIBRIUM CONSTANT FOR THE REACTION
C       C&SO2#CO2&O.5S2
C       FCONST(7)#EQUILIBRIUM CONSTANT FOR THE REACTION
C       C&2CO2#2CO
C       FCONST(8)#EQUILIBRIUM CONSTANT FOR THE REACTION
C       2CO&S2#2COS
C       FCONST(9)#EQUILIBRIUM CONSTANT FOR THE REACTION
C       2COS#CO2&CS2
C       FCONST(19)#EQUILIBRIUM CONSTANT FOR THE REACTION
C       H2&O.5S2&H2S
C       FCONST(20)#EQUILIBRIUM CONSTANT FOR THE REACTION
C       H2O&CO#CO2&H2
C       FCONST(21)#S TO H RATIO
C       FCONST(23)#EQUILIBRIUM CONSTANT OF THE REACTION
C       2SO2 & CH4 # S2 & CO2& 2H2O
C
C       ************************************************
C
0001    FUNCTION CLIMBS(NV,X,IFLAG)
0002    IMPLICIT REAL*8(A-H,O-Z)
0003    DIMENSION X(3),FCONST(50)
0004    COMMON FCONST
C
C       PROGRAM CONTROLLING STATEMENTS
C
```

B.2.2 THE SUBPROGRAMME FOR THERMODYNAMIC ANALYSIS

```
0005            DO 1006 I=1,3
0006            IF(X(I)) 1005, 1006,1006
0007       1005 X (I)=-X(I)
0008       1006 CONTINUE
           C
           C
           C      START CALCULATING DEPENDENT VARIABLES
           C
           C
0009       1000 FCONST (1)=X(1)*(X(2)**0.5)/FCONST(6)
0010            FCONST(2)=X(1)*FCONST(7)**2
0011            FCONST(3)=FCONST(2)*(FCONST(8)*X(2))**0.5
0012            FCONST(5)=FCONST(9)*FCONST(3)**2/X(1)
0013            SUMOXY=2.0*X(1)+2.0*FCONST(1)+FCONST(2)+FCONST(3)
                1+X(3)
0014            FCONST(4)=0.5*SUMOXY*FCONST(10)
0015            FCONST(17)=X(3)*FCONST(2)* FCONST(20)/X(1)
0016            FCONST(18)=(X(2)**0.5)*FCONST(19)*FCONST(18)
0017            FCONST(22)=X(2)*X(1)*(X(3)**2)/(FCONST(23)*
                1FCONST(1)**2)
           C
0018            FCONST(28)= 2.0*X(2)+FCONST(1)+FCONST(3)+2.0*
                1FCONST(5)+FCONST(18)
0019            FCONST(24)=X(1)+X(2)+X(3)+FCONST(1)+FCONST(2)
                1+FCONST(3)+FCONST(4)+FCONST(5)+FCONST(17)+
                2FCONST(18)+FCONST(22)
0020            FCONST(25)=FCONST(28)/SUMOXY
0021            FCONST(26)=2.0*FCONST(4)/SUMOXY
0022            FCONST(27)=FCONST(28)/(2.0*X(3)+2.0*FCONST
                1(17)+2.0*FCONST(18)+4.0*FCONST(22))
0023            FCONST(29)=FCONST(28)/FCONST(30)
           C
           C      CHECK CONVERGENCE
           C
0024            FCONST(14)=(X(1)-(FCONST(12)-X(2)-FCONST(1)
                1-FCONST(2)-FCONST(3)-FCONST(4)-FCONST(5)-
                2FCONST(17)-FCONST(18)-X(3)-FCONST(22)))**2
0025            FCONST(15)=(X(2)-0.5*(FCONST(11)*SUMOXY -
                1FCONST(1) - FCONST(3)-2.*FCONST(15)-FCONST
                2(18)))**2
0026            FCONST(16)=(X(3)-0.5*((2.0*X(2)+FCONST(1)+
                1FCONST(3)+2.0*FCONST(5)+FCONST(18))/FCONST
                2(21)-2.0*FCONST(18)-2.0*FCONST(17)-4.0*
                3FCONST(22)))**2
           C
0027            CLIMBF=0.0
0028            DO 1004 I=14,16
0029            CLIMBF=CLIMBF-FCONST(I)
0030       1004 CONTINUE
0031            RETURN
0032            END
```

B.2.3   UNDERLINE DATA CARD REQUIRED

The following set of cards for each Hill-Climbing pro-
gramme is required:

    (1)   Heading card

    (2)   NV, Nfloat, Nfixed, NPTS, NIND

    (3)   X(I), I=1, NV

    (4)   V(I,J), I=1, NV, J=1,NV, new card for each
             vector

    (5)   Step-size

    (6)   NROT, NCRIT

    (7)   RCRIT, CCRIT

    (8)   Float constants, if any

    (9)   Fixed constants, if any

    (10)   DATA(I,J), I=1,NIND, DATA(6,J), J=1,NPTS,
             new card for each point, if applicable.

Where:

    NV   = no. of independent variables in the hill-
             climb function (in a curve-fitting pro-
             blem, this is the no. of parameters in
             the equation to be fitted to the data)

    NFLOAT = no. of floating-point constants (FCONST
             array)

    NFIXED = no. of fixed-point constants (ICONST
             array)

    NPTS   = no. of experimental points in curve-fitting
             data, if any.

NIND   = no. of independent variables in relation

in curve-fitting problem (ignored if NPTS

=0)

V(-,-)= orthogonal vectors, one vector per column

STSIZE= starting step-size

NROT   = maximum no. of rounds to be carried out

NCRIT   = count criterion for degree of rotation and

overall-change-in-X convergence tests (see

below)

RCRIT, CCRIT:

After each round, the programme prints out a degree of

rotation and an overall movement figure. The degree of

rotation varies between 0 and 1. A large value indicates

a large change in direction of the vectors. A large

change in direction several times (say 6) in succession

can indicate that the peak has been reached. The overall

change is the modulus of the vector joining the latest

point with the point reached at the end of the last round:

that is, it is the overall change in X during the round.

The computation is terminated if the degree of rotation

is greater than RCRIT and the overall change is less than

CCRIT, for NCRIT rounds in succession.

The card formats are: Floating-point cards, 5E15.8

Fixed-point   cards, 15I5

B.4 TYPICAL PRINTOUTS

HILL-CLIMBING PROGRAM - ORIGINAL DATA

EQUILIBRIUM COMPOSITION FOR C-O-S-H SYSTEM AT 1000K-SMELTER GAS-COAL

VALUES
0.67262219D-01 0.32692588D-04 0.1000000D-02

VECTORS
 0.62565552D-01 0.94264084D-01-0.69158965D-01
-0.64548679D 00 0.16467592D 01 0.35394179D 00
-0.54772716D 00 0.13080977D 01 0.30906346D 00

STEP-SIZE
0.50854834D-19

NRNDI NCRI
 20   6

     RCRIT   CCRIT
0.0   0.0

FLOAT CONSTANTS
0.99782754D-09 0.20148803D 00 0.52140799D-02 0.71696463D 00 0.92647963D-04
0.38542542D 06 0.17307687D 01 0.20483660D 02 0.22921957D 00 0.41900000D 01
0.75300000D-01 0.10000000D 01 0.10000000D-02 0.13926436D-07 0.70608073D-04
0.16372575D-04 0.43232870D-02 0.34991754D-02 0.14155558D 03 0.14432315D 01
0.34800000D 00 0.52271258D-05 0.42251931D 12 0.99988199D 00 0.26192992D-01
0.41900000D 01 0.50741662D 00 0.89639374D-02 0.31452412D 00 0.28500000D-01

B.4 TYPICAL PRINTOUTS CONT.

EQUILIBRIUM COMPOSITION FOR C-O-S-H SYSTEM AT 1000K-

SMELTER GAS-COAL

ROTATION	MOVEMENT FUNCTION VALUE	FUNCTION CHANGE
	INDEPENDENT VARIABLES	
0.0	0.0 -0.86994574D-04	0.0
	0.67262219D-01 0.32692588D-04	0.10000000D-02
0.10814761D 00	0.66501325D-18-0.86994574D-04	0.10164395D-19
	0.67262219D-01 0.32692588D-04	0.10000000D-02
0.10000000D 01	0.18715461D-07-0.86994197D-04	0.37652761D-09
	0.67262203D-01 0.32731272D-04	0.10000089D-02
0.99182434D 00	0.14818049D-06-0.86993451D-04	0.74677538D-09
	0.67262194D-01 0.32715102D-04	0.10000190D-02
0.24547470D 00	0.55860706D-05-0.86962164D-04	0.31286725D-07
	0.67261638D-01 0.32684650D-04	0.10005214D-02
0.18303927D-01	0.60903516D-03-0.83542580D-04	0.34195837D-05
	0.67199317D-01 0.34224428D-04	0.10561861D-02
0.20787325D-02	0.21209567D-01-0.44002316D-05	0.79142349D-04
	0.65037941D-01 0.63000631D-04	0.298998950-02
0.30999144D-03	0.48998949D-02-0.62292957F-06	0.37773020D-05
	0.64538153D-01 0.70880115D-04	0.34369889D-02
0.28464408D-02	0.36343785D-04-0.62194853D-06	0.98204048D-09
	0.64541887D-01 0.70750496D-04	0.34336595D-02
0.86696184D-04	0.14252030D-05-0.62194604D-06	0.14859388D-11
	0.64541740D-01 0.70755321D-04	0.34337900D-02
0.13834873D-01	0.24519415D-06-0.62194589D-06	0.15489602D-12
	0.64541716D-01 0.70755347D-04	0.34338122D-02
0.12982060D-02	0.16867600D-05-0.62194541D-06	0.48082816D-12
	0.64541545D-01 0.70757139D-04	0.34339654D-02
0.74422228D-02	0.16125017D-06-0.62194538D-06	0.31799891D-13
	0.64541528D-01 0.70757025D-04	0.34339799D-02
0.21495686D-01	0.59899881D-07-0.62194533D-06	0.45379728D-13
	0.64541522D-01 0.70757915D-04	0.34339855D-02
0.24375747D-01	0.81434292D-08-0.62194532D-06	0.14048150D-13
	0.64541523D-01 0.70757415D-04	0.34339847D-02
0.15772007D 00	0.38805769D-08-0.62194530D-06	0.19158385D-13
	0.64541523D-01 0.70757687D-04	0.34339851D-02
0.99994665D 00	0.91835528D-07-0.62194358D-06	0.17169354D-11
	0.64541525D-01 0.70760957D-04	0.34339825D-02
0.47415841D 00	0.19923151D-06-0.62193685D-06	0.67361598D-11
	0.64541543D-01 0.70757063D-04	0.34339672D-02
0.15552432D 00	0.13600374D-05-0.62189644D-06	0.40404440D-10
	0.64541642D-01 0.70755595D-04	0.34338819D-02
0.69215795D-03	0.24067612D-03-0.61881729D-06	0.30791526D-07
	0.64559100D-01 0.70557078D-04	0.34188184D-02
0.60141119D-03	0.28297866D-04-0.61875176D-06	0.65525795D-10
	0.64557052D-01 0.70571789D-04	0.34205865D-02

B.4   TYPICAL PRINTOUTS   (CONT.)

HILL-CLIMBING PROGRAM - FINISHED DATA

EQUILIBRIUM COMPOSITION FOR C-O-S-H SYSTEM AT 1000K-SMELTER GAS-COAL

VECTORS
-0.72372175D-01 0.51986530D-03 0.62480861D-01
-0.27566035D 00 0.50701454D 00 0.17876947D 00
-0.79959135D 00 0.20432222D 01 0.43555644D 00

STEP-SIZE
0.19858769D-06

FLOAT CONSTANTS
0.14070804D-08 0.19338454D 00 0.73526027D-02 0.69820450D 00 0.19195092D-03
0.38542542D 06 0.17307687D 01 0.20483660D 02 0.22921957D 00 0.41900000D 01
0.75300000D-01 0.10000000D 01 0.10000000D-02 0.14492358D-06 0.33833970D-07
0.43999421D-06 0.14788177D-01 0.17585600D-01 0.14155558D 03 0.14432315D 01
0.34800000D 00 0.63722324D-04 0.42251931D 12 0.99961931D 00 0.76403844D-01
0.41900000D 01 0.35442606D 00 0.25463250D-01 0.89344736D 00 0.28500000D-01

APPENDIX   C

DETERMINATION OF IMPORTANT VARIABLES BY

A PLACKETT-BURMAN DESIGN

APPENDIX   C

DETERMINATION OF IMPORTANT VARIABLES BY A PLACKETT-BURMAN DESIGN

C.1   PLACKETT-BURMAN MATRIX

The experimental design block of the Plackett-Burman type
(40) is usually used as a tool to screen the selected
variables and provide an estimate of their relative signi-
ficance.   These authors proposed a series of basic designs
for as many as 100 experiments.   These designs are balanced
fractional replications of factorial designs in which all
the main effects are confounded with interactions.   Implicit
in such a design, therefore, is the assumption that each
of the variables studied is independent in its response to
the prevailing levels of the other variables.   In many cases
this may not be so and interpretation of the results is by
no means automatic and frequently requires a good apprecia-
tion of the process studied by the experimenter.   The vir-
tue of these designs is the great economy of experimenta-
tion which may be achieved.

In this particular series of experiments a complete study
of four variables at two levels would require 2^4 experi-
ments.   In a Plackett-Burman design, for N experiments per-
formed up to N-1 factors may be evaluated.   There are,
however, certain restrictions in the pattern available and
N must be divisible by the square of the number of levels
at which the variable is studied at two levels, L=2, then
N must be some multiple of 2^2 and if each variable is

studied at three levels then N must be some multiple of 3^2.
Plackett-Burman in their paper provide designs for L=2 for
values of N=8 to N=100 with the exception of N=92. In the
case considered here, for four variables the nearest de-
sign is N=8 and this may be used by treating the three un-
assigned factors as dummies. With caution, these dummies
may be ultilised to provide a measure of the significance
of the variables studied. Fig. C.1 shows a matrix of the
design.

Observation of the matrix shows that each variable occurs
at its high level four times and at its low level four
times. The effect of a variable on the response is simply
the difference between the average value of the response
for the four experiments at the high levels and the average
value of the response for the four experiments at the low
level. This is illustrated in Eq. C.1:

$$E \quad = \quad \frac{R \text{ at } (+)}{4} \quad - \quad \frac{R \text{ at } (-)}{4} \qquad \ldots\ldots C.1$$

where E=effect and R=response or result.

The effect calculated from the above equation is the true
effect of a variable. For example if we consider variable
A, it will be seen that when variable A is at its high
level B is high two times and low two times. Similarly,
when A is at its low level, B is high two times and low
two times. Thus the net effect of changing variable B
cancel out in calculating the effect of A. The remaining

Variables balance in this same way so that the net differ-
ence is only the effect of A.

Variables C, F and G in the design block are dummy varia-
bles. The effects of these dummy variables are obtained
in the same way as the effects of the real variables. In
the absence of interaction and experimental error those
effects should be zero. Any difference from zero repre-
sents either interaction between variables and/or experi-
mental error. If no interaction exists then the error
variance may be calculated from the Eq.C.2:

$$V = \frac{(E_d)^2}{n} \qquad \ldots\ldots C.2$$

where V = the variance of an effect,

E_d = the effect shown by a dummy, and

n = the total number of dummy variables.

The standard error of an effect is defined in Eq. C.3:

$$S.E. = \sqrt{V} \qquad \ldots\ldots\ldots C.3$$

Using the "t" test, the significance of each effect may
then be obtained from Eq. C.4:

$$t = \frac{E}{S.E.} \qquad \ldots\ldots C.4$$

The "t" test is used to assess whether the effect differs
from the standard error by an amount greater than that
attributable to random variation. Usually an effect is

considered as significant if the confidence level is not less than 95%. However, in this type of experimentation it is possible that the value of the standard error may be inflated by interaction effects and therefore it is customary to consider effects as significant if confidence levels are not less than 70%.

A practical example of the application of a Plackett-Burman design to the screening of process variables is provided by Stowe and Mayer (41). In this paper twelve variables were screened in sixteen experiments as a preliminary step in the optimisation of catalyst performance.

C.2   EXPERIMENTAL PROCEDURE

In this series of experiments the general operating procedure is substantially the same as that described in Section 3.2. The order in which the experiments are carried out is randomised to avoid the possibility of bias.

The primary information required for working out the relative significance of the various variables is the objective functions listed in Table C.1. These are the degree of conversion of sulphur dioxide at steady states. From the results of the preliminary runs using activated carbon it is estimated that the time required for approaching a steady state for all cases in this experiment would be less than 20 minutes. To ensure that   steady state had actually been reached, four samples were taken at, and within about

ten minutes after the time when this state was thought
to have been reached. The results obtained from the analy-
sis of the gas samples for the eight runs are shown in
Table C.2. The degree of conversion needed for statisti-
cal analysis was taken as the mean of the four values
obtained from the analysis of the four samples.

In the following section detailed computation of the effects
of variables are given.

TABLE C.1

PLACKETT-BURMAN STATISTICAL BLOCK

RUN	RANDOM	VARIABLE							OBJECTIVE
NO.	ORDER	A	B	C	D	E	F	G	FUNCTION
1	1	+	+	+	−	+	−	−	z_1
2	4	+	+	−	+	−	−	+	z_2
3	7	+	−	+	−	−	+	+	z_3
4	5	−	+	−	−	+	+	+	z_4
5	6	+	−	−	+	+	+	−	z_5
6	3	−	−	+	+	+	−	+	z_6
7	2	−	+	+	+	−	+	−	z_7
8	8	−	−	−	−	−	−	−	z_8

+   Denotes high level of variable

−   Denotes low level of variable

A   Initial SO_2 concentration

B   Temperature level

C   Dummy variable

D   Particle size

E   Flow rate

F   Dummy variable

G   Dummy variable

TABLE C.2a Experimental Results For Statistical Analysis

RUN NO.		1	2	3	4	5	6	7	8
Temp., °C		916	917	770	920	770	767	916	768
Flow Rate, l/min		31.0	26.3	26.9	30.0	30.8	30.6	26.1	26.4
Conc., $\%SO_2$		6.52	6.64	6.9	1.87	6.8	1.78	1.80	1.90
Size, cm		0.078	0.103	0.078	0.078	0.103	0.103	0.103	0.078
Vol. %	SO_2	0.306	0.129	3.44	0.167	4.47	1.31	0.186	1.036
	CO_2	3.86	3.92	3.21	0.81	2.31	0.70	0.96	0.823
(1)	CO	2.67	3.43	0.146	1.66	0.07	0.06	1.52	0.80
	COS	1.65	1.67	0.048	0.20	0.04	−	0.22	−
	SO_2	0.183	0.164	4.07	0.141	4.618	1.14	0.127	1.013
	CO_2	3.78	3.83	2.82	0.826	2.26	0.65	0.097	0.767
(2)	CO	2.90	3.23	0.142	1.95	0.08	0.06	1.53	0.084
	COS	2.05	1.73	0.047	0.195	0.04	−	0.20	−
	SO_2	0.161	0.299	4.23	0.170	4.71	1.18	0.163	1.080
	CO_2	3.480	3.88	2.54	0.89	2.18	0.67	0.907	0.723
(3)	CO	2.84	3.73	0.138	1.91	0.07	0.07	1.56	0.072
	COS	2.14	1.86	0.050	0.19	0.04	−	0.19	−
	SO_2	0.143	0.094	3.86	0.21	4.66	1.16	0.19	1.082
	CO_2	3.52	4.04	2.97	0.81	2.24	0.68	1.012	0.748
(4)	CO	2.82	3.63	0.126	1.92	0.072	0.06	1.55	0.075
	COS	2.08	1.78	0.042	0.20	0.04	−	0.21	−

TABLE C.2b

RUN NO.	1	2	3	4	5	6	7	8
SAMPLE NO.	DEGREE OF CONVERSION OF SO_2, %							
1	95.4	98.1	50.3	91.1	34.2	36.5	89.7	45.5
2	97.2	97.5	41.0	9.25	32.1	35.8	92.9	46.7
3	97.5	96.5	38.6	90.9	30.8	34.0	91.0	43.2
4	97.8	98.6	44.1	89.2	31.5	34.8	89.5	43.0
MEAN	97.0	97.7	43.5	90.9	32.1	35.2	90.8	44.6

C.3 COMPUTATION OF EFFECTS OF VARIABLES

Run No.	Random Order	Variable A	B	C	D	E	F	G	Objective Function
1	1	+	+	+	−	+	−	−	97.0
2	4	+	+	−	+	−	−	+	97.7
3	7	+	−	+	−	−	+	+	43.2
4	5	−	+	−	−	+	+	+	90.9
5	6	+	−	−	+	+	+	−	32.1
6	3	−	−	+	+	+	−	+	35.2
7	2	−	+	+	+	−	+	−	90.8
8	8	−	−	−	−	−	−	−	44.6

Notes:

+ Denotes High level of variable

− Denotes low level of variable

A Initial SO_2 concentration + 6.8% − 1.5%

B Temperature level   + 917°C − 769°C

C Dummy

D Particle size   + 0.103cm − 0.0775 cm

E Flow rate   + 31 1/min − 26 1/min

F Dummy

G Dummy

(A) Effect of Initial SO_2 Concentration − E_A

+	−
97.0	90.9
97.7	35.2
43.2	90.8
32.1	44.6
270.0	271.4

$$E_A = \frac{270.0 - 271.4}{4} = -.4$$

(B)   <u>Effect of Temperature</u> - E_B

+	-
97.0	43.2
97.7	32.1
90.9	35.2
90.8	44.6
376.4	155.1

$$E_B = \frac{376.4 - 155.1}{4} = 55.3 \qquad etc......$$

APPENDIX D

GAS ANALYSIS METHOD

D.1   Column

D.1.1 Separation of SO_2, COS, CS_2 and H_2S

D.1.2 Separation of CO_2, CO, H_2, CH_4 and C_2H_6

D.2   Sampling Method

D.3   Calibration

APPENDIX D

GAS ANALYSIS METHOD

In this work gas chromatography was chosen as the means of analysis. This is because the method is capable of giving a full analysis of a gas sample which contains gases that could vary from several percent to a minute quantity depending on the initial SO_2 concentration and the degree of conversion of SO_2. Moreover, this method offers rapidity in gas analysis.

Samples obtained from the SO_2-carbon reaction were analysed for the following gases: SO_2, CO_2, CO, COS and CS_2. The following additional gases were analysed for samples obtained from the SO_2-coal reaction: methane, ethane, H_2 and H_2S.

Two gas chromatographs were used for gas analysis. They were fitted with thermal conductivity detectors. A Beckman GC-2 gas chromatograph was employed to analyse SO_2, COS, CS_2 and H_2S. This was later replaced by another gas chromatograph fitted with a Gow-Mac thermal conductivity detector. The other gas chromatograph was a Fisher Partitioner. It was used to analyse CO_2, CO, CH_4, C_2H_6 and hydrogen.

D.1 COLUMN

D.1.1 Separation of SO_2, COS, CS_2 and H_2S

It was found that SO_2, COS, CS_2 and H_2S could be separated

satisfactorily by using a Porapak-R column (53). The column was a 3 m x 6 mm O.D. aluminium tubing. The size of the Porapak-R was -80+100 B.S. mesh. Helium was used as carrier gas. In order to get good separation of components the column was maintained at 160°C. The carrier gas flow rate was 20 ml/min and the bridge current 375 mA.

Reactivating the column was found necessary. It was found that the column's reactivity decreased gradually as the number of gas analysis increased. This was indicated by the broader shape and the increase in tailing of the signal representing SO_2. Restoration of its reactivity was achieved by purging the column with helium at 220°C for at least two hours. In practice this purging operation was adopted before every gas analysis to ensure the high and consistent activity of the column.

Generally this gas chromatograph system was satisfactory in analysing SO_2, COS, CS_2 and H_2S. However, for concentrations below 100 ppm accurate and reproduceable determination was difficult. Among these gases, SO_2 was most difficult to determine with accuracy. It was found that at low concentrations the response of SO_2 became rather asymetric coupled with noises and long tails. This could be due to the high reactivity of SO_2 which gave rise to adsorption and desorption problems.

In Table D.1 the approximate retention times of SO_2, COS, CS_2 and H_2S are given. Typical chromatograms obtained from gas analysis are shown in Fig. D.1 and D.2.
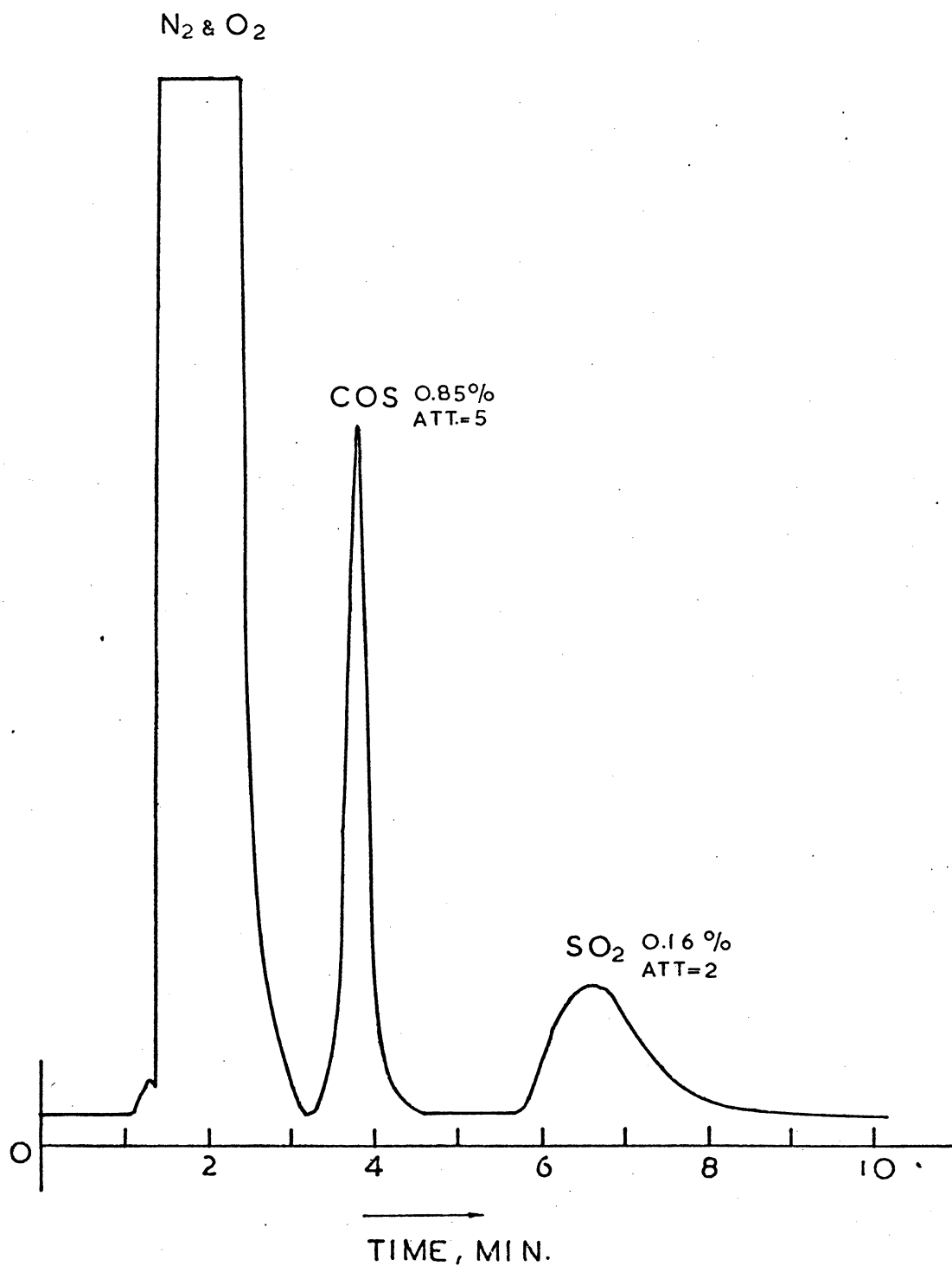
Fig. D.1 Typical Chromatogram for Gas Sample obtained

from SO₂ Reduction with Activated Carbon at

917°C
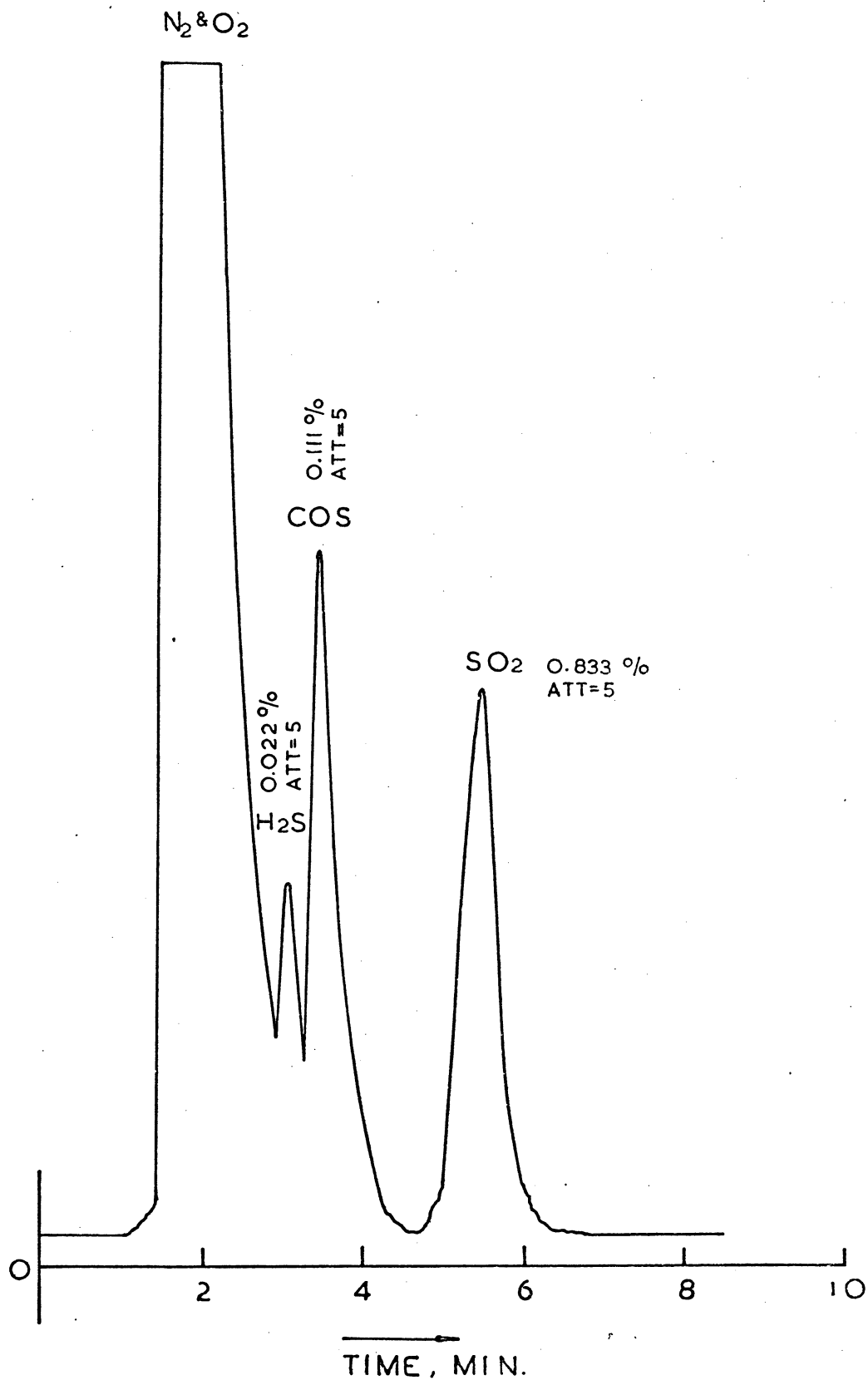
Fig. D.2   Typical Chromatogram for Gas Sample obtained from

SO_2 Reduction with Brown Coal at 900°C

D.1.2 Separation of CO_2, CO, H_2, CH_4 and C_2H_6

Gases CO_2, CO, H_2, CH_4 and C_2H_6 were separated with a matched column made of 6 mm aluminium tubing. The column consisted of two parts connected in series. Column one was 1.5 m long and was packed with HMPA (hexamethylphosphoramide). Column two was 2 m long and was packed with molecular sieve 13X.

HMPA is an organic liquid. It is coated on 60/80 mesh columnpak (chromosorb P) as a partitioning agent. It will gradually bleed away from the column especially under continual use. The life of the column varies from several months to a year depending on the frequency with which it is used. As HMPA bleeds away the retention times of compounds separated will gradually decrease and overlapping of peaks may eventually occur. When this happens a new column is required.

The separating characteristic of molecular sieve was found to be affected by the absorption of water vapour and CO_2. Frequent reactivation was required. This was done by purging the column with nitrogen at 250°C. A typical chromatogram is shown in Fig. D.3.

D.2 SAMPLING METHOD

Gas samples were collected in 250 ml gas sampling bottles. As SO_2 is very reactive and will dissolve in commonly used displacement fluids such as water or sulphuric acid, this method was avoided. The gas sampling bottle was first
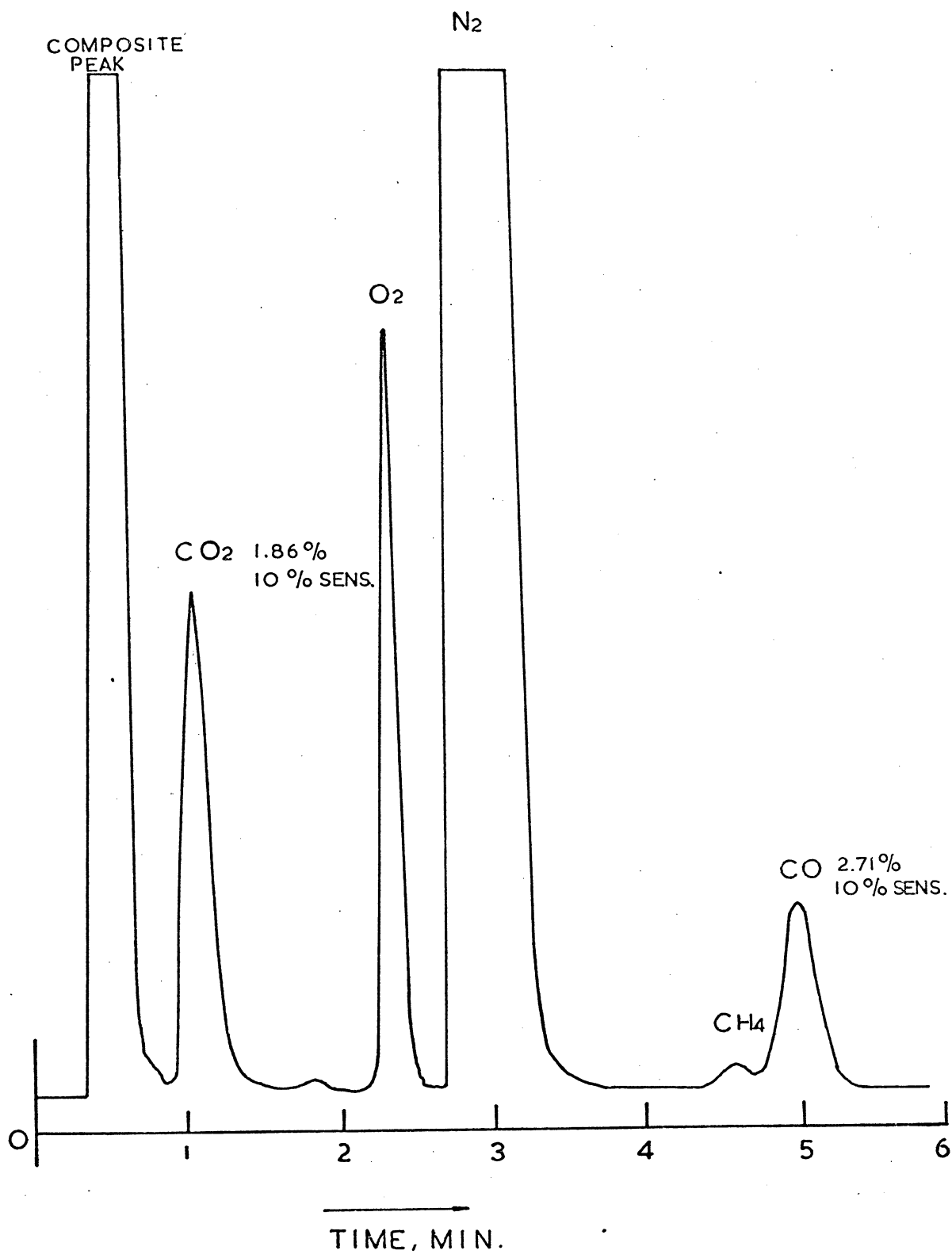
Fig. D.3 Typical Chromatogram for Gas Sample obtained

from SO$_2$ Reduction with Brown Coal at 900°C

evacuated to a known degree and sampling was completed by slowly opening the inlet gas cock.

These bottles were fitted with side arms and rubber septums to allow syringe sample withdrawal. Gas samples could be passed to the chromatograph via the gas sampling valve or through the syringe injection point. The syringe method was found to be reproduceable and since this was more convenient it was used in preference to the sampling valve. 2 ml and 5 ml pressure-lok precision gas syringes were used. The sampling and sample injection procedure was standardised to assist in obtaining reproduceable results. Reproduceability of chromatograph standards in the low concentration range (10 - 100 ppm) was generally better than ± 10 %.

D.3 CALIBRATION

The gas chromatographs were calibrated with standard gases prepared from a gas mixing apparatus as shown in Fig. D.4.

The volume of the apparatus was calibrated accurately. To prepare a standard gas mixture, the apparatus was firstly purged thoroughly with nitrogen. Then a predetermined amount of pure gas was precisely measured with gas syringe and injected into the mixing apparatus.

Peak area (Proportional to the number of counts of the disc integrator) and peak height of signal were used to prepare calibration charts. As peak area is more accurate in concentration determination especially for signals with asymetric peaks, it was used whenever possible. Peak height
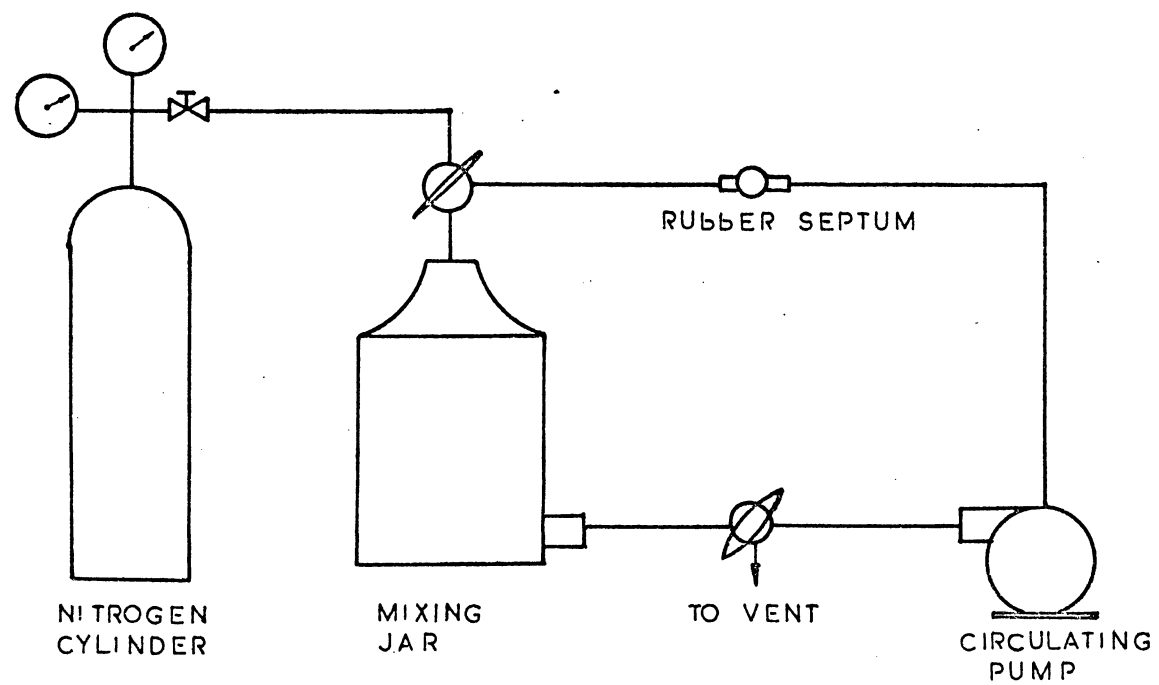
FIG. D4   APPARATUS FOR STANDARD GAS PREPARATION

only was employed to calibrate the Fisher gas chromato-
graph as the recorder was not equiped with a disc
integrator.

Typical calibration charts are shown in Fig.D.6 - D.8.
It can be seen that linear relationships were obtained
for all gases. However, as the slopes of these lines
were sensitive to changes in carrier gas flow rate and
oven temperature and also the column separating character-
istic would change after continual use it was necessary
to recalibrate the gas chromatographs. Recalibration was
simplified by using certified standard gas mixtures from
C.I.G. In every gas analysis these mixtures were in-
jected at the beginning and at the finish of the analysis
to check if there was any change in the slopes of the
calibration curves.

TABLE D.1   RETENTION TIMES OF GAS CHROMATOGRAPHS

Retention Time, min.

Gases	Beckman GC-2	G.C. with Gow-Mac Detector	Fisher Partitioner
SO_2	6.6	5.4	-
COS	3.8	3.2	-
CS_2	5.3	4.8	-
H_2S	3.0	2.2	-
CO_2	-	-	1.1
CO	-	-	5.0
H_2	-	-	0.7
CH_4	-	-	4.2
C_2H_6	-	-	0.9

CONDITIONS USED

Carrier Gas	Helium	Helium	Helium (N_2 for H_2)
Column Temperature	160°C	130°C	Room
Carrier Gas Flow Rate	20 ml/min	20 ml/min	80 ml/min
Bridge Current	375 mA	300 mA	5 mA
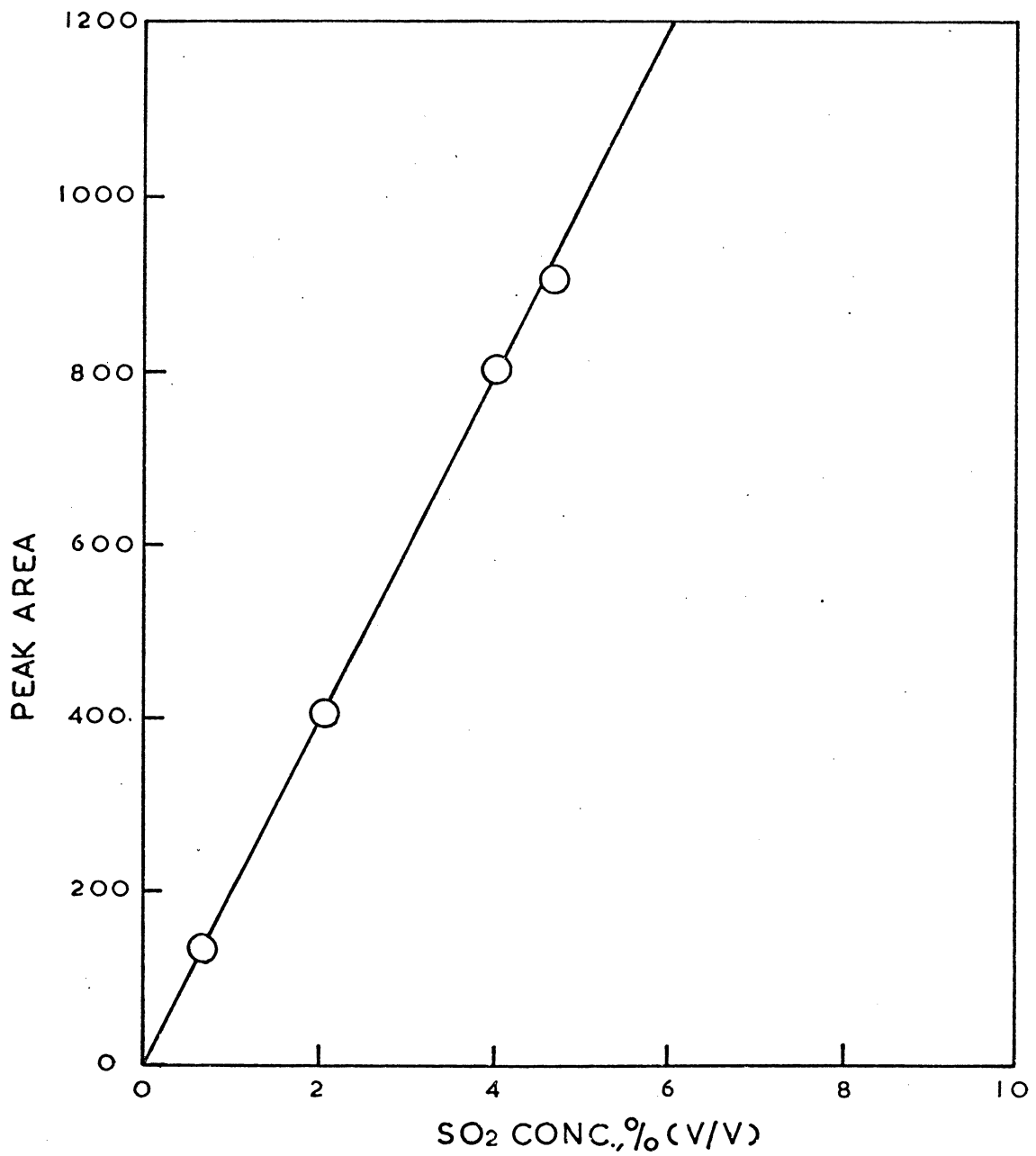
Fig. D.5   SO$_2$ Calibration Curve

G.C.:   Beckman G-2

Att Factor: 20

Sample Size: 2 ml

Column Temp.:   160°C

Carrier Gas: Helium
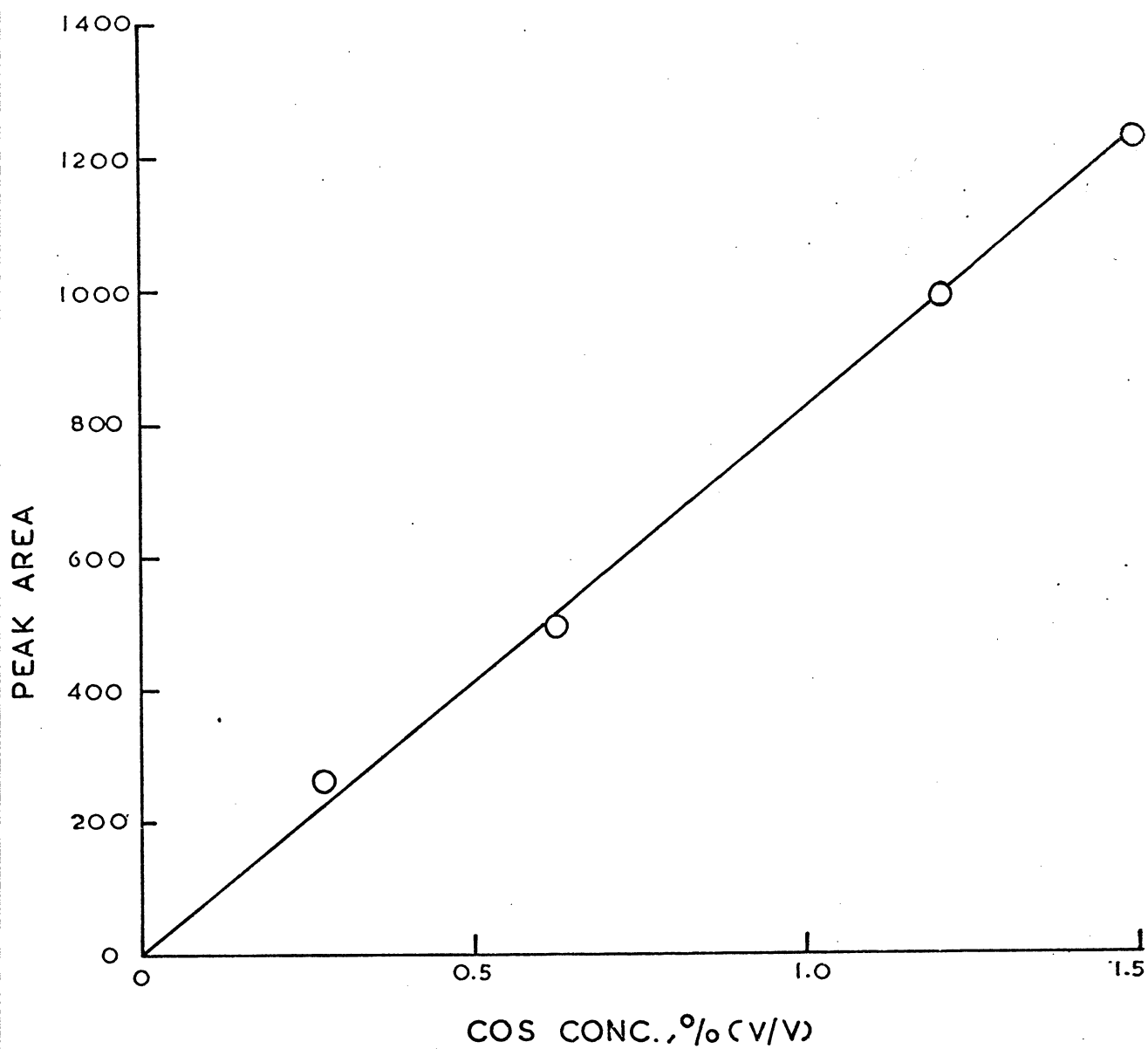
Flow Rate: 20 ml/min

Fig. D.6   Carbon Oxysulphide Calibration Curve

G.C.:   Beckman G-2

ATT. Factor: 10

Sample Size: 2 ml

Col. Temp.:   160°C

Carrier Gas: Helium
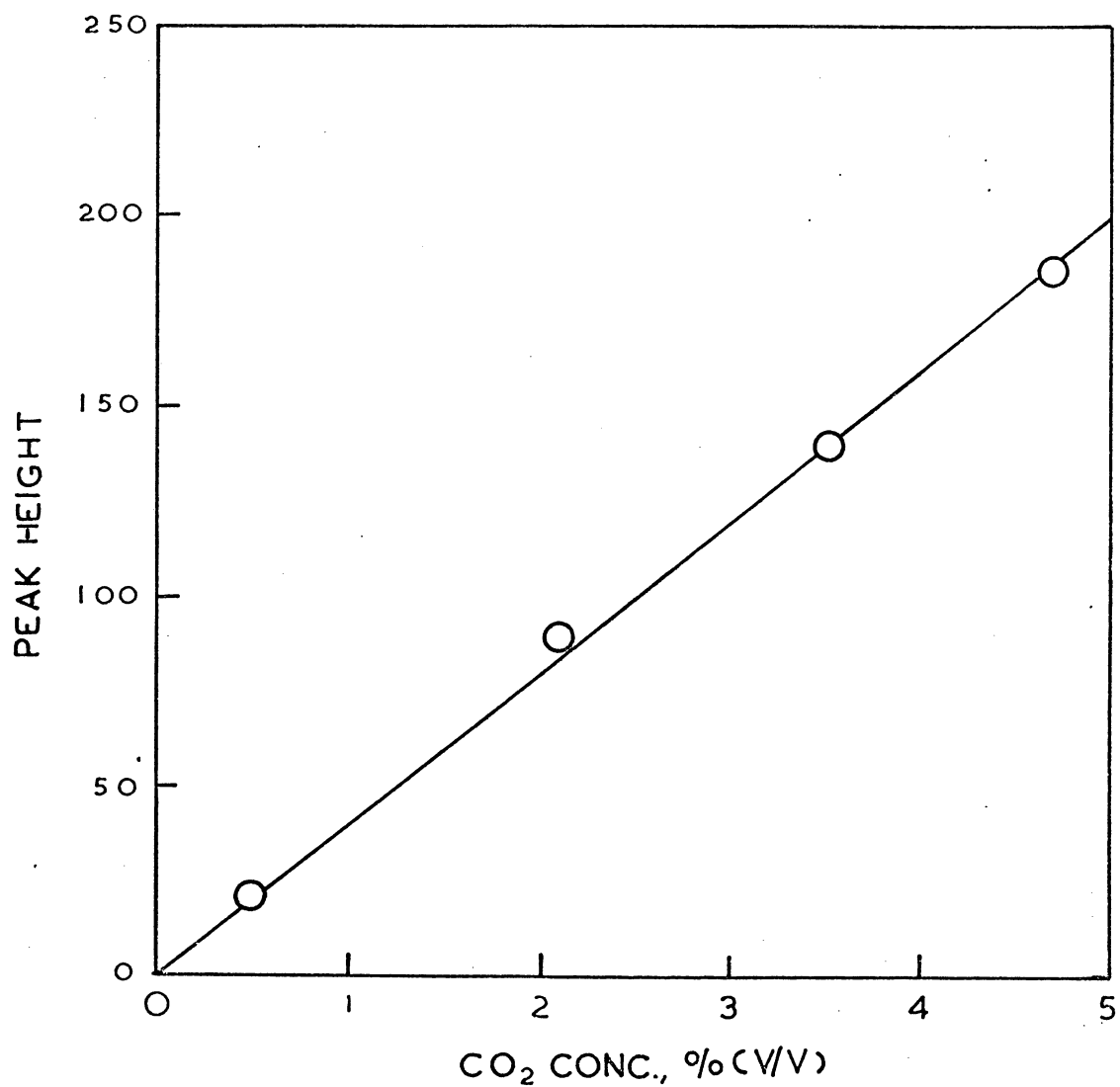
Flow Rate: 20 ml/min

Fig. D.7 Carbon Dioxide Calibration Curve

G.C.:	Fisher Partitioner
ATT. Factor:	4 (25% sensitivity)
Sample Size:	2 ml
Col. Temp.:	20°C
Carrier Gas:	Helium
Flow Rate:	80 ml/min
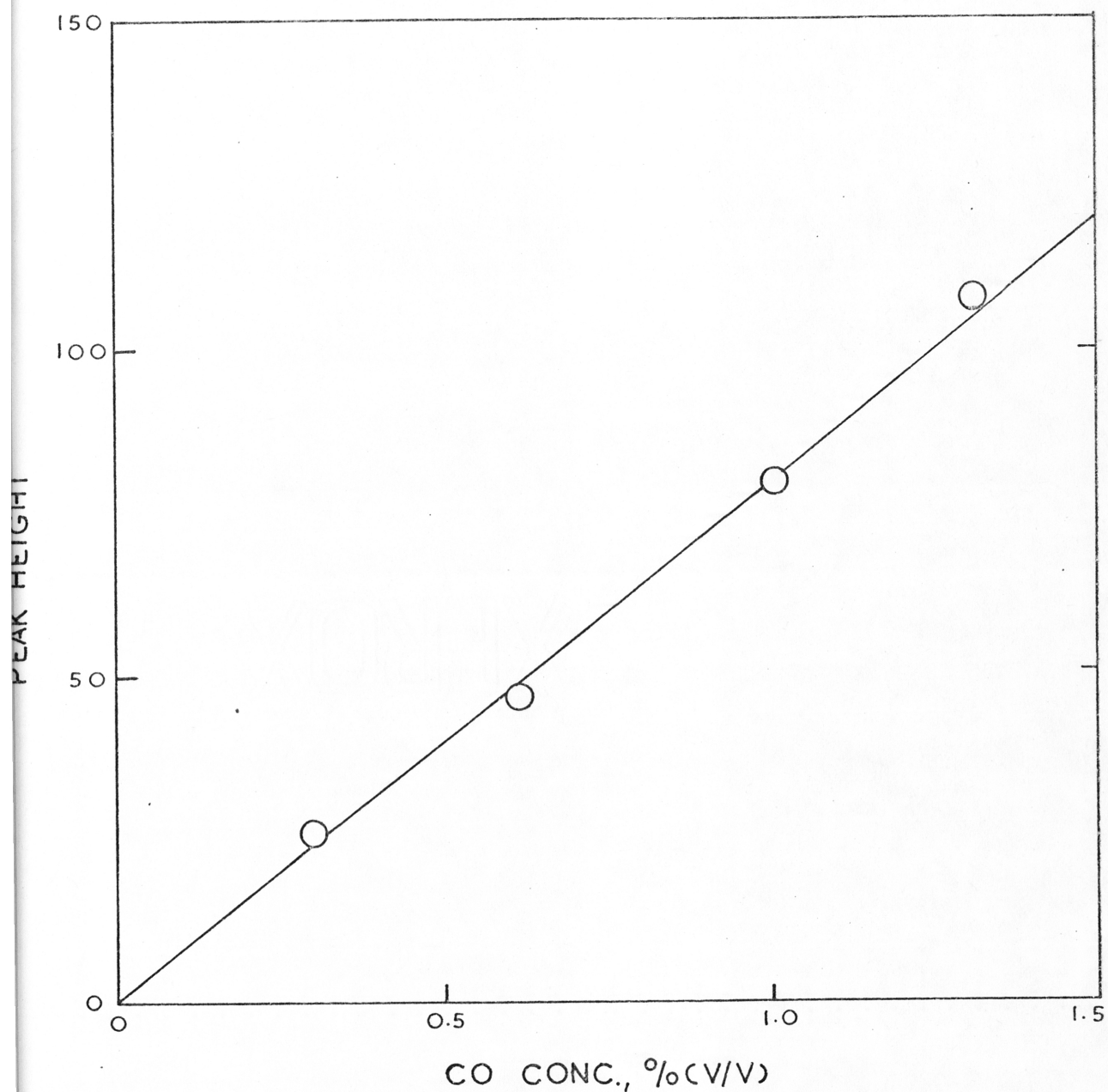
Fig. D.8   Carbon Monoxide Calibration Curve

G.C.:	Fisher Partitioner
ATT. Factor:	100% sensitivity
Sample Size:	2 ml
Col. Temp.:	20°C
Carrier Gas:	Helium
Flow Rate:	80 ml/min

APPENDIX E

EXPERIMENTAL RESULTS OBTAINED FROM SO_2

REDUCTION WITH ACTIVATED CARBON, BROWN

COAL AND ANTHRACITE IN THE SPOUTED BED.

TABLE E.1 REACTION OF SO_2 WITH ACTIVATED CARBON IN A SPOUTED BED

Initial SO_2 Conc. V/v %	Reaction Temp. °C	Contact Time, sec	Reaction Time, min	Outlet Gas Composition, v/v %				SO_2 as % feed SO_2	COS as % feed SO_2
				SO_2	CO_2	CO	COS		
3.84	712	0.079	8	2.530	1.152	0.108	–	65.88	–
			12	2.634	0.742	0.063	–	68.59	–
			16	2.910	0.681	0.072	–	75.78	–
			20	3.218	0.602	0.063	–	83.80	–
			26	3.220	0.575	0.063	–	84.11	–
			30	3.230	0.523	0.073	–		–
3.84	712	0.065	3.0	2.759	0.600	0.193	–	71.85	–
			8	3.065	0.700	0.106	–	79.82	–
			12	3.740	0.528	0.007	–	85.93	–
			16	3.300	0.575	0.005	–	89.32	–
			22	3.430	0.376	0.006	–	89.32	–
			30	3.720	0.311	0.006	–	96.87	–
3.84	801	0.085	3.0	0.335	1.890	0.147	–	8.72	–
			6.0	1.173	1.790	0.130	0.047	30.55	1.22
			10	1.638	2.060	0.112	0.046	42.66	1.20
			15.5	1.654	1.850	0.113	0.046	43.07	1.20
			22	1.561	1.900	0.113	0.041	40.65	1.07
			32	1.553	1.880	0.112	0.041	40.44	1.07
7.12	917	0.078	1	0.171	1.659	2.91	0.035	2.40	0.05
			2	0.129	3.41	4.43	0.160	1.81	2.25
			4	0.163	3.83	4.23	0.848	2.30	11.91
			8	0.299	4.31	3.73	1.710	4.20	24.02
			14	0.094	4.405	3.63	1.700	1.32	24.00
			20	0.123	4.42	3.59	1.760	1.73	24.72

TABLE E.2   REACTION OF SO_2 WITH ANTHRACITE AT 700°C

SO_2 IN   =   3.62 %

REACTION	OUTLET GAS COMPOSITIONS (v/v %)					
TIME (MIN.)	H_2S	COS	SO_2	H_2	CO_2	CO
10	–	–	3.573	0.070	0.044	0.043
20	–	–	3.554	0.097	0.044	0.043
30	–	–	3.573	0.131	0.072	0.066
40	–	–	3.629	0.143	0.061	0.065
60	–	–	3.581	0.062	0.080	0.043
90	–	–	3.484	0.083	0.044	–
120	–	–	3.598	0.053	0.044	–
150	–	–	3.573	0.046	0.043	–
180	–	–	3.598	0.040	0.043	–
212	–	–	3.546	0.012	0.056	–
240	–	–	3.554	0.006	0.070	–
305	–	–	3.601	–	0.078	–

TABLE E.3   REACTION OF SO_2 WITH ANTHRACITE AT 810°C

SO_2 IN = 3.58 %

REACTION TIME (MIN.)	OUTLET GAS COMPOSITION (v/v %)					
	H_2S	COS	SO_2	H_2	CO_2	CO
10	–	–	3.452	0.177	0.109	0.065
22	–	–	3.451	0.194	0.109	0.065
30	–	–	3.488	0.227	0.167	0.096
40	–	–	3.467	0.045	0.130	0.082
60	–	–	3.388	0.026	0.152	0.088
90	–	–	3.311	0.017	0.252	0.097
120	–	–	3.400	0.017	0.234	0.096
150	–	–	3.402	0.017	0.392	0.128
180	–	–	3.397	0.017	0.431	0.144
210	–	–	3.399	–	0.427	0.166
240	–	–	3.389	–	0.412	0.186
300	–	–	4.011	–	0.388	0.161

TABLE E.4   REACTION OF SO_2 WITH ANTHRACITE AT 900°C
SO_2 IN = 3.54 %

REACTION	OUTLET GAS COMPOSITION (v/v %)					
TIME (MIN.)	H_2S	COS	SO_2	H_2	CO_2	CO
10	–	–	3.386	0.184	0.113	0.087
20	–	–	3.379	0.217	0.173	0.115
30	–	–	3.284	0.256	0.236	0.230
40	–	0.013	3.182	0.022	0.387	0.322
60	–	0.013	3.002	0.007	0.394	0.341
90	–	0.019	2.971	0.004	0.462	0.341
120	–	0.026	2.994	0.002	0.495	0.397
150	–	0.021	2.978	0.002	0.508	0.394
180	–	0.099	3.012	–	1.340	0.676
210	–	0.023	2.899	–	0.437	0.349
245	–	0.072	2.976	–	0.472	0.409
300	–	0.004	2.985	–	0.488	0.225

E.5a REACTION OF SO_2 WITH BROWN COAL AT 700°C

SO_2 IN = 3.60 %

REACTION	OUTLET GAS COMPOSITIONS (v/v %)						
TIME (MIN.)	H_2S	COS	SO_2	H_2	CO_2	CO	CH_4
10	–	0.011	2.180	0.055	1.108	0.278	0.312
20	0.054	0.023	1.465	0.063	1.995	0.350	0.420
30	0.119	0.056	0.634	0.073	2.562	0.285	0.374
40	–	0.065	0.461	0.018	2.216	0.284	–
60	–	0.020	1.292	0.011	1.768	0.062	–
90	–	–	2.124	0.025	1.120	–	
120	–	–	2.592	0.002	0.724	–	
150	–	–	2.818	–	0.468	–	
180	–	–	2.857	–	0.261	–	
210	–	–	3.369	–	0.154	–	
240	–	–	3.385	–	0.136	–	
300	–	–	3.521	–	0.071	–	

TABLE E.5b   REACTION OF SO_2 WITH BROWN COAL AT 700°C

INITIAL SO_2 CONC. = 3.60 %

REACTION TIME, MIN.	SO_2 CONV. %	H_2S AS % FEED SO_2	COS AS % FEED SO_2	CO_2/CO
10	39.49	–	0.31	3.986
20	59.31	1.50	0.64	5.70
30	82.39	3.34	1.55	8.99
40	87.19	–	1.83	7.80
60	64.11	–	0.56	28.52
90	41.00	–	–	–
120	27.97	–	–	–
150	21.72	–	–	–
180	20.64	–	–	–
210	6.42	–	–	–
240	5.97	–	–	–
300	2.19	–	–	–

TABLE E.6a   REACTION OF SO_2 WITH BROWN COAL AT 810°C

INITIAL SO_2 CONC. = 4.31 %

REACTION	OUTLET GAS COMPOSITION (v/v %)						
TIME, MIN.	H_2S	COS	SO_2	H_2	CO_2	CO	CH_4
10	0.015	0.039	2.134	0.313	2.060	0.340	0.312
20	0.500	0.128	1.218	0.344	2.712	0.844	0.324
30	0.462	0.174	0.235	0.447	3.572	1.875	0.341
40	-	0.340	0.631	0.091	2.463	1.630	-
60	-	0.206	1.956	0.002	2.255	0.924	-
90	-	0.071	2.980	-	1.109	0.334	-
120	-	-	3.541	-	0.541	0.243	-
135	-	-	3.621	-	0.531	0.206	-

TABLE E.6b   <u>REACTION OF SO_2 WITH BROWN COAL AT 810°C</u>
<u>INITIAL SO_2 CONC. = 4.31%</u>

REACTION TIME, MIN.	SO_2 CONV. %	H_2S AS % FEED SO_2	COS AS % FEED SO_2	CO_2/CO
10	50.39	0.35	0.91	6.06
20	71.76	11.62	2.97	3.21
30	94.55	10.72	4.04	1.91
40	85.36	-	7.90	1.51
60	54.58	-	4.80	2.44
90	31.51	-	1.64	3.32
120	17.84	-	-	2.23
135	15.99	-	-	2.58

TABLE E.7a   REACTION OF SO_2 WITH BROWN COAL AT 900°C

SO_2 IN = 4.12%

REACTION TIME (MIN)	OUTLET GAS COMPOSITIONS (v/v %)						
	H_2S	COS	SO_2	H_2	CO_2	CO	CH_4
10	–	0.072	1.733	0.212	1.695	2.023	0.207
20	0.022	0.111	0.833	0.275	1.859	2.707	0.208
30	0.081	0.130	0.151	0.311	1.993	3.230	0.214
40	–	0.044	2.349	0.015	0.967	0.974	–
60	–	0.019	2.992	0.003	0.737	0.534	
90	–	0.016	3.390	0.003	0.635	0.402	
120	–	0.014	3.284	0.002	0.569	0.301	
158	–	0.004	3.508	–	0.518	0.233	
200	–	–	3.580	–	0.471	0.266	
240	–	–	3.632	–	0.520	0.264	
300	–	–	3.724	–	0.519	0.259	

TABLE E.7 b <u>REACTION OF SO_2 WITH BROWN COAL AT 900°C</u>

<u>INITIAL SO_2 CONC. = 4.12 %</u>

REACTION TIME, MIN.	SO_2 CONV. %	H_2S AS % FEED SO_2	COS AS % FEED SO_2	CO_2/CO
10	57.94	-	1.75	0.838
20	79.78	0.54	2.71	0.687
30	96.34	1.97	3.16	0.617
40	42.99	-	1.67	0.993
60	27.38	-	0.46	1.38
90	17.72	-	0.39	1.58
120	20.29	-	0.34	1.89
158	14.85	-	0.10	2.223
200	13.11	-	-	1.771
240	11.84	-	-	1.97
300	9.61	-	-	2.00

APPENDIX F

ESTIMATION OF THE SIGNIFICANCE OF
THE RATE OF MASS TRANSFER IN THE
SO_2 - C REACTION

F.1   Estimation of Diffusion Coefficient
for Binary Gas Mixture

F.2   Estimation of Mass Transfer Rate
in a Fluidized Bed

F.1 ESTIMATION OF DIFFUSION COEFFICIENT FOR BINARY GAS

   MIXTURE

Assumptions: (1) Carbon particles are surrounded by
                 a film of nitrogen gas.

             (2) Ideal gas law holds.

Now using the theoretical equation based on the modern

Kinetic Theory and the Lennard-Jones expression for inter

molecular forces (58) we have,

$$D_{12} = \frac{0.001858 \ T^{3/2} \ [(M_1 + M_2)/M_1 M_2]^{1/2}}{P\sigma^2_{12} \ \Omega_D} \qquad \dots \dots D.1$$

Where D_{12} = Binary diffusivity cm^2/sec

      M_1, M_2 = Molecular weight, gm

      P = Pressure, atm

      T = Temperature, °K

      σ_{12} = Collision diameter, Angstrom Unit

      Ω_D = Collision integral, dimensionless

From Table 1.3 (58)

              SO_2 : σ_1 = 4.120 ξ_1/K = 335.4

              N_2 : σ_2 = 3.798 ξ_2/K = 71.4

Where ξ_1 , ξ_2 = Maximum attractive energy

          K = Boltzman's constant

             = 1.38 x 10^{-16} ergmol^{-1} °K^{-1}

So,

          σ_{12} = $1/2$ ($\sigma_1 + \sigma_2$) $\dots \dots D.2$

             = 3.955

and

$$\xi_1 = 4.63 \times 10^{-14}$$

$$\xi_2 = 9.86 \times 10^{-15}$$

SO

$$\xi_{12} = \sqrt{\xi_1 \; \xi_2}$$

$$= 2.08 \times 10^{-15} \qquad \ldots\ldots D.3$$

(i)　　AT　　T = 933°K

$$KT/\xi_{12} = 61.9$$

Therefore from Table 1.2 (58)

$$\Omega_D = 0.5583$$

Hence,

$$D_{12} = \frac{0.001858 \; (933)^{3/2} \, [(28+64)/(28\times64)]^{1/2}}{1.0 \times 3.955^2 \times 0.5583}$$

$$= 1.373 \; cm^2/sec$$

(ii)　　AT　　T = 1173°K

$$KT/\xi_{12} = 77.05$$

$$\Omega_D = 0.5377$$

Hence,

$$D_{12} = 2.1 \; cm^2/sec$$

F.2　ESTIMATION OF MASS TRANSFER RATE IN A FLUIDIZED BED

The method given in Reference (57) was used.

(i)　　Data:　P = Pressure = 1.0 atm

T = Temperature = 1173°K

Feed = 4.0% SO_2 in N_2

M_{SO_2} = Molecular weight of SO_2

= 64 gm

U_s = Spouting gas velocity

= 36.6 cm/sec

A = Cross-sectional area

= 11.4 cm^2

D = Column diameter

= 4 cm

H = Bed height

= 6.5 cm

μ_{SO_2} = SO_2 viscosity

= 0.0 44 cps

μ_{N_2} = N_2 viscosity

= 0.054 cps

dp = Particle diameter

= 0.1 cm

E = Voidage of bed

= 0.5

ρ_m = Density of gas mixture

ρ_p = 2.955 x 10^{-4} gm/cm^3

= Density of particle = 1.69 gm/cm^3

(ii) Particle Reynolds Number:

$$N_{Re} = \frac{dp\ G}{\mu(1 - E)}$$

= 4.08

where G = Mass flow rate

(iii) Schmidt Number:

$$N_{sc} = \frac{\mu}{\rho_m D_{12}}$$

= 0.873

(iv) Chilton-Colburn factor:

$$j_D = \frac{K_G \rho}{G} (N_{SC})^{2/3}$$
$$= 5$$

$\therefore \quad K_G$ = Mass transfer coeff.

$$= 2.086 \times 10^{-3} \text{ gm.mole} / \text{sec·cm}^2 \cdot \text{atm}$$

The rate of reactant transfer from the gas stream

per unit carbon particle surface is (assumed 95%

conversion of SO_2):

$$\frac{\text{Rate of reactant transfer}}{\text{Carbon surface area}}$$

$$= 0.000381 \times 0.04 \times 0.95$$

$$= 4.4 \times 10^{-8} \text{ gm.mole} / \text{sec. cm}^2$$

Hence the partial pressure difference needed to

cause transport of reactant at this rate is:

$$\frac{4.4 \times 10^{-8}}{2.086 \times 10^{-3}} = 2.11 \times 10^{-5} \text{ atm}$$

Available reactant potential in the effluent is

$$(1 - 0.95) \times 0.04 = 0.002 \text{ atm}$$

Since only 0.03% of the available potential is required

for mass transport, therefore mass transfer is negligible.

APPENDIX G

COMPUTER PROGRAMME FOR THE

THEORETICAL ANALYSIS OF THE

SO_2-C REACTION IN A SPOUTED BED

G.1   Computer Programme

G.2   Typical Printout

G.1 COMPUTER PROGRAMME

```
       C     THEORETICAL ANALYSIS FOR SO2 REDUCTION IN A
       C     SPOUTED BED USING A TWO-REGION MODEL
       C     THE FOURTH-ORDER RUNGE-KUTTA ITERATION SCHEME
       C     IS USED FOR SOLVING THE SYSTEM EQUATIONS
       C     ***
       C     INDEPENDENT VARIABLE
       C     ***
       C     Z=BED HEIGHT
       C     ***
       C     DEPENDENT VARIABLES
       C     ***
       C     CS=CONCENTRATION OF SO2 IN THE SPOUT
       C     CA=SO2 CONCENTRATION IN ANNULUS
       C     ***
       C     SYSTEM, S HYDRODYNAMIC PARAMETERS
       C     ***
       C     DC=COLUMN DIAMETER
       C     DP=PARTICLE DIAMETER
       C     DI=GAS INLET ORIFICE DIAMETER
       C     DS=SPOUT DIAMETER
       C     SDNSTY=PARTICLE DENSITY
       C     FDNSTY=FLUID DENSITY
       C     BDNSTY=BULK DENSITY
       C     H=TOTAL BED HEIGHT
       C     KR=REACTION RATE CONSTANT
       C     EO=AVERAGE BED VOIDAGE
       C     ES=SPOUT VOIDAGE
       C     US=SPOUTING VELOCITY
       C     VO=GAS VOLUMETRIC FLOW RATE
       C     T=REACTION TEMPERATURE
       C     G=GAS MASS RATE PER UNIT BED CROSS-SECTIONAL AREA
       C     AC=COLUMN CROSS SECTIONAL AREA
       C     AA=ANNULUS CROSS SECTIONAL AREA
       C     AS=SPOUT CROSS SECTIONAL AREA
       C     SUS=SPOUTING VELOCITY IN THE SPOUT
       C     UMF=MINIMUM FLUIDISATION VELOCITY
       C     US=SUPERFICIAL GAS VELOCITY IN THE ANNULUS
       C     UAH=SUPERFICIAL GAS VELOCITY AT Z=H
       C     EMU=VISCOSCITY OF THE GAS
       C     HM=MAXIMUM SPOUTABLE BED HEIGHT
       C     LAMBDA=PARTICLE SHAPE FACTOR
       C     *************
       C
0001         DIMENSION DCSDZ(5),DCADZ(5),COMENT(20),DZ(5)
0002         READ 2007,KOUNT
0003    2007 FORMAT(15)
0004         READ 2000,DZ(1)
0005         READ 2000,ESL,DES
0006         READ 2000,PAMBDA,EKO,ACTENG,BDNSTY,SDNSTY
0007    1016 READ 2005,COMENT
0008    2005 FORMAT (20A4)
0009         PRINT 2006,COMENT
0010    2006 FORMAT(1H1,8X,20A4,/)
0011         READ 2000,ES
0012         READ 2000,CO,VO,H,TR,HM
```

G.1   COMPUTER PROGRAMME CONT.

```
0013           READ 2000,VISCO,EO,DC,DI,DP
0014           PRINT 2001,DZ(I),CO,VO,H,TR,VISCO,EKO
0015           PRINT 2002,ACTENG,BDNSTY,SDNSTY,DC,DI,DP
0016    2000 FORMAT (5E15.8)
0017    2001 FORMAT(1H ,8X,20HITERATION STEP SIZE=,F8.4,/,
          18X,3HCO=E15.5,5X,4H V0=E12.5,5X,2HH=,E12.5,6X,/,
          28X,3HTR=,E12.5,5X,6HVISCO=,E12.5,2X , 4HEKO=,
          3E12.5,4X,/)
0018    2002 FORMAT(1H, 8X, 7HACTENG=,E12.5,1X,7HBDNSTY=E
          112.5,1X,7HSDNSTY=,E12.5,/,8X,3HDC=,E12.5,5X,
          23HDI=,E12.5,5X,3HDP=,E12.5,/)
        C     DEFINE HYDRODRODYNAMIC PARAMETERS INDEPENDENT
        C     OF COLUMN HEIGHT
        C
0019           TEM=TR+273.0
0020           FDNSTY=0.00117*273./TEM
0021           G=16.667*TEM*VO*4.0/(298.*3.1416*DC*DC)*FDNSTY
0022           DS=1.4
0023           AS=3.1416*DS**2/4.0
0024           A=980.665*FDNSTY*(DP*EO)**3
0025           B=150.*VISCO*(1.0-EO)
0026           UMF=2.0*A*SQRT(SDNSTY)/(FDNSTY* DP *B*(1.0+
          1SQRT(1.0+7.0*A/B**2)))
0027           UAH=UMF*(H/HM)
0028           RXC=EKO*2.719**(-ACTENG/(1.987*TEM))
0029           PRINT 2008,DS,UMF,HM
0030    2008 FORMAT(8X,3HDS=,E12.5,5X,4HUMF=,E12.5,4X,3HHM=,
          1E12.5,//)
0031           PRINT 2003
0032    2003 FORMAT(1H ,13X,1HZ,12X,2HCE,10X,4HCONV, 9X,2HCS,
          112X,2HCA,11X,2HES,10X,3HDSS,/)
        C
        C     INITIAL CONDITIONS
0033    2009 CA=CO
0034           C S=CO
0035           Z=0.0
0036           DCS=0.0
0037           DCA=0.0
0038    1000 DCSDZ(1)=.0.0
0039           DCADZ(1)=0.0
        C
0040           DO 1005 K=1,10
0041           Z=Z+DZ(1)
004..   C
        C     DEFINE COLUMN HEIGHT DEPENDENT HYDRODYNAMIC
        C     PARAMETERS
        C
0042           IF(Z-0.3*H) 1020,1021,1021
0043    1020 ZOS=DI*H/(2.0*DS)
0044           TAN=DI/(2.0*ZOS)
0045           DSS=2.0*TAN*(ZOS+Z)
0046           ASS=3.1416*DSS*DSS/4.0
0047           GO TO 1022
0048    1021 DSS=DS
```

G.1 <u>CONT.</u>

```
0049            ASS=AS
0050       1022 IF(Z-2.86) 1006,1006,1014
0051       1014 IF(Z-H)1007,1007,1008
0052       1006 ZO=3.41*DI/DC
0053            DAN=DI/(2.0*ZO)
0054            DCC=2.0*DAN*(Z+ZO)
0055            AC=3.1416*DCC*DCC/4.0
0056            US=16.667*TEM*VO/(298.*AC)
0057            AA=AC-ASS
0058            UA=UAH*(1.0-(1.0-(Z/H))**3)
0059            GO TO 1023
0060       1007 UA=UAH*(1.0-(1.0-(Z/H))**3)
0061            AC=3.1416*DC*DC/4.0
0062            US=16.667*TEM*VO/(298.*AC)
0063       1023 USS=(US*AC-UA*AA)/ASS
           C
           C    START RUNGE-KUTTA ITERATION
           C
0064            DO 1001 L=2,5
0065            GO TO(1002,1002,1002,1002,1003),L
0066       1002 X=2.0
0067            GO TO 1004
0068       1003 X=1.0
0069       1004 CS=CS+DCSDZ(L-1)/X
0070            CA=CA+DCADZ(L-1)/X
0071            ABCA=ABS(CA)
0072            IF(CO-ABCA) 1026,1027,1027
0073       1026 CA=CO
0074       1027 AK=RXC*CS*(1.0-ES)/USS
0075            BK=(( 3.*UAH*(1.0-Z/H)**2/H+6.283*UA*(( DAN )
                1**2*(Z + ZO )-TAN*TAN*(Z+ZOS))/AA)*(CA-CS) +
                2RXC*(1.0-EO)*CA)/UA
0076            DCSDZ(L)=-DZ(1)*AK
0077            DCADZ(L)=-DZ(1)*BK
0078       1001 CONTINUE
           C
0079            DCA=(DCADZ(2)+2.0*DCADZ(3)+2.0*DCADZ(4)+
                1DCADZ(5))/6.0
0080            DCS=(DCSDZ(2)+2.0*DCSDZ(3)+2.0*DCSDZ(4)+
                1DCSDZ(5))/6.0
0081            CS=CS+DCS
0082            CA=CA+DCA
0083       1005 CONTINUE
           C
           C    HERE INTEGRATE SPOUT REGION ONLY
           C    AND CHECK END OF ITERATION
           C
0085       1008 UA=UAH
0086            USS=(US*AC-UA*AA)/ASS
0087            SH=1.25*H
0088            IF(Z-SH)1019,1019,1017
0089       1019 DO 1009 K=1,10
0090            DO 1009 K=1,10
0091            DO 1010 L=2,5
0092            GO TO (1011,1011,1011,1011,1012),L
```

G.1 <u>CONT.</u>

```
0093    1011 X=2.0
0094         GO TO 1013
0095    1012 X=1.0
      C
0096     1013 CS=CS+DCSDZ(L-1)/X
0097          AK=RXC*(1.-ES)*CS/USS
0098          DCSDZ(L)=-DZ(1)*AK
0099     1010 CONTINUE
      C
0100          Z=Z+DZ(1)
0101          DCS=(DCSDZ(2)+2.0*DCSDZ(3)+2.0*DCSDZ(4)+
             1DCSDZ(5))/6.0
0102          CS=CS+DCS
0103     1009 CONTINUE
      C
      C      CALCULATE EXIT CONCENTRATION AND CONVERSION
      C      OF SO2
0104     1015 CE=(UA *AA*CA+USS*ASS*CS)/(US*AC)
0105          CONV=1.0-CE/CO
      C
      C      PRINT DATA
      C
0106          PRINT 2004,Z,CE,CONV,CS,CA,ES,DSS
0107     2004 FORMAT (1H, 7X,7(E12.5,1X))
0108          GO TO 1000
      C
      C      CHECK END OF DATA
      C
0109     1017 IF(ES- ESL) 1024,1025,1025
0110     1024 ES=ES+DES
0111          GO TO 2009
0112     1025 KOUNT=KOUNT-1
0113          IF(KOUNT)3000,3000,1016
0114     3000 STOP
0115          END
```

G.2 TYPICAL COMPUTER PRINTOUT OF RESULTS

```
SO2 REDUCTION WITH CARBON IN A SPOUTED BED AT 770°C
ITERATION STEP SIZE = 0.0100
CO=    0.27540E=-05      VO=0.88000E 01        H=0.70000E  01
TR= 0.77000E  03      VISCO=0.45000E-03 EKO=0.70600E  10


ACTENG=  0.41550E  05  BDNSTY =  0.27550E  00  SDNSTY= 0.50400E  00
DC=  0.39132E  01      DI= 0.63300E  OO    DP=  0.10300E 00
DS=  0.26790E  01      UMF= 0.18065E  02    HM=  0.75400E 01
```

Z	CE	CONV	CS	CA	ES	DSS
0.10000E 00	0.27528E-05	0.43201E-03	0.27529E-05	0.18325E-05	0.86000E 00	0.70954E 00
0.20000E 00	0.27512E-05	0.10050E-02	0.27515E-05	0.18464E-05	0.86000E 00	0.78609E 00
0.30000E 00	0.27492E-05	0.17474E-02	0.27498E-05	0.18543E-05	0.86000E 00	0.86263E 00
0.40000E 00	0.27466E-05	0.26780E-02	0.27478E-05	0.18579E-05	0.86000E 00	0.93918E 00
0.50000E 00	0.27435E-05	0.38183E-02	0.27454E-05	0.18585E-05	0.86000E 00	0.10157E 01
0.60000E 00	0.27397E-05	0.51938E-02	0.27427E-05	0.18566E-05	0.86000E 00	0.10923E 01
0.70000E 00	0.27352E-05	0.68229E-02	0.27395E-05	0.18527E-05	0.86000E 00	0.11688E 01
0.80000E 00	0.27300E-05	0.87268E-02	0.27359E-05	0.18473E-05	0.86000E 00	0.12454E 01
0.90000E 00	0.27239E-05	0.10930E-01	0.27319E-05	0.18405E-05	0.86000E 00	0.13219E 01

Z	CE	CONV	CS	CA	ES	DSS
0.13000E 01	0.26934E-05	0.22016E-01	0.27134E-05	0.18041E-05	0.87000E 00	0.16281E 01
0.14000E 01	0.26828E-05	0.25843E-01	0.27070E-05	0.17926E-05	0.87000E 00	0.17046E 01
0.15000E 01	0.26712E-05	0.30073E-01	0.27000E-05	0.17803E-05	0.87000E 00	0.17811E 01
0.16000E 01	0.26584E-05	0.34725E-01	0.26923E-05	0.17673E-05	0.87000E 00	0.18577E 01
0.16999E 01	0.26443E-05	0.39817E-01	0.26840E-05	0.17535E-05	0.87000E 00	0.19342E 01
0.17999E 01	0.26291E-05	0.45367E-01	0.26750E-05	0.17391E-05	0.87000E 00	0.20107E 01
0.18999E 01	0.26125E-05	0.51389E-01	0.26652E-05	0.17240E-05	0.87000E 00	0.20873E 01
0.19999E 01	0.25945E-05	0.57902E-01	0.26546E-05	0.17083E-05	0.87000E 00	0.20873E 01
0.20999E 01	0.25752E-05	0.64921E-01	0.26432E-05	0.16919E-05	0.87000E 00	0.22404E 01
0.21999E 01	0.25544E-05	0.72459E-01	0.26309E-05	0.16749E-05	0.87000E 00	0.23169E 01

APPENDIX H

CORRELATION OF SOLIDS MIXING DATA

H.1   INTRODUCTION

The particle age distribution data obtained from the
solids mixing study were analysed statistically using
a linear regression method. This is a least squares
method and was written as a subroutine computer
programme.

The raw data (see Table H.1) obtained from the experi-
ment were firstly treated by a main programme, making
them ready for subsequent correlating process using the
subroutine.

H.2 THE MAIN PROGRAMME

```
##FORX52
 LIST PRINTER
  J.FOONG,CHEM.ENG.,POST GRADUATE


C     LINEAR REGRESSION OF SOLIDS MIXING DATA
C     TMEAN IS THE MEAN RESIDENCE TIME
C     TRA IS THE OUTLET TRACER WEIGHT
C     SAM IS THE SAMPLE WEIGHT
C     ADI IS THE INTERNAL AGE DISTRIBUTION
C     EADI IS THE ANTILOG OF ADI
C     F IS THE EXTERNAL AGE DISTRIBUTION
C     DT IS THE DIMENSIONLESS TIME

      DIMENSION F(80), ADI(80), TRA(80), SAM(80), EADI(80)
     1DT(80)
 4000 READ, N
      IF (N), 2000,2000,1000
 1000 CONTINUE
      READ,(DT(I),I=1,N)
      READ,(SAM(I),I=1,N)
      READ,(TRA(I),I=1,N)
C
      PRINT 9
    9 FORMAT (1H1)
      PRINT, (SAM(I),I=1,N)
      PRINT, (TRA(I),I=1,N)
      PRINT 10
   10 FORMAT (1H1,38HINTERNAL AGE DISTRIBUTION VS. DIMEN·
     1SIONLESS TIME)
      PRINT 6
    6 FORMAT (1HO,12X,2HDT,12X,4H ADI,//)
C     DO REGRESSION
      DO 3000 I=1,N
      F(I)=TRA(I)/SAM(I)
      ADI(I)=1.0-F(I)
      PRINT 8, DT(I), ADI(I)
    8 FORMAT (1H,2(F15.8))
      ADI(I)=LOG(ADI(I))
 3000 CONTINUE
C
      CALL LINREG(ADI,DT,N)
      GO TO 4000
 2000 CALL EXIT
      END
```

H.3 THE SUBROUTINE - LINREG

```
      SUBROUTINE LINREG(Y,X,N)
      DIMENSION Y(I),X(I)
      SUMX=0.
      SUMY=0.
      SUMXY=0.
      SUMXX=0.
      SUMYY=0.
      DO 1 I=1,N
      SUMX=SUMX+X(I)
      SUMY=SUMY+Y(I)
      SUMXY=SUMXY+X(I)*Y(I)
      SUMXX=SUMXX+X(I)*X(I)
1     SUMYY=SUMYY+Y(I)*Y(I)
      AN=N
      SXY=SUMXY-(SUMX*SUMY/AN)
      SYY=SUMYY-(SUMY*SUMY/AN)
      SXX=SUMXX-(SUMX*SUMX/AN)
      SSLR=SXY*SXY/SXX
      ANM2=AN-2.
      RESIDS=SYY-SSLR
      REGMS=SSLR
      RESMS=RESIDS/ANM2
      F=REGMS/RESMS
      ANMI=AN-1.
      B=SXY/SXX
      R2=SSLR/SYY
      YMEAN=SUMY/AN
      XMEAN=SUMX/AN
      SE=SQRT(RESIDS/ANM2)
      SB=SE/SQRT(SXX)
      T=B/SB
      A=YMEAN-B*XMEAN
      ONE=1.
      NONE=ONE
      PRINT 3
3     FORMAT(1H1,20HANALYSIS OF VARIANCE)
      PRINT 4
4     FORMAT(1H0,13X,2HSS,11X,2HDF,4X,2HMS,13X,1HF)
      PRINT 5, SSLR,NONE,REGMS,F
5     FORMAT(1H,10HREGRESSION,1X,E14.7,1X,I3,1X,E14.7,1X,E14.7)
      NANM2=ANM2
      PRINT 6,RESIDS,NANM2,RESMS
6     FORMAT(1H ,8HRESIDUAL,3X,E14.7,1X,I3,IX,E14.7)
      NANMI=ANMI
      PRINT 7,SYY,NANM1
7     FORMAT(1HO,5HTOTAL,6X,E14.7,1X,I3)
      PRINT 8,A,B,R2,R,SE,SB,T
8     FORMAT(1HO,3HA= ,F20.5,4H B=   ,F20.5/
     11H ,12HR(SQUARED)= ,F8.5,4H R= ,F8.5/
     21H ,29HSTANDARD ERROR OFESTIMATE = ,E14.7/
     31H ,22HSTANDARD ERROR OF B = ,E14.7/
     41H ,16HT VALUE FOR B = , E14.7)
```

H.3 CONT.

```
    PRINT 9
9   FORMAT (1H1,12X,1HX,19X,1HY,15X,12HY CALCULATED,16X,
   114HY-Y CALCULATED)
    DO  10 I=1,N
    YC=A+B*X(I)
    YDIFF=Y(I)-YC
10  PRINT 11,X(I),Y(I),YC,YDIFF
11  FORMAT(1H ,4E20.7)
    RETURN
    END
```

H.4 TYPICAL PRINTOUT AND EXPERIMENTAL DATA

H.4.1 TYPICAL COMPUTER PRINTOUT

(A) INTERNAL AGE DISTRIBUTION VS. DIMENSIONLESS TIME FOR WHEAT PARTICLES

DT	EADI
.04600	.89158
.21600	.76344
.34500	.65877
.43100	.59717
.69000	.43154
.69300	.29042
1.20600	.23084
1.38000	.20837
1.55200	.14832
1.72500	.11109
1.81000	.13141
.06500	.89809
.13100	.81407
.19600	.75398
.42600	.55858
.58900	.49569
.78500	.35062
.98200	.28568
1.17800	.20584
1.37300	.19726
1.57000	.15070
1.76500	.13098
1.90000	.11276
.09400	.90528
.16400	.84554
.23400	.77963
.42100	.63920
.60900	.51520
.79700	.43220
.98300	.34434
1.17100	.26096
1.35700	.23445
1.54500	.16063
1.73500	.16161
1.92000	.10218
1.94500	.11169
.05900	.94895
.11800	.89710
.17700	.82690
.35400	.68405
.53000	.56670
.70700	.43396
.88300	.35929
1.06000	.29878
1.23700	.23676
1.41400	.20124
1.59000	.16933
1.76800	.13518

H.4.1TYPICAL COMPUTER PRINTOUT CONT.

(B)   ANALYSIS OF VARIANCE (WHEAT PARTICLES)

	SS	DF	MS	F
REGRESSION	2.3791625E+01	1	2.3791825E+01	2.5472571E+03
RESIDUAL	4.2964800E-01	46	9.3401739E-03	
TOTAL	2.4221473E+01	47		

A=   -.02841 B=   -1.14573
R(SQUARED)=   .98226 R=   .99109
STANDARD ERROR OF ESTIMATE = 9.6644575E-02
STANDARD ERROR OF B = 2.2701205E-02
T VALUE FOR B = -5.0470356E+01

(C)

X	Y	Y CALCULATED	Y-Y CALCULATED
4.6000000E-02	-1.1475652E-01	-8.1123043E-02	-3.3633480E-02
2.1600000E-01	-2.6991497E-01	-2.7589848E-01	5.9835100E-03
3.4500000E-01	-4.1737732E-01	-4.2369867E-01	6.3213500E-03
4.3100000E-01	-5.1554809E-01	-5.2223213E-01	6.6840400E-03
6.9000000E-01	-8.4038927E-01	-8.1897825E-01	-2.1411020E-02
6.9300000E-01	-1.2363933E+00	-8.2241546E-01	-4.1397790E-01
1.2060000E+00	-1.4659947E+00	-1.4101790E+00	-5.5816700E-02
1.3800000E+00	-1.5683953E+00	-1.6095374E+00	4.1142100E-02
1.5520000E+00	-1.9083258E+00	-1.8066043E+00	-1.0172150E-02
1.7250000E+00	-2.1973992E+00	-2.0048169E+00	-1.9258230E-01
1.8100000E+00	-2.0294307E+00	-2.1022046E+00	7.2773900E-02
6.5000000E-02	-1.0748432E-01	-1.0289206E-01	-4.5922600E-03
1.3100000E-01	-2.0570302E-01	-1.7851076E-01	-2.7192260E-02
1.9600000E-01	-2.8237736E-01	-2.5298372E-01	-2.9393640E-02
4.2600000E-01	-5.8235474E-01	-5.1650344E-01	-6.5851300E-02
5.8900000E-01	-7.0179123E-01	-7.0325872E-01	1.4674900E-03
7.8500000E-01	-1.0480340E+00	-9.2782334E-01	-1.2021070E-01
9.8200000E-01	-1.2528514E+00	-1.1535337E+00	-9.9317700E-02
1.1780000E+00	-1.5806133E+00	-1.3780983E+00	-2.0251500E-01
1.3730000E+00	-1.6232164E+00	-1.6015172E+00	-2.1699200E-02
1.5700000E+00	-1.8924409E+00	-1.8272276E+00	-6.5213300E-02
1.7650000E+00	-2.0326487E+00	-2.0506464E+00	1.7997700E-02
1.9000000E+00	-2.1824262E+00	-2.2053211E+00	2.2894900E-02
9.4000000E-02	-9.9506682E-02	-1.3611846E-01	3.6611780E-02
1.6400000E-01	-1.6777720E-01	-2.1632011E-01	4.8542910E-02
2.3400000E-01	-2.4892736E-01	-2.9652176E-01	4.7594400E-02
4.2100000E-01	-4.4753600E-01	-5.1077475E-01	6.3238750E-02

X	Y	Y CALCULATED	Y-Y CALCULATED
6.0900000E-01	-6.6319292E-01	-7.2617348E-01	6.2980560E-02
7.9700000E-01	-8.3886359E-01	-9.4157220E-01	1.0270861E-01
9.8300000E-01	-1.0661083E+00	-1.1546794E+00	8.8571100E-02
1.1710000E+00	-1.3433831E+00	-1.3700781E+00	2.6695000E-02
1.3570000E+00	-1.4505035E+00	-1.5831854E+00	1.3268190E-01
1.5450000E+00	-1.8286361E+00	-1.7985841E+00	-3.0052000E-02
1.7350000E+00	-1.8225086E+00	-2.0162743E+00	1.9386580E-01
1.9200000E+00	-2.2809860E+00	-2.2282358E+00	-5.2750200E-02
1.9450000E+00	-2.1920155E+00	-2.2568793E+00	6.4863800E-02
5.9000000E-02	-5.2389473E-02	-9.6017636E-02	4.3628163E-02
1.1800000E-01	-1.0857712E-01	-1.6361617E-01	5.5039050E-02
1.7700000E-01	-1.9006715E-01	-2.3121470E-01	4.1147550E-02
3.5400000E-01	-3.7971607E-01	-4.3401031E-01	5.4294240E-02
5.3000000E-01	-5.6790915E-01	-6.3566018E-01	6.7751030E-02
7.0700000E-01	-8.3479531E-01	-8.3845579E-01	3.6604800E-03
8.8300000E-01	-1.0236215E+00	-1.0401056E+00	1.6484100E-02
1.0600000E+00	-1.2080193E+00	-1.2429012E+00	3.4881900E-02
1.2370000E+00	-1.4406702E+00	-1.4456968E+00	5.0266000E-03
1.4140000E+00	-1.6032148E+00	-1.6484924E+00	4.5277600E-02
1.5900000E+00	-1.7758798E+00	-1.8501423E+00	7.4262500E-02
1.7680000E+00	-2.0011384E+00	-2.0540837E+00	5.2945300E-02

H.4.2 EXPERIMENTAL DATA

TABLE H.1a

Run No.:   1

Particles: Wheat

Bed Height: 18.9 cm

*Particle Mean

Residence time,

$\bar{t}$ = 23.2 min.

Solids feed rate=1.262 kg/min.

Sample No.	$\bar{\theta} = t/\bar{t}$	Sample wt., gm	Tracer wt., gm
0	0	0	0
1	0.064	49.90	5.41
2	0.216	93.72	22.17
3	0.345	73.47	25.07
4	0.431	59.43	23.94
5	0.690	57.70	32.80
6	0.992	45.14	32.03
7	1.206	68.40	52.61
8	1.380	54.42	43.08
9	1.552	61.62	52.48
10	1.725	57.07	50.73
11	1.810	62.40	54.20

* Particle mean residence time is defined as

$$\bar{t} = t \times m/_F$$

where:

    t=   Time, min.

    F=   Solids feed rate, kg/min.

    m=   Bed change, kg.

TABLE H.1.b

Run No.: 2

Particles   Wheat

Bed Height   19.6 cm

Particle Mean

Residence time   30.59 min.

Solids feed rate   1.407 kg/min.

Sample No.	$\bar{\theta} = t/\bar{t}$	Sample wt., gm	Tracer wt., gm
1	0.065	45.05	4.59
2	0.131	69.06	12.84
3	0.196	76.46	18.81
4	0.426	66.83	29.50
5	0.589	68.55	34.57
6	0.785	67.85	44.06
7	0.982	56.32	40.23
8	1.178	61.21	48.61
9	1.373	86.23	69.22
10	1.570	51.89	44.07
11	1.765	80.16	69.66
12	1.900	78.48	69.03

TABLE H.1.c

Run no: 3

Particles: Wheat

Bed Height: 19.6 cm

Particle Mean

Residence Time: 42.75 min.

Solid Feed Rate: 0.686 kg/min.

Sample No.	$\bar{\theta} = t/\bar{t}$	Sample Wt., gm	Tracer Wt., gm
1	0.094	43.79	4.15
2	0.164	78.47	12.12
3	0.234	53.38	11.76
4	0.421	41.36	14.92
5	0.609	60.48	29.32
6	0.797	97.99	55.64
7	0.983	73.25	48.02
8	1.171	69.73	51.53
9	1.359	58.96	45.14
10	1.545	52.62	44.17
11	1.734	59.64	50.00
12	1.720	71.18	63.90
13	1.945	80.43	71.44

TABLE H.1.d.

Run no.:	4
Particles:	Wheat
Bed Height:	18.6 cm
Particle mean Residence time:	17.04 min.
Solids Feed Rate:	1.722 kg/min.

Sample No.	$\bar{\theta} = t/\bar{t}$	Sample Wt., gm	Tracer Wt., gm
1	0.059	32.52	1.66
2	0.118	53.52	5.51
3	0.177	101.33	17.64
4	1.254	75.39	23.82
5	0.530	81.88	25.48
6	0.707	91.38	51.73
7	0.883	79.03	50.63
8	1.060	82.87	58.11
9	1.237	87.11	66.48
10	1.414	68.09	54.38
11	1.590	83.91	69.70
12	1.768	74.46	64.37
12	2.000	77.44	69.13

TABLE H. 2.a

Run No.:	5
Particles:	Millet
Bed Height:	34.9 cm
Particle Mean Residence Time:	85.95 min.
Solids Feed Rate:	1.2 lb/min (0.545 kg/min)

Sample No.	$\bar{\theta} = {}^t/\bar{t}$	Sample Wt., gm	Tracer Wt., gm
1	0.058	4.788	0.277
2	0.117	1.733	0.110
3	0.175	1.370	0.161
4	0.234	1.365	0.215
5	0.349	1.415	0.470
6	0.466	1.609	0.667
7	0.582	1.509	0.728
8	0.698	1.423	0.755
9	0.815	1.923	1.214
10	0.931	1.466	0.986
11	1.047	1.639	1.181
12	1.164	1.415	1.080
13	1.280	1.640	1.287
14	1.397	1.617	1.276
15	1.514	1.443	1.224

TABLE H.2.b

Run No.:   6
Particles: Millet
Bed Height: 34.95 cm
Particle Mean
Residence Time: 31.12 min.
Solids Feed Rate: 1.512 kg/min.

Sample No.	$\bar{\Theta} = {}^{t}/\bar{t}$	Sample Wt., gm	Tracer Wt., gm
1	0.064	3.133	0.015
2	0.161	2.330	0.224
3	0.257	1.928	0.356
4	0.386	1.883	0.566
5	0.514	1.932	0.759
6	0.643	1.528	0.639
7	0.804	1.963	1.114
8	0.965	1.675	1.032
9	1.117	1.850	1.293
10	1.350	1.801	1.391
11	1.575	2.027	1.656

APPENDIX I

SOLIDS CIRCULATION RATE

I.1 INTRODUCTION

In a multiple spouted bed solids are found to move from
one spout region to another over the top of the bed and
through the interface of the two regions. The latter
mode of solid transportation was thought to be negligible
compared to the former. Actual measurements were needed
to substantiate this conjecture.

I.2 METHODS OF EXPERIMENT

The internal circulation and blending rates of the bed
material of a fluidised bed can be determined by using a
bed composed of two regions of characteristically differ-
ent particles and measuring the time required for the two
regions to blend completely into a homogeneous bed (87,89).
This technique was found suitable by Chaterjee (85) for
determining the internal circulation rate of a spouted bed.
It appears that the method can also be adopted for measur-
ing the solids crossing rate through the interface of two
spout regions.

I.2.1 Experimental Apparatus

A multiple spouted bed with three spout regions was con-
structed. The bed was half-sectional with a clear front
made of perspex. The bottom of the bed was flat. The
three gas inlet orifices were 1.27 cm diameter and 15.24 cm
apart (equivalent to a 15.24 cm dia. column bed). Two
pieces of removable metal sheets were used to separate one

spout region from another. A solid sampling point was provided in the middle of the centre spout region. Schematically, the bed is the same as that given in Fig. 4.1, (see. Fig. I.1).

Two types of materials, wheat and millet were used for the experiment. Tracer was prepared by dyeing some of the wheat and millet with water soluble dye. The tracer was initially kept in the centre spout region. Two runs in duplicate were carried out for these materials. The cross-flow rate of particles through the interfaces of these spout regions could be evaluated by means of material balances. These are given below.

I.2.2 Solids Cross-Flow Model

The process of particle cross-flow is illustrated in Fig. I.2

Assumptions:

  (i) Solids are perfectly mixed in every region.

  (ii) Equal cross-flow rates at all spout interfaces.

For the tracer in the centre spout region:

$$S_1 \, {}^{dx}/dt = W(y-x) \qquad \ldots\ldots I.1$$

For the two side-spout regions:

$$S_2 \, {}^{dy}/dt = W(x-y) \qquad \ldots\ldots I.2$$

The initial conditions are:

  $t = 0$

  $x = a$

  $y = b = 0$

Fig. I.1 Photograph of the half-sectional bed with three spouts

where,

S_1: Total weight of bed material in centre
spout region

S_2: Total weight of bed material in the two
side-spout region

a: Fractional weight of tracer material at t=0
in centre of spout region

x: Fractional weight of tracer material at time
=t in centre spout region

y: Fractional weight of tracer material at time
=t in outside spout region.

b: Fractional weight of tracer material at t=0 in
outside spout region.

W: Material cross-flow rate.

Now (1) + (2) gives

$$S_1 \, ^{dx}/dt + S_2 \, ^{dy}/dt = 0 \qquad \ldots\ldots I.3$$

Integrate (4) gives

$$S_1 \, x - S_1 \, a + S_2 \, y = 0$$

i.e. $\quad y = \; ^{S_1}/S_2 \; (a-x) \qquad \ldots\ldots I.5$

Substitute (5) in (1) and integrate gives:

$$Ln \; \frac{a}{(1 + S_{1/S_2})x - (S_{1/S_2})a} = W(^{1}/S_1 + ^{1}/S_2)t$$

$$\ldots\ldots I.6$$

If the total tracer in the whole bed is equal to the
total solids initially in the centre spout region ,
then $\qquad a = 1.0$
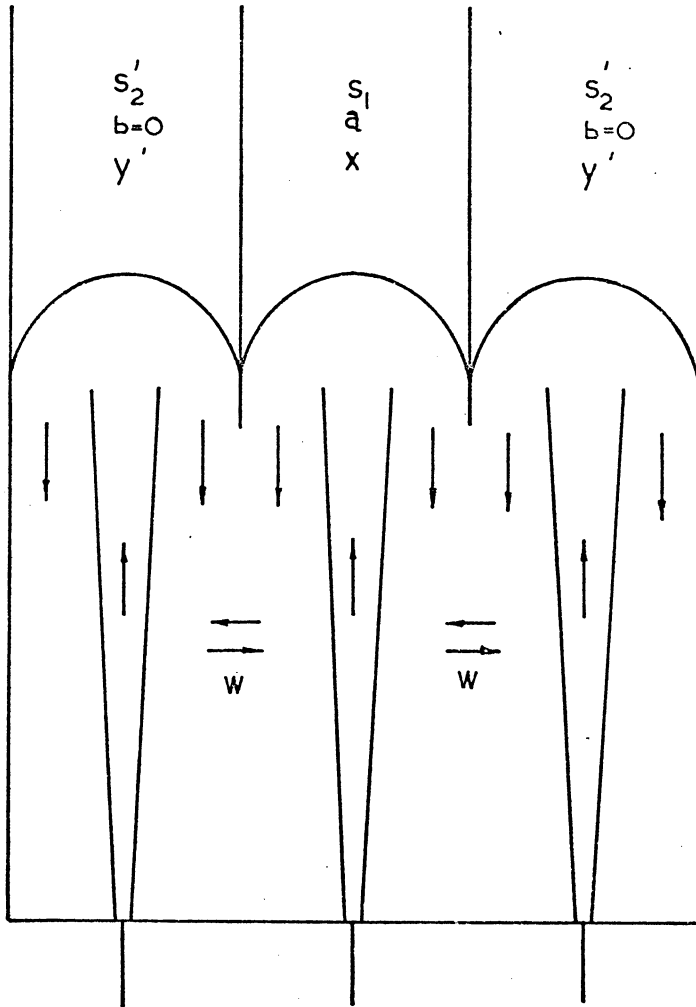
Fig. I.2 Flow Model for Solids Cross - Flow Study

Symbols:

S_1:   Total weight of bed material in centre spout region

$S_2'=\frac{1}{2}S_2$:   Total weight of bed material in the outside spout region.

a: Fractional weight of tracer material at t=0 in centre spout region

x: Fractional weight of tracer material at time=t in centre spout region

$y'=\frac{1}{2}y$ Fractional weight of tracer material at time=t in outside spout region

b: Fractional weight of tracer material at t=0 in in outside spout region

w: Material cross-flow rate

Equation (6) becomes

$$\text{Ln} \frac{S_2 \,/(S_1 + S_2)}{x - S_1/(S_1 + S_2)} = W(\frac{1}{S_1} + \frac{1}{S_2})t \quad \ldots\ldots I.7$$

From equation (7), the cross-flow rate, W, can be obtained from the slope, $W(\frac{1}{S_1} + \frac{1}{S_2})$ of the plot $\text{Ln}[S_2/(S_1 + S_2)/(x - S_1/(S_1 + S_2)]$ vs t.

I.3 EXPERIMENTAL PROCEDURE

   (1)   Isolate the spout regions with the two sheet
          metal partitioners.

   (2)   Fill the centre spout region with tracer and
          the two side-spout regions with solids. The
          weights of all materials are known.

   (3)   Keep all the regions in a spouting stage and
          adjust air flow rate about 5% above the mini-
          mum spouting flow rate.

   (4)   Quickly lift the two partitioners to the
          surface of the bed and start timing.

   (5)   Collect samples at suitable intervals for
          analysis.

I.4 ANALYSIS OF RESULTS

The samples collected from the experiment were weighed,
then the tracer separated from the main sample and weighed.
This information and the corresponding sampling times were
then fed into a computer for linear regression analysis.
The subroutine LINREG (see Appendix H) was again employed.
The simple main computer programme is given in the follow-
ing section.

In Fig. I.3 the actual data and lines of best fit are given.
The solids cross-flow rates obtained by determining the
slopes of the lines are given as follows:

Bed Material	Bed Height, cm	Cross-Flow kg/hr
Wheat	20.30	4.89
Millet	34.29	2.03

Thus the cross-flow of solids through spout interface
appears to be rather low. The rapid solids mixing
observed in the study of solids age distribution was due
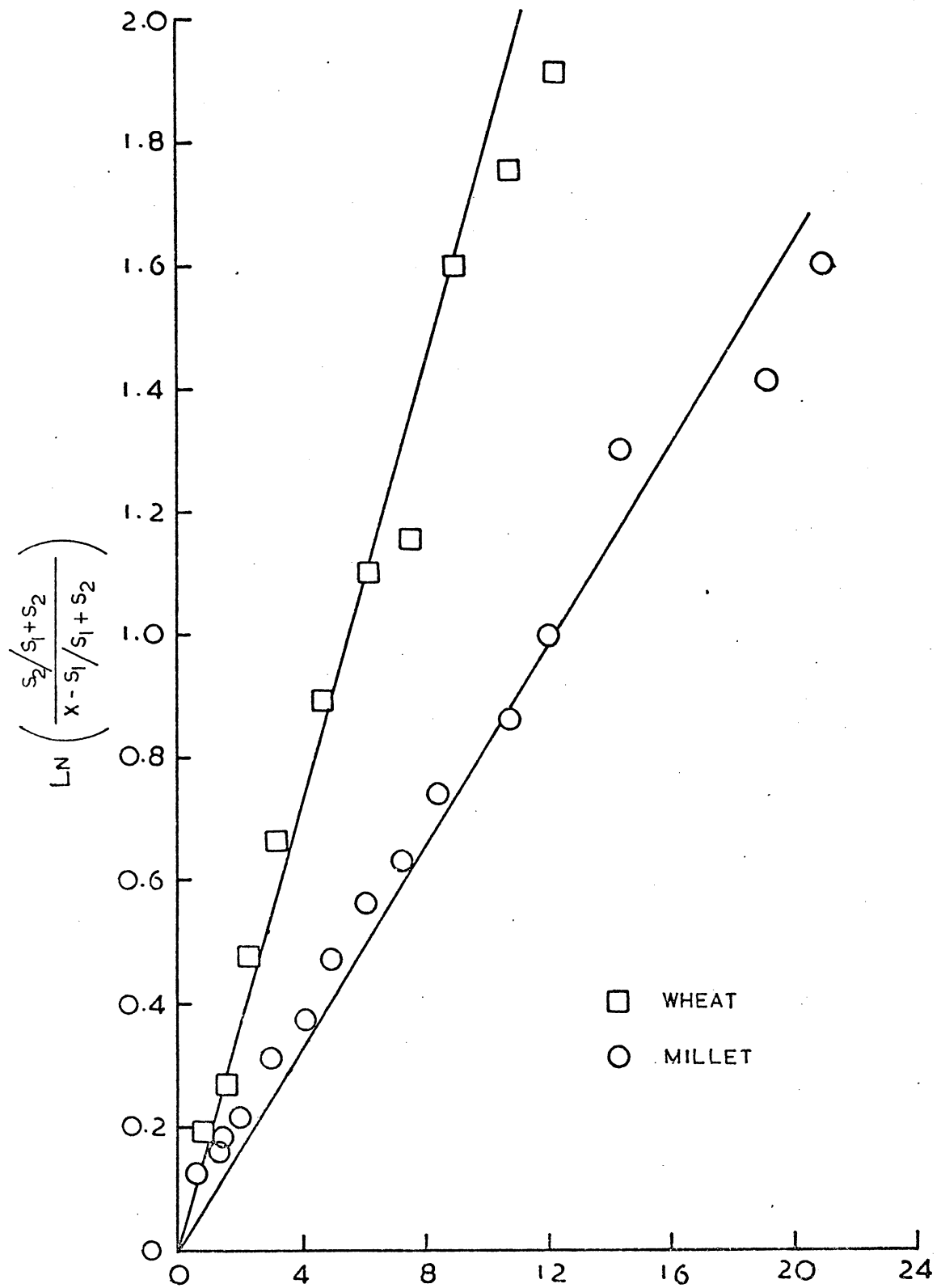mainly to solids transport over the surface of the bed.

Fig. I.3 Linear fitting of solids cross-flow data

I.5 COMPUTER PROGRAMME

```
FORX52
**S.K. FOONG, CHEM. ENG. POSTGRADUATE.
*LIST PRINTER
*DIAGNOSTICS


C
C     LINEAR REGRESSION OF MULTISPOUT BED
C     INTERNAL MIXING DATA
C     -SYMBOLS-
C     S1 IS THE TOTAL WEIGHT OF BED MATERIAL IN THE
C     CENTRAL SPOUT REGION
C     S2 IS THE TOTAL WEIGHT OF BED MATERIAL IN THE
C     OUTER SPOUT REGION
C     SAM IS THE WEIGHT OF SAMPLE
C     TRA IS THE WEIGHT OF TRACER
C     TRAPC IS THE FRACTIONAL WEIGHT OF TRACER
C
C
      DIMENSION SAM(30),TRA(30),TRAPC(30),TIME(30)
      DIMENSION X(30), Y(30), HEADER(20)
    1 READ,N
      IF (N) 14,14,2
    2 CONTINUE
      READ 3, HEADER
    3 FORMAT (20A4)
      READ, S1,S2
      READ,(TIME(I),I=1,N)
      READ,(SAM(I),I=1,N)
      READ,(TRA(I),I=1,N)
C
      PRINT 4, HEADER
    4 FORMAT(1H1,4X,20A4,//,10X,4HTIME,6X,6HSAMPLE,6X,6HTRACER
     1,//)
      DO 6 I=1,N
      PRINT 5,TIME(I),SAM(I),TRA(I)
    5 FORMAT(1H ,8X,F6.2,3X,F9.4,5X,F7.4)
    6 CONTINUE
C
      TRAINF  =  S1/(S1+S2)
      ZINF  = S2/(S1+S2)
C
      DO 13 I=1,N
      TRAPC(I) =TRA(I)/SAM(I)
      X(I)=(1.0/S1+1.0/S2)*TIME(I)
      IF (I-1) 7, 7, 8
    7 ARGUMT = 1.0
      GO TO 9
    8 ARGUMT = ZINF/(TRAPC(I)-TRAINF)
    9 IF (ARGUMT) 10, 10, 12
   10 PRINT 11, I
   11 FORMAT (1H0,1X,48HSOMETHING IS WRONG,MATE.Y(K) SET
     1EQUAL TO ZERO.,5X, 4HI = , I3)
      Y(I) = 0.0
      GO TO 13
```

CONT.

```
 12 Y(I)=LOG(ARGUMT)
 13 CONTINUE
C
    CALL LINREG(Y,X,N)
C
    TO TO 1
 14 STOP
    END

00003 0001
00013 10000000-1
00023 00000000RR
 00033      SAM 00323  00333    TRA 00623 TRAPC 00933
```

I.6 TYPICAL COMPUTER PRINTOUTS

BED MATERIAL = MILLET

TIME	SAMPLE	TRACER
0.00	3.0000	2.8000
2.00	3.0603	2.8345
6.00	2.9980	2.6637
8.00	1.8130	1.5680
12.25	1.7060	1.3907
16.50	2.2608	1.7948
20.00	1.8174	1.3626
25.00	1.7079	1.2144
30.00	1.6692	1.1515
35.00	1.8785	1.2215
40.00	1.9796	1.2620
45.00	1.8432	1.1345
50.00	1.7930	1.0390
60.00	1.7570	.9080
80.00	1.8151	.9004
88.00	1.9578	.9078

ANALYSIS OF VARIANCE

	SS	DF	MS	F
REGRESSION	3.4263900E+00	1	3.4263900E+00	1.1491617E+03
RESIDUAL	4.1743000E-02	14	2.9816428E-03	
TOTAL	3.4681330E+00	15		

A=   .08608   B=   .07424
R(SQUARED) =   .98796   R=   .99396
STANDARD ERROR OF ESTIMATE = 5.4604421E-02
STANDARD ERROR OF B =   2.1901846E-03
T VALUE FOR B =   3.3899290E+01

X	Y	Y CALCULATED	Y-Y CALCULATED
0.0000000E-99	0.0000000E-99	8.6085370E-02	-8.6085370E-02
4.8000000E-01	1.1729296E-01	1.2172330E-01	-4.4303400E-03
1.4400000E+00	1.8303555E-01	1.9299918E-01	-9.9636300E-03
1.9200000E+00	2.2652758E-01	2.2863711E-01	-2.1095300E-03
2.9400000E+00	3.2466061E-01	3.0436773E-01	2.0292880E-02
3.9600000E+00	3.6987966E-01	3.8009835E-01	-1.0218700E-02
4.8000000E+00	4.7059801E-01	4.4246474E-01	2.8133270E-02
6.0000000E+00	5.6814933E-01	5.3155958E-01	3.6589750E-02
7.2000000E+00	6.2590516E-01	6.2065443E-01	5.2507300E-03
8.4000000E+00	7.4364222E-01	7.0974927E-01	3.3892950E-02
9.6000000E+00	7.8470606E-01	7.9884411E-01	-1.4138050E-02
1.0800000E+01	8.5977223E-01	8.8793896E-01	-2.8166730E-02
1.2000000E+01	9.9637991E-01	9.7703380E-01	1.9346110E-02
1.4400000E+01	1.2903117E+00	1.1552234E+00	1.3508830E-01
1.9200000E+01	1.4102131E+00	1.5116027E+00	-1.0138960E-01
2.1120000E+01	1.6320640E+00	1.6541545E+00	-2.2090500E-02

APPENDIX J

MATERIALS USED IN SPOUTED BED EXPERIMENTS

MATERIALS USED IN SPOUTED BED EXPERIMENTS

The materials used for the experiment were wheat, rape

seed, coal, gravel and mixtures of rape seed and wheat.

Their physical properties are listed in Table J.

The densities were determined by using a pycnometer.

The bulk densities were determined by weighing the bed

charge and measuring the static bed height after the

bed had been through a spouting cycle. Results obtained

in this manner were found to be consistent from run to run.

The effective particle diameters were obtained from the

sieve analysis using the following expression

$$D_p = \frac{1}{\sum\limits_{i=1}^{n} x_i / d_{pi}}$$

where,

D_p = particle diameter

x_i = mass fraction of particles of size d_{pi}

D_v = particle equivalent diameter

$n = \dfrac{\text{Specific surface of particle}}{\text{Specific surface of sphere of same diameter}}$

Specific
Surface = Surface area of particles per unit of mass

This definition has been found to be the best method of

characterising the diameter of mixed-size particles (87).

The shape factors were calculated by Brown's expression

(88).

$$\emptyset = \left(\frac{1}{n}\right) \frac{D_p}{D_v}$$

TABLE J

MATERIAL	B.S. MESH SIZE	APPARENT DENSITY, gm/c.c.	BULK DENSITY, gm/c.c.	MEAN DIAMETER cm.	SHAPE FACTOR
Rape Seed	-7+14	1.068	0.665	0.189	1.0
Wheat	-1/4+8	1.356	0.765	0.320	0.84
Coal	-5+14	1.362	0.738	0.196	0.87
Gravel	-5+18	2.625	1.360	0.169	0.82
Millet	-10+18	1.327	0.693	0.119	0.83
(Rape Seed + Wheat)	-1/4+14	1.212	0.726	0.255	0.92
Polythene I	-7+14	0.96	0.560	0.211	0.87
Polythene II	$-\frac{1}{8}+10$	0.96	0.600	0.249	0.84

LIST OF SYMBOLS

a	Coefficient as defined in Eq. 4.1a
A_a	Cross-sectional area of the annulus of a spouted bed, cm^2
A_s	Cross-sectional area of the spout of a spouted bed, cm^2
C	Product concentration or instantaneous concentration of reactant, mole/c.c.
C_a	Reactant concentration in the annulus, mole/c.c.
C_e	Reactant concentration at outlet of spouted bed, mole/c.c.
C_o	Feed concentration, mole/c.c.
C_s	Reactant concentration in the spout, mole/c.c.
C_{aH}	Reactant concentration in an annulus at bed height=H , mole/c.c.
$C_{s\bar{H}}$	Reactant concentration in the spout at bed height=$\bar{H}$, mole/c.c.
D_c	Column diameter, cm
D_i	Gas inlet orifice diameter, cm
D_p	Particle diameter, cm
D_s	Spout diameter, cm
D_v	Equivalent diameter of particle, cm
d_{pi}	Particle diameter of size fraction, x_i, cm
F_{Ao}	Initial mass flow rate of reactant A , mole/sec
g	Acceleration of gravity, cm/sec^2
H	Bed height, cm
$\bar{H}$	Spout height, cm
H_m	Maximum spoutable bed height, cm
I	Internal age distribution function
K	Constant as defined in Eq. 4.3
K_1, K_2	Reaction rate constant as defined in Eq. 1.1

List of Symbols cont.

K_r	Reaction rate constant based on volume of solids, sec^{-1}
N	Number of mole
ΔP_s	Spouting pressure drop across bed, KPa
r	Reaction rate of reactant mole/sec
S_p	Surface area of particle, cm^2
t	Time, sec
$\bar{t}$	Mean residence time, sec
V, V_r	Bed volume, c.c.
V_b	Volume of backmix region, c.c.
V_p	Volume of plug flow region, c.c.
v	Volumetric flow rate, c.c./sec
$\bar{v}_a$	Spouting velocity in the annulus, cm/sec
v_{mf}	minimum fluidization velocity, cm/sec
v_{ms}	Minimum spouting velocity, cm/sec
$\bar{v}_s$	Spouting velocity in the spout, cm/sec
v_s	Spouting velocity, cm/sec
$\bar{v}_{aH}$	Velocity of gaseous reactant at bed height=H, cm/sec
$\bar{v}_{s\bar{H}}$	Velocity of gaseous reactant at bed height=$\bar{H}$, cm/sec
X	Degree of conversion
x_i	Mass fraction of particles of size d_{pi}
z	Bed depth, cm
dz	Differential bed depth, cm

LIST OF SYMBOLS (cont.)

A_o	Cross-sectional area of the inlet of a spouted bed, cm^2
a	Fractional weight of tracer material at t=0 in the centre spout region
b	Fractional weight of tracer material at t=0 in outside spout region
D_{12}	Binary diffusivity, cm^2/sec
E	Effect of a variable (Eq.C.1)
E_d	Effect of a dummy variable (Eq.C.2)
F_f^o	Standard free energy, cal/mole
K_e	Equilibrium constant
K	Botzman's constant used in calculation associated with Eq.D.1
M_1, M_2	Molecular weight, gm
p	Partial pressure, atm
R	Gas constant
r_A	Rate of reaction with respect to reactant A, mole/sec
S_1, S_2	Total weight of bed material in the centre spout region and the two outside spout regions respectively, gm
T	Temperature, ^oK
"t"	"t" test as defined in Eq.C.4
v_r	Radial gas percolation velocity, cm/sec
V	Variance of an effect (Eq.C.2)
x	Fractional weight of tracer material at t=t in centre spout region
y	Fractional weight of tracer material at t=t in outside spout region
W	Material cross-flow rate, gm/sec

GREEK LETTERS

β	(beta)	Angle of particle internal friction
θ	(theta)	Dimensionless time
λ	(lambda)	As defined in Eq. 4.3
ρ_b	(rho)	Bulk density of particle, gm/c.c.
ρ_f	(rho)	Fluid density, gm/c.c.
ρ_p	(rho)	Apparent density of particles, gm/c.c.
ϕ_s	(phi)	Particle shape factor
ε_s	(Epsilon)	The spout void fraction
ε_a	(Epsilon)	The annulus void fraction
ε_{mf}	(Epsilon)	Void fraction of bed at minimum fluidization
ε_o	(Epsilon)	Static bed void fraction
μ	(mu)	Viscosity of fluid, gm/cm·sec

GREEK LETTERS (cont.)

σ_{l2} (sigma)   Collision diameter, Angstrom
                                  unit

Ω_{D} (omega)   Collision integral, dimensionaless

$\xi_{l}, \xi_{2}, \xi_{l2}$ (xi)   Maximum attractive energy between
                                  two molecules, ergs.

REFERENCE

1. National Air Pollution Control Administration, "Air Quality Criteria for Sulphur Oxides", U.S. Clearing House Fed. Science and Tech. Inform., Report No. PB190252, 1968.

2. National Industrial Pollution Control Council, "Air Pollution by Sulphur Oxides", U.S. Clearing House Fed. Sci. & Tech. Inform., Report No. Com-71-50235, 1971.

3. Robinson, E, and Robbins, R.C., "Air Pollution Control", Part II, Chapter I (Ed. W. Strauss), Wiley and International, 1972.

4. Thomson, W.A. and Strauss, W., "Total Emission to the Australian Atmosphere", Clean Air, Feb., 1973, pp. 18-20.

5. Redmond, J.C., Cook, J.C. and Hoffman, A.A.J., "Cleaning the Air: The Impact of the Clean Air Act on Technology", I.E.E.E. Press, 1971, pp. 115.

6. Slack, A.V., "Sulphur Dioxide Removal from Waste Gases", Noyes Data Corp., 1971.

7. Dibbs, H.B., "Methods for the Removal of Sulphur Dioxide from Waste Gases", Department of Mines and Resources, Mines Branch, Ottawa, Canada, 1971.

8. Leonard, J.W. and Cockrell, C.F., "Basic Methods of Removing Sulphur from Coal", Mining Cogr. Jour., Vol. 56 (12), 1970, p. 65.

9. Davey, T.R.A., "The Sulphur Problem and The Non-Ferrous Metal Industries in Australia", Pace, August, 1973, pp. 20-27.

10. Lepsoe, R., "Chemistry of Sulphur Dioxide Reduction - Thermodynamics", I. & E. C., Vol. 30 (1), 1938, pp. 92 - 100.

11. Lepsoe, R., "Chemistry of Sulphur Dioxide Reduction - Kinetics", I.& E.C., Vol. 32, No. 7, 1940, pp. 910-918.

12. Potts, H.R. and Lawford, E.G., "Recovery of Sulphur from Smelter Gases by the Orkla Process at Rio Tinto", Trans. Inst. Min. Metall., Vol. 58, 1949, pp. 427 - 516.

13. Barton, R.K., "The Low Temperature Carbonisation of Coal in a Spouted Bed with Particular Reference to Rates of Devolatization", Ph.D.Thesis, Uni. of N.S.W., 1968.

14. Rigby, G., "The Low Temperature Carbonisation of Coal in a Spouted Bed with Particular Reference to Prediction of Exit Char Volatile Matter", Ph.D. Thesis, Uni. of N.S.W., 1968.

15. Siller, C.W., "Carbon Disulphide from Sulphur Dioxide and Anthracite", I. & E.C., Vol. 40, No. 7, July, 1948 pp. 1227-1233.

16. Owen, A.J., Sykes, K.W. and Thomas, D.J.D., Trans. Faraday Soc., Vol. 47, 1951, pp. 419-428.

17. Kellogg, H.H., "Equilibria in the System C-O-S and C-O-S-H as Related to Sulphur Recovery from Sulphur Dioxide", Metallurgical Trans., Vol. 2, August 1971, pp. 2161 - 2169.

18. Biswas, A.K., Roy, N.C. and Rao, M.N., "Conversion of Waste Sulphur Dioxide into Sulphur and Carbon

Disulphide", Indian Jour. Technol., Vol. 6, May, 1968, pp. 157-158.

19. Giberson, R.C. and Tingey, G.L., "The Reduction of Sulphur Dioxide with Graphite", U.S. Atomic Energy Comm., 1968 BNWL-SA-1849.

20. Stacy, W.O., Vastola, F.J. and Walker, P.L., Jr., "Interaction of Sulphur Dioxide with Active Carbon", Vol. 6, 1968, pp. 917-923.

21. Walker, P.L.Jr., Rusinko, F. Jr. and Austin, L.G., "Advances in Catalysis", Vol. 11, Academic Press, New York (1959), pp. 133-221.

22. Sappok, R.J. and Walker, P.L. Jr., (Removal of Sulphur Dioxide from Flue Gases Using Carbon at Elevated Temperatures", Jour. Air Poll. Assoc., Vol. 19, No. 11, 1969, pp. 856-861.

23. Sinha, R.K. and Walker, P.L. Jr., "Removal of Sulphur Dioxide Flue Gases Using Calcined Anthracite at Elevated Temperature", A.I.CH.E. Symposium Series, Vol. 68(126), 1972, pp. 160-166.

24. Malmstrom, R. and Tuominen, T., "High Temperature Reduction of Sulphur Dioxide Gases with Pulverised Coal", Advan. Extr. Met. Refi Proc., Int., Symposium (1971), Pub. (1972), Ed. M.J. Jones, Inst. Min. Metall., London, pp. 529-542.

25. Fleming, E.P. and Fitt, T.C., Ind. Eng. Chem., Vol. 42, 1950, p. 2249.

26. Averbukh, T.D. Radivilov, A.A. and Baknia, N.P., "Thermodynamics of Reduction of Sulphur Dioxide by

Methane", Zh. Priki. Khim, Vol. 43, No. 1, 1970,,
pp. 35 -43.

27.   Averbukh, T.D., Radivilov, A.A. and Baknia, N.P.,
"Reduction of Sulphur Dioxide by Methane in Presence
of Carbon and Carbon in Presence of Steam", Zh.
Priki. Khim., Vol. 43, No. 2, 1970, pp. 228-236.

28.   JANAF Thermodynamic Tables, U.S. Dept. of Commerce,
2nd. Ed., Nat. Bureau of Standard, 1971.

29.   Berkowitz, J. and Chupka, W.A. Jour. Chem. Phys.,
Vol. 40, No. 2, 1964, p. 287.

30.   Meyer, B. Ed., "Elemental Sulphur", P. 127, Inter-
science, New York, N.Y., 1965.

31.   Drowart, J. et. al., Z. Phys. Chem., Vol. 55, 1967,
pp. 314-319.

32.   Gamson, B.W. and Eikins, R.H., Chem. Eng. Progr.,
Vol. 49, No. 4, 1953, p.206.

33.   Munro, A.J.E. and Madison, E.G., Brit. Chem. Eng.,
Vol. 12, No. 3, 1967, p.364.

34.   Yodis, A.W., "Sulphur from Smelter Gas by Reduction
of Sulphur Dioxide", Paper presented at the 158th
National A.C.S. Meeting, 1969.

35.   Holub, R., Piok, P. and Macak, J., "Thermodynamic
Equilibrium in the System Solid Carbon - Gaseous
SO_2", Chem. Industry, Vol. 23/48, No. 1, 1973,
pp. 14-17.

36.   Blackwood, J.D. and McCarthy, D.J., "The Kinetically
Effective Stoichiometry of Reactions in the Carbon-
Sulphur Dioxide System", Australian Jour. Chem.,
Vol. 26, 1973, pp. 723-731.

37. Van Zeggeren, F., and Storey, S.H., "The Computation of Chemical Equilibrium", Cambridge University Press, 1970.

38. Mathur, K.B. and Gishler, P.E., "A Technique for Contacting Gases with Coarse Solids Particles", A.I.CH.E., Jour., Vol. 1, No. 2, June, 1955, pp.157-164.

39. Malek, M.A. and Lu B.C.-Y., "Pressure Drop and Spoutable Bed Height in Spouted Bed", Ind. Eng. Chem., Process Design and Development, Vol. 4, No. 1, Jan., 1965, pp. 123-128.

40. Plackett, R.L. and Burman, J.P., Biometrika, Vol. 33, pp. 303-325.

41   Stowe, R.A. and Mayer, R.P., "Efficient Screening of Process Variables", Ind. and Eng. Chem., Vol. 58, No. 12, Feb., 1966, pp. 36-40.

42. Levenspiel, O., "Chemical Reaction Engineering", John Wiley & Sons, Inc., 1962.

43. Kunii, D. and Levenspiel, O., "Fluidization Engineering", John Wiley & Sons, Inc., 1969.

44. Mamuro, T. and Hattori, H., "Flow Pattern of Fluid in Spouted Beds", Journ. Chem. Eng., Japan, Vol. 1, No. 1, Feb., 1968, pp. 1-5.

45. Mathur, K.B. and Epstein, N. "Dynamics of Spouted Beds", Advances in Chem. Eng., in Press.

46. Thorley, B., Saunby, J.B., Mathur, K.B. and Osberg, G.L., "An Analysis of Air and Solids Flow in a Spouted Wheat Bed", Can. Jour. Chem. Eng., Vol. 37, No. 5, Oct., 1959, pp. 184-192.

47. Mathur, K.B. and Lim, C.J., "Vapour Phase Chemical
     Reaction in Spouted Beds : A Theoretical Model",
     Chem. Engg. Science, 1974.

48. Ergun, S., "Fluid Flow Through Packed Column", Chem.
     Engg., Progress, Vol. 48, No. 2, Feb., 1952, pp. 89-94.

49. Meisel, G.M. "Sulphur Recovery", Jour. of Metals,
     May, 1972, pp. 31-39.

50. McKee, A.G. and Co., "Systems for Control Emissions,
     Primary Non-ferrous Smelting Industry", Vol. IIV,
     National Air Pollution Control Admin., Contract PH
     86-65-85, Clearing House for Red. Scientific & Tech.
     Inform. PB 184885, June, 1969, Appendix B.

51. Semrou, K.T., "New Processes for Recovery of Sulphur
     Dioxide from Smelter Gases", Symposium on Air Pollution
     from the Production of Copper, Lead and Zinc, Am.
     Inst. Chem. Engrs. and Inst. Mexi. de Ingenieros
     Quimicos, August, 1970.

52. Blackwood, J.D. and McCarthy, D.J., "Production of
     Sulphur Compounds by Reaction of Carbon and Sulphur
     Dioxide", Proc. Australas, Inst. Min. Metall., No. 249,
     March, 1974, pp. 25-30.

53. Bailey, J.B.W., Brown, N.E. and Phillips, C.V., "A
     Method for the Determination of CO, CO_2, SO_2, COS,
     O_2 and N_2 in Furnace Gas Atmospheres by Gas
     Chromatography", Analyst, Vol. 96, June, 1971, pp.
     447-451.

54. Collins, A.C., "Atmosphere Pollution by Sulphur
     Dioxide", Rep. Progress Applied Chemistry, Vol. 55,
     1970, pp. 643-663.

55. Spedding, P.L., "Corrosion by Atmospheric Sulphur

Dioxide", Australian Corrosion Eng., Sept., 1971, pp. 27-36.

56.   Jones, L.H.P. and Cowling D.W., "Effects of Air Pollution on Plants", 39th Annual Conference, National Soc. of Clean Air, U.K., 1972.

57.   Satterfield, C.N. and Sherwood T.K., "The Role of Diffusion in Catalysts", Addison Wesley Reading, Mass., 1963.

58.   Hirschfelder, J.O., C.F. Curtis and R.B. Bird, "Molecular Theory of Gases and Liquids", Wiley, N.Y., 1954.

59.   Becker, H.A. "An Investigation of the Laws Governing the Spouting of Coarse Particles", Chem. Engg. Science, Vol. 13, No. 4, June, 1961, pp. 245-62.

60.   Davidson, J.F. and Harrison, D. (Editors), "Fluidization", Chapter 17, Academic Press 1971.

61.   Becker, H.A. and Sallan, H.R., "Drying Wheat in a Spouted Bed on the Continuous, Moisture-Controlled Drying of Solid Particles in a Well-Mixed Isothermal Bed", Chem. Engg. Sci., Vol. 13, 1960, pp. 97.

62.   Cowan, C.R., Peterson, W.S. and Osberg, G.L. "Drying of Wood Chips in a Spouted Bed", Pulp and Paper Magazine of Canada, Vol. 58, Dec., 1957, p. 138.

63.   Nemeth, J. and Pallai, I. "The Spouted Bed Method and its possible Utilizations", Magyar Keimtnook Lavja, Vol. 2, 1970, pp. 74-82.

64.   Peterson, W.A. "Spouted Bed Dryers", Can.Jnr.Chem. Engg., Vol 40, No. 5, Oct., 1962, pp. 226-30.

65.   Fissons Fertilizers Ltd., Levington, U.K.

66. Bowers, K.H., Stevens, J.W. and Suckling, R.D., British Patent No. 855809, filed 1959, granted 1960.

67. Heiser, A.L., Lowenthal, W. and Singiser, R.E., U.S. Patent Nos. 3, 112,220, filed 1960, granted 1963.

68. Singiser, R.E., Heiser, A.L. and Pritting, E.B., "Air Suspension Tablet Coating", Chem. Engg. Progr., Vol. 62, No. 6, June, 1966, pp. 107-111.

69. Berquin, Y.F., U.S. Patent No. 3,231,413, filed 1962, granted 1964.

70. Berquin, U.F. "Nouveau Procede de Granulation et son Application dans le Domains de la Fabrication des Engrains", Genie Chimique, Vol. 86, 1961, pp. 45-47.

71. Berti, L.P. "Operational Criterion of a Spouted Bed Oil Shale Retort". D.Sc. Thesis, Colorado School of Mines, Golden, Colorado, U.S.A., 1968.

72. Buchanan, R.H. and Manurung, F. "Experiences in Fluidization. Spouted Bed Low-Temperature Carbonization of Coal" British Chem. Eng.., Vol. 6, June, 1961, pp. 402-403.

73. Barton, R.K., Rigby, G.R. and Ratcliffe, J.S., "The Use of a Spouted Bed for the Low Temperature Carbonization of Coal", Mech. and Chem. Trans. Inst. of Engrs., Aust., Vol. 4, 1968, pp. 105-112.

74. Madonna, L.A., Lama, R.F. and Brisson, W.L. "Solid-Air Jets", Brit. Chem. Engg. Vol. 6, No. 8, Aug., 1961, pp. 524-528.

75. Lefroy, G.A. and Davidson, J.F., "The Mechanics of Spouted Bed", Trans. Inst. Chem. Engrs., Vol. 47,

1969, pp. T120-128.

76.   Malek, M.A., Madonna, L. and Lu, B.C.Y., "Estimation of Spout Diameter in a Spouted Bed", Industrial and Engg. Chemistry Process Design and Development, Vol. 2, No. 1, Jan., 1963, pp. 30-34.

77.   Manurung, F., "Studies in the Spouted Bed Technique with Particular Reference to the Application to Low Temperature Coal Carbonization", Ph. D. Thesis, Uni. of N.S.W., 1964.

78.   Volpicalli, G., Ross, G. and Massimilla, L., "Gas and Solids Flow in Bi-Dimensional Spouted Beds", Proceedings Eindhoven Fluidization Symposium, 1967, pp. 123-133.

79.   Hunt, C.H. and Brennan, D., "Estimation of Spout Diameter in a Spouted Bed", Aust. Chem. Engg., Vol. 6, No. 3, March, 1965, pp. 9-15.

80.   Reddy, K.V.S. and Smith, J.W., "Spouting Mixed Particle-Size Beds", Can. Jnr. of Chem. Engg., Vol. 42, No. 5, Oct., 1964, pp. 206-210.

81.   Kugo, M., Watanbe, N., Uemaki, O. and Shibata, T., "Drying of Wheat by Spouted Bed", Bull. Hokaido Uni., Japan.

82.   Bowling, K. McG. and Watts, A., "Determination of Particle Residence Time in a Fluidized Bed", Theoretical and Practical Aspects, Aust. Jnr. of Appl. Science, Vol. 12, No. 4, Dec., 1961, pp. 413-427.

83.   Chaterjee, A., "Effect of Particle Diameter and Apparent Particle Density on Internal Solid Circulation Rate in Air-Spouted Beds", Ind. Engg., Chemistry,

Process Design and Development, Vol. 9, No. 4, 1970, pp. 521-526.

84. Cholette, A. and Cloutier, L., "Mixing Efficiency Determinations for Continuous Flow Systems", Can. Jnr.Chem. Engg., Vol. 37, June, 1959, pp. 105-112.

85. Zenz, F.A. and Othmer, D.F., "Fluidization and Fluid Particle Systems", Reinhold, N.Y., 1960, p. 290.

86. Van Heerden, C., Nobel, A. and Van Krevelen, D.W., "Studies On Fluidization I - The Critical Mass Velocity", Chem. Engg. Science, Vol. 1, No. 1, 1951, pp. 37-49.

87. Brown, G.G. et al - "Unit Operations", p. 77 - John Wiley & Sons Inc., New York, 1955.

88. Leva, M. and Grummer, M., Chem. Engg. Progr. Vol. 48, 1952, P. 307.

89. Gorshtein, A.E. and Mukhlenov, I.P., Zh. Priki Khim., Vol. 37, 1964, p. 1889.

90. Gorshtein, A.E. and Mukhlenov, I.P., Zh, Priki Khim, Vol. 40, 1967, p. 2469.

91. Mikhailik, V.D., "Collected Works on Research on Heat and Mass Transfer in Technological Processes and Equipment", p. 37, Naukai Teknika B.S.S.R., Minsk, 1966

92. Malek, M.A. and Lu, B.C.-Y, "Heat Transfer in Spouted Beds", Can, Jour. Chem. Engg., Vol. 42, No. 1, Feb., 1964, pp. 14-20.

93. Zabrodsky, S.S. and Mikhailik, V.D. "Collected Papers on Intensification of Transfer of Heat and Mass in Drying and Thermal Processes", Naukai Teknika BSSR, 1967, p. 130.

94. Klassen, J. and Gishler, P.E., "Heat Transfer from

Column Wall to Bed in Spouted, Fluidised and
Packed Systems", Can. Jour. Chem. Engg. Vol. 36,
(1), Feb., 1958, pp. 12-18.

95. Ghosh, B. and Osberg, G.L., "Heat Transfer in Water
Spouted Beds", Can. Jour. of Chem. Engg., Vol. 37(6),
Dec., 1958, pp. 205-207.

96. Uemaki, O. and Kugo, M., Kagaku Kogaku, Vol. 31, 1967,
p. 348.

97. Barton, R.K. and Ratcliffe, J.S., "The Rates of Devola-
tilization of Coal Under Spouted Conditions", Mech.
& Chem. Engg. Trans., I.E.(Aust.), Vol. 5, May, 1969,
pp. 35-41.

98. Mathur, K.B. and Gishler, P.E., "A Study of the
Application of the Spouted Bed Technique to Wheat
Drying", Jour. of Appl. Chemistry, Vol. 5 (11), Nov.,
1955, pp. 624-636.

99. Mathur, K.B. and Epstein, N., "Momentum, Heat and
Mass Transfer in Spouted Beds, a Critical Review",
Presented on the 20th Annual Conf. of the Comm. Soc.
Chem. Engg. Oct., 1970.

100. Uemaki, O. and Kugo, M., Kagaku Kogaku, Vol. 31,
1967, p. 48.

101. Mathur, K.B. and Gishler, P.E. Paper presented to
the C.I.C. Annual Conf., Quebec, (1955), private
communication.

102. Quinlan, M. and Ratcliffe, J.S., "Consequential
Effects of Air Drying Wheat - Spouted Bed Design and
Operation", Mech. & Chem. Eng.. Trans., Inst. Engrs.
(Aust.), Vol. MC6 (1), May, 1970, pp. 19-24.

103. Romankov, P.G. and Rashkovskaya, N.B., "Drying in a Suspended State", 2nd Ed., Chem. Publishing House, Leningrad Branch (1968), in Russia.

104. Rosenbrock, H.H. and Storey, C., "Computational Techniques for Chemical Engineers", Pergamon, 1966.

105. Uemaki, O, Fugikawa, M. and Kugo, M., "Vapour Phase Hydrogenation of Propylene - Pyrolysis of Petroleum Fractions (Naptha Heavy Oil, Crude Oil) for Production of Ethylene and Propylene using Externally Heated Spouted Bed", Kogyo Kagaku Zasshi, Vol. 73 (3) 1971, pp. 453-461 (Japan).

106. Uemaki, O., Fugikawa, M. and Kugo, M., "Pyrolysis of Petroleum (Kerosine, Heavy Oil and Crude Oil) Using an Externally Heated Two-Spouted Bed", Kogyo Kagaku Zasshi, Vol. 74 (5), 1971, pp. 733-738. (Japan).

107. Ozawa, M., "Spouted Bed Reduction of Iron Ore", Tatsu-to-Hagane, Vol. 59, No. 3, 1973, pp. 361-369 (Japan).

CHARACTERISTICS OF MULTIPLE SPOUTED BEDS

By: S-K. FOONG+,   R.K. BARTON*   and   J.S. RATCLIFFE+
         M.Sc.   Ph.D.   M.Sc.,Ph.D.

ABSTRACT

Basic characteristics of multiple spouted beds were
investigated. Bed instability was noted and was found
to be dependent on bed height and D_p/D_i ratio. The
optimal ratio was found to lie within 0.09 - 0.13. General
correlations developed for single spouted beds were proven
applicable to multiple spouted beds. A solids-flow model
based on the concept of "mixed models" was developed for
the bed.

+ Respectively, postgraduate student and Professor of
   Chemical Engineering, the University of New South Wales.

* Technical Director of Ajax Chemicals, Division of Searle
   Australia Pty. Ltd., N.S.W.

1. INTRODUCTION

Fluidization is a well established process for contacting
particulate solids with fluids. With coarse and uniform-
sized granular solids, however, fluidized beds show a
marked tendency towards slugging because of the growth of
large bubbles. To overcome this difficulty, Mathur and
Gishler (Ref. 1) developed the "spouted bed" technique in
1954. The phenomenon of spouting has been exhaustively
described elsewhere (Ref. 1,2,3,21).

Since its inception, the process has been used for drying
wheat (Ref. 1,4) wood chips (Ref. 5) and peas, lentils and
flax (Ref. 7). This technique has also been successfully
applied to the drying of other materials such as activated
carbon, superphosphate, gelatine and pharmaceuticals (Ref.
6). Due to its unique properties, the technique has also
been found useful for a variety of seemingly-unrelated pro-
cesses, such as cooling (Ref. 8), blending (Ref. 9) and
coating (Ref. 10,11) of various materials, granulation of
fertilizers and other products (Ref. 12,13), pyrolysis of
shale (Ref. 14) and carbonization of coal (Ref. 15,16).

It appears, therefore, that the method has been quite widely
accepted as a useful means for fluid-solid contacting. Its
application to a commercial process, however, would gener-
ally require a larger capacity than can be handled by a
single spouted bed. Also, from the viewpoint of plant eco-
nomics it is obvious that the fixed costs of one large bed

would be lower than for a number of smaller beds having
a similar throughput. The obvious solution is scale up,
however, scale up of spouted beds is not straightforward.
For example, it has been shown that for satisfactory opera-
tion of spouted bed systems the column diameter to parti-
cle size ratio should be in the range 25-200 (Ref. 6).
This imposes severe limitations on the maximum bed diam-
eter. The largest column recorded in the literature has a
diameter of 610 mm (Ref. 5,7,17). Although this does not
represent an upper limit an order of magnitude separates
the diameters of practical spouted beds and fluidized beds.

There are two alternatives which could be used for over-
coming this limitation:

    (a)   Staging a number of units and maintaining a
           counter current flow of fluid and solids.

    (b)   Using a multiple spouted system.

The former was demonstrated by Madonna et al (Ref. 18),
using a system of four stages. The latter is not reported
in the literature. The aim of this work, therefore, was
to make a detailed study of the multiple spouted bed system.

2. EXPERIMENTAL

2.1 Preliminary Study

Two dimensional beds have been widely used in the study of
fluidization. The half-sectional bed as shown in Fig. 1
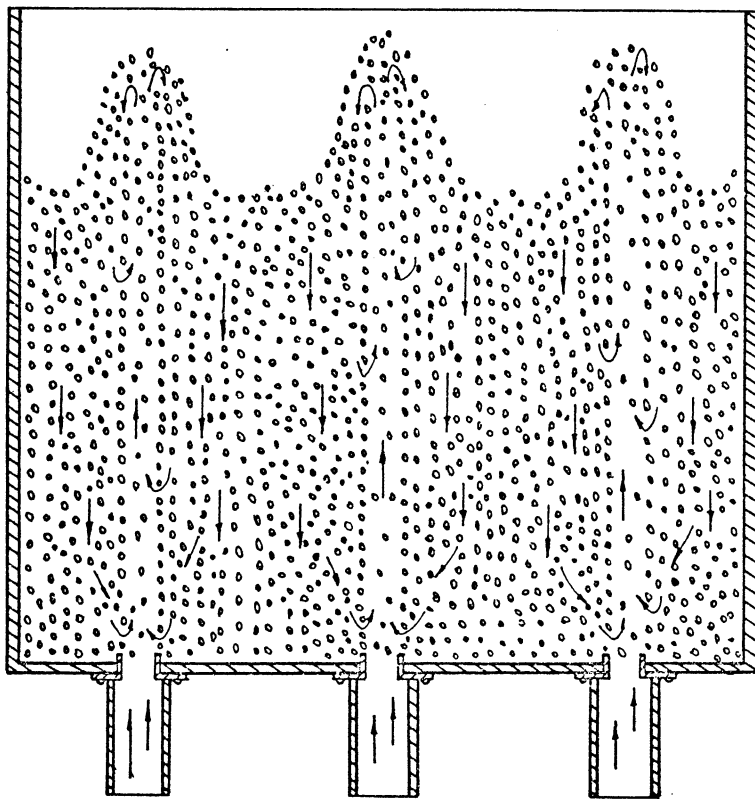
Fig. I   Schematic Diagram of a Multiple
              Spouted Bed

has found equal favour in the study of spouting (Ref. 1,17, 19,20) where it has been shown to behave as a full column. Initial work on the multiple spouted bed was conducted using a flat bottom, clear front, half-sectional bed with three 12.7 mm diameter gas inlets. Gas supplied to the gas inlets was controlled individually. The materials used in the study were wheat, rape seed and millet.

The mechanism of obtaining an active multiple spouted bed was found to resemble that of a single spouted bed. This bed is shown schematically in Fig. 1. It should be noted that there is a constant exchange of material between spouts. This occurrence is a result of material being transported over the bed top and the cross-flow of material through annular interfaces as the material descends.

The effect of the separation of gas inlets on spout stability was studied by varying the separation between gas inlets from 38 mm centres to 228 mm centres. With the spouts at 38 mm centres the bed became unstable as the spouts tended to merge and interfere while at 228mm centres solids mixing was poor. Satisfactory solids circulation appeared to be obtainable at 76 mm separation. However, this is still rather close to the unstable spout separation.

Further qualitative experiments were carried out in a column with two gas inlets. This column had a flat bottom and dimensions of 300 mmx150mmx1500mm. The gas inlet orifices were placed at 150mm centres and projected 3 mm above the bed floor, a practice which has been found to improve

bed stability (Ref. 21). Bed behaviour was observed with
various bed materials at various bed heights. The materials
employed were wheat, rape seed, millet and polythene pellets.
(See Table II for their physical properties). From these
runs, it was found that in most cases the bed tended to be-
come unstable as the bed height was increased. Two combined
effects seemed to be responsible for bed instability, namely,
spout pulsation and regression. The former appeared to be
associated with spouting all the time and increased in am-
plitude and frequency as the bed height increased. The
latter set in at a greater bed depth and seemed to have the
same tendency as the former. When the spout started to
pulsate and regress, an uneven bed level resulted as each
spout possessed its own pulsation and regression frequency.
Thus, a slight disturbance in the air flow to the bed would
usually cause one of the spouts to collapse.

The effect of spout pulsation and regression on bed sta-
bility was further investigated by operating the bed with
a removable baffle inserted vertically between spouts.
Under these conditions the bed acted as two single spouted
beds. The phenomenon of pulsation and regression was
again observed. This finding is in accordance with obser-
vations recorded by other workers (Ref. 18,20,22). It
appears, therefore, that spout instability is inherent to
the process. This has been normally overlooked in single
spouted beds because of the lack of any apparent ill-effect
on the process.

An attempt was made to stabilize the bed using baffles to

partially isolate neighbouring spouts from one another. These baffles extended to the static height of the bed but of course allowed interchange of bed material from one spout region to another during operation, over the top of the baffles. However, this was found ineffective in stabilizing the bed because there was still sufficient interaction between spouts, due to spout regression and pulsation, to cause one of the spouts to collapse.

Gas inlet orifice sizes were next varied from 6 to 25 mm diameter. The following observations were made with respect to bed stability:

(a) Wheat

Wheat was the largest bed particle used in the experiment. It had an effective diameter of 3.2 mm. Stable beds were achieved with orifices larger than 25 mm diameter.

(b) Rape Seed and Polythene Pellets I and II

For rape seed (1.9mm), polythene I (2.2mm) and polythene II (2.5mm) stable beds were achieved with orifices larger than 19 mm.

(c) Millet

For millet 1.2mm stable beds were obtained with orifices larger than 13 mm diameter.

During these runs it was seen that when suitable orifice sizes were used spout pulsation and regression although still present appeared to be at a minimum. Also, spout shape was better defined and spouting could be maintained

at flow rates close to the minimum spouting velocity.
Respouting of the bed after collapse was also found to be
easier. Therefore it appears that bed stability is depen-
dent on particle size as well as on inlet orifice size.
Table I summarized the results of these runs. From this
Table the optimal effective particle diameter to orifice
diameter ratios (D_p/D_i) are thus:

Material	Optimum Ratio, D_p/D_i
Wheat	0.126
Rape Seed	0.092
Millet	0.094
Polythene I	0.111
Polythene II	0.131

The range of optimal D_p/D_i ratios (0.092 - 0.131) is
quite narrow. It is probable that these ratios are not
true optimums because orifice diameter could only be
varied discretely. These results suggest, however, that
for maximum bed stability the ratio would probably have
to lie within the above range. It was necessary to check
results obtained in a three dimensional bed.

2.2 Design and Operation of the Experimental Multiple Spouted Bed

The three dimensional bed was constructed such that one
spout was completely surrounded by others. This was
achieved by arranging seven spouts on a 150mm triangular
pitch. The central spout was then free from wall effects

and would be typical of the majority of spouts in an industrial size multiple spouted bed. All measurements were therefore related to this spout.

The bed consisted of a 456x416x150 mm open topped, flat bottom timber box. Like the two-spout bed the spout orifices projected 3mm above the flat bottom. A weir of adjustable height was fitted to one side of the bed to control bed height at any pre-determined level.

The spouting air was supplied by a positive displacement blower capable of delivering 4.53 m^3/min (N.T.P.) of air at 69 kPa. An automatic pressure relief valve was employed to regulate pressure in the 0.85 m^3 capacity air receiver. A line from this receiver fed the seven spouting points through a set of calibrated rotameters and control valves. These valves allowed individual control of air flow to each gas inlet. A sufficiently long calming section of pipe was used between the control valve and the spout orifice to damp out any turbulence in the air flow.

A solids feed system was incorporated in the equipment. This consisted of a 0.085 cubic meter vibra-feed hopper mounted on platform scales, an engaging chamber and a disengaging cyclone. This system was needed for continuous running. In this operation, solids were fed from the hopper and pneumatically transported to one side of the top of the bed. A complete flow diagram of the experimental system is shown in Fig. 2.
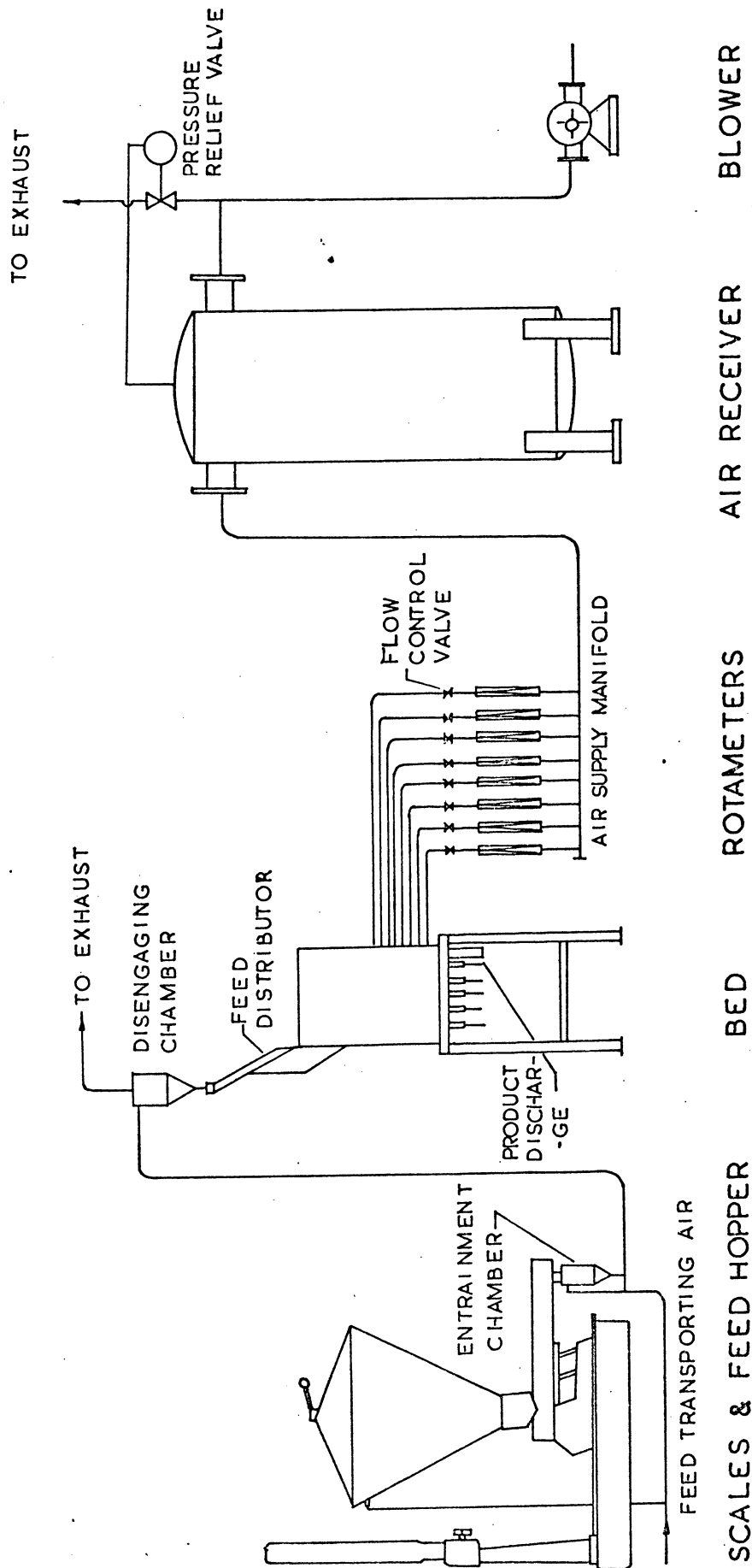
Fig. 2   Flow Diagram of the Experimental Multiple Spouted Bed System

The choice of a 150 mm separation between each orifice followed from the two-dimensional work since satisfactory solids circulation was likely when 13mm orifices were used. Furthermore, larger orifices could be used in the bed without changing the separation.

In the literature, reports on single spouted beds are mainly concerned with beds having conical bases, however, for multiple spouted beds, a more practical design is flat bottomed. The main shortcoming of this design lies in the fact that a zone of stagnant solids with a cone-like inner boundary is formed at the base. However, this zone was found to decrease in volume with increasing air flow and bed height (Ref. 23). Spouting stability was not affected by this design (Ref. 24).

3. RESULTS AND DISCUSSION

3.1 Effect of D_p/D_i Rations on Bed Stability - Qualitative Results

Earlier it was established that in a two-spout bed the D_p/D_i ratios appeared to have important controlling effects on bed stability. Experiments were then carried out in the three dimensional multi-spout bed with the aim of verifying this experience. Bed stability was observed using different D_p/D_i ratios. Bed materials used in the experiments were the same as those employed in the two-spout experiments. It was found that the bed behaved very much the same as the two spout bed. Again spout regression and pulsation was

observed. The effect on the stability of this bed appeared
to be more severe than that of the two-spout bed. This is
because of the higher degree of interaction between spouts
in a three dimensional bed. D_p/D_i ratios which gave
stable spouting for the two-spout bed were also found to
give stable spouting for this bed.

3.2   Quantitative Characterisation of the Bed

In order to characterise the bed, studies of hydrodynamic
characteristics such as pressure drop across the bed, mini-
mum spouting velocity, maximum spoutable bed height and
solids mixing are desirable. System variables usually used
in these studies are the flow rate of the spouting fluid,
column diameter, fluid inlet orifice diameter, particle
size, particle density and shape, fluid density and bed
height. In the present study, column diameter and fluid
density were constant since only one spouted bed was in-
vestigated and air only was used as the spouting fluid.
Furthermore, the inlet orifice diameter was also held con-
stant. The need for a larger inlet orifice diameter for
particles with larger effective diameter as indicated in
Table I presented problems with air supply. As a result
of this, it was decided to use 1.3mm diameter orifice
only. This enable larger particles to be spouted at reason-
able bed heights. This, on the other hand, gave less
stable beds when materials larger than millet were spouted.
However, experience obtained from the earlier model studies

indicated that the effect of instability on spouting

pressure drop, minimum spouting velocity and solids mixing

pattern was insignificant.

3.2.1 Pressure Drop Across the Spouted Bed

The spouting pressure drop of the centre spout was deter-

mined using the materials listed in Tables II. Manurung's

equation (Ref. 21) for spouting pressure drop was employed

to correlate the spouting pressure drop data. This correla-

tion was developed by considering P_s to approach the fluid-

ized pressure drop as the bed depth increases to infinity.

$$\lim_{\frac{L}{D_c} \to \infty} \frac{\Delta P_s}{L \rho_b} = 1$$

The above limit is transformed into the following linear

equation:

$$\frac{L \rho_b}{\Delta P_s} = 1 + a \left(\frac{D_c}{L}\right) \qquad \ldots\ldots(1a)$$

By evaluating "a" from experimental data, Manurung obtained

the following correlation which was found to fit the data

with an average deviation of 12 percent.

$$\Delta P_s = \frac{L \rho_b}{1 + 0.81 \frac{(\tan \beta)^{1.5}}{\phi^2} \left(\frac{D_c D_p}{D_1}\right)^{0.78} \left(\frac{D_c}{L}\right)} \qquad \ldots\ldots(1b)$$

This equation is general for a wide range of particles and

column variables in single spout beds and so has been used

to correlate the multiple spouted bed data. The only

problem is to define D_c (column diameter) for a multiple

spouted bed. This has been considered as follows: For a

bed with more than one gas inlet, the cross section of

each "spout region" generally is non-circular. The effec-

tive diameter of each region is thus defined as being

equivalent to the diameter of a cylinder having the same

cross sectional area as the spout region. For the present

case (the spout region under consideration was taken as a

150 mm square). The effective diameter of this square is

170 mm.

Fig. 3 relates the experimental and calculated pressure

drop. The agreement is seen to be good.

3.2.2   Minimum Spouting Velocity

Minimum spouting velocity is one of the most important

hydrodynamic variables in the spouting process. Although

it has been the subject of over a dozen investigations, a

satisfactory general correlation for predicting this para-

meter has still not been developed. This is due to the

fact that minimum spouting velocity is dependent on the

properties of solids and fluid as well as bed geometry.

The problem is therefore inherently more complex than in

either fluidization or pneumatic transport, with the re-

sult that most investigators have had to resort to empiri-

cism for correlating experimental results. Nevertheless,

some of the correlations proposed are sufficiently general
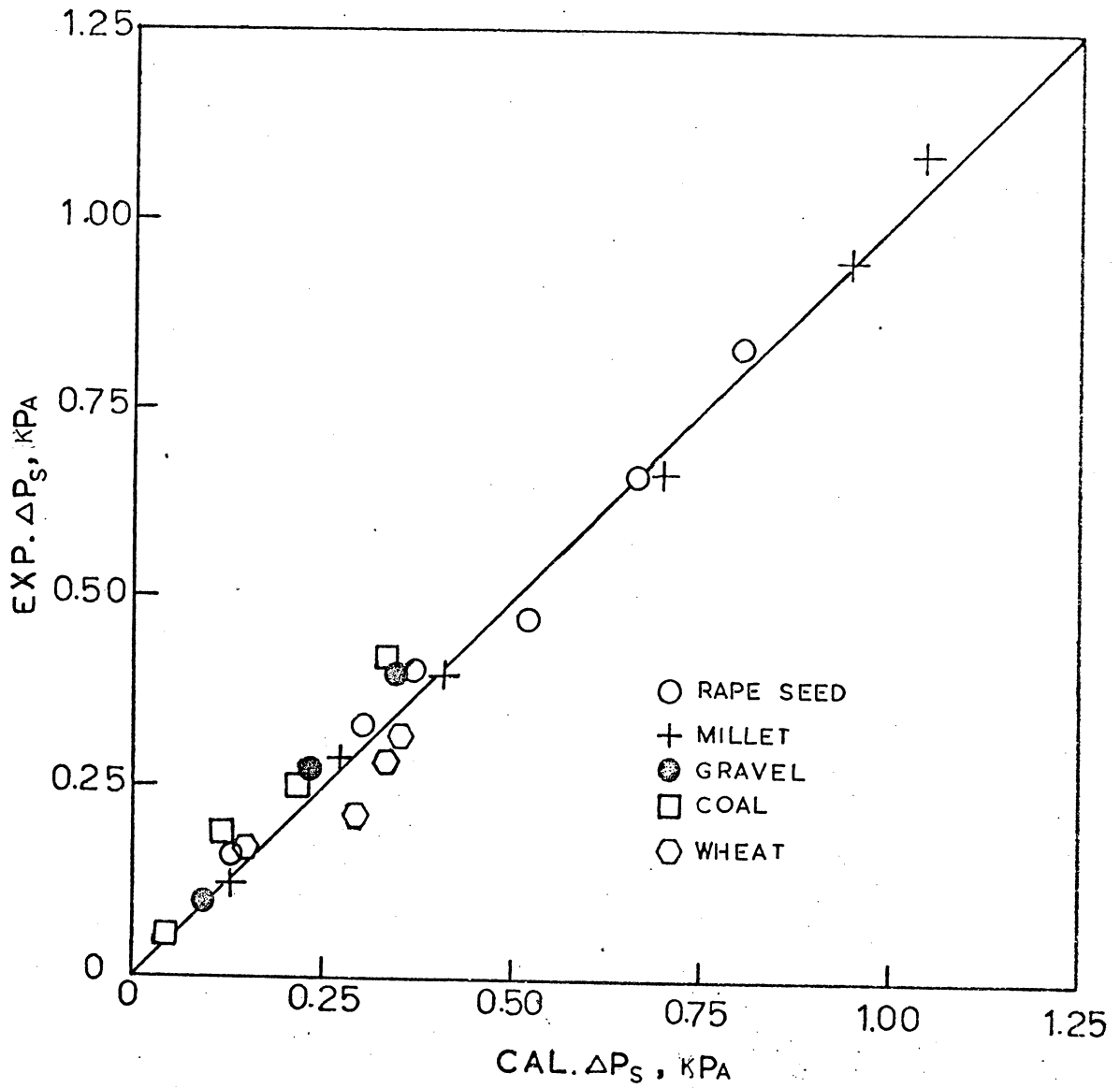
to be of practical value.

Fig. 3 Comparison of Experimental and Calculated Spouting
Pressure Drop

Mathur and Epstein (Ref. 3) compared the validity of correlations proposed by Mathur and Gishler (Ref. 1), Becker (Ref. 2), Manurung (Ref. 21) and Reddy and Smith (Ref. 25). The conclusion was that the first correlation (i.e. Mathur and Gishler's) although the most simple in form gave the most reliable prediction of the minimum spouting velocity for common materials, over a wide range of practical conditions. This equation is given as follows:

$$V_{ms} = \left(\frac{D_p}{D_c}\right)\left(\frac{D_i}{D_c}\right)^{1/3} \sqrt{2gL \frac{(\rho_p - \rho_f)}{\rho_f}} \quad \ldots (2)$$

Comparison of the predicted results and the experimental data obtained from the centre spout is shown in Fig. 4. From this diagram it appears that most of the experimental data have a tendency of deviating more from the predicted as bed height is increased. This is due, to the higher gas rate required to maintain a spouting bed when D_i does not fall in the optimum region. Therefore it appears that a correlation which was developed for a single spouted bed may be used for a stable multispout bed.

3.2.3 Maximum Spoutable Bed Height

Maximum spoutable bed height is defined as the height of a bed above which a spout cannot be formed. The maximum spoutable bed height could not be easily determined in this system because of the large amount of air required. However, useful information could be derived from the results obtained from the two-spout bed.

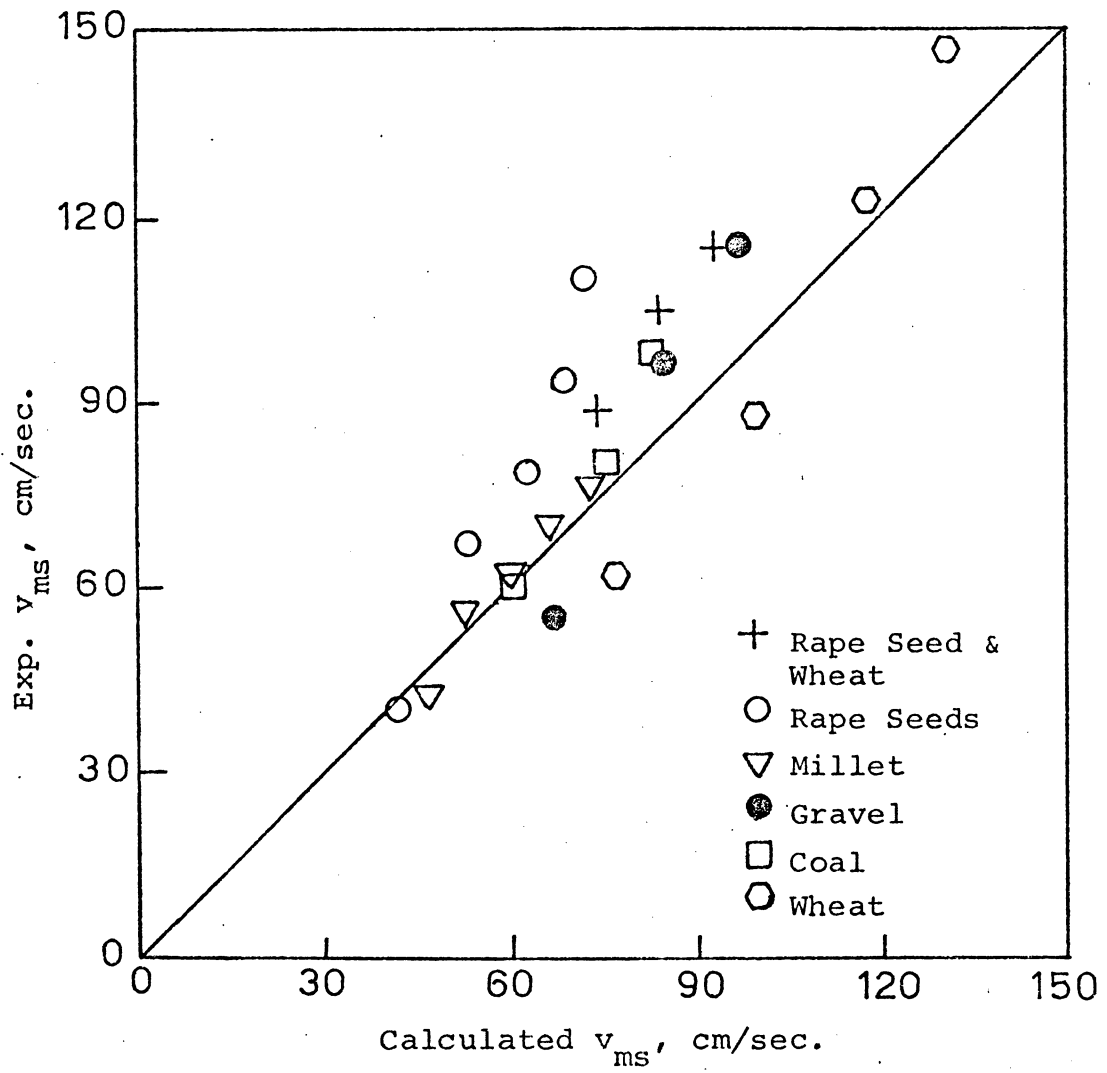In Table 1, maximum spoutable bed heights for wheat, rape

Fig. 4   Comparison of Experimental and Calculated Min.

Spouting Velocity

seed and millet are listed.

Malek and Lu (Ref. 26) employed a wide range of materials
and different column diameters (i.e. 100,150 and 225mm) for
investigating the maximum spoutable bed height. The
following correlation was proposed:

$$\frac{L_m}{D_c} = K\left(\frac{D_c}{D_p}\right)^{0.75} \cdot \left(\frac{D_c}{D_i}\right)^{0.40} \cdot \left(\frac{\lambda2}{\rho_p^{1.2}}\right) \quad \ldots\ldots(3)$$

where

$$K = 0.105 \text{ for air}$$

$$\lambda = 0.205 \; S_p/V_p{}^2/3$$

By using this correlation, maximum spoutable bed heights
for wheat, rape seeds and millet under the "optimal
conditions" are respectively 720mm, 975mm and 1360mm.
Higher maximum spoutable bed heights for a single spouted
bed is not surprising as spout interaction plays a very
influential role in multiple spouted beds.

3.3.3   Solids Mixing

In order to compare further the performance of multi and
single spout beds a study of solid mixing was carried out.
A solids flow model was developed and compared with pub-
lished data.

A stimulus-response technique was utilised for the study.
This technique uses a tracer which can be introduced into
the system in the form of a step change, a pulse, a ramp
or a sinusoidally varying input. Tracer concentration is
then monitored at the exit of the vessel. Several types

of tracers have been used in studies of this type. The
choice of the most suitable tracer depends on the applica-
tion and the size of the equipment under study. For
solids, methods involving coloured or tagged particles
have been the most popular (Ref. 27,28). In the present
situation the use of a step function involving a coloured
tracer was employed.

A series of residence time distribution runs was carried
out using wheat and millet as bed material, and the bed
heights were respectively 200mm and 350 mm.

To commence a run the bed was initially filled with coloured
particles to the operating level whilst spouting. The
spouting air was then adjusted to about 5% above the mini-
mum spouting gas rate. At time zero, non-coloured feed
was introduced at a pre-determined rate and product samples
taken at regular intervals for approximately two mean resi-
dences times. These samples were then weighed and tracer
and non-tracer separated. The weight fraction of tracer
was then determined.

As an aid to developing the solids flow model some visual
observations were conducted using the three-spout half-
sectional perspex model. It was found that the feed
particles entered the annular region of the bed on the side
opposite the product outlet and moved downward to the
spout where they were rapidly transported to the fountain
region at the top of the bed. Some of the particles then

re-entered the annular section of the bed where the cycle

was repeated, and some migrated to the neighbouring spouts

as they descended from the fountain. It was also noted

that some degree of cross flow took place at the annular

sections between spouts. However, as the circulation of

particles in a spouted bed is high (Ref. 29) the extent of

particle mixing would seem to be determined by the random

movement of particles travelling from spout to spout over

the bed top. The concept of "mixed models" originally

proposed by Cholette and Cloutier (Ref. 30) and Levenspiel

(Ref. 31) has been used to characterize the multispout bed.

This model considers the system as consisting of the follow-

ing kinds of regions: plug flow region, backmix region,

dispersed plug flow regions and deadwater regions. In

addition to the above regions, mixed models may used the

following kinds of flow: by-pass flow, recycle flow and

cross flow.

From the experimental data an internal age distribution

function, I, diagram was constructed (Fig. 5). The

following expression was obtained with a standard error of

estimate of 0.08.

$$\mathrm{Ln}\ I = \mathrm{Ln}\ (1 - {}^{C}/_{C_o}) \qquad \ldots\ldots(4)$$
$$= 0.02 - 17\theta$$

After matching the above expression with various conceptual

mixed models, the model which consisted of a relatively

large voluem of backmix region, a portion of deadwater

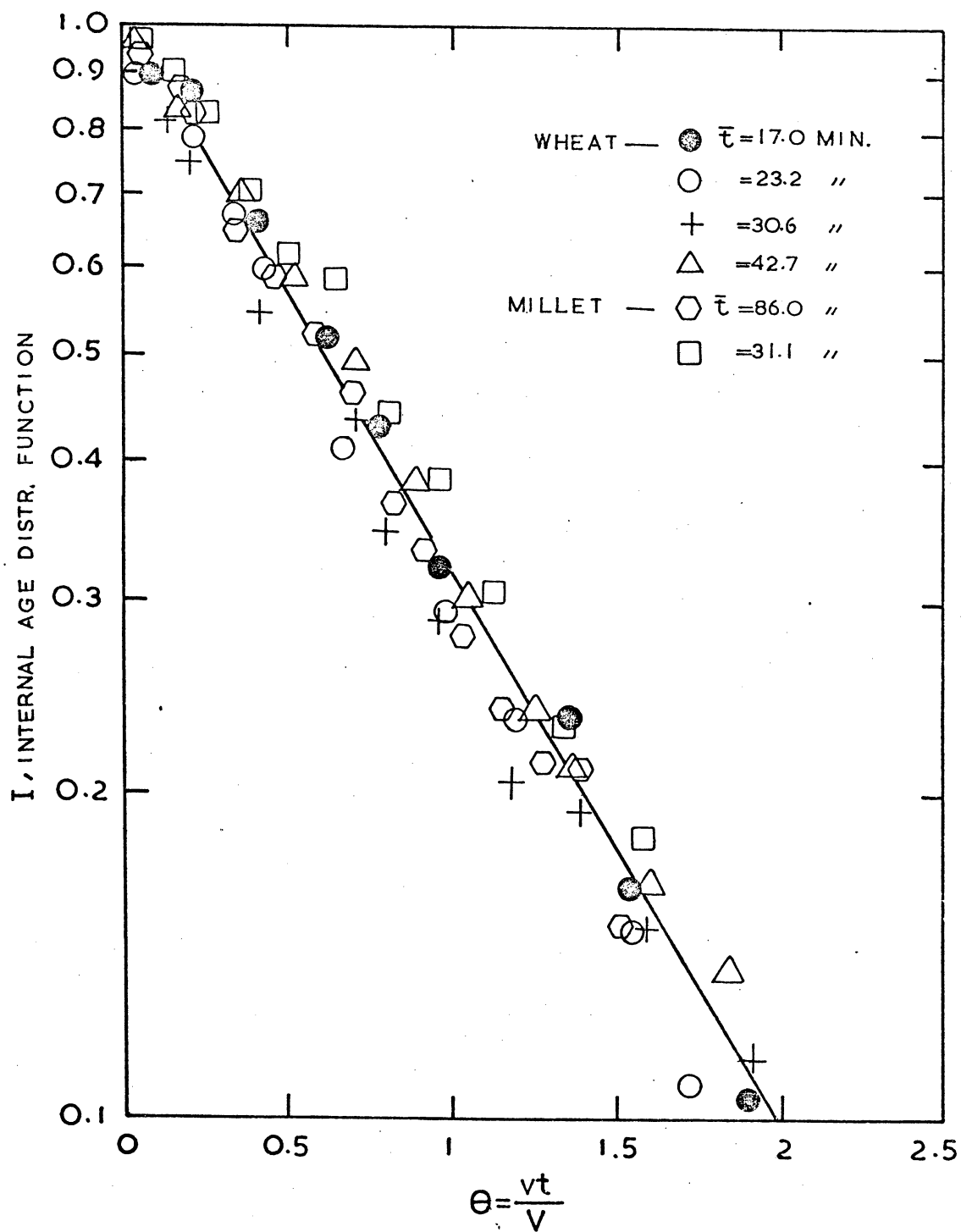region, some plug flow region and negligible bypass flow

Fig. 5 Internal Age Distribution Function Diagram

appeared to give the line of best fit. The model is
shown schematically in Fig. 6.

Mathematically the model can be shown to be derived
from the following expression (Ref. 31):

$$I = \text{Exp} \ [-V/V_b \ (\theta - V_p/V)] \quad \ldots\ldots (5)$$

From eq. (4)

$$-V/V_b \ (\theta - V_p/V) = 0.02 - 1.17\theta$$

and so eq. (5) becomes

$$I = \text{Exp} \ [-1/0.855 \ (\theta - 0.017)] \quad \ldots (6)$$

From the above relationship, the total volume of the bed,
therefore, comprised 85.5 percent of completely mixed re-
gion, 1.7 percent of plug flow region and 12.8 percent of
deadwater region. Cross flow at the annular sections be-
tween spouts was also estimated using the method given by
Zenz and Othmer (Ref. 32). As expected the magnitude of
cross flow was quite low, being of the order of 4.55 kg/hr.
This rate is too low to account for the rapid mixing of
the entire bed material observed in the experiment. It
is estimated that if solids cross-flow is the only mode
of solids transport then it would take about one hour to
exchange 95% of the bed material between adjacent spout
regions. Hence, it is proposed that the bed material in
a continuous flow multiple spouted bed is transported
mainly by overflow of solids at bed surface from one spout
region to another.

Internal circulation of a spout region is an important
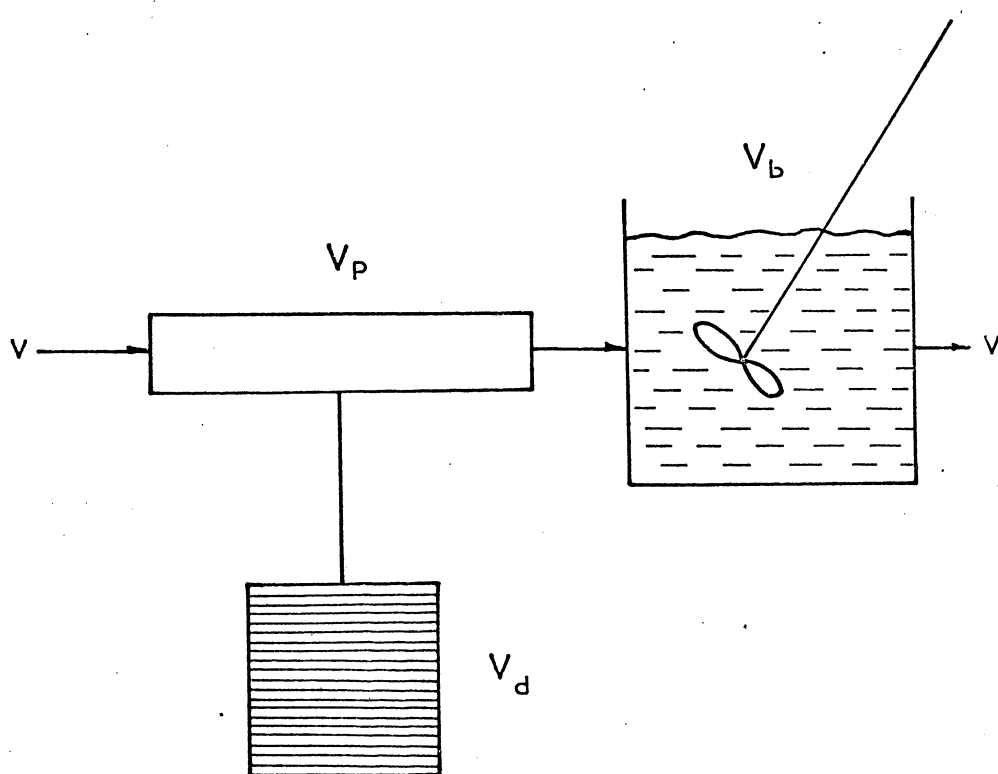factor contributing to formation of a well mixed multiple

FIG. 6   SOLIDS-FLOW MODEL

spouted bed. Chaterjee (Ref. 29) utilised the same method in studying the internal circulation rate of a single spout bed. An empirical correlation was thus proposed. Application of correlation to the present situation gave an internal circulation rate of about 1000 kg/hr.

Kuga et al. (Ref. 27) studied the effects of orifice size, spouting gas velocity, bed height and mean residence time on solids mixing in a 150 mm single spouted bed, and concluded that under all conditions investigated the bed was essentially a perfect mixed system. Although it could be true that for higher bed depths the plug flow element may become larger, as was shown by Barton et al. (Ref. 16), the validity of this model should not be significantly affected.

4. CONCLUSION

The experimental work reported in this paper has shown that the multiple spouted bed was inherently unstable due to the tendency of the spouts towards pulsation and regression. Bed stability was found to be dependent on the D_p/D_i ratio as well as bed height. For satisfactory design and operation of a multispout bed the ratio of D_p to D_i would probably have to be in the range of 0.09 - 0.13.

It has also been shown that generally correlations developed for single spouted beds could be used for the characterisation of multispouted beds operated within the stable regime.

A flow model of solids for this system was developed using the concept of "mixed models". Comparison of the model with those for a single spouted bed suggest that this model could be applicable to situations beyond the present experimental range.

5.   ACKNOWLEDGEMENT

TABLE I

Effect of Gas Inlet Diameter on Bed Stability

Material	Orifice Diameter, mm.	Maximum Spoutable Bed Ht., mm.	D_p/D_i	Remarks
Wheat	13	–	0.252	unstable
	19	–	0.168	unstable
	25	720	0.126	stable
	29	605	0.112	stable
Rape Seed	13	–	0.146	unstable
	19	585	0.092	stable
	25	500	0.074	stable
Millet	9.5	–	0.125	unstable
	13	1410	0.094	stable
	19	1110	0.063	stable
	25	830	0.047	stable
Polythene I	13	–	0.176	unstable
	19	635	0.111	stable
	25	560	0.832	stable
Polythene II	13	–	0.196	unstable
	19	640	0.131	stable
	25	600	0.098	stable

APPENDIX

Materials Used

The materials used for the experiment were wheat, rape seed, coal, gravel and mixtures of rape seed and wheat. Their physical properties are listed in Table II.

The apparent densities were determined by using a pyknometer. The bulk densities were determined by weighing the bed charge and measuring the static bed height after the bed had been through a spouting cycle. Results obtained in this manner were found to be consistent from run to run.

The effective particle diameters were obtained from the sieve analysis using the following expression:

$$D_p = \frac{1}{\sum\limits_{i=1}^{n} x_i / d_{pi}}$$

This definition has been found to be the best method of characterising the diameter of mixed-size particles (Ref. 33).

The shape factors were calculated by Brown's expression (Ref. 34):

$$\phi = \left(\frac{1}{n}\right) \frac{D_p}{D_v}$$

where

n = $\dfrac{\text{specific surface of particle}}{\text{specific surface of sphere of same diameter}}$

D_v = particle equivalent diameter

specific surface = surface area of particles per unit of mass

TABLE   II

Physical Properties of Bed Material

Material	Apparent Density (gm/cc)	Bulk Density (gm/cc)	Mean Diameter mm.	Shape Factor
Rape Seed	1.06	0.66	1.9	1.0
Wheat	1.35	0.76	3.2	0.84
Coal	1.36	0.74	2.0	0.87
Gravel	2.62	1.36	1.7	0.82
Millet	1.32	0.69	1.2	0.83
Polythene I	0.96	0.56	2.2	0.87
Polythene II	0.96	0.60	2.5	0.84
Rape Seed & Wheat	1.21	0.72	2.5	0.92

LIST   OF   SYMBOLS

a   Coefficient in (1a)

C   Product concentration

C_o Feed concentration

D_c Column diameter

D_i Diameter of gas inlet orifice

D_p Particle diameter

D_v Equivalent particle diameter

d_{pi} Particle diameter of size fraction, x_i

g   Acceleration of gravity

I   Internal age distribution function

K   Constant as defined in Equation 3

L   Bed height

L_m Maximum spoutable bed height

ΔP_s Spouting pressure drop across bed

S_p Surface area of particle

t   Time

$\bar{t}$ Mean residence time

V   Bed volume

V_b Volume of backmix region

V_p Volume of plug flow region (or volume of particle defined in Equation 3)

V_{ms} Minimum spouting velocity

v   Volumetric flow rate

x_i Mass fraction of particles of size d_{pi}

GREEK   LETTERS

β	(beta)	Angle of particle internal friction
θ	(Theta)	Dimensionless time
ρ_b	(rho)	Bulk density of particle
ρ_f	(rho)	Fluid density
ρ_p	(rho)	Apparent density of particle
ϕ	(phi)	Particle shape factor
λ	(lambda)	As defined in Equation 3

REFERENCES

1. Mathur, K.B. and Gishler, P.E., -A Technique for Contacting Gases with Coarse Solid Particles - A.I.Ch.E. Journal, Vol. 1, No. 2, June, 1955, pp 157.64.

2. Becker, H.A. -An investigation of the laws governing the spouting of Coarse Particles - Chem. Engg. Science, Vol. 13, No. 4, June, 1961, pp 245-62.

3. Davidson, J.F. and Harrison, D. (Editors) - Fluidization, Chapter 17, Academic Press 1971.

4. Becker, H.A. and Sallan, H.R. - Drying Wheat in a Spouted Bed on the Continuous, Moisture-Controlled Drying of Solid Particles in a well-mixed Isothermal Bed - Chem. Engg. Science, Vol 13, 1960, p 97.

5. Cowan, C.R., Peterson, W.S. and Osberg, G.L. -Drying of Wood Chips in a Spouted Bed. Pulp and Paper magazine of Canada, Vol. 58, Dec., 1957, p 138.

6. Nemeth, J. and Pallai, I. -The Spouted Bed Method and its Possible Utilizations. Magyar Keimtnook Lavja, Vol. 2, 1970, pp 74-82.

7. Peterson, W.A. - Spouted Bed Dryers. Can. Jnr. Chem. Engg., Vol. 40, No. 5, Oct., 1962, pp 226-30.

8. Fissons Fertilizers Ltd., Levington, U.K.

9. Bowers, K.H., Stevens, J.W. and Suckling, R.D., British Patent No. 855809, filed 1959, granted 1960.

10. Heiser, A.L., Lowenthal, W. and Singiser, R.E., U.S. Patent Nos. 3, 112, 220, filed 1960, granted 1963.

11. Singiser, R.E., Heiser, A.L. and Pritting, E.B., Air

Suspension Tablet Coating. Chem. Engg. Progr., Vol. 62, No. 6, June, 1966, pp 107-111.

12. Berquin, Y.F., U.S. Patent No. 3,231,413, filed 1962, granted 1964.

13. Berquin, Y.F. - Noveau Procede de Granulation et son application dans le domains de la Fabrication des Engrains. Genie Chimique, Vol. 86, 1961, pp 45-47.

14. Berti, L.P. - Operational Criterion of a Spouted Bed Oil Shale Retort. D.Sc. Thesis, Colorado School of Mines, Golden, Colarado, U.S.A., 1968.

15. Buchanan, R.H. and Manurung, F. - Experiences in Fluidization. Spouted Bed Low-Temperature Carbonization of Coal. British Chem. Engg., Vol. 6, No. 6, June, 1961, pp 402-3.

16. Barton, R.K., Rigby, G.R. and Ratcliffe, J.S. - The Use of a Spouted Bed for the Low Temperature Carbonization of Coal - Mech. and Chem. Trans. Inst. of Engrs. Aust., Vol. 4, 1968, pp 105-112.

17. Thorley, B., Saunby, J.B., Mathur, K.B. and Osberg, G.L. - An Analysis of Air and Solids Flow in a Spouted Wheat Bed - Can. Jnr. Chem. Engg. Vol. 37, No. 5, Oct., 1959, pp 184-192.

18. Madonna, L.A., Lama, R.F. and Brisson, W.L. - Solid-Air Jets. Brit. Chem. Engg., Vol. 6, No. 8, Aug., 1961, pp 524-28.

19. Lefroy, G.A. and Davidson, J.R. - The Mechanics of Spouted Bed, Trans. Inst. Chem. Engrs., Vol. 47, 1969, pp T120-128.

20. Malek, M.A., Madonna, L. and Lu, B.C.Y. - Estimation of Spout Diameter in a Spouted Bed. Industrial and Engg. Chemistry Process Design and Developemtn, Vol.2, No. 1, Jan., 1963, pp 30-34.

21. Manurung, F. - Studies in the Spouted Bed Technique with Particular Reference to the Application to Low Temperature Coal Carbonization, Ph.D. Thesis, Uni. of N.S.W., 1964.

22. Volpicalli, G., Ross, G. and Massimilla, L. - Gas and Solids Flow in Bi-Dimensional Spouted Beds. Proceedings Eindheven Fluidization Symposium, 1967, pp 123-33.

23. Hunt, C.H. and Brennan, D. - Estimation of Spout Diameter in a Spouted Bed. Aust. Chem. Engg., Vol. 6, Nos. 3, March, 1965, pp 9-15.

24. Mathur, K.B., Epstein, N. - Dynamics of Spouted Beds, Advances in Chemical Engineering (in press).

25. Reddy, K.V.S. and Smith, J.W. - Spouting Mixed Particle-Size Beds. Can. Jnr. of Chem. Engg., Vol. 42, No. 5, Oct ., 1964, pp 206-10.

26. Malek, M.A. and Lu, B.C-Y. - Pressure Drop and Spoutable Bed Heights in Spouted Bed. Ind. Engg. Chemistry Process Design and Development, Vol. 4, No. 1, Jan, 1965, pp 123-128.

27. Kugo, M. Watanabe, N. Uemaki, O. and Shibata, T. - Drying of Wheat by Spouted Bed. Bull. Hokaido Uni., Japan.

28. Bowling, K. McG. and Watts, A. - Determination of Particle Residence Time in a Fluidized Bed - Theoretical

and Practical Aspects. Aust. Jnr. of Appl. Science, Vol. 12, No. 4, Dec., 1961, pp 413-27.

29. Chaterjee, A. - Effect of Particle Diameter and Apparent Particle Density on Internal Solid Circulation Rate in Air-Spouted Beds. Ind. Engg., Chemistry, Process Design and Development, Vol. 9, No. 4, 1970, pp 521-526.

30. Cholette, A. and Cloutier, L. - Mixing Efficiency Determinations for Continuous Flow Systems. Can. Jnr. Chem. Engg., Vol. 37, June, 1959, pp 105-112.

31. Levenspiel, O. - Chemical Reaction Engg., New York, John Wiley and Sons Inc., 1964.

32. Zenz, F.A. and Othmer, D.F. - Fluidization and Fluid Particle Systems- Reinhold, N.Y., 1960, p 290.

33. Van Heerden, C., Nobel, A. and Van Krevelen, D.W. - Studies on Fluidization I - The Critical Mass Velocity. Chem. Engg. Science, Vol. 1, No. 1, 1951, pp 37-49.

34. Brown, G.G. et al. - Unit Operations, p 77 - John Wiley and Sons Inc., New York, 1955.